ISSN 0970 - 3268

The journal of the Indian Association of Sedimentologists

First Online Volume

Dinasaur egg nest in Lamenta Formation

The journal of the Indian Association of Sedimentologists

ISSN 0970 - 3268

Managing Editors:

G. M. Bhat
Bashir Ahmed Lone

The JIAS is leader in its field and publishes ground-breaking research from across the spectrum of sedimentology, sedimentary geology and sedimentary geochemistry and allied braches of sedimentary research. It also publishes review articles, editorials, conference reports, tributes, etc. It is currently distributed to over universities and research laboratories in India and abroad. Access to the complete electronic journal archive over the past five years comes free of cost. Subscribers also have the option to buy the printed journal at subsidized cost.

TABLE OF CONTENTS

ARTICLES

First online volume
Jour. Indian Association of Sedimentologists, Vol. 35, No. 1 (2018), pp.3-4
ISSN 0970-3268

Report

National conference on "Basin dynamics, facies architecture and palaeoclimate" and 34th Convention of Indian Association of Sedimentologists

M. A. Quasim*, M. Albaroot, Asma A. Ghaznavi and Zuhi Khan
Department of Geology, Aligarh Muslim University, Aligarh - 202002
*E-mail: adnanquasim@gmail.com

The 34th convention of Indian Association of Sedimentologists (IAS) and national conference on "Basin dynamics, facies architecture and palaeoclimate" was held at the Sant Gadge Baba Amravati University (SGB), Amravati, Maharashtra, India. More than ninety oral presentations including seven keynotes were delivered by researchers with ninety five extended abstracts and three abstracts for the Young Sedimentologist Award competition. The inauguration ceremony was presided over by Dr. Murlidhar G. Chandekar, Vice Chancellor, SGB Amravati University, Amravati.

Prof. M. Raza, General Secretary, IAS expressed his pleasure for a good participation in the convention and outlined the vision and mission of IAS to reach maximum researchers every year in order to develop a strong platform for geoscientist interaction and exchange of ideas. Dr. D.M. Mohabey, Ex. DDG, GSI, Northern Region, Lucknow appreciated the organizers in putting up a year-long effort in organizing such an event. Prof. G.N. Nayak, President of IAS emphasized that much deliberation cater advance aspects of the sedimentological studies to be addressed by young minds. Prof. G.M. Bhat, Vice President, IAS, added that the platform should be fully utilized by the researchers to convey their ideas in a systematic and detailed manner. He stressed that feedback should be positively incorporated by the participants in improving their future research ventures. The inaugural session ended with vote of thanks by Dr. Ashok K. Srivastav, Convener, IAS, where he thanked all the participants, delegates and dignitaries. He also expressed his gratitude towards all the technical staff, faculty members and students of SGB University for their endless effort in organizing the event

On day one, three keynote addresses were presented by Dr. A.K. Singhvi, Honorary Scientist, PRL, Ahmedabad "Correlation of terrestrial and marine sedimentation records during the Quaternary: some conceptual issues", Dr. Rajwant, Scientist-E, SERB, New Delhi "Research challenges and opportunities for pursuing career in earth and atmospheric sciences", and Dr. D. M. Mohabey, Ex. DDG, GSI, Northern Region, Lucknow, "Is Deccan Volcanism responsible for termination of Indian Late Cretaceous Dinosaurs?",

Two technical sessions were conducted on first day based on "basin dynamics, climate through time and space and resource potential of sedimentary basins" and "Facies architecture and depositional environments". In the last technical session on first day three young sedimentologists presented and defended their research work for the Young Sedimentologist's Award.

Day second started with keynote address by Dr. A.V. Joshi Professor, Department of Geology, M. S. University of Baroda, Vadodara, delivered a keynote address on "Infratrappean sequences (Maastrichtian) of Narmada Basin, western India: repository of terminal Cretaceous

events - A review". Another keynote address was presented by Dr. B. P. Singh, Professor, CAS in Geology, Banaras Hindu University, Varanasi, on "Evolution of the western Himalayan foreland basin".

Technical session-III was based on petrology and technical session-IV was on hydrogeology, remote sensing and GIS, technical session-V on stratigraphy and paleobiology and technical session-VI on Quaternary basins of India, surface and subsurface processes.

The third day of the conference was devoted for the fieldwork in Salbardi area of Betul, Madhya Pradesh where Lower Gondwana and Lameta Formation are exposed. The Lameta Formation of Salbardi area typifies the fluvio-lacustrine environment and bears dinosaur eggs nest.

Participants of the 34th Convention of Indian Association of Sedimentologists Salbardi area

Dinosaur egg nest in Lameta Formation

First online volume
Jour. Indian Association of Sedimentologists, Vol. 35, No. 1 (2018), pp.5-22
ISSN 0970-3268

Late Paleozoic-Early Triassic Mega Sequences of Southern Pangea Supercontinent: Their Climate and Tectonic Regime between Panthalassa and Tethys: an overview

S. M. Casshyap and Helmut Wopfner*
Department of Geology, Aligarh Muslim University, Aligarh (Retd.)
*Geological Institute, University of Cologne, Germany (Retd.)
smcasshyap@gmail.com

Abstract: The contiguous assembly of continental plates in southern Pangea, comprising South America, Afro-Arabia, India, Antarctica and Australia constituted original "Gondwana", bounded by Panthalassa in the south and Tethys to the north. The sedimentary sequences overlying the super continental crust at Pangean stage have been referred to as Pangea Mega Sequence (PMS), the term is synonymous with the term "Lower Gondwana" of Indian stratigraphy ranging in age from Permo-Carboniferous to Early Triassic, exhibiting similar characters across the whole of Gondwana . During the Permo-Triassic extreme climatic variations across Gondwana were experienced beginning with Gondwana glaciation in the Late Carboniferous to Early Permian, followed by warm to semi-humid, and arid to hot conditions by the Late Permian-Early Triassic. The depositional period of PMS was equally governed by three contrasting tectonic regimes: i) compressive conditions on the Panthalassan edge of Gondwana plates along the southern margin; ii) corresponding trans-pressional sags forming interior cratonic basins of southern Africa, and iii) transtension and rifting experienced in the north along the Tethys margin and adjoining intracratonic basins. The resultant glacial and non-glacial facies developed are exemplified in the corresponding Gondwana sediment assemblage of peri/intracratonic tectonic basins of southern Pangean supercontinent. Stratigraphic setting, lithofacies, depositional environments and climatic history of the aforesaid sequences are reviewed in selective basins of Afro-Arabia, India, Antarctica, Australia, and detached blocks of East and Southeast Asia. The striking similarities between the lithofacies indicate matching climate/depositional conditions and similar timing of tectonic pulses. A synthesis of records on the direction of Permian glacial transport and paleocurrents of succeeding fluvial system in different basins of southern Pangea reveals a radial paleodrainage pattern in central-eastern Gondwanaland as in Antarctic highland, directed towards SW in South Africa, N in India, NW in West Australia, and SE in Eastern Australia. The paper explains the causes of climatic changes, the influence of pole drifting and arrangement of seas and continent.

Introduction

Pangea which was the latest supercontinent to form during 450-320 Ma and existed from Late Paleozoic to Early-Middle Mesozoic era, assembled, existing micro-continents affected by Early Paleozoic orogeny and fold belts. In contrast, to present earth and distribution of continental mass, much of Pangea was in southern hemisphere with contiguous assembly of continental plates comprising South America, Africa, India, Antarctica and Australia, which constituted original "Gondwana" bounded by a super ocean Panthalassa in the south and Tethys to the north. The sedimentary sequences overlying the super continental crust at the Pangea stage have been referred to as Pangea Mega Sequence (PMS). The term is synonymous with the term Lower Gondwana of Indian stratigraphy which embraces rock sequences ranging in age from Permo-Carboniferous to Early Triassic exhibiting similar facies and sedimentary characters across the whole of southern Pangea. Figure 1 represents the reconstruction of Gondwana display the major occurrences of Late Paleozoic-Early Triassic depositional basins including localized depocentres of Arabia, as detached Gondwana derived blocks (Wopfner,2012).The review treaties with climatic developments and tectonic regimes as recorded in the sedimentary sequences of the aforesaid depositional basins from Africa

south of equator, through India, Antarctica and Australia.

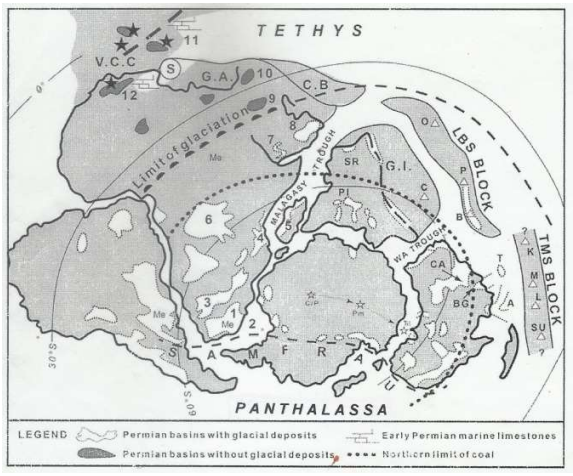

Figure: 1. Reconstruction of of southeren Pangean supercontinent / Gondwana in Early Permian time depicting distribution of with Late Carboniferous –Early Triassic sediments (=Pangean Mega Seqence /PMS), distinguishing between basins with or without glacigene deposits. Dashed curve shows the approximate northern limit of glaciation; dotted curve shows limit of coal formation. Numerals identify the following basins; 1. Karoo; 2.Falkland ; 3. Kalhari; 4. Ruhuhu (Southern Tanzania); 5. Morondava (Medagascar); 6. Congo; 7. Yemen; 8. South Oman; 9. Saudi Arabia; 10. Levante; 11.South Alpine Terrine (Collio-Etsch- Carni); 12. Morocco (after Wopfner, 2012). Gondwana derived Blocks including LBS: Lhasa-Baoshan-Shan; TMS: Tengchong-Malay-Sumatra. Open stars refer to position of Permian South Pole.

Evolutionary factors: climatic variations and tectonic regimes

During the end of Paleozoic/ beginning of Mesozoic extreme climatic variations across Gondwana were experienced, from great Gondwana glaciation when, glaciers flourished at places upon Gondwana in the Late Carboniferous–Early Permian, to warm to semi humid, and arid to hot climate by the Late Permian–Early Triassic. In Afro-Arabia, India, and Australia glaciers advanced to 40° paleo-latitude creating a steep gradient between them and hot– humid environment in the vicinity of equator. Synchronous deglaciation associated with a eustatic rise of sea level in the Early Sakmarian was followed by warm climate and increased humidity resulting in the formation of the large coal swamps/coal deposits between the South Pole and about 50° paleo-latitude succeeded by increasing aridity and hot climate towards equator in the north (Fig. 1), as exemplified by the Gondwana sediments in the various cratonic basins across southern supercontinent. The depositional period of PMS was equally influenced by three contrasting tectonic regimes: (i) the compressive system of the Samfrau Geosyncline dominated the Panthalassan margin of Gondwana in the south, resulting in the linear fold system extending from South America and Africa via Antarctica to eastern Australia (Veevers and Powell, 1994); (ii) corresponding trans-pressional sags controlling the adjoining interior cratonic basins of southern Africa; and, iii) the compressive conditions along the Panthalassan edge contrasted with the northern margin of Gondwana where extension and transtension prevailed and rifting was experienced along the Tethys margin (Sengor, 1998), which is in the adjoining intracratonic basins. The resultant glacial and non-glacial facies realms developed in the corresponding depositional sequences are reviewed from Karoo Super group and equivalents of South Africa, Tanzania, Madagascar, Arabia, southern Alpine terrine, Lower Gondwana and equivalents of India, Antarctica, Australia, and detached Gondwana derived blocks of East and Southeast Asia.

Karoo super group: Stratigraphy, lithofacies and depositional environment

South Africa

The post-Numarian PMS in African continent south of Paleozoic equator is referred to as the Karoo Super group and its coeval equivalents (Fig. 2). The stratigraphic

sequence of the Karoo Super group is demonstrated in figure 3. In the southern part of South Africa, Karoo sedimentation took place in the subsiding fore-deep of the

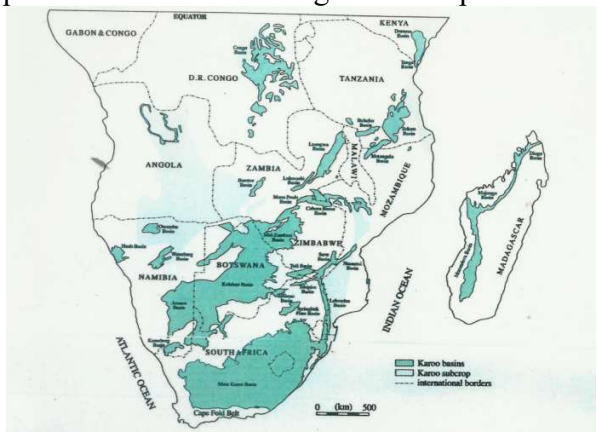

Figure: 2. Distribution of Karoo Basin in south-central Africa (after Wopfner, 2002).

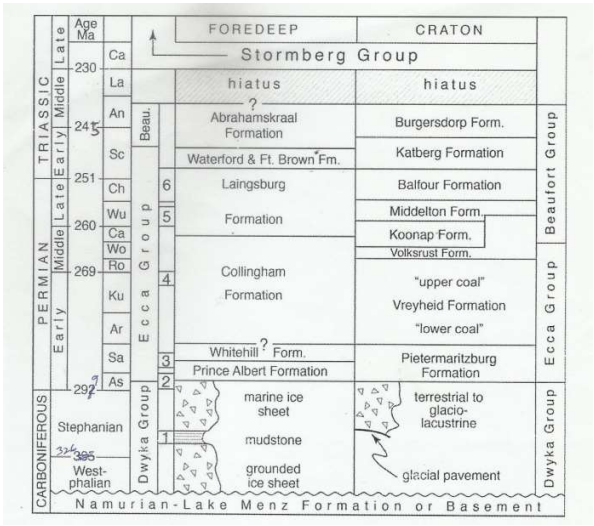

Figure: 3. Map of Afro-Arabia showing northern limit of glacial and MTS (Median Thermal Swell). The ridge separated rift basins in the east and sag basins in the west and supported the regional center of glaciation. Arrows indicate the direction of ice movement from local highlands (after Rust, 1874; Wopfner, 1994).

Samfrau convergence (Catuneanu et al., 2005), but northern part extended onto the cratonic basins due to trans-pressional sags and rifting. A complex system of N-NE trending rift basins extended from Namibia/Botswana towards eastern parts of Africa, whereas large sag basins developed in the Congo, in Angola and in Gabon. These two settings were separated by an N-NE trending structural highs (Stratten, 1970; Wopfner, 1994). Much of this undulating terrain in south and central Africa was a focus of Permo-Carboniferous glaciation (Rust, 1975 & Visser,1997), with glacial movement and periglacial melt water streams directed from NE to SW towards fore-deep (Fig. 4). The Gondwana glaciation has left indubitable traces over parts of southern Africa and Arabia.

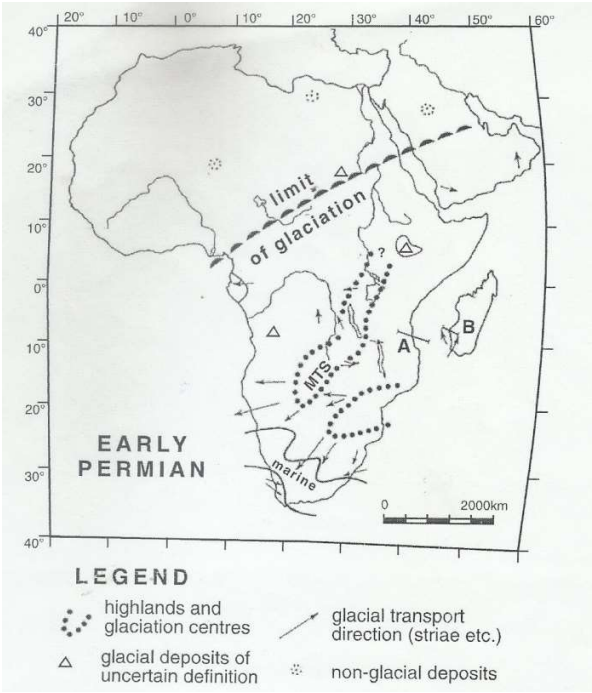

Figure:. 4. Simplified stratigraphic columns of the Karoo Basin in South Africa, demonstrating marked facies change between the fore deep in the SW and terrestrial environment in the NE and N of the basin (Wopfner, 2012).

The field evidence for the lower limit is provided in the southern Karoo Basin, where tillites of the Dwyka Group rest uncomfortably on the Lower to Middle Carboniferous Namurian strata (Fig. 4) which, display of no evidence of glacial activity. The post-glacial Ecca Group contain the terminal deposits of the glacigene succession and comprises clastic

sequences of the fore-deep including turbidites and banded siliciclastics, organic-rich mudstones and cherts of a deep marine environment represented by Prince Albert, White Hall, Collingham and Lainsburg Formations. The shallow marine Waterford and Fort Brown Formations conclude the Ecca succession in the southern Karoo Basin. However, on the cratonic shelf situated northeast and north of the fore-deep, the Ecca Group consists of terrestrial deposits beginning with the Petermartizburg Formation in the lower part comprising dark grey, carbonaceous siltstones and shale of fresh water origin. It is succeeded by the Vryheid Formation which harbors the coal deposits of southern Africa.

East Africa

The Permian sag and rift basins of south-central Africa representing Karoo sequence extend SW-NE from Namibia/Botswana, Zambia, Mozambique and Tanzania in the east (Fig. 2) (Wopfner & Kreuser, 1986). These basins were part of the complex rift system of the Malagasy (Madagascar).

Tanzania

One of the most complete sequences of the Karoo super group is that of Ruhuhu basin in SW Tanzania (Figs. 2, 7). The classical sequence is referred to as the Songea Group, with lithological subdivisions as shown in Figure 5 (Wopfner & Jin, 2009). Deposition was controlled by climatic and tectonic events resulting in five distinctive coal-bearing depositional cycles, (Casshyap et al., 1987; Wopfner and Casshyap, 1997). The sedimentary succession begun with the deposition of the Permo-Carboniferous glacigene Idusi Formation, comprising basal tillites, overlain by reworked glacial debris, slumped diamictites. The succeeding coal-bearing Mchuchuma Formation with thin coal seams initiated with medium to coarse cross-bedded sandstone (Mpera Sandstone Member) representing the humid phase of deglaciation. The overlying Mbuyura Formation embarks with red beds and cross-bedded scrap Sandstone Member representing floodplain and channel deposits of braided rivers in response to rising rift shoulders. It is succeeded by an assemblage comprising coal measures of the Mhukura Formation, overlain by the Ruhuhu and Usili Formations, consisting of calc marls, dolomites with stromatolitic limestone representing deposition in alkaline lakes (Fig.5). The Pangean sequence of Tanzania was concluded by Early Triassic fluviatile Kingori Sandstone, with a short evaporative event developed due to hot and semi-arid conditions represented by the Manda Beds.

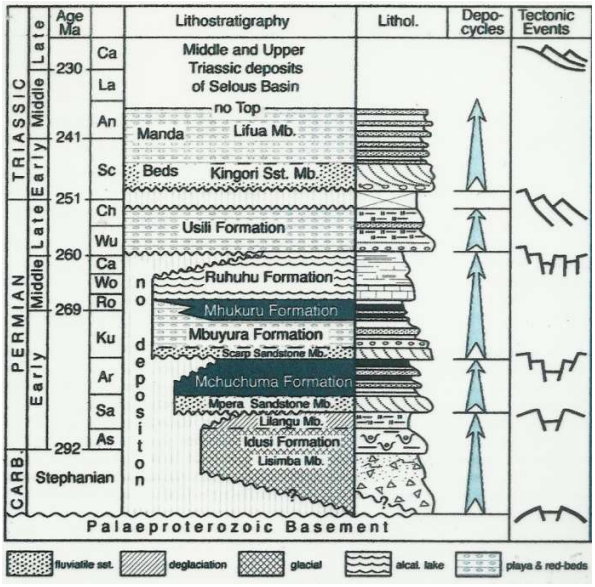

Figure: 5. Simplified stratigraphy, depositional cycles and tectonic phases of the Songea Group (PMS) of Ruhuhu basin, Southern Tanzania. Solid black colured beds depict coal measure formations (after Wopfner and Jin, 2009).

Madagascar

During the Pangean stage, Madagascar was situated opposite Eastern Africa including Tanzania (Fig 2,). Structurally, western Madagascar represents a mirror image of Permian rift system of eastern Africa

(Wopfner, 1994; Catuneanu et al., 2005). Thus, it is not the Permian – Early Triassic PMS sequences of the Island resemble those of the Karoo super group of eastern Africa.

In the Morondava Basin of western Madagascar, the succession is subdivided into three major lithology units consisting of Sakola, Sakamena and Isalo Groups, in ascending order. The Sakola Group comprises the glacigene deposits identical to that of the Idusi Formation of Tanzania, succeeded by coal measures, cross-bedded red beds, and marine limestone at the top. These correspond to Mchuchuma, Mbuyura, Mhukura, and Ruhuhu Formations of the Songea Group of Tanzania (Catuneanu et al., 2005). A tectonic event near the Middle–Late Permian boundary separates the Sakola from the overlying Sakamena Formation with an unconformity (Wopfner and Jin, 2009).

The Majunga Basin in the NW of Madagascar contains similar rock assemblage as the Morondava Basin but towards the top occur intercalated marine limestones (Lower Sakamena). Their fauna includes the similar cephalopod as that of the Salt Range of Pakistan suggesting southward extension of Tethys forming the Malagasy (Madagascar) Trough.

Arabian Peninsula

Isolated outcrops of PMS as time-equivalent to Karoo deposits occur in Yemen and Oman in southern Arabian Peninsula (Figs. 2, 7). Polished and striated pavements overlain by boulder tillites with faceted clasts have been observed in South Yemen (Kruck and Thiele, 1983) and in the South Oman (Braakman et al., 1982), indicating flawless evidence of continental glaciers in southern part of Arabian peninsula in Late Paleozoic time. The Oman succession of glacigene deposits is similar to the Idusi Formation of Tanzania and is termed the Alkhalata Formation of the Haushi Group (Fig. 6). It is topped by the black bituminous mudstones of the Rahab Shale. The latter has characteristic oil-bearing signatures (Levell et al., (1986). The Rahab Shale is followed by shallow marine deposits of Lower Gharif Formation. The succeeding sequence of Khuff Formation consisting of evaporates was deposited in shallow shelf sea which transgressed most of the Arabian Peninsula (Alsharan, 2006).

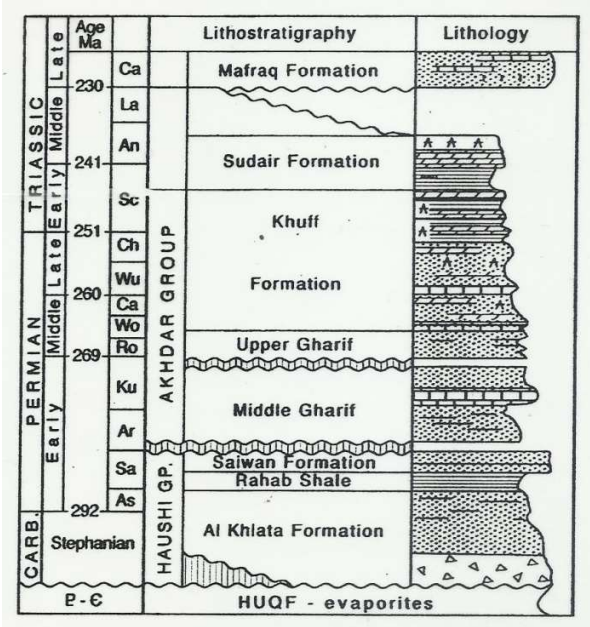

Figure: 6. Generalized stratigraphic columns of PMS of Southern Oman (after Alsharan, 2006; Wopfner and Jin, 2009).

Africa north of the glacial front

Based on the dispersal of northernmost exposures of glacigene sediments, Wopfner and Casshyap (1997) identified the northern limit of Late Paleozoic glaciation as a convex line extending from west-central Africa through Arabian Peninsula towards east-southeast (Figs. 2, 3). The non-glacial rock assemblage equivalent to PMS occur as isolated outcrops between glacial front and equator across the northern Africa as outlined below.

Central Saudi Arabia outcrops

Lying at the northern periphery of the line of glacial front (Fig. 2), isolated outcrops of

PMS in Central Saudi Arabia spectacle terminal facies of non-glacial/proglacial assemblage (Al-Laboun, 1987). The Permian succession is established by the dolomite-anhydrite beds of the Khuff Formation. This sequence is present in the subsurface of the Central Arabia Basin. Similar isolated outcrops of non-glacial sediments occur north of Saudi Arabia near Gulf of Suez and Sinai, Nagev, in Libiya, Tunisia, and Morocco in the NW near equator (Fig. 1). These sediments developed in localized sags and/or rifted basins consist of occasional conglomerate, sandstone, red beds, and evaporates suggestive of warm, hot to arid climate, which is not unlikely due to their proximity to equator.

Lower Gondwana and equivalents
Peninsular India

The Gondwana basins of Peninsular India, confined to three major linear elongated tracts, developed on the Archaean basement along a northerly paleoslope from the highlands to the south and southeast including the uplands of Eastern Ghats and ancestral mountains of Eastern Antarctica (Casshyap, 1973; 1976). Besides exposed rocks in the linear belts (Fig.7), the Gondwana sediments in Rajmahal Basin, Eastern Raniganj Basin, Upper Assam and western Satpura Basin, occur in subsurface under the Rajmahal Traps/Deccan Traps and below the recent alluvium cover. Occurrence of isolated outliers of Talchir glacial deposits and Karharbari/Barakar coal measures in the proximity of basins are, suggestive of wider extent of original exposures beyond the existing margins of the basins (Casshyap et al., 1993; Mitra, 1993). It is quite obvious, that the original Gondwana basins were extensive than exposed within the three major basins of Peninsular India.

Tectonic Setting

The Gondwana strata is low-dipping (5-10º), though steep dip occur in places and near boundary faults where rocks are locally folded. The Gondwana sediments were deposited in half-graben/failed rift structures and preserved in subsiding rifted basins bounded on their southern or northern margins by high-angle normal faults (Casshyap, 1979; Casshyap and Tewari, 2001; Verma and Singh, 1979).

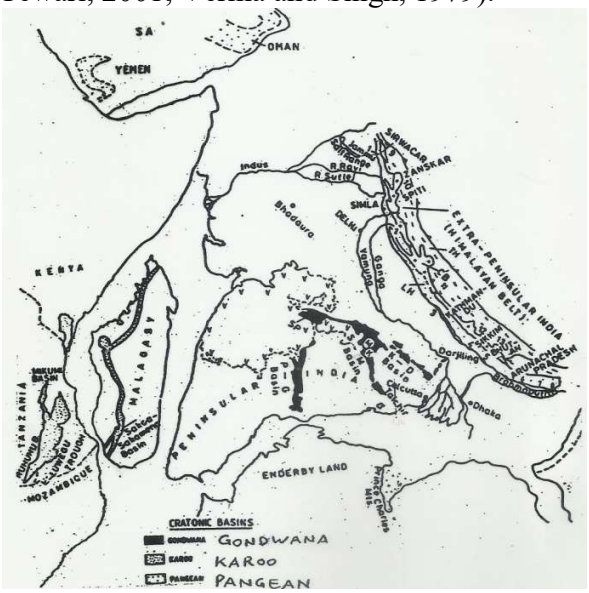

Figure: 7. Assembly of India in the Early Permian, showing exposures of Gondwana rocks in three major Linear belts in Peninsular India and in Lesser and Tethys Himalaya of Extra-Peninsular region. Also shown are areas of exposures of Karoo and equivalent rocks in Madagascar, Tanzania, Yemen, and Oman of South Arabia . Alphabets in Extra-Peninsular India refer to TH, Tethys Himalaya; CB, Crystalline Belt; LS, Lesser Himalaya.

Some of these faults truncated the exposed coal measures abruptly along the boundary, as perceived in Jharia (Mahuda sub-basin) and Singrauli Basins (Casshyap, 1979, 1981a; Casshyap et al., 1993).

Stratigraphic setting

The cratonic Gondwana basins are developed in the Damodar and Son-Mahanadi Valleys, including 1-30 coalfields (Fig 8). Besides, coalfields of less productive deposits occur in Pranhita – Godavri, and Satpura Basins in west-central India. These basins (coalfields), representing a thick pile (average

thickness 2200 m) of the Permo-Triassic Lower Gondwana sequence (Fig. 9), provide a prolonged history of sedimentation (Casshyap,1977; 1981b). The stratigraphic and lithofacies sections of Permian Gondwana (Damuda Group) are displayed in figure 9.

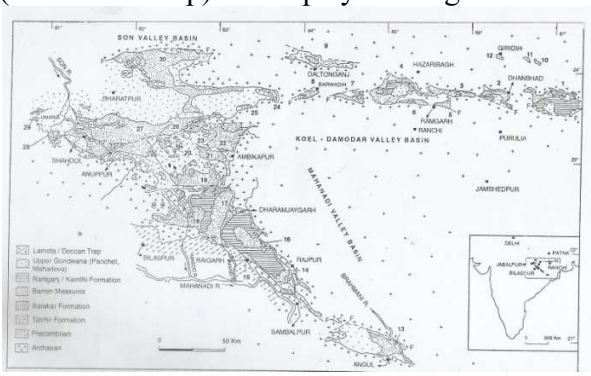

Figure: 8. Geological map showing the distribution of Gondwana rocks in the Koel-Damodar and Son -Mahanadi basins. Inset shows location of the basins. Numbers 1-30 refer to coalfields: (after Casshyap and Tewari, 1984; Ramakrishnan and Vaidyanadhan, 2008, fig. 7.2)

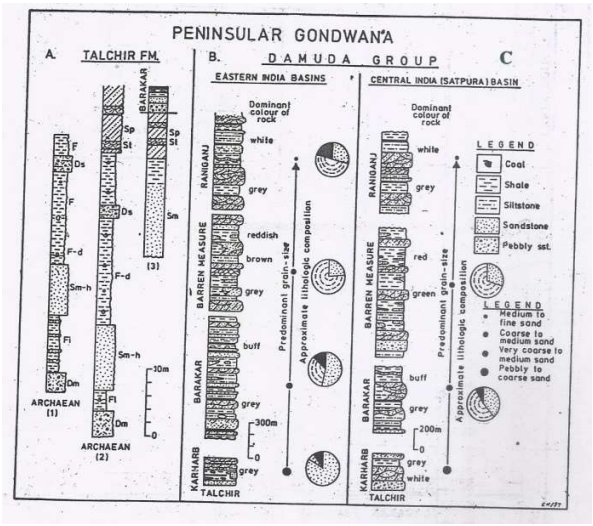

Figure: 9. Generalized stratigraphic sections of Permian Gondwana showing lithofacies, grain size and sedimentary structures : A. Glacial and glacigene sequence in Talchir Formation, measured at different locations between Korba and Ambikapur in Son-Mahanadi basin; B. Generalised sections of fluvial deposits of the damuda group in Koel-Damodar and Son-Mahanadi basins (C. Similar sections from Central India, Satpura basin (after Casshyap and Srivastava, 1988; Casshyap, 1999).

Lithofacies and Depositional Environments

Glacial Facies

Glacigene facies of the Talchir Formation comprising boulder tillite and diamictite in the lower part were laid down by grounded ice in glacially scoured depressions and striated pavements on the Archaean basement (Smith, 1967). Subsequent melt waters deposited reworked stratified tills with thin inter-beds of cross-bedded sandstone, shale, with or without dripstones. The glacigene facies of the Talchir Formation comprising boulder tillite and diamictite in the lower part is grounded ice in glacially scoured depressions and striated pavements on the Archaean basement (Smith, 1967ltstone, with or without drop stones in the overlying assemblage (Fig. 9). Unlike the Dwyka tillites, the Talchir tillites/diamictites seldom exceed 2m in thickness. Lithofacies characters of Talchir Formation, depositional environments, paleoice and paleoflow transport have been studied (Casshyap, 1970, 1981b; Casshyap and Qidwai, 1971; Casshyap and Tewari, 1982; Casshyap and Srivastava, 1988; Casshyap et al., 1993; Frakes et al., 1975).

Post-glacial Fluviatile facies

The succeeding post-glacial sediments of coal-bearing Karharbari, Barakar and Raniganj Formations of Damuda Group, are products of extensive fluviatile system intercepted by swamps and lakes, deposited as channel sand bars and overbank fine clastics, resulting in the development of repeated sequences of cross-bedded sandstones, shale/siltstones carbonaceous shale, and coal (Casshyap, 1977, 1981a; Casshyap & Tewari, 1984, 1988). These coal measures are intervened by mid - Permian Barren Measures/Motur Formation exhibiting similar lithofacies and depositional environments (Casshyap & Tewari, 2001). Unlike other PMS basins of Pangean supercontinent, the Damuda Group is conspicuous by the recurring fining upward cycles/cyclothems terminated by coal of

varying magnitude (Casshyap, 1970; Casshyap and Kumar, 1987; Casshyap et al., 1993). The cyclical characters of the Barakar coal measures have been established statistically by applying Entropy in Markov chain analysis based on measured sections and available borehole data (Casshyap and Khan, 1981).

The succeeding Early Triassic Panchet Formation is separated from the underlying Damuda Group by an unconformity (Casshyap, 1999; Casshyap and Tewari, 2001). Its variants are the Pachmarhi Sandstone in the Satpura Basin, Upper Pali Formation of Umaria, and middle and upper parts of the Kamthi Formation in the Kamptee and Pranhita-Godavari basins. Occurrence of coarse clastics, including pebble beds and coarse arkosic sandstone in the basal part, suggest a new episode of tectonic upliftment and readjustment of paleoslope. The Panchet Formation accomplishes the Lower Gondwana (PMS). It is separated from younger Mesozoic rocks by the mid-Triassic hiatus.

The depositional environments of post-glacial Permo-Triassic Gondwana facies were alluvial plains drained by river systems which were braided during the early stages of Karharbari Formation. The system became progressively meandering through Barakar to Raniganj (Middle to Upper Permian), and later changed to braided pattern during deposition of the Lower Triassic Panchet/ Pachmarhi, as depicted in the depositional models (Fig. 10) (Casshyap and Khan, 1981; Casshyap and Tewari, 1984; 1988).Based on the striking similarities between the facies and the onset of the sequence boundaries of the PMS (Lower Gondwana) of Peninsular India and those of eastern Africa (Tanzania/Zambia) indicate an identical climatic/depositional conditions and analogous timing of tectonic pulses, although post-depositional rifting and/or boundary faults played a greater role in the control of peninsular basins (Casshyap, 1999; Wopfner and Jin, 2009).

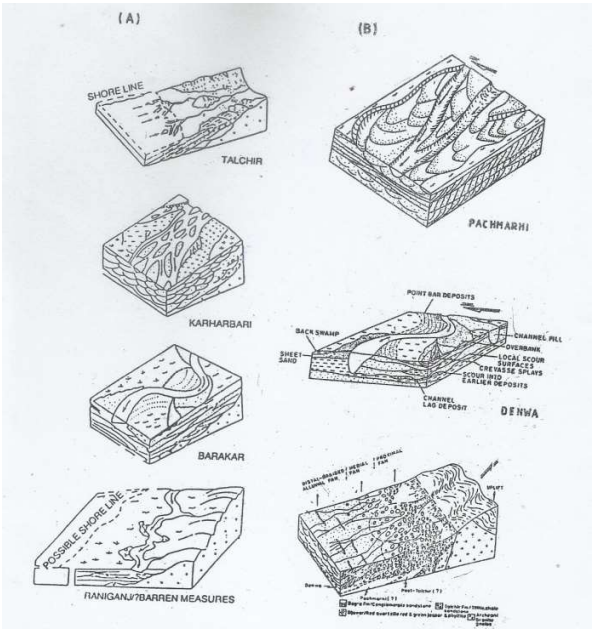

Figure: 10 Schematic depositional models of Gondwana sedimentation showing changing pattern of fluvio-glacial and fluvial system from Talchir, Karharbari to Pachmarhi (after Casshyap and Khan, 1981; Casshyap and Tewari, 1988).

Intermittent Marine Incursions

Following deglaciation of the Early Permian glacier, low lying areas of fluvial environments were locally intercepted by intermittent incursion of the Tethys sea from northeast into Peninsular Gondwana basins at/ or near the top of Talchir and other formations, along linear belt of the Lesser Himalaya.

Extra-Peninsular India

The Pangean successions of Extra-Peninsular India are, Lesser Himalaya and Tethyan Himalaya. The lesser Himalaya features is in conjoint with cratonic Gondwana facies, including a coal-bearing succession, whereas the Tethyan Himalaya demonstrate the stronger marine influence and, in places, are associated with acid volcanic rocks (Acharyya et al., 1979).

Lesser Himalaya

Isolated outcrops of Late Paleozoic succession in the Lesser Himalaya occur in

continuous linear belt from Arunachal Pradesh to central Nepal via Bhutan and Darjeeling in the northeast (Fig. 7}. The Rangit tectonic window in Sikkim, comprising the succession correlated with the Gondwana super group of Peninsular India: the Rangit Pebble Slate is equivalent to the Talchir Formation, and the overlying assemblage is coeval to the formations of the Damuda Group.

Tethyan Himalaya

The bulk of the sediments of the Tethys Himalayan belt is marine and has been reliably correlated with the Peninsular India and Arunachal (Nakazava and Kapoor, 1979). The Tethyan zone extends from Kashmir to Spiti, into Lhasa block of Tibet and Baoshan and Tengchong blocks in Southwest China (Casshyap, 1999). These Gondwana succession dominated by thick continental basalt succeeding the glacigene succession (Gaetani and Garzanti, 1991; Wopfner and Casshyap, 1997).

Gondwana derived blocks

These are the Late Carboniferous to Early Permian glacigene marine deposits followed by the remarkable postglacial sequence (Fig.10), now organized in the form of a long belt (Fig.11), the western part of which is bounded between the former the Gondwana continent including India and northern continent, and includes Baoshan and Tengchong blocks of western Yunan bordering northern Myanmar, and Gangdise {Lhasa} and Qiangtang {Tibet} block. The eastern part constitutes the Sibumasu Block of Southeast Asis. The Baoshan and Tengchong blocks of western Yunan, separated by well-defined tectonic lineament, display well developed Late Paleozoic-Mesozoic sequence. The basal formation of Baoshan block comprises diamictite, tillite, and mudstone containing Brachiopods of Stephanian to Asselian age, overlain by thick basalt with intercalations of limestone. Similar sequence constitutes the Tengchong block. Both the blocks are deliberated to be of glaciomarine origin and, hence of Gondwana affinity. Besides, the sequences in Gangdise (Lhasa) and Qiangtang are of glaciomarine origin. Likewise, the presence of Gondwana affinity in parts of Southeast Asia has been remarked. The comprehensive term Sibumasu Block is considered to be composed of the Shan state of Mynamar, western and Northwestern Thailand and Western Malaysia and Sumatra (Metcalfe, 1988). It is believed that Sibumasu was adjacent to Gondwana through the Carboniferous and found striking similarities of the Paleozoic succession with that of Western Australia. Sibumasu was rifted off from the Gondwana in the earliest Permian to collide with south China in the Late Triassic.

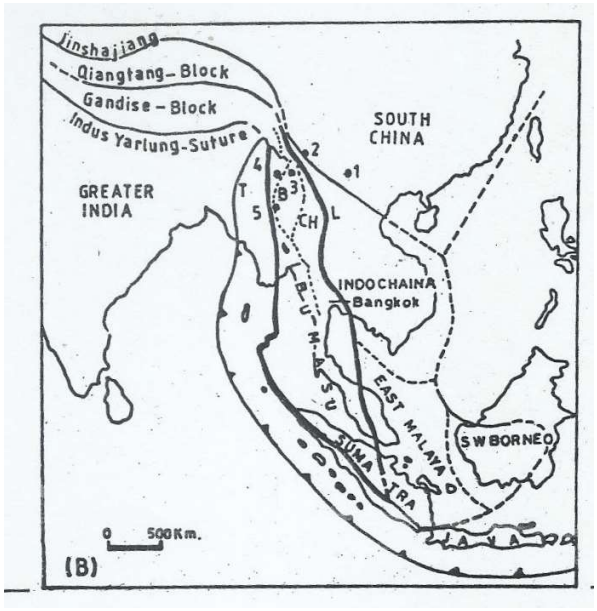

Figure: 11. Map showing Gondwana derived tectonic blocks characterized by glacigene and succeeding rocks showing Gondwana affinity in East and Southeast Asia. Alphabets refer to: B, Baoshan-Shan unit; T, Tengchong unit; CH, Chanling-Menglian unit. Numerals depict localities forming part of Sibumasu Block : 1. Kumming; 2, Dali; 3, Baoshan; 4, Tengchong (Yunan); 5, Mandlay (Myanmar) (after Wopfner and Jin, 2009).

Antarctica

The rifted/fault-bounded Permo-Triassic Gondwana sediments have been reported, in isolated outcrops, from Ellsworth Mountains, Pensacola Mountains, Ohio Range, Queen Maud Range, besides South Victoria Land (Fig. 12). These sediments were developed radially in (?) pericratonic basins on the coastal periphery around the East Antarctic Paleoupland (Trans Antarctic Mountains) in the proximity of East Coast of India, southern Africa, and southwest Australia. On the other side of the centrally located Paleoupland, close to the Ross Ice Shelf, occurred the Beardmore Glacier terrain (Fig. 12), displaying a well-developed Permo-Triassic glacigene and post-glacial succession of Antarctica (Barrett,1969). The 2600 m-thick Beacon sequence comprises eight formations: the Alexandria Formation (? Devonian), the Pagoda, Mackellar, Fairchild and Buckley Formations (Permian), the Fremouw and Falla Formations (Triassic), and the Triassic?-Jurassic Prebble Formation. The bulk of the sediment of Mackellar and Fairchild Formations are of terrestrial origin, consisting of interbedded current-bedded sandstones shale and siltstones, including arkosic sandstones, deposited by southeasterly flowing streams. The Buckley Formation is a crudely cyclic coal-bearing sequence embedded with fossil leaves and stems of *Glossopteris*. The Triassic Fremouw and Falla assemblages are sandstone-shale cyclic sequences. The depositional environments were generally Fluviatile, lacustrine and paludal, with northwesterly paleoflow direction. Most other radial Glacier systems (basins) on either side of the East Antarctic Paleoupland, such as Beaver Lake, Shacklelton, Nimrod, Darwin, Victoria Land exhibit selective Gondwana facies.

Australia

In Australia, rock successions of PMS (Gondwana) have been deposited in three distinct tectonic settings: collision and fore deep environments of the Hunter-Bowen Fold Belt along the east coast, transcurrent sag basins in the central part, and rift and fault-bounded basins of West Australian Trough along the west coast of the continent, including Collie and Perth Basin in SW, Carnarvon, Canning, and Bonaparte Gulf Basins in NW. In Eastern Australian fold-belt setting, the basal Permian to Early Triassic PMS succession comprises in ascending order: Lower Marine, Greta Coal Measures, and Upper Marine Formations in Lower to Middle Permian, Singleton Formation in Late Permian, and Narrabeen and Hauksbury Formations in Early to Middle Triassic. However in Tasmania in the southeast, the bulk of the equivalent glacigene and periglacial sequence is dominated by marine sediment of Panthalassa margin (Wopfner, 2012). In West Australia, coal measures in Permian assemblage occur only in the south (Perth Basin) and carbonate formation was restricted to some thin bands of limestones, mainly in northern basins. Glacial deposits consisting of tillites, debris flows are known to occur in the Permian sequence of Bonaparte Gulf and Canning basins in the northwest (Wopfner, 1999, 2001).

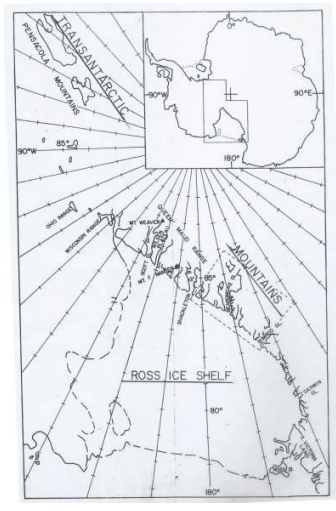

Figure: 12. Outline map of the central Trans Antarctic Mountains (East Antarctic Paleoupland) showing Beardmore Glacial Area. Inset shows entire map of Antarctica (after Barrett, 1969, fig. 1).

Paleodrainage and paleoslope

India

The glacial transport in the scoured depressions/valleys in the underlying Archaean terrain was directed from southeast to northwest, though locally intercepted by subsidiary lobes descending transversely or obliquely from adjoining highlands, as interpreted from the associated glacigene facies (Casshyap, 1973; Casshyap and Tewari, 1982; Casshyap and Srivastava, 1988). The succeeding paleodrainage pattern of postglacial fluvial system was, likewise, directed predominantly from southeast to northwest in practically all the major basins throughout the deposition of Permo-Triassic Gondwana sediments, as reconstructed by Casshyap (1973,1977, 1981b, and Mitra, 1991), and corroborated subsequently (Fig. 13) by Veevers and Tewari (1995, fig. 7.11). The consistent direction of glacial transport and paleocurrents imply that the paleoslopes in all the Gondwana basins were predominantly directed from southeast to northwest. However, during Upper Permian in the Damodar Valley, the paleocurrents were

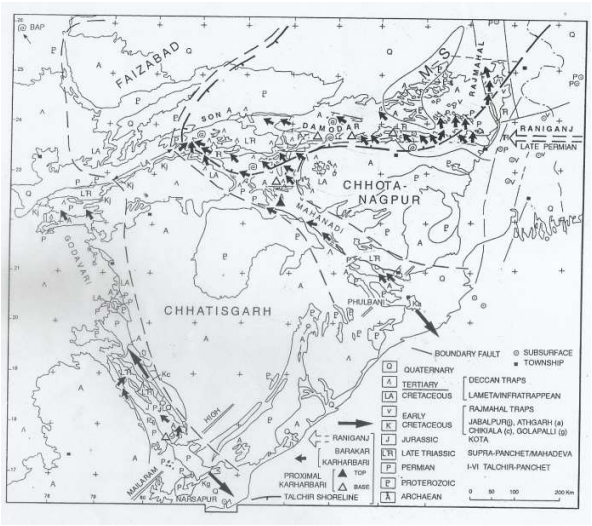

Figure: 13. Paleocurrent dispersal map of Permian Karharbari, Bokaro, and Raniganj Formations in the Gondwana basins of Peninsular India (Veevers and Tewari, 1995).

directed from east-southeast to west-northwest, possibly towards the Tethyan shoreline (Casshyap & Kumar, 1987).

Local deviations/reversals in paleoflow directions in different formations and areas suggest contribution by local tributary channels from adjoining highlands. Significantly, the northwesterly directed Permo-Triassic Gondwana drainage was abruptly truncated along the faulted northern margins of the Singrauli and Satpura basins, which strongly questions their existing northern limits, apparently terminated by the Son-Narmada Lineament, and call for a critical review (Casshyap et al., 1993; Casshyap, 1999).

Radial Paleodrainage System in Gondwanaland

The figure 14A displays a comprehensive master map demonstrating, a radial paleodrainage system in Gondwanaland around the East Antarctic Paleoupland, as reconstructed by Tewari and Veevers (1993) and modified by Veevers and Tewari (1995, fig. 40). Among noteworthy features are, along the periphery of Antarctica inferring connections of paleo-ice and flow azimuths between Antarctica and bordering continents of South Africa, India, and Australia (Fig 14 B). The flow azimuths in the Permian Gondwana/Karoo sediments are radially directed southwest and west in the Karoo Basin of South Africa, northward in Mahanadi and Godavari Basins of east coast of India, northwest in West Australia, and southeast in Eastern Australia (Powell and Li, 1994; Veevers and Tewari, 1995, fig. 41). The perimeter of the radial drainage for fluvial deposition was at about 30^{o} paleolatitudes in India and adjoining continents as marked by dotted curve in Figure 14B.

Based on above perspective it is inferred that the Permian paleodrainage system, including glacial lobes and melt-water fluvio-glacial network, developed in elevated terrains

of the East-Central Antarctica, descended downhill along valleys radially towards coastal periphery, connecting with respective paleodrainage of the aforesaid low-lying depositional basins of the bordering continents of South Africa, India, and Australia, resulting in the radial paleodrainage system of Gondwanaland.

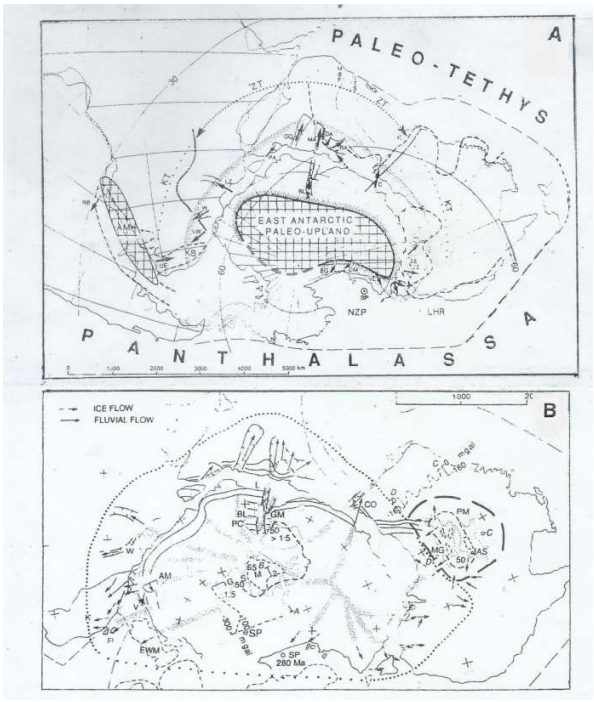

Figure: 14. A) Radial drainage system in central-eastern Gondwanaland around the East Antarctic Paleoupland (Trans Antarctic Mountains) . Full arrows indicate the azimuths of Permian and fluvial transport (after Tewari and Veevers, 1993; Veevers and Tewari, 1995, fig. 40). Alphabets refer to: **Antarctica**: BL, Beaver Lake; BG, Beardmore Glacial Area; DM, Darwin Mountain; VL, Victoria Land. **India:** M, Mahanadi; DA, Damodar; RA, Rajmahal; GO, Godavri; P, Palar; RNGI, restore northern edge of Greater India. **South Africa**: LZ, Lower Zambezi; W, Waterberg; VR, Vryheid; KB, Karoo Basin; UE Upper Ecca; Am. Atlanctic Mountain. **Australia**: C, collie; SEAUS, southeastern Australia. Curves indicate: ZT, Zambezian or fault-bounded terrain; KT, Basement of Karoo basin (Rust, 1975). B) Large radial drainage system . Generalised arrows showing fluvial flow azimuths, depicting connections with adjoining continents (Powell and Li, 1994; Veevers and Tewari, 1995, fig. 41).

Paleoclimate history

Afro-Arabia

During Permo-Triassic, Africa and Arabia extended from area proximal to the South Pole into lower latitudes so that the regions near the Tethyan margin remained free of ice cover during the Gondwana glaciation (Fig. 1). Drifting of Permian pole was an important factor, among others, for governing the Permo-Triassic climatic changes during Pangean/Gondwana sedimentation from Afro-Arabia through India to Antarctica/Australia.

Glacial Climate

The onset of the Pangean depositional succession was synonymous to the Late Paleozoic glaciation in the southern supercontinent of Gondwana. The question of whether the South African glacial deposits (Dwyka Group) resulted from a single sub-polar ice sheet emanating from Antarctic highlands and/or from individual glacial centers (Visser, 1997), or from a large ice sheet covering Antarctica and Samfrau, with coalescing centers in South Africa (Wopfner and Diekmann, 1996), is still a matter of debate. The basal boulder tillite facies of Karoo Basin developed extensively from fore deep in the south to cratonic shelf areas towards north and northeast (Fig. 2). In the neighboring areas of Mozambique, Zambia, Tanzania, and Madagascar in Central and East Africa which were not at much lower latitudes, the glacial deposits of the Idusi Formation of Ruhuhu basin of Southwest Tanzania resulted from plateau type glaciers, with lodgment tills and reworked glacial debris (Wopfner and Kreuser, 1986). Further north, Southern Arabia was situated at lower latitude; consequently, the glacial deposits in Oman formed as repeated intertounging flow tills, slurred debris and turbidities (Levell et al., 1988). The evidences presented in this paper indicate that the glacier front In Afro-Arabia extended to about 40^{o} paleolatitudes (Figs. 1, 3). Synchronous deglaciation associated with a eustatic rise of sea level in

the Early Sakmarian was followed by retreat of glaciers, and warm climate and increased humidity, which is a wide spread event across the southern Pangea.

Transition to Warmer Climate

In southern half of Africa, deglaciation and the retreat of glaciers is followed by the Ecca and Songea Groups respectively, comprising fluviatile sandstones, shale, and carbonaceous shale embedded with *Glossopteris* flora. This flora along with the overlying coal seams suggests high precipitation rate and prolific plant growth, providing the biomass for peat accumulation and coal formation. In Africa coal formation extended to about 55^{o} palaeolatitude which approximates the limit on other parts of Gondwana (Fig. 1). Coal formation ceased in South Africa when temperature increased in the Middle Permian, ushering in the deposition of the Beaufort Group. North of the 'coal-line', climate became rapidly dryer, warmer and semi-arid. In Arabia this trend is evidenced by the evaporate and anhydrite beds in the Middle Gharif and Lower and Middle Khuff Formations of Oman .

Warm to hot, semi-arid to arid climate

This phase, characterized by elevated temperatures, is exemplified by the Permo-Triassic Songea and Ruhuhu Groups of Tanzania, comprising repeated red bed facies of shale and sandstones, and stromatolitic limestones/dolomites which are interpreted as the product of hot, arid to semi-arid climate. There was a distinct gradient from the warm semi-arid climate dominating the environment of the Beaufort Group in southern Africa, to the arid to hotter conditions on the Arabian Peninsula, northern Africa, and terminating to the evaporate conditions in the South Alpine Terrine close to the northern margin of Tethys at the end of Permian.

India

The Gondwana Basins of Peninsular India were at same latitude as those of East Africa and Madagascar (Fig. 3). Consequently they experienced a similar climatic history.

Glacial and Transitional Phase

Climatic development during the depositional event of the Talchir Formation is exemplified by the glacigene successions in the Damodar, Son-Mahanadi, Pench Valley, and other basins as investigated by Casshyap and Qidwai (1971), Casshyap and Tewari (1982), and Casshyap and Srivastava (1988). Deglaciation phase and retreat of Talchir glaciers was followed by the development of periglacial melt water streams, lakes and ponds, comprising channel sandstones, eskers, and varvites with or without drop stones. The Extra-Peninsular glacial and proglacial successions were deposited at lower latitude close to Tethyan margin of Gondwana. The presence of Eurydesmas and Bryozoa/Mollusc fauna in several parts with occurrence of *Gangamopteris* flora suggestive of cool climate during the period of Talchir sedimentation up to the top layers, date to the Early Sakmarian.

Postglacial Phase

The postglacial phase was marked by a cool, temperate climate during deposition of alluvial fan and braided river facies of the Lower Permian Karaharbai and Barakar Formations, which abound in fresh to slightly weathered feldspar. The recurrence of fining upward cycles topped by coal seams with prolific *Glossopteris, Gangamopteris* and related flora indicate seasonal warming of climate. The red coloured Barren Measures provide the first signs of a hot/warm, humid climate during the Middle Permian throughout Peninsular India, followed by the Upper Permian Raniganj coal measures dominated by *Glossopteris*, suggestive of reversal to cooler, mild climate (Casshyap and Kumar, 1987). The coastline facies of Lesser Himalaya and

the shelf facies of Tethyan Himalaya which succeed the glacigene deposit abound in carbonate and fine clastics. They are indicative of warm temperate climate. The Triassic period represented by Panchet/Pachmarhi Formations comprises pebbly sandstone and red- and yellow shale, suggesting a seasonally warm, semi-arid and humid climate.

Antarctica, Australia

The retreat of glaciers was a synchronous Gondwana-wide event. The Early Permian Mackeller Formation of the Beardmore Glacier area, comprising black carbonaceous, interbedded with turbidities is suggestive of deglaciation phase in Antarctica. Simultaneous was the onset of the formation of coal beds in Gondwana, including the Buckley Coal Measures of Antarctica and the formation of red beds (Wopfner and Casshyap, 1997). Middle Permian fossil forests and plant assemblages demonstrate that the Late Artinskian onward, Antarctica was vegetated and free of glaciers as was Gondwana (Wopfner, 2012).

In Eastern Australia, the Permo-Carboniferous glaciomarine/glacigene deposits succeeded by a sequence including Permian Lower and Upper Gretra Coal Measures and Permo-Triassic Singleton Formation are associated with terrestrial deposits of Permo-Triassic Narabeen and Hauksbury Formations. Similar facies characterized the Permian Perth Basin in the south and other basins of northwest Australia. Of particular significance is the deglaciation facies in both the Canning and Bonaparte Gulf basins, consisting of thick black carbonaceous lutites (Wopfner, 1999). Above characteristics are suggestive of a climatic regime similar to that of East Africa, Extra-Peninsular India, and neighboring Antarctica.

DISCUSSION

Causes of Glaciation and Climatic Change

A northward drift of Afro-Arabia and/or of Gondwana as a whole towards the equator was assumed to explain the amelioration of post-Sakmarian climate (Scotese and Langford, 1995, and others), which was, however, a physical impossibility as the African continent was attached to Antarctica till Jurassic. In the Late Paleozoic/Early Permian, the paleo-south pole for Gondwana was placed on or near central Antarctica in the vicinity of present South Pole (Powell and Li, 1994). During the Permian, however, the pole moved towards Australia to reach a position in southeastern Australia in the Early Triassic (Powell and Li, 1994) (Fig 1). Thus, southerly pole shift towards southeast Australia resulted in pole-ward expansion of central latitudinal tropical belts to influence climatic change (Wopfner and Jin, 2009), as evidenced by the coal formation and paucity of red beds in the Permian basins of Australia, supporting its closer position to South pole (Fig. 1).

Alternative perspectives have been proposed in the context of climatic variations. Crowell (1978) proposed that the southern supercontinent was oriented during this time that its north shore received onshore moist winds from the Tethys Sea and its southern shore on the edge of Panthalassa received precipitation originating from an ice-free sub-polar ocean (Fig. 15). The ice age apparently ended when strong circulation of air and ocean currents parallel to latitudes in the Early Mesozoic. Thus, besides pole drifting the arrangement of seas and continents with respect to the air circulation may be an important cause of ice sheet and glaciation.

Conclusion

The contiguous assembly of continents from South America, Africa, via Antarctica, India to Australia, forming Late Paleozoic-Early Mesozoic Pangean supercontinent, named as Gondwana, bounded by Panthalassa in the south and Tethys in the north, developed

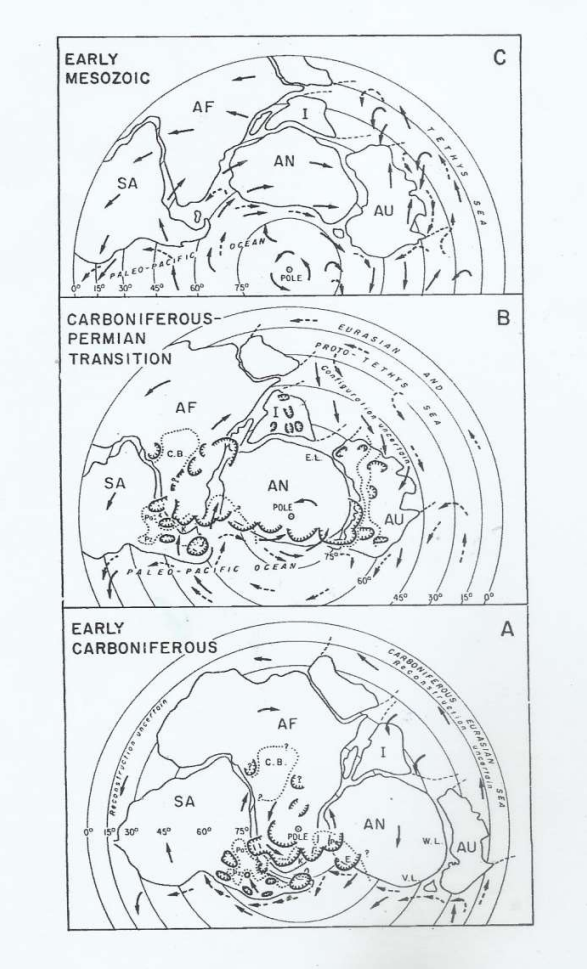

Figure: 15. Schematic diagrams showing the position of Gondwana: (A) during the Early Carboniferous;(B) near the time of the Carboniferous-Permian transition; and (C) Early Mesozoic. Ocean currents shown as dashed arrows, winds as soilid arrows, epeiric seas as bounded by dotted line, and ice centres with hatured lines Alphabets indicate: AF, Africa; AN, Antarctica; AU, Australia; CB, Congo Basin; E, Ellsworth Range; I, India; K, Karoo Basin; PA, Parana Basin; Pa, Pensacola Mt.; SA, South America; V.L., Victoria Land; W.L., Wilkes Land (after Crowell,1978, fig.5).

multiple depositional basins to provide a prolonged history of sedimentation. The Permo-Triassic mega-assemblage so developed and referred to as Pangean Mega Sequence (PMS), the term synonymous with the term Lower Gondwana of Indian stratigraphy, exhibits striking similarities of lithofacies in response to similar if not identical paleoclimate through space and time.

A micro shift of Afro-Arabia or of Gondwana as a whole towards the equator was assumed to explain the amelioration of the post-Sakmarian/postglacial climate. Northerly shift of Permian Africa, however, was a remote possibility as stated earlier. Besides, pole drifting the arrangement of Permian seas and continents with respect to the air-ocean circulation is probably an cause of glaciation.

References

Acharyya, S.K., Shah, S.C., Ghosh, S.C and Ghosh, R.N. (1979). Gondwana of Himalaya and its Stratigraphy. *Proc. IV Intern. Gondwana Symposium, 1977*, Geol. Surv. India, Calcutta, 2, 420-430.

Al-Laboun A.A. (1987). Unaytah Formation: a new Permian-Carboniferous Unit in Saudi Arabia. *Amer.Assoc. Petrol. Geol.,* Bull. 71, 29-38.

Alsharan, A.S. (2006). Sedimentological character and hydrocarbon parameters of the Middle Permian to Early Triassic Khuff Formation. *United Arab Emirates. GeoArabia*, 11, 121-158.

Archbold, N.W. (2001). Post-Gondwana, Early Permian (Asselan-Sakmarian-Artinskian) correlations. *In:* Weiss, R. H. (Ed.) *Contributions to Geology and Palaeontology of Gondwana in Honour of Helmut* Wopfner. Geological Institute, University of Cologne, 29-33.

Barrett, Peter (1969). Stratigraphy and Petrology of the mainly flluviatilePermian and Triassic Beardmore Glacier Area, Antarctica. *Institute of Polar Studies, The Ohio State University, Columbus Ohio, USA,* Report No. 34, August 1969, 1-132.

Braakman, J.H., Levell, B.K., Martin,T.H., Potter,T.L. and Van Vliet,A. (1982). Late Palaeozoic gondwana glaciation in Oman, *Nature*, 299, 48-50.

Casshyap, S.M. (1970). Sedimentary cycles and environments of deposition of the Barakar Coal Measures of Lower Gondwana, India. *Jour. Sedimet. Petrol.* 40, 1302-1317.

Casshyap, S.M. (1973). Paleocurrents and paleogeographic reconstruction of the Barakar (Lower Gondwana) sandstones of Peninsular India. *Sediment. Geol.,* 9, 283-303.

Casshyap, S.M. (1976). Paleocurrents and continent assembly: a compaarision from Permian coal Measures of South Africa, Antarctica, India, and

Australia. Abstract: *25th Intern Geol. Congr Sydney,* 238-239.

Casshyap, S.M. (1977). Sedimentation trends in Gondwana basins. Key Paper, *IV Intern. Gondw. Symp., Geol. Surv. India, Calcutta*, 1-34.

Casshyap, S.M. (1979). Paleocurrents and basin framework: an example from Jharia coalfield. *Proc. IV Intern. Gondw. Symp. India, 1977, Geol. Surv. India,* Calcutta**,** 2, 826-842.

Casshyap, S.M. (1981a). Lithofacies analysis of Late Permian Raniganj coal measures (Mahuda basin) and their paleogeographic implications. *In: Cresswell, M.M. & Vella, P. (Eds.) Gondwana Five,* A. Balkema, Rotterdam, 29-83.

Casshyap, S.M. (1981b). Paleogeography and paleodrainage of the Son Valley Gondwana basins, Madhya Pradesh. In: *Valdiya, K.S., Geology of Vindhyachal.* Hindustan Publ. Corp., Delhi, 132-142.

Casshyap, S.M. (1999). Southern Pangea Gondwana / Karoo super sequence of India and neighboring Cratonic platforms of Central Gondwanaland: Stratigraphy, sedimentation and paleogeograph*y. Presidential Address, ESS Section, 86th Session of Ind. Sci. Congress, 1999, 1-51.*

Casshyap, S.M & Qidwai, H.A. (1971). Paleocurrent analysis of Lower Gondwana sedimentary rocks, Pench Valley coalfield, Madhya Pradesh (India). *Sediment. Geol*., 5, 135-145.

Casshyap, S.M. & Khan, Z.A. (981) Entropy in Markov chain analysis of Late Paleozoic cyclical coal measures of East Bokaro basin, Bihar, India. *Jour. Mathem. Geol.,* 13, 153-162.

Casshyap, S.M. and Khan, Z.A. (1982). Paleohydrology of Permian Gondwana streams in Bokaro basin, Bihar, India. *Jour. Geol. Soc. India,* 23, 419-430.

Casshyap, S.M &Tewari, R.C. (1982). Facies analysis and paleogeographic implications of a Late Paleozoic glacial outwash deposit, Bihar, India. *Jour. Sediment. Petrol.,* 52, 1243-1256.

Casshyap, S.M & Tewari, R.C. (1984). Fluvial models of the Lower Permian coal measures of Son-Mahanadi and Koel-Damodar Valley basins, India, *Spl. Publ. Intern Assoc. Sedimentology*, 7, 121-147.

Casshyap, S. M., Kreuser, T. & Wopfner, H. (1987). Analysis of cyclic sedimentation in the Lower Permian Mchuchuma coalfield (Southwest Tanzania). *Geol. Rundschau,* 76. 869-863.

Casshyap, S.M. and Kumar, Ajay. (1987). Fluvial architecture of the Upper Permian Raniganj coal measure in the Damodar basin, Eastern India. *Sediment. Geol*. 51, 181-213.

Casshyap, S.M & Srivastava, V.K. (1988). Glacial and postglacial Talchir sedimentation in Son-Mahanadi Gondwana basin: paleogeographical reconstruction. In: McKenzie, G.D. (Ed.) *Gondwana Six, Amer. Geophy. Union, Monograph*, 41, 167-182.

Casshyap, S.M & Tewari, R.C. (1988). Depositional model and tectonic evolution of Gondwana basins. The *Paleobotanist,* 16, 59-66.

Casshyap, S.M. and Tewari, R.C. (2001). Lithofacies and sedimentation of Mid. Permian Lower Gondwana red beds of eastern Peninsular India. In; Weiss, R.H. (Ed.) *Contributions to Geology and Palaeontology of Gondwana in Honour of Helmut Wopfner*. Geological Institute, University of Cologne, 63-72.

Casshyap, S.M., Tewari, R.C. and Srivastava, V.K. (1993). Origin and evolution of intracratonic Gondwana basins and their depositional limits in relation to Narmada-Son Lineament. In: Casshyap, S.M., Valdiya, K.S., Khain, V.V., Milanovsky, E.E. and Raza, M. (Eds.), *Rifted Basins and Aulacogens: Geological and Geophysical Approach*. *Gyaanodaya Prakashan, Nainital, India*, 200-215.

Catuneanu, O, Wopfner, H., Cairncross, B., Rubidge,B.S., Smith, R.M.H. and Hancox, P.j. (2005). In:Catuneanu, O., Guirand, R., Eriksson, P. , Thomas, B., Shone, R., Key, R (Eds.) The Karoo basin of south-central Africa: Phanerozoic Evolution of Africa. *Jour. of African Earth Sciences,* 43, 211-253.

Crowell, J.C. (1978). Gondwana glaciation, cyclothems, continental positioning and climatic change. *American Jour. Sci.,* 278, 1345-1372.

Frakes, L.A., Kemp, E.M. and Crowell, J.C. (1975). Late Palaeozoic glaciation: Part VI, Asia. *Geol. Soc. America Bull.,* 86. 454-464.

Gaetani, M. and Garzanti, E. (1991). Multicyclic history of the Northern India continental margin (North-West Himalaya). Ameriican *Assoc. Petrol. Geol. Bull.* ica75, 1427-1446.

Kruck,W. and Thiel, J.C. (1983). Late Palaeozoic glacial deposits in the Yemen. *Geologisches Jharbuch (B),* 46, 3-29.

Levell, B.K., Braakman, J.H and Rutten, K.W. (1988). Oil-bearing sediments of Gondwana glaciation in Oman. *American Assoc. Petrol. Geol. Bull*., 72, 775-796.

Lopez- Gamundi (1997). Glacial-Post-glacial transition in the Late Palaeozoic basins of southern South America*. In: Martini, I.P. (Ed.) Deglaciation and global changes: Quaternary, Permo-Carboniferous and Proterozoic*. *Oxford University Press, Oxford*, 147-168. 2, 409-416.

Metcalfe, I. (1988). Origin and assembly of Southeast Asian continental terrannes. In: Audley-Charles, *M.G. and Hallam,A. (Eds.) Gondwana and Tethys.Geol. Soc., London*, Special Publ., 37, 101-118.

Mitra, N.D. (1991). The sedimentary history of Lower Gondwana coal basins of Peninsular India. In: Ulbrich, H. and Rocha Campus, A.C. (Eds.) *Gondwana Seven, Proc. Seventh Gondwana Symposium, Institute of Geosciences, Universidade de Sao Paulo*, 273-288.

Mitra, N.D. (1993). Tectonic history of Lower Gondwana basins of Peninsular India. In: *Casshyap, S.M.,Valdiya, K.S., Khain,V.K., Milanovsky, E.E. and Raza, M. (Eds.) Rifted basins and Aulacogens; Geological and Geophysical Approach.* Gyanodaya Prakasan, Nainital, 216-221.

Nakazava, K and Kapoor, H.M. (1979). Correlation of the marine Permian in the Tethys and Gondwana.*Proc. IV Intern Gondw. Symp., Calcutta*, 2 409-416.

Powell, C.M. and Li, Z.X. (1994) Reconstruction of the Panthalassan margin of Gondwanaland. In: Veevers J.J. and Powell, C.McA (Eds.) *Permian-Triassic Pangean Basins and Foldbelts along the Panthalassan Margin of Gondwanaland. Geol. Soc. of America, Boulder, Memoir* 184, 5-10.

Rust, L. C. (1975). Tectonic and sedimentary framework of Gondwana basins in southern Africa. In: Campbell, K.S.W. (Ed.) *Gondwana Geology. Australian National University Press, Canberra*, 537-564.

Scotese, P.Z. and Langford, R.P. (1995). Pangea and the Palaeogeography of the Permian. *In: Scholle, P.A., Peryt, T.M. and UlmerScholle, D.S. (Eds.) The Permian of Northern Pangea. Vol. I: Palaeogeography Palaeoclimatic Stratigraphy.* Spriger, Berlin, 3-19.

Sengor, A.M. (1998). Die Tethys: vor hundert jahren und heute. *Mitteilungen der Osterreichischen Geologischen Gesellschaft*, 89,5-177.

Smith, A.J. (1969). Evidence of a Talchir (Lower Gondwana) glaciation: striated pavement and boulder Bed at Irai, central India, *Jour. Sediment. Petrol*., 33, 739-750.

Smith, R.M.H., Eriksson, P.G. and Botha, W.J. (1993). A review of the stratigraphy and sedimentary environments of the Karoo-aged basins of Southern Africa. *Jour. African Earth Sci,* 16, 143-169.

Stratton, T. (1970). Tectonic framework of sedimentation during the Dwyka period in South Africa. *Second Gondwana Symp. Proceedings and Papers, Pretoria, South Africa*, 483-490.

Taveren-Smith, R. (1982). Prograding coastal facies associations in Vryheid Formation (Permian) at Effingham Quarries, near Durban, South Africa. *Sediment. Geol*., 32, 111-140.

Tewari, R.C. and Veevers, J.J. (1993). Gondwana basins of India occupy the middle of a 7500 km sector of Radial valleys and loibes in central-eastern Gondwana. *Gondwana Eight*, Balkema, Rotterdam, 507-512.

Veevers, J.J. and Powell, C.M. (Eds.) (1994). Permian-Triassic Pangean Basins and Foldbelts along the Panthalassan Margin of Gondwanaland. *Geol. Soc. America, Boulder*, Memoir 184.

Veevers, J.J. and Tewari, R.C. (1995). Gondwana Master Basin of Peninsular India. *Geol. Soc. America,* Memoir 187, 72p.

Verma, R.P. and Singh, V.K. (1979). A chronology of tectonics and igneous activity in Damodar Valley coalfields. *Proc. IV Intern. Gondw. Symp., 1977, Geol. Surv. India, Calcutta*, 2, 901-907.

Visser, J.N.J. (1989). The Perm-Carboniferous Dwyka Formation of Southern Africa: deposition by a predominantly sub-polar marine ice sheet. Palaogeog., Palaoclimat.,Palaoecol., 118, 213-243.

Visser, J.N.J. (1997). A review of the Permo-Carboniferous glaciation in Africa. In: *Martini, I.P. (Ed.) Deglaciaation and Global changes: Quaternary, Permo-Carboniferous and Proterozoic. Oxford University Press, Oxford*, 169-191.

Wopfner, H. (1991). Extent and timing of the Late Palaeozoic glaciation in Africa. *Festschrift Karl* Brunnacker*, University zu Koln,* 82, 447-453.

Wopfner, H. (1994). The Malagasy Rift, a chasm in the Tethyan margin of Gondwana. *Jour. Southeast* Asia *Earth Sci.,* 9, 456-461.

Wopfner, H. (1999). The Early Permian deglaciation event between East Africa and northwestern Australia. *Proc. of the Tenth Gondwana Symp., Cape Town. Jour. of African Earth Sci*, 29, 77-90.

Wopfner, H. (2002). Tectonic and climatic events controlling deposition in Tanzanian Karoo basins. *Jour. African Earth Sci.* 34, 167-17.

Wopfner, H. (2012). Late Palaeozoic-Early Triassic deposition and climates between Samfrau and Tethys: A review. *Geol. Soc., London Special Publication published online, Nov. 26, 2012*:10. 1144/SP, 376.4.

Wopfner, H. and Kreuser, T. (1986). Evidence for Late Palaeozoc in Southern Tanzania. *Palaeogeog., Palaeoclimat., Palaeoecol*., 56, 256-275.

Wopfner, H. and Diekmann, B. (1996). The Late Palaeozoic Idusi Formation of Southwest Tanzania: A Record of change from glacial to postglacial conditions. *Jour. African Earth Sci*., 22, 575-595.

Wopfner, H. and Casshyap, S.M. (1997). Transition from freezing to subtropical climates in the Permo- Carboniferous of Afro-Arbia and India. In: Martini, I.P. (Ed.) *Deglaciation and Global changes: Quaternry, Permo-Carboniferous and Proterzoic. Oxford University Press, Oxford,* 192-212.

Wopfner, H. and Jin, X.C. (2009). Pangean Mega sequences of Tetyan Gondwana-margin reflect global changes of climate and tectonism in Late Paleozoic and Early Triassic times – a review. *Paleoworld,* 18, 169-192.

First online volume
Jour. Indian Association of Sedimentologists, Vol. 35, No. 1 (2018), pp.23-35
ISSN 0970-3268

Sedimentary Record of Forced Regression Along The Margin of Kutch Basin: Terminal Cenozoic Succession (Sandhan Formation), Western India

Shubhendu Shekhar, Avinash Shukla and Pramod Kumar
Department of Geology, Center for Advanced Studies, University of Delhi, Delhi 110007

Abstract: The sedimentation of Cenozoic successions of Kutch took place in passive margin sag-basin over the stable continental shelf, primarily controlled by relative sea-level fluctuations vis-à-vis siliciclastic supply/carbonate production. The basin-wide two-tier unconformity bounded clastic dominated Sandhan Formation is deposited in shallow marine (~135m, lower part) to fluvial environment (~157m, upper part). The discontinuous exposures along cliff/banks of Kankawati River (type section) and Kharod River provided an excellent opportunity for detailed sedimentological and sequence stratigraphic analysis. The fluvial forced regressive sediments are very rare in rock records because of subsequent transgression and erosion. The total 11 facies were identified (Miall, 1985 classification) viz. **Gm, Gmm, Gp, Gt, Sh, Sp, St, Sm, Fsm, Fl,** and **P** are grouped into three Facies Association (FA): 1. **Channel and Channel Fill FA;** occurs at the base, characterized by **Gm, Sh** and **Sp** facies with vertically and laterally amalgamated stacked tabular sheet sandstone bodies with concave upward erosional base, individual sandstone sheet shows the fining upward trend with channel-lag. 2. **Sandy and Gravel Bar FA;** characterized by fining upward tabular sandstone bodies (**Sh** and **Sp**) overlain by the cycle of coarse poorly sorted massive gravel fining upward to trough cross-stratified sandstone. Towards downstream section multistoried stacked sheet of trough cross-stratified gravel beds are overlain by the planar stratified gravel bed (**Gm, Gt** and **Gp**). 3. **Overbank Fines and Floodplain FA;** characterized by **Fl, Fsc,** and **P** elements and by 5-6m thick massive deposit of lithofacies **P** in the upper part of the succession, dominated by abundant root penetration structures and extensive pedogenic features with calcrete/ferricrete layers, indicates a major break in sedimentation and sequence boundary. The Sandhan Formation is characterized by the wave-dominated TST overlain by normal regression/progradation of HST followed by the forced regressive deposit of FSST. The FSST is bounded at the base by a basal surface of forced regression, characterized by cobble/pebble horizons followed by abundant fluvial channel lags occurring at the top of HST. The low dipping shelves are very sensitive to sea-level changes and subjected to inundate/expose a large part of the shelf in small fluctuations. The abrupt fall in the sea-level exposed a large part of the continental shelf and older HST prism provided the sufficient slope for the braided fluvial system to develop. The relative sea-level never reached to its previous extent which leads the preservation of forced regressive deposits. The final withdrawal of shoreline shifted the depositional milieu westward and sedimentation/basin closed at the onland part of Kutch.

Keywords: Sandhan Formation, Falling Stage Systems Tract, Channel and Channel Fill, Sandy and Gravel bar, Overbank Fines and Floodplain.

Introduction

The falling stage systems tract develops during falling limb of sea level curve is characterized by shoreface wedge or fluvial sediments having distinct offlap strata of partially attached or detached lobes (Bera et al. 2008; Hunt, 1992; Hunt and Tucker, 1992). Initially, it was assumed that due to the overall erosive regime during base-level fall there was no sedimentation on the exposed part of the shelf (Van Wagoner et al. 1987; Vail, 1987: Mitchum, et al. 1977). The deposits of forced regression driven by fall in sea level was recorded by many (Plint (1988, 1991; Plint and Norris, 1991; Ainsworth, 1994; Hunt, 1992; Hunt and Tucker, 1992; Nummedal, 1992 etc). This systems tract was introduced by Hunt and Tucker (1995) as Forced Regressive Wedge Systems Tract (FRWST), later renamed as Falling Stage Systems Tract (FSST) and comprehensive explanation was given by Plint and Nummedal (2000) and introduced to the original tripartite classification of depositional sequences (Vail, 1987; Posamentier and Vail, 1988). This is the only systems tract in the depositional sequence which has no direct correlation of sediment supply and relative sea-level fluctuations, however, systems tract develop due to the high rate of sea-

level fall irrespective of rate of sediment supply. Its development is controlled by shelf geometry, slope, tectonics, climate, magnitude of relative sea-level fall characterized by general high rate of sedimentation. The preservation potential of this systems tract is very low because of extensive erosion along the depositional profile to lowest sea level (Coe et al., 2005) or erosion from the subsequent transgressive event, therefore, in rock record FSST are rare. The FSST can experience the marine or fluvial influences depending upon the rate of base-level fall.
This study aims at process based sedimentological and stratigraphic analysis of the upper part of the Sandhan Formation for its depositional and sequence stratigraphic interpretation. The basin-wide two-tier unconformity bounded terminal Cenozoic Sandhan Formation is clastic dominated succession deposited in shallow marine (~135m) followed by the fluvial environment (~157m) is considered as 'sequence', comprised of wave-dominated TST overlain by HST and followed by fluvial deposits of forced regressive FSST. The distinctive location and subsequent sea-level cycle provided an opportunity to develop FSST in the upper part of Sandhan Formation.

Geological Setting

The Kutch basin evolved as a passive margin sag-basin during Cenozoic, exposed along the western margin of Kutch, India. The sedimentation initiated after Deccan volcanism is exposed along narrow coastal plain trending NNW-SSE separated by various magnitude of unconformity, non-conformity or paraconformity. The sedimentation took place on the tectonically undisturbed continental shelf so the beds are almost flat to low dipping at 1-3° towards SSW to NW (Fig: 1). Because of almost flat topography, Cenozoic successions are mainly exposed along cliffs and banks of rivers. The sedimentation in the passive margin setting is controlled by relative sea-level fluctuations vs. the rate of siliciclastic supply/carbonate production without large-scale tectonic hindrance is divided into various formations (Table: 1). The terminal Cenozoic formation of Kutch is designated as Sandhan Formation is siliciclastic dominated. The age of the Sandhan Formation is not clear because of the absence of age-diagnostic fauna, instinctively, the Pliocene age is assigned to it because of a prominent break in sedimentation above Lower-Middle Miocene and according to the order of superposition (Biswas, 1992). Nearly 292m thick Sandhan Formation is exposed along cliffs and banks of Kankawati (type section) and Kharod River with several exposure gaps towards upper part. The Sandhan Formation is bounded by basin-scale unconformity, the lower unconformity above Chhasra Formation is characterized by the conglomerate bed and upper contact with Sub-recent sediments is identified by regional and laterally persistent paleosol horizon. According to Biswas (1992), the depositional environment of Sandhan Formation is interpreted to be supra littoral to deltaic or foreshore environment.

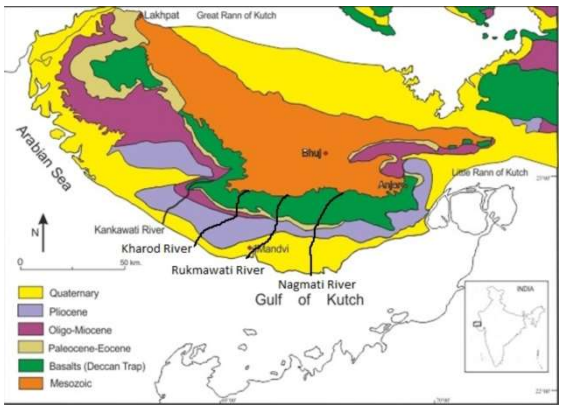

Figure: 1. Geological map of the Kutch basin (After Biswas, 1992).

Methodology

The mainstay of the present study is outcrop process based sedimentology, stratigraphic observation for the purpose of depositional environment and sequence stratigraphic analysis of upper part of

Sandhan Formation. The detailed fieldwork was carried out along Kankawati

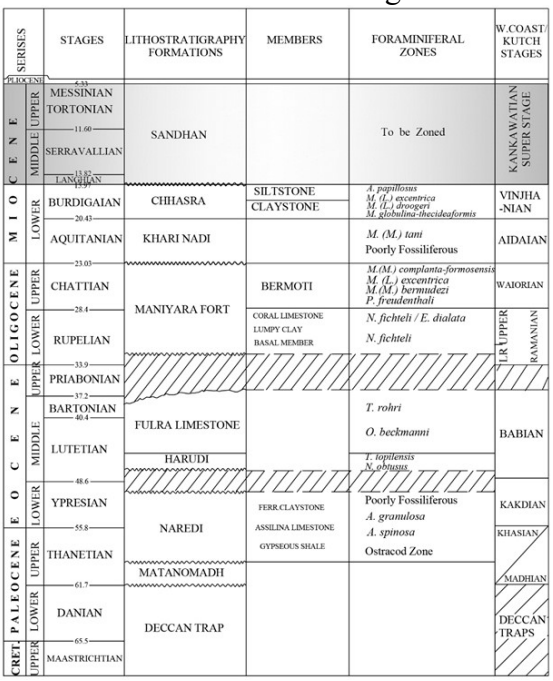

Table: 1. Cenozoic stratigraphy of Kutch Basin (after Biswas, 1992).

River (type section) and Kharod River sections to document lithology, grain size, colour, sedimentary structures, bed geometry and nature of contact. Wherever possible, the beds were traced along strike and down dip to understand the geometry and lateral continuity. The standard procedure was applied to stratigraphic and sedimentological observations and information was used to prepare graphic-log of the two river sections. The identified facies are clubbed into facies association for depositional environment interpretation. The samples were collected for petrographic analysis.

Facies Analysis

The introduction of facies in sedimentology has changed the way of looking at the sedimentary rocks. The process-based sedimentological analysis of sedimentary succession is now exclusively conducted through the facies analysis. The facies are distinctive lithounits deposited under the particular depositional condition and reflect process operated at the time of its deposition and modification later on. The facies can be identified through their distinct lithology, texture, grading, sedimentary structures, bed geometry and biogenic contents etc. The process operated during the deposition of particular lithounits can suggest depositional environment through the genetically related facies (follows Walther's Law) into facies association (Walker, 1979). However; facies association can have a very progressive and dynamic shift through time (Walker, 1984; Reading, 1986; 1996; Posamentier and Walker, 2006). The process-based sedimentological and stratigraphic analysis is carried out in the upper part of the Sandhan Formation (~157m) to identify facies, facies association for the interpretation of depositional environment. Studied stratigraphic interval is dominated by granular/pebbly to coarse-grained sandstone and occasional gravel beds. The coarse sandstone bodies are overlain by the fine siltstone or mudstone at places. The sandstones are arkosic to sub-arkosic in nature and comprises of angular to sub-angular grains with a dominant proportion of orthoclase feldspar. The lithofacies name were assigned according to the scheme provided by facies classification of Miall (1985, 1996). Total 11 lithofacies were identified in the field (Table: 2).

Facies Association: 1
Channel and Channel Fill Facies Association

This facies association occurs at the base of the studied section are characterized by the stacked tabular sheet sandstone bodies with distinct concave upward erosional base. The thickness of individual sheet ranges from 2-3m, fining upward trend with coarse channel lag at the base. Sandstone sheets are vertically and laterally amalgamated. Disorganized coarse channel lag (**Sm)** facies (Fig. 2.A), is overlain by the **St, Sp** and **Sh** Facies. At places, **Fsm** is encased between sheet sandstone indicating frequent channel shift.

Gravel Facies

Facies Code	Lithofacies	Description	Interpretation
Gmm	Coarse grained poorly sorted matrix supported gravel facies	This facies consist of poorly sorted gravels and pebbles supported by the poorly sorted sandy matrix. Massive to crudely bedded. Elongate lobate geometry. Thickness of the lobes is ~75 cm. Imbrication is absent. (Fig. 3.B).	This facies suggests deposition by the non-cohesive sediment gravity flow. High viscosity lead to the lobate geometry.(Miall , 1996).
Gt	Trough cross-stratified gravel facies	Shallow scoop shaped trough cross-stratified gravel bodies having erosional base filled with the lag deposit of coarse granule to pebble size grains which fines upward.Erosional troughs are overlain by diffused multistoried gravel sheet (Fig.3.A).	Trough cross stratification indicate the migration of transvers dunes with curved crest (Miall, 1985).
Gp	Planar cross-stratified gravel facies	Poorly sorted planar cross stratified gravels typically overlie the Gmm and Gt facies in the section. Cross set thickness are less than 1m.(Fig. 2.E).	Transverse bedform, deltaic growth from older bar remnants (Miall, 1996).
Gm	Massive to crudely planer-stratified gravel facies	This facies is characterized by the stacked sheet of the poorly sorted gravels bodies, often overlain by the Gp and Gt facies (Fig. 2.E).	Deposition by longitudinal bar in relatively shallow flow, high stage of flow. Diffused sheet (Hein & Walker, 1977). Grow upward and downstream during episodes of high water and sediment discharge to form longitudinal bar (Rust, 1972).

Sand Facies

Facies Code	Lithofacies	Description	Interpretation
Sh	Medium grained horizontally laminated sandstone facies	Tabular medium to coarse grained poorly sorted planar laminated sandstone. Each unit of the sandstone bodies are 2-3m thick. (Fig. 2.B).	Represent the upper plane bed condition at the transition from subcritical to supercritical flow (Miall, 1996).
Sp	Planar cross stratified sandstone	Coarse to medium grained tabular cross stratified sandstone. Grain size and set thickness reduces upward. (Fig. 2.C).	Form by the migration of 2D dunes (Miall,1996)), migration of ripples in upper flow regime. Sand waves generate planar cross-bedding (Smith, 1970, 1971).
St	Trough cross stratified coarse grained sandstone, often pebbly facies	Characterized by large scale cross strata in poorly sorted sandstone. Grain size and set thickness reduces upward. Thickness of large set is up to 3o cm which reduces upward to 1o cm. cross strata are oriented in the same direction. (Fig. 2.D)	Migration of the curved crested transverse and longitudinal dunes on the channel floor.
Sm	Massive, pebbly sandstone	Very coarse grained poorly sorted pebbly sandstone. Pebbles are present in the matrix of poorly sorted sand and have rounded to angular shape. Measured thickness of this facies is 40-50 cm (Fig. 2.A).	It has been envisaged as a channel lag deposit. It can also be a product of rapid deposition from heavily loaded flow, possibly a flash flood scenario (Pflüger and Seilacher, 1991).

Fine Grained Clastic Facies

Facies Code	Lithofacies	Description	Interpretation
Fsm	Mud, Silt	Massive silty mudstone bed above the poorly sorted sandstone body. Thickness is around 2-3m (Fig. 3.D).	Overbank fines, abandoned channel (Miall, 1996).
Fl	Mudstone interbedded with fine silt and sand.	Tabular bodies of laminated mud interbedded with rippled fine silt and sand. Overall thickness of the facies is about 4-5m with individual mud and silt layers being 50-75cm thick (Fig. 3.C).	Ovebank fines, back swamp deposit, bar top deposits (Bridge, 2006).
P	Paleosol associate with calcrete nodules	Fine mud deposits marked by the pedogenic features with distinct root penetration structure indicative of soil formation. Occurs at uppermost part of the section (Fig. 2.E-F).	Floodplain deposits exposed for considerable period of time. Soil with chemical precipitation (Miall, 1996).

Table: 2. The facies description of Sandhan Formation and its interpretation

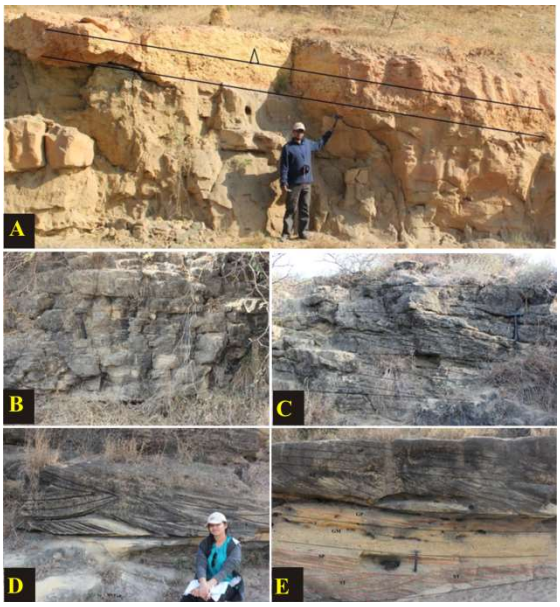

Figure: 2. Outcrop photographs of fluvial facies identified in the field. **(A.)** Massive pebbly sandstone with channel lag (**Sm**) **(B.)** Planar Laminated sandstone (**Sh**). **(C.)** Tabular cross stratified sandstone (Sp). **(D.)** Trough cross stratified sandstone, Curved bounding surfaces and trough sets have been marked (**St**). **(E.)** Gravel Bed characterized by lithofacies **Gm** and **Gp**.

Interpretation

The sediments deposited in the channels are left behind as river migrate laterally across their floodplain. This lateral migration continues till the river avulses. After the avulsion river abandons their old channel and follows a new pathway across the floodplain. As the aggradation rate increases, these isolated lenses of the abandoned channel sediments will amalgamate into sheet-like bodies due to lateral migration of the channel. Lateral migration of the channels is represented by the vertically and laterally amalgamated sheet sandstone bodies in the rock record (Church and Rood, 1983; Crowley, 1983). Mudstone Facies above the sheet sandstone body mark the channel fill succession deposited by the vertical aggradation. The fining-upward trend with a related decrease in cross set thickness clearly shows the temporal decrease in flow strength.

Facies Association: 2

Sandy and Gravel Bar Facies Association

The 3-4m thick tabular bodies of fining-upward planar to crudely cross-stratified sandstone occur above channel element. The vertical stacking of a number of lithofacies **St, Sp, Sh, and Sr** is present (Fig. 2.B-D). The fining-upward succession with a reduction in set thickness upward and change in structure from cross set to ripples was observed. The facies association is repetitive in nature and individual cycle is overlain by another cycle of pebbly to coarse sandstone with large trough cross-stratification with reduction in set thickness and grain size in up section. This facies association is most common in middle part and share major part of stratigraphic section. In the upstream section, it occurs stratigraphically above the multistoried stacked sheet sandstone whereas, in the downstream section it occurs stratigraphically above the gravel sheet facies.

In the downstream part trough cross-stratified sandstones are overlain by the crudely bedded massive gravel. The lithofacies gives way to facies **Gp** and **Gm** (Fig. 2.E) with clast imbrications. This gravel layer is overlain by **St→Sp→Sh→Sr** facies shows a cyclic deposition of lithofacies each consisting of **Gm, Gp, Gt, Sp, Sh** and capped by **Sr**. The trough set thickness varies from 15-25 cm. In downstream part above facies are overlain by the medium to large scale low angle trough cross-stratified sandstone bed capped by the tabular cross-stratified to planar bedded sandstone. The troughs are characterized by the coarse granule to pebble size grains at the base of the foresets, with fining upward trend as well as a decrease in the size of the trough set thickness. These planar beds are overlain by another cycle characterized by coarse gravel-rich large scale trough beds, which shows a fining upward trend and have a lateral extent of ~10m.

Further downstream two major outcrops were identified. The lower one is characterized by trough cross-stratified gravel, **Gt** (Fig. 3.A), overlain by the massive gravel bed, **Gm**, overlain by the facies sequence as described above. Trough set thickness is ~30cm which reduces to 15cm in upward section. The upper bar is characterized by the gravel sheet. Each sheet consists of facies **Gm→Gt→Gp**. The gravel sheet are occasionally capped by the thin layer of fine sandstone. The layer of sediment gravity flows is also associated with these facies and occur as an elongate lobe dominated by the lithofacies **Gmm** (Fig. 3.B).

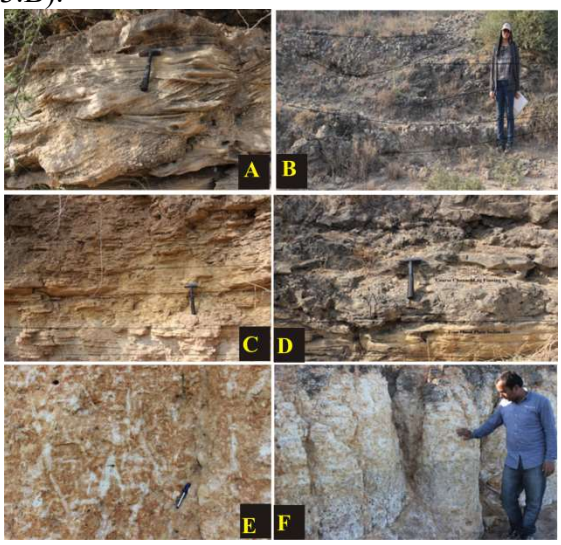

Figure: 3. Outcrop photographs of fluvial facies identified in the field. (A.) Trough cross stratified gravel forming gravel bar (Gt). (B.) Sediment gravity flow showing an elongated lobe geometry (Lithofacies Gmm). (C.) Inter-laminated mud, sit and sandstone (Fl). (D.) Floodplain sediment above channel characterized by mud, silt (Fsm). (E.) Paleosol with root penetration structures (P). (F.) Calcrete layers associated with the paleosol.

Interpretation

The lower part of the facies association is characterized by dune scale planer cross bedding may have formed by the migration of transverse bar. Transverse bars and sand waves are known to produce planar cross bedding (Smith, 1970, 1972; Levey, 1978; Blodgett and Stanley, 1980). The middle part of the section dominated by the trough-cross bedding has been showing the result of migration of dunes in the deeper part of the channel which is overlain by planar-cross strata. Vertical stacking of different bedform type indicates frequent changes in the flow regime. Longer term changes reflect aggradation and reduction in water depth (Miall, 1985). It is supported by the field evidence of fining-upward succession associated with a reduction in set thickness. Each repeating cycle shows a reduction in flow strength with fine rippled sand overlying the trough-cross bed.

In the downstream part trough-cross stratified sandstone overlain by the crudely bedded massive gravel and the cyclic succession of the facies, **St→Sp→Sh→Sr** were identified as the product of the growth, migration and lateral and downstream accretion of lobate unit bars. The bar head regions are deposited as a result of accretion of fronts of unit bars and bar tails by accretion of sides of lobate unit bars (Hein and Walker, 1977; Bridge, 2006). Individual unit bars showing a temporal reduction in flow strength. In the downstream section, flow strength decreases further as fine sediments begin to appear as interpreted as bar top facies possibly deposition in very shallow water on top of the bars.

The outcrops of gravel beds are identified as the gravel longitudinal bars. During the episode of high water and sediment discharge gravel sheet grow upward and downstream to form gravel longitudinal bars (Rust, 1972). Sheet and clast accumulation tend to result in fining up succession as observed in the field. The repeated cycle of the bed indicates the bar migration downstream (Gustavson, 1978). The geometry of the gravel bar bedform has been modeled as multistoried sheet of 10's of meter thick flat/erosional surface between each set (Miall, 1986). Deposits of gravity flows occur as narrow, elongate lobes and typically associated with the gravel bars (Miall, 1996).

Facies Association: 3

Overbank fines and Floodplain Facies Association

In the upstream section, 5-6m thick silty mudstone deposit are incased in the sheet sandstone bodies. In the downstream section the outcrop of sheet/tabular fine silt interbedded with mud (lithofacies **Fl** and **Fsm**) overlain the trough-cross stratified sandstones (Fig. 3.C-D). The silt layer is represented by the horizontal laminations due to deposition through suspension settling. The silt layers are characterized by the ripple lamination and ripple scale cross stratification. Occasional ferruginous layers and desiccation cracks observed in the mudstone.

Uppermost part of the succession is marked by the 4-5m thick massive mudstone deposit. It is dominated by the abundant root penetration structure and marked by the extensive pedogenic features which indicate the soil formation (Fig.3.E). It also shows the succession of calcrete/ferricrete layers towards the top (Fig.3.F). This facies is the uppermost deposition facies of the Sandhan Formation and is directly overlain by the recent Quaternary sediments.

Interpretation

It is inferred that deposition took place away from the channels by the vertical accretion of the fine clastic sediments. The most active vertical accretion environments occur along high-energy channels with sandy floodplains that can be destroyed catastrophically by large floods and subsequently reconstructed by overbank deposition (Schumm and Lichty, 1963; Burkham, 1972; Nanson, 1986). Fine silt and sand layer suggest that deposition took place under low energy condition from suspension settling of fine-grained sediments. Small-scale ripples and cross stratification present in the silt layer suggest traction transport process during occasional high energy condition. Paleosol succession preserved at the uppermost part of the succession suggests the seasonal/longer term drying out of the floodplain.

Depositional Environment

The three facies associations were identified through outcrop based facies analysis along the Sandhan Formation viz. Channel and Channel Fill Facies Association, Sandy and Gravel Bar Facies Association, and Overbank fines and Floodplain Facies Association. Channel and Channel Fill Facies Association characterized by a stacked sheet of poorly sorted medium to coarse-grained sandstone with fining upward character represented by **Gm, Sh** and **Sp** facies. The Sandy and Gravel bar Facies Association is characterized by fining upward tabular sand bodies comprised of **Sh** and **Sp** facies. The fining-upward cycles of gravel culminate at the top by **Sp** or **St** Facies. Mid-channel bar is formed by the accretion of unit bars **St** and **Sp**, which are capped by the overbank fines facies **Fl** in the downstream sections. Gravel bar Facies Association are characterized by multi-storied stacks of trough cross stratified gravel overlain by the planar stratified gravel of **Gm, Gt** or **Gp** facies. Gravel bar facies interspersed with sediment gravity flow deposits. The Overbank fines and Floodplain Facies Association represent the minor fraction and are characterized by the lithofacies **Fl, Fsm** and paleosol **P** facies in the upper part of the succession. The coarse-grained sandstone, gravels, abundant trough-cross stratification, very rare preservation of the current ripples and erosive bounding surface indicate the high energy condition of the flow. Many basin margins are characterized by the wedges of gravel deposit, commonly these are deposited by the distributary fluvial system (Miall, 1996). Associated sediment gravity flow deposit and minor thickness of fine-grained deposit (low water and overbank sedimentation) also indicate the high energy stream flow (Miall, 1996). Multi-storied channels, multi-storied gravel

sheets, the absence of floodplain levee complex and lateral accretion character indicate the braided character of fluvial deposits. The absence of complete open marine and estuarine sediment inter-tonguing with fluvial sediments and high energy condition inferred from the above sedimentological evidence suggests that the deposition of the upper part of the Sandhan Formation took place in unincised, unconfined gravel-bed braided river system. Sufficient slope for the braided river system to develop is provided by the abrupt fall in relative sea-level led to the exposure of large part of the continental shelf and highstand prism of previous deposits.

Sequence Stratigraphic Framework

Sequence stratigraphy is a novel concept of sedimentary record that provides a predictive model of basin fill architecture. The paradigm uses unconformities or their correlative conformities to split sedimentary succession into unconformity-bounded sequences at different scales. The concept was first developed for the siliciclastic environment for passive margin basins where evidence of sea-level fluctuation and sedimentary fill can be better preserved and documented in the stratigraphic record. Being an association of genetically related strata bounded by unconformity or their correlative conformity; the process based sedimentology and facies analysis is a backbone for sequence stratigraphic analysis. Identification of sequence boundary is the first step in sequence analysis. The two-tier unconformity-bounded succession of Sandhan Formation is considered as a sequence. The lower sequence boundary with Chhasra Formation is clearly observed in river sections under study as an undulating erosional surface with a conglomerate bed, can be traced at basinal-scale. The contact implies a fall in relative sea-level, exposure of the depositional substrate and the development of a subaerial unconformity. The unconformity between the two formations defines a plane across which depositional pattern changed and a large shift in depositional environment noticed at basin-wide scale and thus marks a sequence boundary. The upper sequence boundary with overlying sub-recent sediments is characterized by the thick and regional occurrence of paleosol horizon with abundant root penetration and calcretes. The thick formation of paleosol requires landscape stability associated with the physical, chemical and biological transformation of exposed sediments (Kraus, 1999) thus indicates an episode of non-deposition/unconformity. The development of paleosol in marginal marine to shallow marine environments is controlled by base-level fall and subaerial exposure of shelf (Lander et al., 1991; Webb 1994; Wright 1994; Van Wagoner, 1995). The fall reaches its maximum extent at the end of the forced regression (Helland et al., 1992), however, the type of paleosol developed at sequence boundary is dependent on fluctuating base-level and prevailing climate (Write and Marriott, 1993; Tandon and Gibling, 1994). The unconformity-bounded Sandhan Formation is divided into transgressive systems tract (TST), highstand systems tract (HST) and falling stage systems tract (FSST) separated by standard sequence stratigraphic surfaces (Fig.4). The study section lies at the shallow shelf where lowstand systems tract (LST) are typically absent and TST directly overly on sequence boundary/transgressive surface (Baum and Vail, 1988). The base of FSST is demarcated by the basal surface of forced regression, characterize the base of all the deposit that accumulates during the forced regression of the shoreline (Hunt and Tucker, 1992). This surface marks the boundary between the normal regressive strata below and the forced regressive strata above. This surface is very prominent if the rate of relative sea-level fall is high and shelf slope is very gentle. The distinct and extensive fluvial deposits

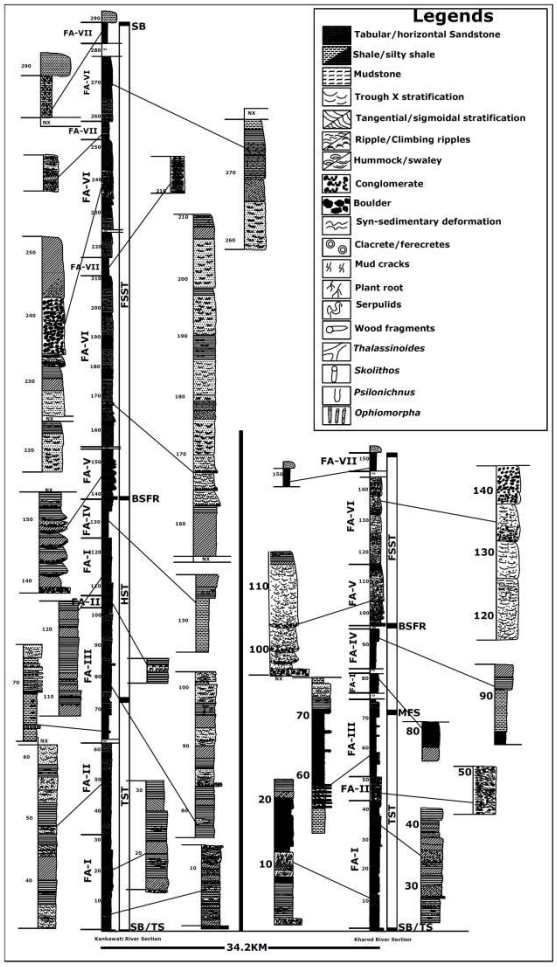

Figure: 4. Sedimentary log of Sandhan formation along Kankawati and Kharod River, showing Facies Associations and Sequence stratigraphic elements

above HST is separated through the basal surface of forced regression is characterized by multiple channel stacking and channel fill sediments (Fig: 5. A). The immediate incision of the fluvial channel above highstand deposits led to abrupt facies break which argues for relative sea level fall. The fluvial erosion due to relative sea-level fall eventually truncates earlier highstand strata (Plint and Nummedal, 2000). Whereas FSST is bounded at the top by composite surface may include subaerial unconformity or its correlative conformity (Hunt and Tucker, 1992). The distinct 11 facies of fluvial environment is clubbed into three facies associations are designated as forced regressive deposits of FSST (Fig. 6). The FSST is overall coarsening and shallowing upward strata of an offlap pattern. The occurrence of distinct overbank and floodplain sediments with abundant channels and bars indicates unconfined braided fluvial system. The abundance of large grain size and gravity deposits suggests intermittent high energy during occasional flash flood condition (Fluger and Seilacher, 1991; Wright and Marriott, 1993).

The continental shelf of western India around Kutch is wide (~375km) which tapers down southwards. The slope of the shelf is around 1-3° towards SSW. This geometry of shelf generates very low slope due to which minor fluctuation in base level can inundate or expose the wide area of the shelf. The preservation potential of shallow marine falling stage systems tract is inversely proportional to the magnitude of base level fall (Catuneanu, 2006). In the case of low magnitude fall in base level when the shoreline does not reach the shelf edge the forced regressive shelf sediments get preserved between the basal surface of forced regression and subaerial unconformity (Catuneanu, 2006). The fluvial system also common in the upper part of HST, however, HST fluvial system is characterized by lowest energy fluvial system of stratigraphic sequence. It is commonly sluggish, meandering type, characterized by a channel of moderate to high sinuosity (Catuneanu, 2006). In the absence of topographic relief, HST fluvial system does not form braided pattern until affected by tectonics or climate-driven high discharge of clastic supply. The LST sediments are coarse grain deposits and can develop a braided pattern. The occurrence of the regional unconformity at the upper part of Sandhan Formation (Fig. 5. B) exclude the possibility of LST sediments as it is bounded by correlative conformity at the base, not by the basal surface of forced regression and topped by the transgressive surface of marine erosion, not by the subaerial unconformity. The argument for fluvial sediments of Sandhan Formation to assign lowstand

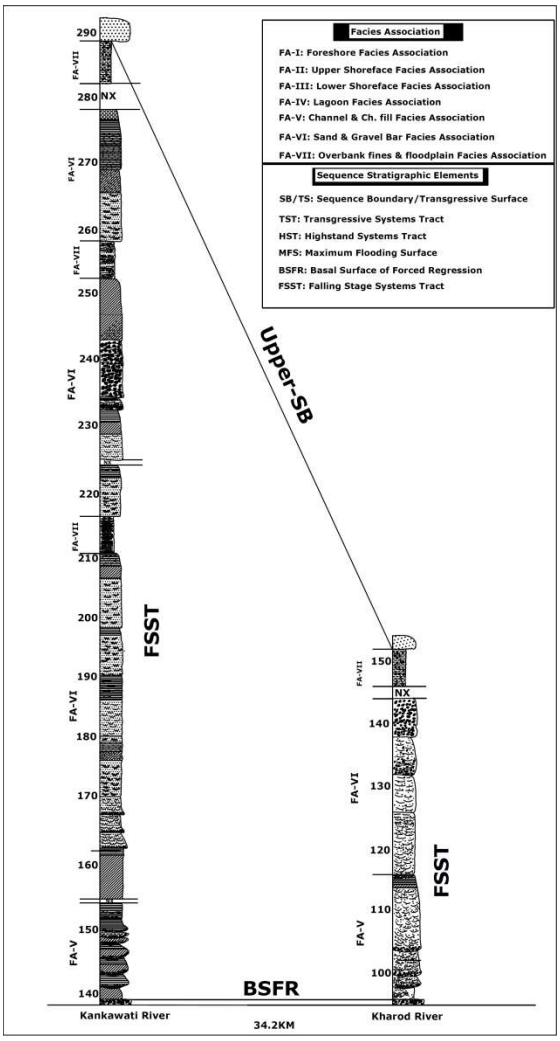

Figure: 6. Sedimentary logs showing the correlation of FSST of Sandhan Formation between Kankawati and Kharod River sections.

deposits is not valid in this situation. Moreover, the development of LST is restricted at shelf slope or shelf edge area. The unincised fluvial system of the falling stage is now documented as having a more common occurrence in the rock record than originally inferred by early standard sequence stratigraphic models. There are specific conditions in the shallow marine basin with a gently sloping ramp or margin of continental shelf setting where the forced regressive shoreline does not fall below the elevation of shelf edge (Posamentier, 2001). The fluvial deposits of upper part of Sandhan Formation are characterized by unincised braided pattern, deposited on the gentle sloping shelf of Kutch is affected by relative sea-level fall, however, fall does nor exceeded beyond shelf edge provided opportunity to preserve FSST sediments. The subsequent sea level rise after Sandhan Formation does not raise up to an extent to rework/erode the FSST sediments.

Conclusions

1. The sedimentary succession of the upper part of Sandhan Formation deposited in unincised, an unconfined braided system characterized by three Facies Associations: Channel and Channel Fill, Sandy and Gravel Bar and Overbank fines and Floodplain, affected by episodic high energy environment.
2. The combined effect of HST prism and shelf provided the sufficient slope for the deposition of braided fluvial sediments.
3. The thick accumulation of paleosol at the uppermost part of succession formed due to end of base level fall, geomorphic stability and extensive pedogenic processes, indicates a large break in sedimentation.
4. The specific location of FSST in the base provided the opportunity to preserve the forced regressive sediments. The sea-level not increased afterward, depositional milieu shifted basin-ward and sedimentation stopped/closed in the onland part of Kutch.

Acknowledgments

The author (Pramod Kumar) acknowledges the financial support provided by University of Delhi under Research and Development Grants during 2014 and 2015. We acknowledge Prof. M. G. Thakkar and Gaurav Chauhan (KSKV Kutch University) for their support during the field.

References

Ainsworth, R. B. (1994). Marginal marine sedimentology and high resolution sequence analysis; Bearpaw–Horseshoe Canyon transition, Drumheller, Alberta. Bulletin of Canadian Petroleum Geology. 42, 26-54.

Baum, G. and Vail, P. (1988). Sequence stratigraphic concepts applied to Paleogene outcrops, Gulf and Atlantic Basins. In: Sea level changes: an integrated approach. C. Wilgus, B.S. Hastings, C.G. Kendall, H.W. Posamentier, C.A. Ross, and J.C. Van Wagoner (eds.). SEPM Special Publication. 42, 309-327.

Bera, M.K., Sarkar, A., Chakraborty, P.P., Loyal, R.S. and Sanyal, P. (2008). Marine to continental transition in Himalayan foreland. GSA Bulletin; 120 (9-10): 1214–1232.

Biswas, S.K. (1992). Tertiary Stratigraphy of Kutch. Journal of the Palaeontological Society of India. 37, 1-29.

Blodgett, R.H. and Stanley, K.O. (1980). Stratification, bedforms and discharge relations of the Platte River system, Nebraska. J. Sediment. Petrol. 50, 139-148.

Bridge, J.S. (2006). Fluvial facies models: recent developments. Special Publication Society of Sedimentary Geology. 84, 84-170.

Burkham, D. E. (1972). Channel changes of the Gila River in Safford Valley, Arizona: U.S. Geological Survey, Professional Paper. 24, 655p.

Catuneanu, O. (2006). Principles of Sequence Stratigraphy. 1st Edition, Elsevier, Oxford, 1-374 p.

Church, M., and Rood, K. (1983). Catalogue of alluvial river channel regime data, University of British Columbia, Department of Geography Vancouver, BC. 99p

Coe, A.L., Boescence, D.W., Church, K.D., Flint, S.S., Howell, J.A. And Wilson, R.C. (2005). The sedimentary record of the sea-level change: The Open University, Cambridge: Cambridge University Press, 285 p.

Crowley, R.D. (1983). Large scale Bed configurations (Macroform), Platt River Basin Colorado and Nebraska- Primary structure and formative processes: Geological society of America Bulletin. 94, 117-133.

Fluger, P. and Seilacher, A. (1991). Flash flood conglomerates. In: G. Einsele, W. Ricken and A. Seilacher, (Eds.), Cycles and Events in Stratigraphy, Springer-Verlag, Berlin, New York. pp. 383-391.

Gustavson, T.C. (1978). Bedforms and stratification types of modern gravel meander lobes, Nueces River, Texas. Sedimentology. 25, 401-426.

Hein, F.J. and Walker, R.G. (1977). Bar evolution and development of stratification in the gravelly, braided Kicking Horse River, British Columbia. Can. J. Earth Sci. 14, 562-570.

Helland H. W., Lomo, L., Steel, R., and Ashton, M. (1992). Advance and retreat of the Brent delta: recent contributions of the depositional model. In. Geology of the Brent Group A. C.

Hunt, D. (1992). Application of sequence stratigraphic concepts to the Urgonian Carbonate Platform, SE France. Ph.D. Thesis, University of Durham, p. 410

Hunt, D. and Tucker, M. E. (1992). Stranded parasequences and the forced regressive wedge systems tract: deposition during base level fall. Sedimentary Geology. 81, 1-9.

Hunt, D., and Tucker, M. E. (1995). Stranded parasequences and the forced regressive wedge systems tract: deposition during base level fall – reply. Sedimentary Geology. 95, 147-160.

Lander, R. H., Bloch, S., Mehta, S., and Atkinson, C. D. (1991). Burial diagenesis of paleosols in the giant Yacheng gas field, People's Republic of China: bearing on illite reactivation pathways. Journal of Sedimentary Petrology. 61, 256–268.

Levey, R.A. (1978). Bedform distribution and internal stratification of coarse-grained point bars, Upper Congaree River, South Carolina. In: Fluvial Sedimentology (Ed. A.D. Miall) (Eds.), Canadian Society of Petroleum Geologists. Memoir 5, 105-127.

Kraus, M. J. (1999). Paleosol in clastic sedimentary rocks: their geologic implication. Earth Science Reviews. 47, 47-70.

Miall, A.D. (1977). A review of the braided river depositional environment. Earth Sci. Rev. 13, 1-62.

Miall, A.D. (1978). Facies types and vertical profile models in braided river deposits: a summary. In: A.D. Miall, (Eds.), Fluvial Sedimentology. Can. Soc. Pet. Geol., Mem. 5, 597-604.

Miall, A.D. (1985). Architectural-element analysis: a new method of facies analysis applied to fluvial deposits. Earth Sci. Rev. 22, 261-308.

Miall, A.D. (1988). Reservoir heterogeneities in fluvial sandstones: lessons from outcrop studies. Am. Assoc. Petr. Geol. Bull. 72, 682-697.

Miall, A.D. (1992). Alluvial deposits. In: R.G. Walker, N.P. James, (Eds.), Facies Models-Response to Sea Level Change. Geological Association of Canada. pp. 119-142

Mitchum, R. M. Jr; Vail, P. R. and Sangree, J. B. (1977). Seismic stratigraphy and global

changes of sea level, part 6: stratigraphic interpretation of seismic reflection patterns in depositional sequences. In: C. E. Payton, (Ed). Seismic stratigraphy-applications to hydrocarbon exploration. American Association of Petroleum Geologists Memoir. 26, 117-133

Mitchum, R.M., Jr. (1977). Seismic stratigraphy and global change of sea level, glossary of term used in seismic stratigraphy. In seismic stratigraphy- application to hydrocarbon exploration. American Association of petroleum Geologist, Memoir 26, 205-212.

Nanson, G.C, Rust, B.R and Taylor, G. (1986). Coexistent mud braids in an arid zone river: Cooper Creek, Central Australia. Geology 14, 175-178.

Nummedal, D. (1992). The falling sea-level systems tract in ramp settings. In SEPM Theme Meeting, Colorado. p. 50.

Plint, A. G. (1988). Sharp-based shoreface sequences and "offshore bars" in the Cardium Formation of Alberta; their relationship to relative changes in sea level. In: Wilgus, C. K.; Hastings, B. S.; Kendall, C. G. St C.; Posamentier, H. W.; Ross, C. A.; Van Wagoner, J. C. (Eds.) Sea level changes-an integrated approach. SEPM Special Publication. 42, 357-370.

Plint, A. G. (1991). High frequency relative sea level oscillations in Upper Cretaceous shelf clastics of the Alberta foreland basin: possible evidence of a glacio-eustatic control? In: D. I. M. Macdonald, (Eds.) Sedimentation, tectonics and eustacy. Association of Sedimentologists Special Publication.12, 409-428.

Plint, A. G. and Norris, B. (1991). Anatomy of a ramp margin sequence: facies successions, paleogeography and sediment dispersal patterns in the Muskiki and Marshybank Formations, Alberta foreland basin. Bulletin of Canadian Petroleum Geology. 39, 18-42.

Plint, A. G., and Nummedal, D. (2000). The falling stage systems tract: recognition and importance in sequence stratigraphic analysis. In Sedimentary Response to Forced Regression,

Posamentier, H. W. (2001). Lowstand alluvial bypass systems: incised vs. unincised. American Association of Petroleum Geologists Bulletin. 85, no. 10, 1771–1793.

Posamentier, H. W. and Vail, P. R. (1988). Eustatic controls on clastic deposition II–sequence and systems tract models. In: Sea Level Changes–An Integrated Approach, C. K. Wilgus, B. S. Hastings, C. G. St.C. Kendall, H. W. Posamentier, C. A. Ross and J. C. Van Wagoner, (Eds.), SEPM Special Publication. 42, 125–154.

Posamentier, H.W. and Walker R.G. (2006) eds., Facies Models Revisited: SEPM, Special Publication 84, p. 19–83.

Reading, H.G. (1986).Sedimentary environments and facies, 2nd edn. Blackwell, Oxford

Reading, H. G. (1996). Sedimentary Environments: Processes, Facies and Stratigraphy. Third Edition, Blackwell Science, pp. 1-688.

Rust, B.R. (1972). Structure and process in braided river. Sedimentology. 18, 221-245.

Schumm, S.A., and Lichty, R. W. (1963). Channel widening and floodplain construction along Cimarron River, southwestern Kansas: U.S. Geol. Survey Prof. Paper 352-E

Smith, N.D. (1970). The braided stream depositional environment: comparison of the Platte River with some Silurian clastic rocks, North-Central Appalachians. Bull. Geol. Soc. Am. 81, 2993- 3014.

Smith, N.D. (1972). Some sedimentological aspects of planar cross-stratification in a sandy braided river. J., sedini. Petrol. 42, 624-634.

Tandon, S. K., and Gibling, M. R. (1997). Calcretes at sequence boundaries in upper Carboniferous cyclothems of the Sydney Basin, Atlantic Canada. Sedimentary Geology. 112, 43–67.

Vail, P. R. (1987). Seismic stratigraphy interpretation procedure. In: Bally, A. W. (Ed). Atlas of seismic stratigraphy. American Association of Petroleum Geologists Studies in Geology. 27, 1-10.

Van Wagoner, J. C. (1995). Sequence stratigraphy and marine to non-marine facies architecture of foreland basin strata, Book Cliffs, Utah, U.S.A. In: Van Wagoner, J. C.; Bertram, G. T. ed. Sequence stratigraphy of foreland basin deposits. American Association of Petroleum Geologists, Memoir 64,137-223.

Van Wagoner, J. C., Mitchum, R. M., Posamentier, H. W. and Vail, P. R. (1987). An overview of sequence stratigraphy and key definitions. In: A. W. Bally, Editor, Atlas of Seismic Stratigraphy, volume 1, Studies in Geology vol. 27, American Association of Petroleum Geologists pp. 11–14.

Walker R.G. (1979). Facies models. Geological Association of Canada. Geosci Can Reprint Series, 1.

Walker R.G. (1984) Facies model, 2 nd edn. Geological Association of Canada. Geosci Can Reprint Series, 1.

Webb, G. E. (1994). Paleokarst, paleosol, and rocky-shore deposits at the Mississippian-Pennsylvanian unconformity, northwestern Arkansas. Geological Society of America Bulletin. 106, 634-648.

Wright, V. P. (1994). Paleosols in shallow marine carbonate sequences. Earth-Science Reviews. 35, 367–395.

Wright, V. P., and Marriott, S. B. (1993). The sequence stratigraphy of fluvial depositional systems: the role of floodplain sediment storage. Sedimentary Geology. 86, 203–210.

First online volume
Jour. Indian Association of Sedimentologists, Vol. 35, No. 1 (2018), pp.36-46
ISSN 0970-3268

Petrochemical characterization of Argada seam of South Karanpura Coalfield, Jharkhand, India

Alok K. Singh* & Mrityunjay K. Jha
Rajiv Gandhi Institute of Petroleum Technology, Raebareli, Uttar Pradesh, 229010, India
*Email: asingh@rgipt.ac.in

Abstract: South Karanpura Coalfield is a part of the master Gondwana basins of India. It is semi-elliptical in shape and located in the western part of the Damodar Valley, Ramgarh district, Jharkhand. The area comprises different formations of Lower Gondwana. Pillar coal samples have been collected from the working mine face of Argada coal seam. On the basis of megascopic study, coal samples having similar characteristics were clubbed together to form a single composite sample. The petrographic analysis shows that these coals are vitrinite rich followed by inertinite and liptinite maceral group. Mineral matters are represented by carbonates, followed by argillaceous minerals and pyrite. At microlithotype level, these coals are vitrinertite rich followed by vitrite, duroclarite and inertite. Carbominerites are represented by carbankerite followed by carbargillite, while the concentration of carbopolyminerite and carbopyrite are insignificant. The vitrinite reflectance characterizes these coals as sub-bituminous 'B' to high volatile bituminous 'C' in rank. The maceral and microlithotypes concentration suggests that the coals of Argada seam have evolved under alternate oxic to anoxic moor conditions.

Keywords: Petrography, Maceral, Microlithotype, Rank , South Karanpura, Argada Seam

Introduction

The lower Gondwana system has a unique importance in the Indian energy scenario due to the presence of significant coal reserves in different coal bearing sedimentary basins. Main coal bearing basins of India are Damodar Valley, Mahanadi Valley, Son Valley, Satpura, Pranhita - Godavari Valley, Wardha Valley etc. South Karanpura is one of the major coalfields of Damodar valley and it is located in Ramgarh district of Jharkhand (Figure 1). This coalfield covers an area of 195 square kilometers (Raja Rao, 1987). There are 13 coal seams exposed in the area. In the present study, Argada coal seam has been taken into consideration for the detail petrochemical characterization, which is the thickest coal seam of this coalfield. Studies of South Karanpura Coalfield and adjoining areas are mainly attempted by Sedimentologists, paleontologists and paleobotanists but studies on coal deposits of the area are least attended by the researchers. Although few petrographic and geochemical data on South Karanpura coals were published by Ganju (1955), Marshall (1959) and Pareek, (1969) but these data were generated by the workers based on sporadic samples. The previous studies lack a systematic sampling collection and a detailed regional approach. In the present study, an endeavor has been made to find out the detailed organic petrographic and geochemical variation along the vertical section of Argada seam and based on the petrographic constituents depositional condition of the coals have been discussed. This study reveals vital information about

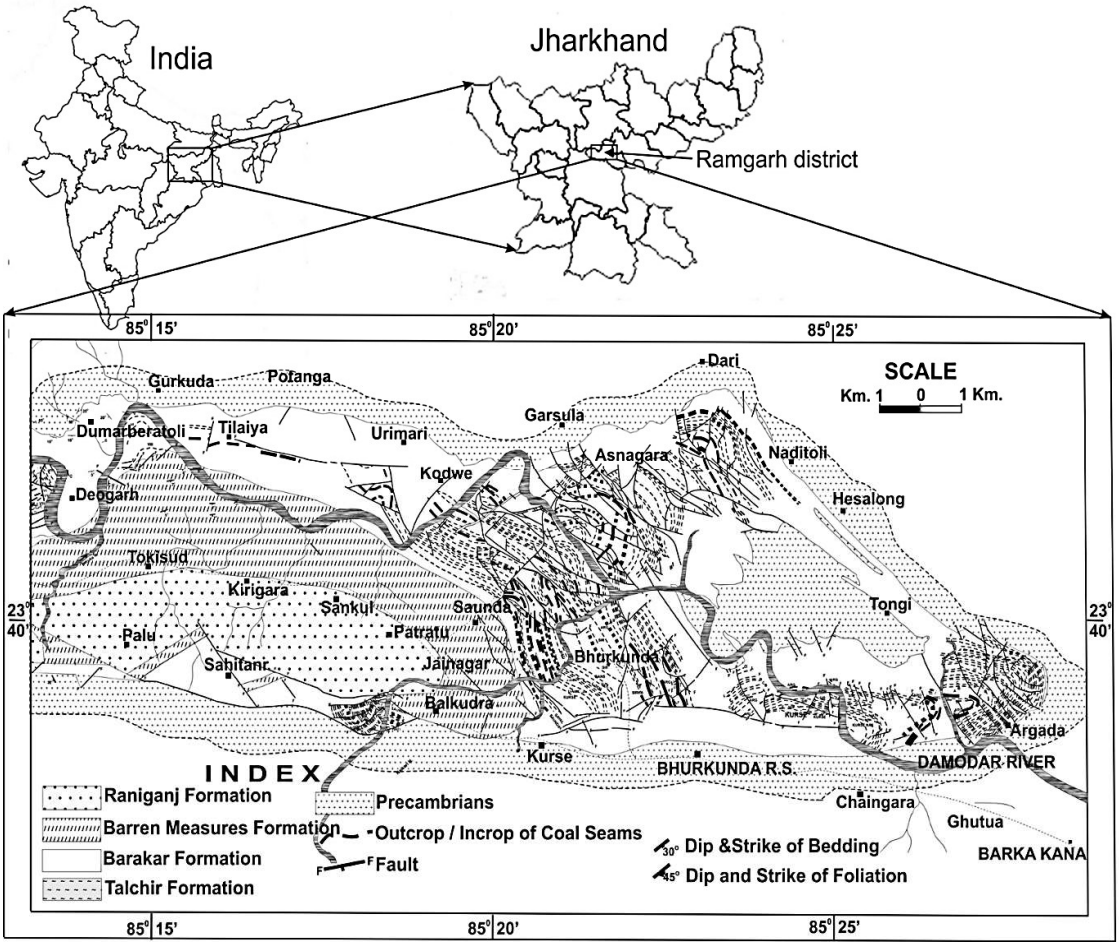

Figure 1. Geological map of Argada area, South Karanpura Coalfield, Jharkhand (Modified after Raja Rao, 1987).

the coal of the area and it can also be helpful for suggesting the proper utilization of these coals.

Geological setting

South Karanpura Coalfield is a part of the east-west aligned Damodar-Koel group of basins and contains different formations of Lower Gondwana (Figure1). The metamorphics forming the basement rock, which are exposed all along the periphery of the area. It includes rocks such as granite, gneisses, mica schist, quartzite and very few occurrences of limestone. Talchir rocks composing of greenish shales and tillites conformably lie on the basement. The Talchir tillites are made up of angular to sub-angular pebbles of quartz, quartzite or granite. Karharbari formation having main rock type as pebbly to coarse-grained sandstone forms an unconformable contact with Talchir formation. Barakar is the main coal-bearing horizon of the area. According to the stratigraphic order it is above Karharbari, but at most places it directly overlies on metamorphics. It covers the most part of the coalfield. The barren measure is exposed at the central part of the coalfield and comprises of medium grained sandstones, siltstones, ironstone, micaceous and carbonaceous shale. It forms a gradational contact with Barakar formation. Raniganj formation resides in the south-central part of the coalfield and forms a conformable contact with Barren measure. There are several faults present in the area. The Barakar formation is the main coal-bearing horizon and contains several coal seams. There are few coal seams also present in the underlying Karharbari formation. Raniganj formation does not contain significant coal seams. Argada seam is the most important and thickest seam of this coalfield, it is a

part of the Barakar formation. At different parts of the area, thickness of Argada seam varies from 12.1 m to 30.7 m. The lithological succession of the area is described in Table 1 (after Raja Rao, 1987).

Age	Series	Formation	Lithology	Approximate thickness in (m)
Early Cretaceous		Intrusive	Lamprophyre and dolerite dykes and sills.	
Late Permian	Damuda	Raniganj	Fine-grained sandstones; grey, medium to coarse grained, calcareous sandstones; mudstones; carbonaceous shale; a few thin coal seams	610
Middle Permian		Barren Measures	Medium grained sandstones; siltstones; micaceous and carbonaceous shales; ironstone shales.	304-457
Early Permian		Barakar	Coarse-grained sandstone, shales; various economic coal seams	1053
Early Permian		Karharbari	Pebbly to coarse-grained sandstones, shales and coal seams	74
Early Permian to Late Carboniferous	Talchir	Talchir	Olive green shales/ green mudstones; fine to medium-grained sandstones; conglomerate; rhythmites and diamictites.	3-16
Precambrian		Basement	Granite, gneisses, mica-schist, quartzite and limestone	

Table 1. Generalized stratigraphy sequence of South Karanpura Coalfield (after Raja Rao, 1987).

Methodology

During the present investigation coal samples (more than 60 samples) have been collected from the working faces of Argada main coal seam following the pillar sampling method. The megascopic characterization of the coal samples has been done according to Diessel's classification of banded coal (Diessel, 1965). Coal samples having the similar megascopic characteristics have been clubbed together and form the composite band. The coal samples were crushed to < 18-mesh size for petrography and < 72-mesh size for chemical analysis. The polished particulate coal mounts were prepared by using cold setting compound, without pressure. The study was carried out on an advanced petrological microscope with fluorescence attachment and MSP 200 photometry system. The identification of maceral has been carried out as per the recommendation of the International Committee for Coal Petrology (1963, 1971, 1975, 1998, 2001), Stach et al. (1982) and Taylor et al. (1998). To identify different macerals such as dark vitrinite and unstructured liptinite more precisely, the macerals analysis was carried out in both incident white light as well as under fluorescence light. Qualitative and quantitative analysis of

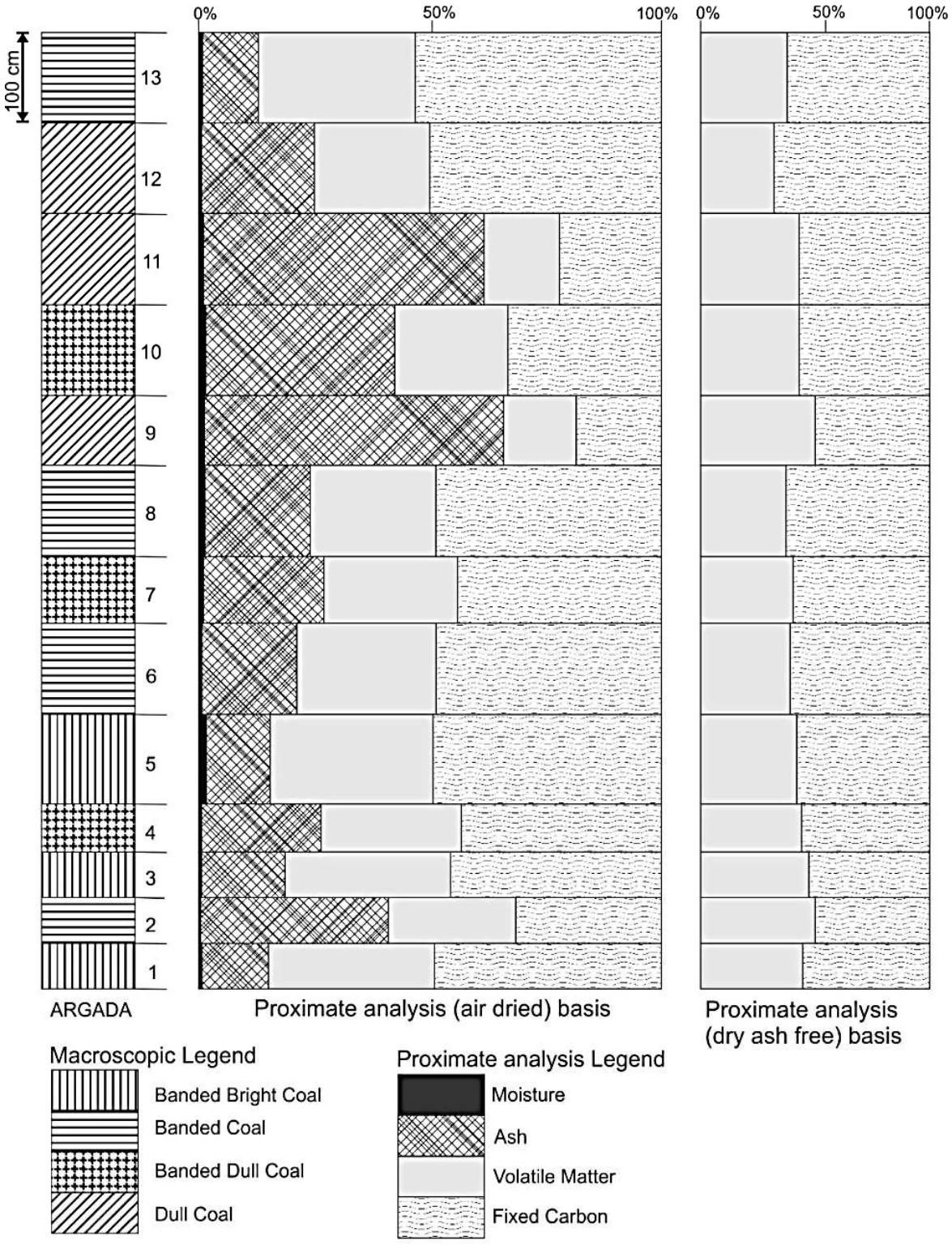

Figure: 2. Macropetrographic section and proximate analysis (air-dried basis and dry ash free basis) seam profiles of Argada Seam, South Karanpura Coalfield, Jharkhand.

maceral and microlithotype counting was done simultaneously. The random virtinite reflectance measurement was carried out as per the ISO standard (ISO 7404-5, 2009) on the scratch free collotelinite patches. All the coal samples were subjected to proximate analysis using Indian Standard (1984).

Chemical characteristics of argada coal seam

Coals of Argada seam exhibit low moisture (0.19 to 1.51 %) and moderately high ash (12.77 to 64.99 %) contents. In these coals, volatile matter varies between 15.99 and 36.63 % (32.62 to 48.57 % daf basis) while the fixed carbon ranges from 17.74 to 53.19 wt% (51.43 to 67.38% daf basis) (Table 2) and (Figure 2).

Proximate Analysis	**Range**		**Mean**
	Minimum	**Maximum**	
Moisture	0.19	1.51	0.76
Ash	12.77	64.99	29.62
Volatile Matter	15.99	36.63	28.16
Fixed Carbon	17.74	53.19	41.47
Volatile Matter (daf basis)	32.62	48.57	41.01
Fixed Carbon (daf basis)	51.43	67.38	58.99

Table 2. Proximate analysis result (in wt%) of coals of Argada seam, South Karanpura Coalfield, Jharkhand.

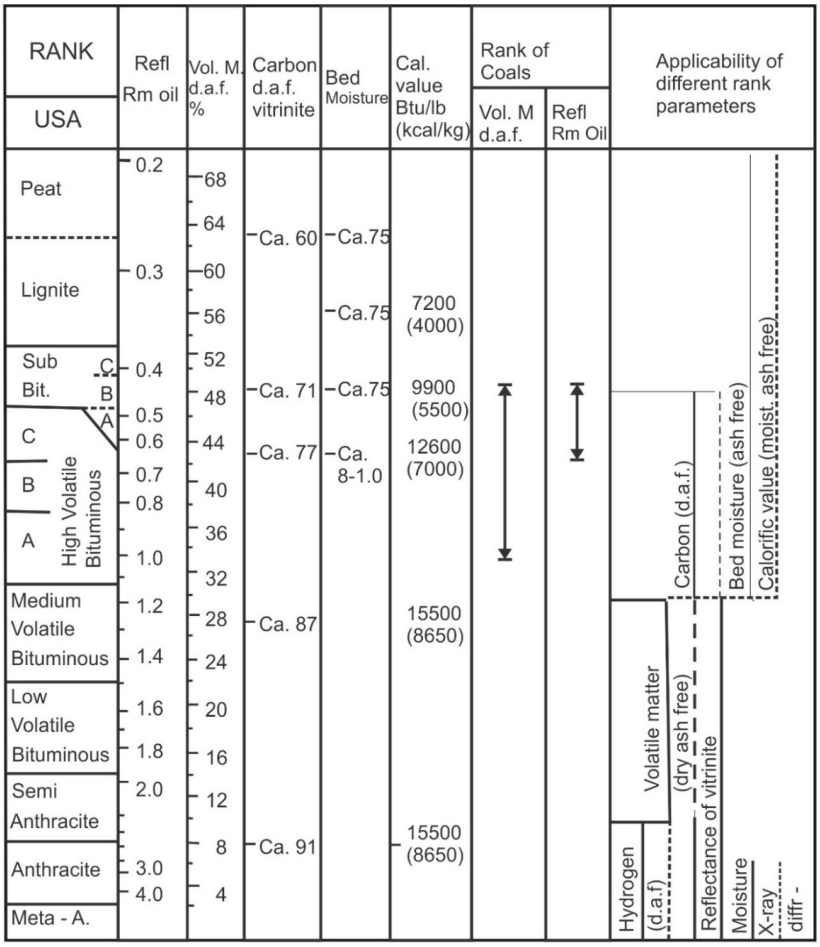

Figure 3. Rank of coals of the Argada seam, South Karanpura coalfield, Jharkhand on the basis of V.M. (d.a.f.) and vitrinite reflectance in the scheme representing the different stages of coalification according to North American (ASTM) classification and their distinction on the baiss of different physical and chemical parameters. The last column shows the applicability of various rank parameters to different coalfication stage (modified after Stach et al., 1982).

Petrographic characteristics of coal

Macropetrographic characteristics

The coals of Argada seam are banded in nature. The megascopic characteristics of this coal seam have been described using the classification of Diessel (1965) for banded coals. Banded coal is the dominant band followed by dull coal, banded dull coal and banded bright coal in Argada coal seam (Figure 4). Banded coals are present all over the seam and contribute to the major portion of the thickness of the seam. Dull coals are generally limited to the top of the seam. These bands are hard and compact in nature and dull appearance with a higher specific gravity than other lithotypes. Banded bright coal and Banded dull coal occurs approximately in equal proportion. In the Argada seam, generally banded bright coals are present at the bottom of the seam sections whereas banded dull coal is found in intervals from bottom to top.

Micropetrographic characteristics

Maceral analysis

All the three group of macerals vitrinite, liptinite and inertinite are present in these coals. Quantitative analysis of the microscopic constituents is given in Table 3. The Figure 4 represents the variation of macerals along the macropetrographic seam profile of Argada seam.

Vitrinite group

Coals of Argada seam are vitrinite rich. All the sub-macerals of the vitrinite group (telinite, collotelinite, vitrodetrinite, collodetrinite, gelinite and corpogelinite) occur in these coals. Telinite is present in good amount. The cell cavities/lumens of telinite are generally found to be filled with gelinite but sometimes with resin and mineral matter (Figure 5A). Collotelinite is the most dominant maceral of this group (Table 3). Its colour varies from light grey to moderate grey. It occurs as thick and thin bands and commonly shows a fragmentary nature and cracks (Figure 5B). The gelinite in these coals are found acting as infilling material within the cell lumens or cracks and cavities. Oval to crescentic shaped corpogelinites has also been detected. These generally exhibit the same colour as collotelinite but comparatively higher relief and reflectance. Vitrodetrinites are found in high concentration commonly associated with other macerals showing attrital nature. Collodetrinite is found sometimes forming groundmass for other macerals (inertodetrinite, sporinite etc.) and dispersed nature minerals such as argillaceous minerals and carbonates (Figure 5C). In some samples pseudovitrinite is also found, having very light grey colour and higher reflectance than collotelinite in the same coal. Few occurrences of dark vitrinite are also detected showing darker colour and low reflectance. They exhibit orange to brown fluorescence due to impregnation by hydrogen rich bituminous substances.

Liptinite group

Sporinite is the most dominant maceral of the liptinite group. They occur as elongated thread-like bodies. Tenui (thin walled) (Figure 5D), sporinite are dominant than crassi sporinite (thick walled) (Figure 5E and 5F). Both mega and micro spores are observed but microspores are more common. Under white light, they look darker while under fluorescence light they show yellow to orange colour of moderate intensity. Generally, thick wall of the spore is generated as a protective cover against dehydration, hence thin wall of sporinite represent wet environment (Diessel, 1992). Cutinite also occurs in these coals as thread-like bodies with serrated margins. They exhibit colour of dark grey in incident white light but show a yellowish orange to light brown colour under fluorescence light (Figure 5G). Round to oval shaped resinite of variable size are found as isolated or as cell fillings (Figure 5H). They are dark grey to black under

white light but show greenish yellow colour under fluorescence light. Detrital remains of structured liptinites (sporinite, cutinite and resinite) form a significant amount of liptodetrinite in the sample. Unstructured liptinites are represented by bituminite, fluorinite and exsudatinite. Exsudatinite is found occupying few voids and cracks. They exhibit black colour under white incident light and greenish yellow colour under fluorescence light. Teichmüller, (1986) marks it, as an indicator of first coalification jump and beginning of bituminization. Fluorinite is rarely present in coals of the Argada seam.

Inertinite group

Coals of Argada seam contains appreciable amounts of inertinites. Inetrodetrinite followed by semifusinite are the most dominant macerals of this group present in the samples. Fusinite is characterized by very high reflectance as well as very well-preserved cellular structure. Most of the times cell cavities are empty, sometimes they are filled with mineral matter (Figure 6A). Both pyro-and degrado-fusinite have been recorded. Bogen structure formed due to collapsed cell cavities and sieve structures are seen at various instances (Figure 6B). Semifusinites are having colour variation from light grey to white and recognized by their poorly preserved cell structure (Figure 6C). Macrinite occurs mostly as rounded to oval bodies showing white colour with reflectance as like fusinite (Figure 6D). In these coals, inertodetrinite is a common maceral constituting less than 10 micrometer fragments of other inertinites such as fusinite, semifusinite and macrinite (Figure 5C). Micrinite having a characteristic white dot-like appearance with size less than 2 microns are also observed in few samples (Figure 5A). The quantitative occurrence of inertinite macerals is shown in Table 3.

Mineral matter

Coals of Argada seam contain a significant portion of visible mineral matter. Argillaceous, carbonate and various sulphide minerals are easily recognizable mineral constituent of this seam. In general, the carbonate minerals are more dominant mineral matter and occurs as a dispersed form, as groundmass (Figure 6G) whereas various carbonate nodules are also observed (Figure 6H). Argillaceous minerals are also present in a high amount and characterized by their dark black colour. They occur as lenticular bodies, microbands and as infillings of fissure, crack, cleat and cell cavities of fusinite (Figure 6F). Pyrites are found as disseminated particles as well as discrete grains sometimes they also occur as fissure fillings.

Microlithotype analysis

At the microlithotype level, coals of Argada seam are vitrinertite rich, followed by vitrite, duroclarite and inertite. Vitrinertite-V is more common than vitrinertite-I and forms most of the vitrinertite microlithotype. In these coals, duroclarite is generally represented by a combination of vitrinite, inertinite and liptinite group of macerals, among which vitrinite macerals are more dominant than liptinite and inertinite combined. Variation of different microlithotype along the seam profile is represented in Figure 4.

Carbominerite represents a combination of macerals and mineral matter (Mukhopadhyay & Hatcher, 1993). Coals of the study area are marked by carbankerite followed by carbargillite while the concentration of carbopolyminerite and carbopyrite are insignificant. Frequency distribution of microlithotype composition (in vol. %) is given in Table 4.

MACERAL	Range	Mean

	Minimum	Maximum	
VITRINITE	20.20	68.60	39.51
Telinite	0.80	12.20	5.15
Collotelinite	2.60	41.60	18.65
Vitrodetrinite	6.00	21.40	11.17
Collodetrinite	1.00	6.00	3.55
Corpogelinite	0.20	1.80	0.69
Gelinite	0.00	0.80	0.24
Dark Vitrinite	0.00	1.20	0.43
Pseudovitrinite	0.00	0.20	0.04
LIPTINITE	5.80	12.20	8.88
Sporinite	1.80	7.80	4.49
Cutinite	0.40	1.80	0.82
Resinite	0.20	1.80	0.86
Alginite	0.00	0.00	0.00
Suberinite	0.00	0.20	0.03
Liptodetrinite	1.20	3.60	2.08
Fluorinite	0.00	0.20	0.02
Exsudatinite	0.00	1.80	0.55
Bituminite	0.00	0.40	0.14
INERTINITE	21.40	53.60	35.55
Micrinite	0.00	2.80	0.98
Macrinite	0.00	2.60	0.95
Semifusinite	3.00	20.20	8.77
Fusinite	2.60	19.80	7.23
Sclerotinite	0.00	0.00	0.00
Inertodetrinite	8.40	34.60	17.77
MINERAL MATTER	20.20	68.60	39.51
Argillaceous mineral matter	0.40	19.20	6.74
Carbonate mineral matter	0.20	40.80	8.71
Pyrite	0.20	1.40	0.73

Table 3. Maceral and mineral matter composition (in vol. %) in coals of Argada seam, South Karanpura Coalfield, Jharkhand.

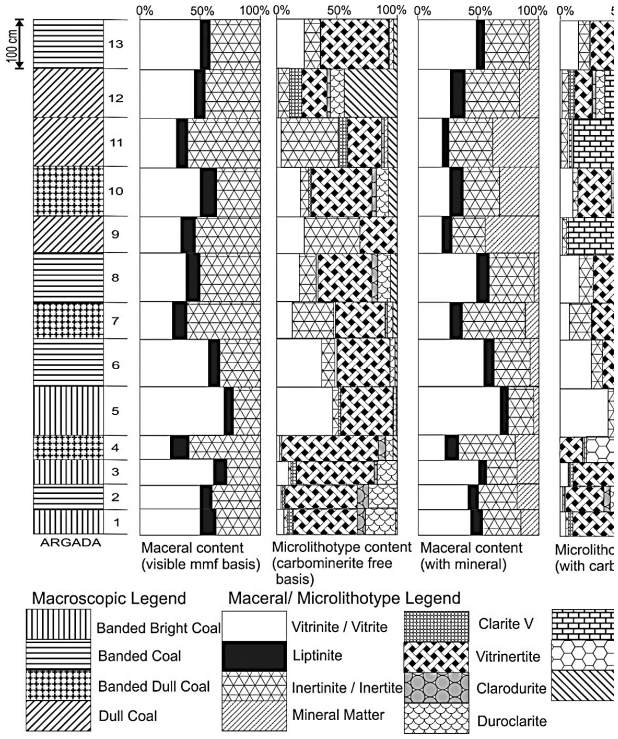

Figure 4. Macropetrographic section and microscopic (maceral and microlithotype) seam profiles of Argada seam, South Karanpura coalfield, Jharkhand

Microlithotype group	Range		Mean	Range (mmf basis*)		Mean (mmf basis)
	Minimum	Maximum		Minimum	Maximum	
Monomaceral	0.81	43.53	16.72	3.51	70.04	30.47
Vitrite	0.40	39.06	11.37	1.56	45.81	15.78
Liptite	0.00	0.22	0.03	0.00	0.31	0.02
Inertite	0.40	18.02	6.23	1.02	47.07	14.66
Bimaceral	1.92	53.22	32.07	26.68	83.33	55.96
Clarite V	0.00	7.32	2.00	0.00	10.31	2.96
Clarite E(L)	0.00	0.94	0.24	0.00	1.25	0.28
Vitrinertite V	1.44	37.20	19.91	10.00	55.19	33.82
Vitrinertite I	0.24	12.20	7.21	3.34	29.82	12.96
Durite I	0.00	29.05	4.59	0.00	40.94	5.39
Durite E(L)	0.00	1.65	0.44	0.00	1.94	0.54
Trimaceral	0.24	26.80	9.21	3.14	34.81	13.58
Vitrinertoliptite	0.00	2.00	0.60	0.00	3.34	1.07
Clarodurite	0.00	5.40	2.07	0.00	9.22	3.31
Duroclarite	0.00	19.60	6.54	0.00	25.26	9.20
Carbominerite	14.73	92.81	44.27			
Carbankerite	0.23	86.09	26.94			
Carbopyrite	0.00	1.60	0.50			
Carbopolymineritе	0.47	5.13	2.40			
Carbargilite	0.60	72.73	18.38			

Table 4. Microlithotype and carbominerite composition (in vol. %) in coals of Argada seam, South Karanpura Coalfield, Jharkhand

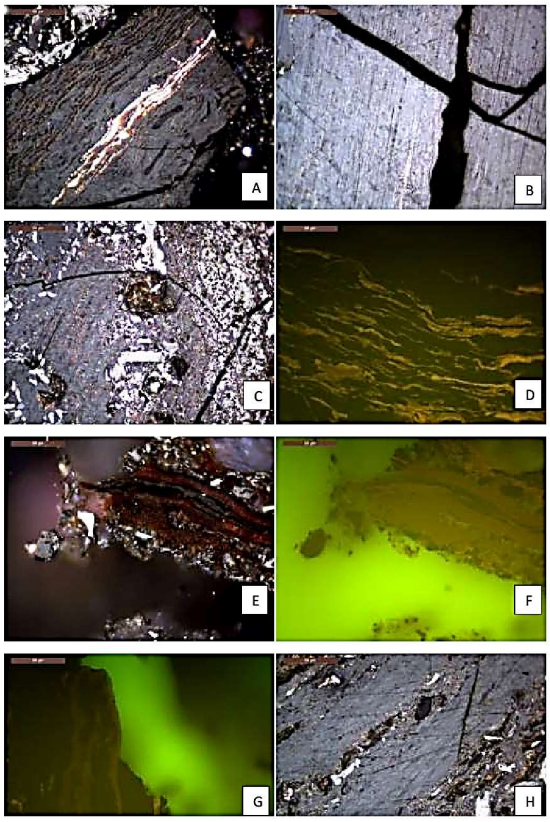

Figure 5. Representative photomicrographs of macerals of Argada seam (scale bar= 50 µm). A) Telinite, cell lumens filled with micrinite, B) Collotelinite with mineral matter filled in crackes, C) Collotelinite and collodetrinite with inertodetrinite, D) Tenui-type sporinite in fluoresecence light, E) Megasporinite in white incident light, F) Megasporinite in fluoresecence light, G) Cutinite with serrated margin in fluorescence light, H) Oval shaper resinite occurring with collotelinite

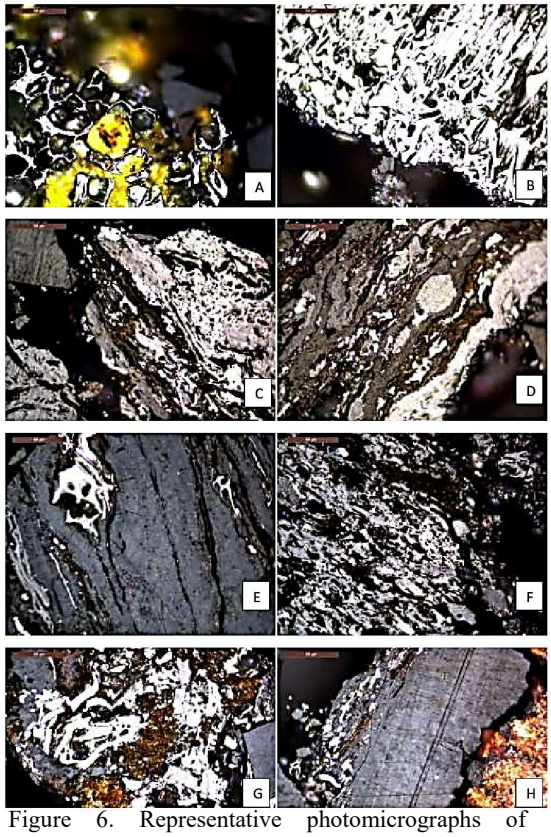

Figure 6. Representative photomicrographs of macerals of Argada seam (scale bar= 50 µm). A) Fusinite cell cavities filled with carbonate minerals, B) Pyro-fusinite, C) Semifusinite occurring with sporinite, D) Oval shaped macrinite with inertodetrinite and collotelinite, E) Secretinite, F) Semifusinite cell cavities filled with argillaceous minerals, G) Dispersed nature carbonate minerals, H) Part of a carbonate nodule at bottom left surrounded by collotelinite.

Evolution of coals of argada seam

An attempt has been made to discuss the evolution of coals of the Argada seam. Since these coals are minerals rich and minerals are directly related with the paleodepositional condition. Hence, the coal petrography-based depositional model proposed by Singh & Singh, (1996) for Permian coal is chosen to discuss the evolutionary condition of these coals. This model suggests that the most of the coals of Argada seam have evolved under alternate oxic to anoxic moor conditions (Figure 7). Few of the samples present at the top of the seam lies outside the zone of alternate oxic to anoxic moor condition and suggest an oxic (dry) moor with a rapid influx of water. The model is also justified by the alternate formation of more and less inertinite due to the fluctuation of the water table.

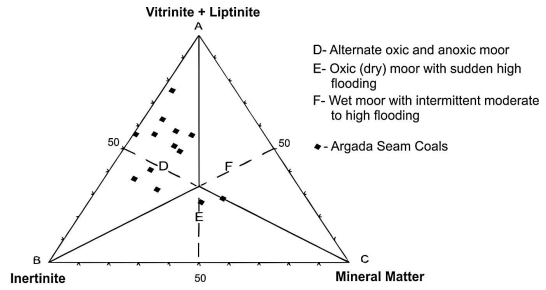

Figure 7. Depositional conditions of Argada coal seam based on maceral and mineral matter content (after Singh and Singh, 1996).

Evolution of coals of argada seam

An attempt has been made to discuss the evolution of coals of the Argada seam. Since these coals are minerals rich and minerals are directly related with the paleodepositional condition. Hence, the coal petrography-based depositional model proposed by Singh & Singh, (1996) for Permian coal is chosen to discuss the evolutionary condition of these coals. This model suggests that the most of the coals of Argada seam have evolved under alternate oxic to anoxic moor conditions (Figure 7). Few of the samples present at the top of the seam lies outside the zone of alternate oxic to anoxic moor condition and suggest an oxic (dry) moor with a rapid influx of water. The model is also justified by the alternate formation of more and less inertinite due to the fluctuation of the water table.

Conclusion

Coals of Argada seam of South Karanpura Coalfield are vitrinite-rich followed by inertinite and liptinite. The vitrinite reflectance indicates these coal as to sub-bituminous 'B' to high volatile bituminous 'C' in rank. Disseminated nature clay and carbonate minerals, carbonate nodules and few fragments of pyrite are the main visible mineral matter found in these coals. At microlithotype level, these coals are characterized by a high amount of vitrinertite followed by vitrite, duroclarite and inertite. Carbominerite is characterized by carbankerite followed by carbargillite while the concentration of carbopolyminerite and carbopyrite is insignificant. The microscopic constituents of these coals suggest its evolution in an alternate oxic and anoxic moor condition due to repeated seasonal variation.

Acknowledgement: The authors are thankful to the Director, Rajiv Gandhi Institute of Petroleum Technology (RGIPT), Jais, Amethi, Uttar Pradesh, India, for providing the necessary facilities and financial assistance to MKJ. The help rendered during sampling, by the officials of the Central Coalfields Limited is thankfully acknowledged.

References

Diessel, C.F.K. (1965). Correlation of macro- and micropetrography of some New South Wales Coals. Proceedings of the 8th Commonwealth Mining and Metallurgical Congress, Melbourne, Australia, Vol. v6, 669-677.

Diessel, C. F. K. (1992). Coal-Bearing Depositional Systems. Springer Verlag, Berlin. 721 pp.

Ganju, P.N. (1955). Petrology of Indian Coals: Memoirs of the Geological Survey of India, vol.83, 101 pp.

IS (Indian Standard 1350 Part - I), (1984). Methods of Test for Coal and Coke- Proximate Analysis. 5–18.

International Committee for Coal Petrology, (1963). International Handbook of Coal Petrography, 2nd ed. Centre National de Recherche Scientifique, Paris.

International Committee for Coal Petrology, (1971). International Handbook of Coal Petrography. 1st Supplement to 2nd edition. Centre National de Recherche Scientifique, Paris.

International Committee for Coal Petrology, (1975). International Handbook of Coal Petrography. 2nd Supplement to 2nd edition. Centre National de Recherche Scientifique, Paris.

International Committee for Coal and Organic Petrology, (1998). The new vitrinite classification (ICCP System 1994). Fuel 77, 349–358.

International Committee for Coal and Organic Petrology, (2001). The new inertinite classification (ICCP System 1994). Fuel 80, 459–471.

ISO 7404-5, 2009. Methods for the Petrographic Analysis of Coal- Part 5: Methods of Determining Microscopically the Reflectance of Vitrinite. International Organization for Standardization, Geneva, Switzerland, 1–14.

Marshall, C.E. (1959). Petrology and preparation of certain (Permian) coal seams of India: Economic Geology, vol. 54, 20-56.

Mukhopadhyay, P. K., & Hatcher, P. G. (1993). Composition of coal. In: Hydrocarbons from coal: AAPG Studies in Geology, 38, 79-118.

Murthy, S., Tripathi, A., Chakraborti, B., & Singh, U. P. (2014). Palynostratigraphy of Permian succession from Binja Block, South Karanpura Coalfield, Jharkhand, India. Journal of Earth System Science, 123(8), 1895-1906.

Pareek, H. S. (1969). The Application of Coal Petrography to Coking Property of Indian Coals. Economic Geology, 64, 809–821.

Raja Rao, C. S. (1987). Coalfields of India, Bulletins of the Geological Survey of India, A, 45, 336 pp.

Singh, M. P., & Singh, P. K. (1996). Petrographic characterization and evolution of the Permian coal deposits of the Rajmahal basin, Bihar, India. International Journal of Coal Geology, 29(1-3), 93–118.

Teichmüller, M. (1986). Organic petrology of source rocks, history and state of the art. Organic Geochemistry, 10, 1-3.

First online volume
Jour. Indian Association of Sedimentologists, Vol. 35, No. 1 (2018), pp.47-56
ISSN 0970-3268

Provenance, processes and productivity through spatial distribution of the surface sediments from Kongsfjord to Krossfjord system, Svalbard

Shabnam Choudhary*, G. N. Nayak[*] and N. Khare[**]
*Department *of Marine Sciences, Goa University, Goa – 403 206, India*
***Ministry of Earth Sciences, Govt. of India, New Delhi*
gnnayak@unigoa.ac.in ; gnnayak57@gmail.com

Abstract: Krossfjord-Kongsfjord is a glacial fjord system in West Spitsbergen (Svalbard archipelago) situated adjacent to the Arctic and Atlantic water mass, a suitable site to study the effect of climate change on the environment. To understand the sedimentary characteristics, depositional processes, source and their implications on productivity in the fjord, spatial variations of grain size, organic carbon, nitrogen, phosphorus, biogenic silica and calcium carbonate in the surface sediments were studied. Grain size showed the dominance of fine-grained sediment (silt and clay) suggesting relatively quieter hydrodynamic conditions prevailing in the fjord. The nutrient (C, N, P and BSi) concentrations in surface sediments of both the fjords show a clear spatial gradient with lower values in the glacier-dominated inner fjord and higher values towards the outer fjord as high turbidity towards the fjord head diminishes the expanse of the photic zone leading to low primary productivity close to the glacier fronts. Along Krossfjord, the C: N ratio varied from 1.01 to 26.37 and along the Kongsfjord the C: N ratio varied from 6.67 to 17.00 indicating the derivation of the organic matter from both terrestrial as well as marine sources with increasing marine influence towards the fjord mouth. Carbonate production in this region is low and the calcium carbonate occurring here may be of detrital origin. Sediment grain size seems to be a dominant controlling factor in the distribution of organic and inorganic matter in Krossfjord-Kongsfjord system.

Keywords: Surface sediment, nutrients, Krossfjord-Kongsfjord, hydrodynamics

Introduction

Fjords are considered as a link between the ocean and the land through cross-shelf exchanges, which result in circulation and mixing in the fjords (Nilsen et al., 2008). The fjords on the west coast of Spitsbergen balance Atlantic, Arctic, brine and freshwater inputs, which are sensitive indicators of environmental changes (Nilsen et al., 2008). One of the fjord system affected by a warm current is Kongsfjord-Krossfjord system-a suitable site for studying glacial history and palaeoclimate. Changes in climate influence the currents flowing in the fjord and which will be reflected in the distribution pattern of environmental parameters inducing changes in composition and abundance of organic matter throughout the fjord.

It has been documented that apart from serving as a tool for studying depositional environment, transport pathways, remineralization and past climate conditions, source characterization of the sedimentary organic matter is required to estimate the deposition of marine and terrigenous organic matter (Stein and MacDonald, 2004). Various geochemical proxies such as C/N ratio of sedimentary organic matter (Meyers, 1997, 2003; Stein and MacDonald, 2004; Schubert and Calvert, 2001), specific biomarkers (Fahl and Stein, 1999) and Rock-Eval parameters (Peters, 1986) are used to identify relative composition of land and marine-derived components of organic matter. However, a multiproxy approach for identification of source and composition of organic matter is rare due to which factors controlling spatial variations of different biogeochemical parameters are rarely identified. Despite previous investigations (Stein et al., 1994; Shetye et al., 2011; Kumar et al., 2016; Koziorowska et al., 2017), the source of sediments, processes involved during and after sediment deposition and their implications on productivity in the recent past still remain unclear primarily on account of proxy specific limitations.

In the present study, we have investigated the spatial variability of sediment grain size, organic elements and calcium

carbonate within Krossfjord-Kongsfjord system with water depths ranging from 41 m to 332 m situated at the west coast of Svalbard to understand the source, depositional processes and productivity in the recent past.

Study Area

Kongsfjord-Krossfjord is a glacial fjord system in the Arctic that opens onto a submarine glacial trough in the western Svalbard shelf, called Kongsfjordrenna (Fig.1). This system is located between 78º50'-79º30'N and 11º-13ºE. The orientation of the southern arm of the fjord system, Kongsfjord, is south-east to north-west, whereas the northern arm Krossfjord is north to south (Kumar et al., 2014). The length of the Kongsfjord is 20 km and its width varies from 4–10 km (MacLachlan

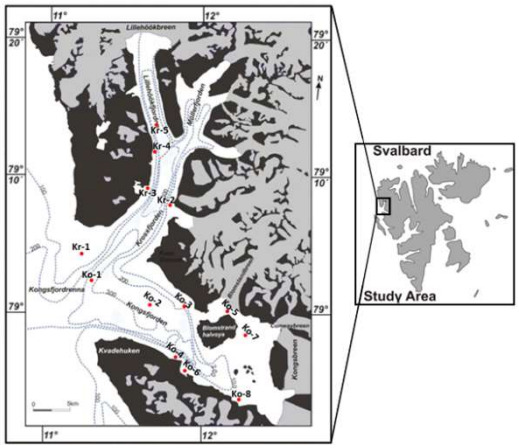

Fig.1 Map showing the study area (modified after Svendsen et al., 2002)

et al., 2010) with the deepest point of 394 m. The Krossfjord is narrower (3–6 km) and longer (~30 km) compare to Kongsfjord, with a maximum depth of 374 m (Svendsen et al., 2002). The total volumes of Kongsfjord and Krossfjord have been estimated to be equal to 29.4 and 25 km^3, respectively (Ito and Kudoh, 1997).

The climate of Svalbard is strongly influenced by the atmospheric circulation, Arctic sea ice extent and ocean currents. Western Spitsbergen is flanked by a northerly warm West Spitsbergen Current (WSC), with Atlantic water mass (AW). The presence of these currents towards the mouth of the fjord give rise to fronts and instabilities associated with them causes exchange of warm saline shelf transformed Atlantic water with the cold freshwater from the glacial discharge. The western Spitsbergen Current (WSC) causes ice-free conditions along the west coast throughout the year and partially ice-free waters north of Svalbard even during winter (Vinje, 1982). The prevailing winds are from NE to the SE sectors, except during summer (Forland et al., 1997).

The Kongsfjord-Krossfjord system lies close to a major tectonic boundary separating the Cenozoic fold and thrust belt of western Spitsbergen to the southwest and the Northwestern Basement province to the northeast (Svendsen et al., 2002). The northern side of the fault zone consists of pre-Devonian metasediments and igneous rocks, whereas towards south Late Palaeozoic sedimentary strata, such as carbonates, conglomerates and calcareous sand-stones are found (Streuff, 2013). Mostly, the coastal part of the fjord system is covered with unconsolidated deposits of Quaternary age which includes moraines, marine shore and fluvial deposits (Kumar et al., 2014). Glacial processes like active glacial, hydro-glacial, periglacial and coastal processes have modified the landforms of this area.

Both of these fjords are largely influenced by the presence of tidewater glaciers: Lilliehookbroon at the head of Krossfjord (Lilliehookfjord) and five other calving glaciers along its eastern coast. Glaciers like Kronebreen and Kongsvegen at the head of Kongsfjord and Conwaybreen and Blomstrandbreen on the northern coast influence the fjord. Mass balance studies from these fjords have shown that the major contribution of fresh water into the fjord comes from the glacial discharge (MacLachlan et al., 2007) since precipitation plays a limited role.

Materials and Methods

Sampling and collection

Thirteen surface sediment grab samples were collected at various water depths from Kongsfjord and Krossfjord during August 2016 (Table1). Surface sediment samples were collected using stainless steel Van Veen Grab sampler using the workboat "MS Teisten" to understand the source, depositional processes, productivity and trace the glaciomarine contrast along the fjords. Samples were labeled and brought back to the laboratory in a frozen condition for analysis. In the laboratory, samples were dried at 60ºC in the oven and used for further analysis.

Sample name	Water Depth (m)	Latitude (ºN)	Longitude (ºE)
Kr-1	285.00	79.0675	11.2193
Kr-2	130.00	79.1346	11.7843
Kr-3	180.00	79.1535	11.6501
Kr-4	189.00	79.1995	11.6928
Kr-5	265.00	79.2337	11.6894
Ko-1	332.00	79.0365	11.2955
Ko-2	180.00	79.0081	11.6083
Ko-3	283.00	79.0087	11.7887
Ko-4	235.00	78.9510	11.8278
Ko-5	41.70	79.0073	12.1797
Ko-6	302.00	78.9403	11.9622
Ko-7	90.00	78.9725	12.3309
Ko-8	70.10	78.9045	12.2300

Table 1. Sampling depth and Location

Laboratory analysis

The samples were analyzed for grain size using pipette method (Folk, 1968) which is based on Stoke's settling velocity principle. Total Carbon (TC) and Total Nitrogen (TN) was estimated using elemental analyzer (Elementar, Vario isotope cube). The analytical precision for TN and TOC are ±0.31% and ±0.30% (1σ standard deviation) obtained by repeatedly running Sulfanilamide as the standard. Total Inorganic carbon (TIC) was measured by using UIC carbon coulometer. Total organic carbon (TOC) was calculated by subtracting TIC from TC. Calcium Carbonate ($CaCO_3$) was computed as TIC *8.333. The sediment for total phosphorus (TP) analysis was digested using HF-HNO_3-$HClO_4$ mixture and brought to liquid phase as adopted by Yu et al. (2013) and further determined following the procedure given by Murphy and Riley (1962), where the intensity of phosphomolybdenum blue complex was measured at 880 nm using UV-1800(Shimadzu) visible spectrophotometer. The accuracy of phosphorus analysis was determined using a digested sample of JLK-1 and obtained a recovery of 98%. Biogenic silica (BSi) from the freeze-dried sample was extracted using 25 ml of 1% Na_2CO_3 in an 85ºC water bath for 5 hours and measured by the wet alkaline extraction method, modified by Mortlock and Froelich (1989) and Muller and Schneider (1993) where intensity of blue silico-molybdenum complex was measured at 810 nm using UV-1800 (Shimadzu) visible spectrophotometer. Duplicate measurements were conducted on each sample and relative error was noted to be less than 3%.

Results

Distribution of Sediment components

Sand, silt and clay vary in the Krossfjord in the range from 5.70 to 21.24%, 43.15 to 61.04% and 20.00 to 48.27% respectively, with the average value of 10.46%, 52.95% and 36.59% respectively. Among sediment components silt is predominant. Sand is highest at station Kr-2 due to its close proximity to the D'Arodesbreen glacier, silt shows decreasing trend from station Kr-5 to Kr-1 while clay exhibits an increasing trend from station Kr-5 to Kr-1. Along the Kongsfjord, sand, silt and clay vary from 5.66 to 33.78%, 29.69 to 53.35% and 32.27 to 50.67% respectively, with the average value of 18.21%, 42.22% and 39.57% respectively. Silt is dominant amongst the sediment components. Station

Ko-8, Ko-6, Ko-5 and Ko-4, except station Ko-7, show a high concentration of sand as compared to the other stations due to their glacial fed and proximal location to the coast while station Ko-3, Ko-2 and Ko-1 show comparatively lower concentration as they are located away from the glacier and the coast. However, station Ko-1 shows higher sand as compared to the station Ko-7, Ko-3 and Ko-2 possibly due to the presence of Ice-rafted debris (IRD) which disturbs the current sorted grain size fraction (Hass, 2002). Silt and clay exhibit an increasing trend from station Ko-8 to Ko-1. Further, the data on sediment components of surface sediments from Krossfjord and Kongsfjord is presented in figure 2.

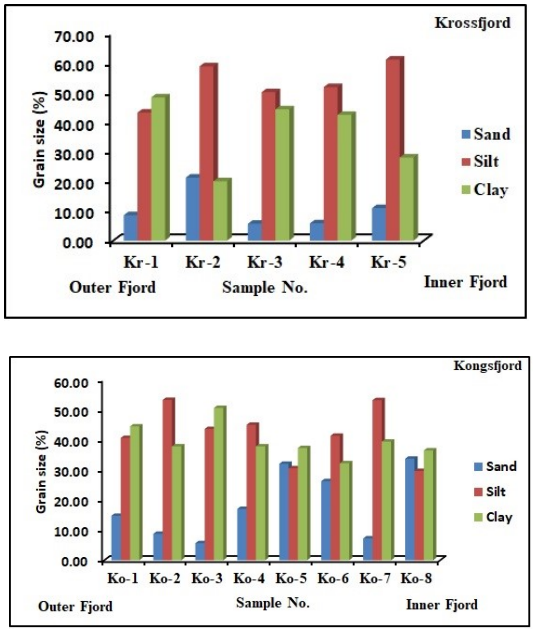

Fig.2. Variation in sediment components along Krossfjord (Kr) and Kongsfjord (Ko).

Distribution of organic elements (C, N, P and BSi)

TOC and TN concentration vary within a range from 0.04% to 1.70% and 0.04 % to 0.17% respectively (Table 2**)** along the Krossfjord**.** TOC (1.70%) and TN (0.17%) are highest at station Kr-1 while least concentration of TOC (0.04%) at station Kr-4 and TN (0.04%) at station Kr-4 and Kr-5 is noted (Fig.3a). TP varies from 0.019 to 0.023 % (Table 2). High concentration is at station Kr-1 while least concentration is at station Kr-2 and Kr-5. BSi varies from 2.74% to 4.19%. High concentration of BSi is at station Kr-1 and least concentration is at Kr-5 (Fig. 3a).

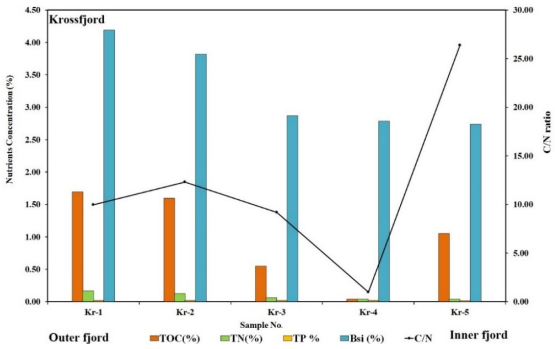

Fig.3a. Distribution of total organic carbon (TOC), total nitrogen(TN), total phosphorus(TP), biogenic silica (BSi) and C/N ratio in surface sediments of Krossfjord (Kr).

Along the Kongsfjord, TOC and TN vary from 0.20% to 1.74% and 0.03% to 0.17% (Table 2**).** TOC (1.74%) and TN (0.17%) are highest at station Ko-1 and least concentration of TOC (0.20%) and TN (0.03%) at station Ko-7. TP varies from 0.017% to 0.061%. Ko-5 shows high concentration while Ko-7 shows the lowest concentration. BSi varies from 1.42% to 4.03%. High concentration of BSi is noted at station Ko-1 and least concentration at station Ko-8 (Fig.3b**).**

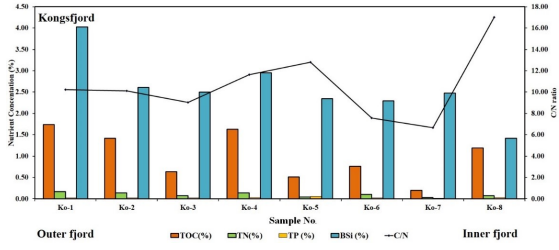

Fig.3b. Distribution of total organic carbon (TOC), total nitrogen (TN), total phosphorus (TP), biogenic silica (BSi) and C/N ratio in surface sediments of Kongsfjord (Ko).

Sample	Sand (%)	Silt (%)	Clay (%)	TOC (%)	TN (%)	C/N	TP (%)	BSi (%)	$CaCO_3$ (%)
Kr-1	8.58	43.15	48.27	1.70	0.17	9.98	0.023	4.19	10.95
Kr-2	21.24	58.76	20.00	1.60	0.13	12.31	0.019	3.82	10.91
Kr-3	5.70	50.03	44.27	0.55	0.06	9.19	0.022	2.87	4.32
Kr-4	5.84	51.76	42.40	0.04	0.04	1.01	0.021	2.79	4.91
Kr-5	10.96	61.04	28.00	1.05	0.04	26.37	0.019	2.74	13.79
Ko-1	14.78	40.69	44.53	1.74	0.17	10.23	0.019	4.03	9.00
Ko-2	8.78	53.35	37.87	1.41	0.14	10.10	0.022	2.61	12.54
Ko-3	5.66	43.67	50.67	0.63	0.07	9.03	0.022	2.50	4.81
Ko-4	17.06	45.07	37.87	1.63	0.14	11.62	0.029	2.95	11.60
Ko-5	32.06	30.61	37.33	0.51	0.04	12.81	0.061	2.34	15.56
Ko-6	26.32	41.41	32.27	0.76	0.10	7.57	0.024	2.29	9.94
Ko-7	7.26	53.27	39.47	0.20	0.03	6.67	0.017	2.48	13.24
Ko-8	33.78	29.69	36.53	1.19	0.07	17.00	0.026	1.42	12.00

Table 2 Sediment components, TOC, TN, TP, BSi and $CaCO_3$ content along Krossfjord and Kongsfjord.

Distribution of Calcium carbonate

In general, the carbonate content of the surface sediments is relatively low, most of the values are lower than 15% (Table 2). Calcium Carbonate ($CaCO_3$) varies within a range from 4.32% to 13.79% along the Krossfjord. $CaCO_3$ (13.79%) is highest at station Kr-5 while least concentration (4.32%) at station Kr-3. Along the Kongsfjord, $CaCO_3$ varies from 4.81% to 15.56%. Ko-5 station exhibits a high concentration of $CaCO_3$ while least concentration is exhibited by station Ko-3.

Discussion

Sources and transport mechanism of sediment components

In the Krossfjord-Kongsfjord system, in general, coarse-grained sediments depicts increasing trend from the mouth (outer fjord) towards the head (inner part of the fjord) indicating that the coarser grains are deposited close to the glacier front which corresponds to glacial deposition due to the retreat of glaciers in the study area. This suggests warm conditions in the region due to which coarse-grained particles have been transported to the fjord through physical (glacial) weathering of rocks present in the catchment area. While the finer fractions are transported by the surface waters to the central and outer part of the fjord (Fig.2). Overall, sediment grain size shows the dominance of fine-grained sediment (silt and clay) in both the fjords suggesting deposition from water column suspensions. The freshwater runoff from calving and ablation of the glacier, melting of sea ice and precipitation increases the turbidity in the inner fjord, and thus diminishes the vertical extent of the euphotic zone (Keck et al., 1999).

Further, an attempt has been made to infer the hydrodynamic conditions of the depositional environment using textural analysis. For this purpose, a ternary diagram (Fig.4) proposed by Pejrup (1988) has been used. The hydrodynamics are distinguished in the diagram into four sections labeled as I to IV. Section I indicates the very calm hydrodynamic condition and section II to IV indicate increasingly violent hydrodynamic conditions. Further, sections A to D

provides an environment with respect to the size of the sediments. When the data was plotted, surface sediments collected from Krossfjord mostly falls between section III(C) and III(D) with a single point being part of II(D) indicating less calm to less violent conditions prevailed facilitating deposition of finer sediments. In the Kongsfjord, all the data points lie between section II(C), II(D), III(C) and III(D) indicating not much variation in sediment size and deposition environment. Therefore, quieter hydrodynamic conditions prevailing in the fjord system from the glacier front to the mouth of the fjord which is responsible for the deposition of finer grained sediments towards the outer fjord. In addition,

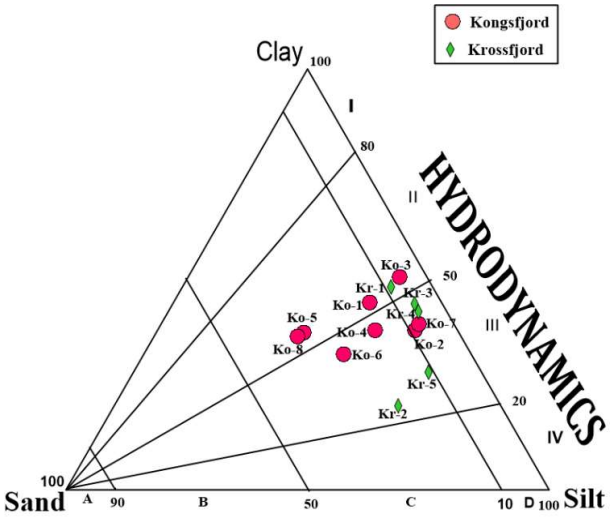

Fig.4. Triangular diagram for classification of hydrodynamic conditions of a) Kongsfjord and b) Krossfjord (after Pejrup, 1988).

factors like glacier outflow and temperature-salinity stratification (aggregation of fine particles) lead to the offshore transportation of fine-grained material (Zaborska et al., 2006).

Biogeochemical proxies in fjord sediments

Organic carbon content in the surface sediment shows an increasing trend towards the mouth of the Krossfjord and Kongsfjord (Table 2). The total nitrogen concentration in surface sediments follows a similar increasing trend. TOC and TN in surface sediments of both the fjords shows a clear spatial gradient with lower values in the glacier-dominated inner fjord and higher values towards the outer fjord due to the high turbidity towards the fjord head, which gives rise to a shallow photic zone close to the glacier fronts (Shetye et al., 2011). Consequently, algae become light limited and Eilertsen et al. (1989) suggested that during the summer, algal biomass decreased due to increased grazing in the inner part of the fjord. High input of sediment-loaded glacial meltwater deteriorates growth of phytoplanktons during summer (Svendsen et al., 2002), therefore, low organic matter in the inner part of the fjord resulted in lower primary productivity. A steep gradient in the deposition of sediment and grain size sorting from inner fjord to the outer fjord may also have played a role in their distribution. It is well established that the finer particles of the sediments provide, large surface area, thus having high adsorption capacity (Siraswar and Nayak, 2012; Fernandes and Nayak, 2017) which is supported by increase in organic carbon and finer sediments in the outer fjord and coarser sediments and low organic carbon in the inner fjord.

A strong correlation between TOC and TN exist in the surface sediments of Krossfjord (r^2=0.69) and Kongsfjord (r^2=0.84) suggesting that the contribution of inorganic nitrogen to the total nitrogen pool is negligible in Krossfjord-Kongsfjord system (Kim et al., 2011). TP fluctuates without any particular trend in both the fjords. TOC and TN show poor association with TP indicating a differential pathway for phosphorus. BSi shows an increasing trend from inner fjord towards the outer fjord indicating high productivity towards the outer fjord. The nutrient (C, N, P and Si) concentrations in the inner fjord are low may be due to less concentration of organic matter, possibly because of the proximity of glacier as glacial meltwater is low in nutrient

concentrations and also diluted possibly by the presence of coarse-grained sediments. All geochemical proxies TN, TOC and BSi show similar variations from outer fjord to inner fjord indicating their common source. The close relationship between BSi and other nutrient parameters could confirm that sedimentary organic matter is predominantly derived from the natural source and anthropogenic organic input did not significantly influence the organic matter.

Source of organic matter in fjord sediments

The C: N ratio has been widely used to trace sources of organic matter (marine vs. terrestrial) in Arctic environments (Stein and Macdonald, 2004). Organic matter derived from higher plants is typically characterized by a higher C: N ratio (>20; Meyers and Ishiwatari,1993) as compared to the organic matter derived from marine organisms (6-9; Muller, 1977) as terrestrial organic matter contains a high percentage of non-proteinaceous material (cellulose and lignin). According to Bordowskiy (1965) and Hedges et al. (1986), C: N ratios of marine organic matter are around 6 whereas terrigenous organic matter has C: N ratios of >15. Along Krossfjord, the C: N ratio in sediments varies from 1.01 to 26.37 and along the Krossfjord the C: N ratio varies from 6.67 to 17.00 (Table 2) suggesting the mixed source of organic matter derived from terrestrial as well as marine source increasing marine influence towards the fjord mouth. High terrestrial organic matter (TOM) supply to the fjord corresponds to the meltwater discharge and glacial erosion processes. The contribution of organic matter from the vegetation cover seems to play a minor role since the area is glaciated and small areas provide favorable ground for plant growth. A higher proportion of marine organic matter (MOM) towards the mouth of the fjord reflects the dominant influence of nutrient-rich Atlantic water inflow is indicated by a high temporal variability in annual primary productivity (4—180 gC m^{-2} yr^{-1}) (Hop et al., 2002). Both the fjords show higher C: N values in shallower regions because of the presence of high amount of terrestrial material and their association with coarse-grained sediment suggesting grain size to be a dominant factor regulating the distribution of organic matter. Winkelmann and Kneis (2005) suggested that C: N values of marine surface sediments off Spitsbergen, were substantially affected by a contribution of inorganic nitrogen, which accounted for up to 70% of the total nitrogen content. This indicated that relatively low C: N values are possibly due to the high amount of inorganic nitrogen present in fine-grained sediments. However, in the present study, TOC shows a strong correlation with TN indicating that most of the nitrogen was associated with organic carbon and it can be considered as a measure of organic nitrogen suggesting a negligible contribution of inorganic nitrogen to the total nitrogen pool as reported by Kim et al., 2011.

Factors controlling Carbonate content

Variations in carbonate content are mainly controlled by dissolution during its journey through the water column, dilution by the non-carbonate fraction and terrigenous matter and/or productivity changes (Stein et al., 1994). In general, in polar regions, CO_2 dissolution is high which leads to increase in carbonic acid concentration which in turn explains the low $CaCO_3$ content. The $CaCO_3$ concentration is associated with coarse grain size where with increasing sand fraction towards the head of the fjord calcium carbonate increased. While the $CaCO_3$ content is low towards the mouth of the fjord due to increased clay loads which caused dilution of carbonates. Association of carbonate with coarse-grained sediment in the surface sediments of the fjord indicates that it is of detrital origin derived from the weathering of rocks present in the catchment area of the fjord

(Midproterozoic and Proterozoic metamorphic rocks, mainly marble towards north and south of Kongsfjord respectively).

Conclusions

The sediment size decreases with increasing distance from the glacier fronts and shows the dominance of fine-grained sediment (silt and clay) in both the fjords suggesting deposition from water column suspension indicating the relatively quieter hydrodynamic condition. The sediment seems to have been released from physical and mechanical (glacial) weathering. Organic matter concentration increases with increasing distance from the glaciers. C/N ratio suggests that the inner fjord region is dominated by terrestrial source while marine source becomes dominant away from the glaciers. Grain size seems to be a controlling factor regulating the distribution of organic matter. High concentration of nutrients C, N, P and BSi towards the mouth of the fjord away from the glacier suggests the influence of Atlantic water mass in western Spitsbergen. Carbonate concentration in this region is low (< 15%) due to increased clay loads which caused dilution of carbonates. The carbonate is mainly of detrital origin derived from the weathering of rocks present in the catchment area.

Acknowledgment

The authors place on record thanks to the Director, National Centre for Antarctic and Ocean Research (NCAOR), Goa, for providing the opportunity to participate to one of the authors (SC) in Indian Arctic programme and Ministry of Earth Sciences (MOES) for providing the logistic support required for the collection of samples. One of the authors (SC) thanks the University Grant Commission (UGC), for providing a fellowship. The authors thank Dr. Manish Tiwari, Scientist; Mr. Shubham Tripathi, Dr. P.V. Bhaskar, Scientist; Ms. Melena Augusta, Scientist, ESSO-NCAOR, Goa for kindly extending the instrumental facility of C-N analyzer and Coulometer.

References

Bordowskiy, O.K. (1965). Sources of organic matter in marine basins. *Marine Geology*, 3-5 31.

Eilertsen, H.C., Taasen, J.P. and WesIawski, J.M. (1989). Phytoplankton studies in the fjords of West Spitsbergen: physical environment and production in spring and summer. *Journal of Plankton Research*, *11* (6), 1245-1260.

Fahl, K. and Stein, R. (1999). Biomarkers as organic-carbon-source and environmental indicators in the Late Quaternary Arctic Ocean: problems and perspectives. *Marine Chemistry*, *63* (3), 293-309.

Fernandes, M.C. and Nayak, G.N. (2017). Geochemistry of mudflat and mangrove sedimentary environments, within tropical (Sharavati) estuary, Karnataka coast, India. *Journal of Indian Association of Sedimentologists,* 34(1-2), 103-119.

Folk, R.L. (1968). Petrology of Sedimentary rocks. Austin, Texas, Hemphills, 177.

Forland, E.J., Hanssen-Bauer, I. and Nordli, P.O. (1997). *Orographic precipitation at the glacier Austre Broggerbreen*, *DNMI Rep. 02/97 Klima.*

Hass, H.C. (2002). A method to reduce the influence of ice-rafted debris on a grain size record from northern Fram Strait, Arctic Ocean. *Polar research*, *21* (2), 299-306.

Hedges, J.I., Clark, W.A., Quay, P.D., Richey, J.E., Devol, A.H. and Santos, M. (1986). Compositions and fluxes of particulate organic material in the Amazon River. *Limnology and Oceanography*, *31* (4), 717-738.

Hop, H., Pearson, T., Hegseth, E.N., Kovacs, K.M., Wiencke, C., Kwasniewski, S., Eiane, K., Mehlum, F., Gulliksen, B., Wlodarska-Kowalczuk, M. and Lydersen, C. (2002). The marine ecosystem of Kongsfjorden, Svalbard. *Polar Research*, *21* (1), 167-208.

Ito, H. and Kudoh, S. (1997). Characteristics of water in Kongsfjorden, Svalbard. *Proceedings of 509 the NIPR Symposium on Polar meteorology and Glaciology. 11, 211-232*.

Keck, A., Wiktor, J., Hapter, R. and Nilsen R. (1999). Phytoplankton assemblages related to physical gradients in an Arctic glacier fed fjord in summer. ICES *Journal of Marine Science*,56, 203-214.

Kim, J.H., Peterse, F., Willmott, V., Kristensen, D.K., Baas, M., Schouten, S. and Sinninghe Damste, J.S. (2011). Large ancient organic

matter contributions to Arctic marine sediments (Svalbard). *Limnology and Oceanography*, *56* (4), 1463-1474.

Koziorowska, K., Kulinski, K. and Pempkowiak, J. (2017). Distribution and origin of inorganic and organic carbon in the sediments of Kongsfjorden, Northwest Spitsbergen, European Arctic. *Continental Shelf Research*, 1-150, 27-35.

Kumar, P., Pattanaik, J.K., Khare, N., Chopra, S., Yadav, S., Balakrishnan, S. and Kanjilal, D. (2014). Study of ^{10}Be in the sediments from the Krossfjorden and Kongsfjorden Fjord System, Svalbard. *Journal of Radioanalytical and Nuclear Chemistry*, *302* (2), 903-909.

Kumar, V., Tiwari, M., Nagoji, S. and Tripathi, S. (2016). Evidence of Anomalously Low δ^{13}C of marine organic matter in an Arctic Fjord. *Scientific reports*, *6*, 36192.

MacLachlan, S.E., Cottier, F.R., Austin, W.E. and Howe, J.A. (2007). The salinity: δ^{18}O water relationship in Kongsfjorden, western Spitsbergen. *Polar Research*, *26* (2), 160-167.

MacLachlan, S.E., Howe, J.A., Vardy, M.E. (2010). Morphodynamic evolution of Kongsfjorden-Krossfjorden, Svalbard, during the Late Weichselian and Holocene. *Geological Society, London, Special Publications*, *344* (1), .195-205.

Meyers, P.A. (1997). Organic geochemical proxies of paleoceanographic, paleolimnologic, and paleoclimatic processes. *Organic geochemistry*, *27* (5-6), 213-250.

Meyers, P.A. (2003). Applications of organic geochemistry to paleolimnological reconstructions: a summary of examples from the Laurentian Great Lakes. *Organic geochemistry*, *34* (2), 261-289.

Meyers, P.A. and Ishiwatari, R. (1993). Lacustrine organic geochemistry—an overview of indicators of organic matter sources and diagenesis in lake sediments. *Organic geochemistry*, *20* (7), 867-900.

Mortlock, R.A. and Froelich, P.N. (1989). A simple method for the rapid determination of biogenic opal in pelagic marine sediments. *Deep Sea Research. Oceanography Research Papers,* 36 (9), 1415–1426.

Muller, P.J. (1977). C/N ratios in Pacific deep-sea sediments: Effect of inorganic ammonium and organic nitrogen compounds sorbed by clays. *Geochimica et Cosmochimica Acta*, *41* (6), 765-776.

Muller, P.J. and Schneider, R. (1993). An automated leaching method for the determination of opal in sediments and particulate matter. *Deep Sea Research Part I: Oceanography Research Papers*, 40 (3), 425–444.

Murphy, J.A.M.E.S. and Riley, J.P. (1962). A modified single solution method for the determination of phosphate in natural waters. *Analytica Chimica Acta*, 27, 31–36.

Nilsen, F., Cottier, F., Skogseth, R. and Mattsson, S. (2008). Fjord–shelf exchanges controlled by ice and brine production: the interannual variation of Atlantic Water in Isfjorden, Svalbard. *Continental Shelf Research*, *28* (14), 1838-1853.

Pejrup, M. (1988). The triangular diagram used for classification of estuarine sediments: a new approach. In de Boer, P.L., van Gelder, A., Nios, S.D., (Eds) *Tide-influenced sedimentary environments and facies. (*Reidel, Dordrecht), 289-300.

Peters, K.E. (1986). Guidelines for evaluating petroleum source rock using programmed pyrolysis. *AAPG bulletin*, *70* (3), 318-329.

Siraswar, R.R. and Nayak, G.N. (2012). Distribution of Sediment Components and Metals in Recent Sediments within Tidal Flats along Mandovi Estuary. *Journal of Indian Association of Sedimentologists*, *31* (1&2), 33-44.

Schubert, C.J. and Calvert, S.E. (2001). Nitrogen and carbon isotopic composition of marine and terrestrial organic matter in Arctic Ocean sediments: implications for nutrient utilization and organic matter composition. *Deep Sea Research Part I: Oceanographic Research Papers*, *48* (3), 789-810.

Shetye, S., Mohan, R., Shukla, S.K., Maruthadu, S. and Ravindra, R. (2011). Variability of Nonionellina labradorica Dawson in surface sediments from Kongsfjorden, West Spitsbergen. *Acta Geologica Sinica (English Edition)*, *85* (3), 549-558.

Stein, R. and MacDonald, R.W. (2004). In: Stein, R. and MacDonald, R.W. (Eds.) The organic carbon cycle in the Arctic Ocean, 8, 315-322.

Stein, R., Grobe, H. and Wahsner, M. (1994). Organic carbon, carbonate, and clay mineral distributions in eastern central Arctic Ocean surface sediments. *Marine Geology*, *119* (3-4), 269-285.

Streuff, K. (2013). Master's thesis in Geology, Department of geology, University of Tromso, Norway.

Svendsen, H., Beszczynska-Moller, A., Hagen, J.O., Lefauconnier, B., Tverberg, V., Gerland, S., Borre Orbaek, J., Bischof, K., Papucci, C., Zajaczkowski, M. and Azzolini, R. (2002). The physical environment of Kongsfjorden–Krossfjorden, an Arctic fjord

system in Svalbard. *Polar research*, *21* (1), 133-166.

Vinje, T. (1982). Frequency distribution of sea ice in the Greenland and Barents Seas, 1971-80. *Norsk Polarinstitutt Arbok,* 57-61.

Winkelmann, D. and Knies., J. (2005). Recent distribution and accumulation of organic carbon on the continental margin west off Spitsbergen. *Geochemistry Geophysics Geosystems.* 6: Q09012.

Yu, Y., Song, J., Li, X., Yuan, H., Li, N. and Duan, L. (2013). Environmental significance of biogenic elements in surface sediments of the Changjiang estuary and its adjacent areas. *Journal of Environmental Science, 25 (11)*, 2185–2195.

Zaborska, A., Pempkowiak, J. and Papucci, C. (2006). Some sediment characteristics and sedimentation rates in an Arctic Fjord (Kongsfjorden, Svalbard). *Annual Environmental Protection*, *8*, 79-96.

First online volume
Jour. Indian Association of Sedimentologists, Vol. 35, No. 1 (2018), pp.57-76
ISSN 0970-3268

Geochemistry of the Archaean metasedimentary rocks of the Bundelkhand Mauranipur-Babina greenstone belt, central India: Implications for provenance characteristics

Ausaf Raza* and M.E.A. Mondal
Department of Geology, Aligarh Muslim University, Aligarh-202002, India
*Geologist, Geological Survey of India (GSI)
Jhalana Dungri, Jaipur- 302004
Rajasthan, India.
Contact No. +91-7023047345
E-mail: ausafraza2@gmail.com

Abstract: Metasedimentary rocks occurring as minor components of Mauranipur- Babina greenstone belt of the Bundelkhand craton were analyzed for major oxides and trace elements to constrain the composition and weathering history of their provenance and the tectonic setting prevailing at the time of deposition. On the basis of mineralogy and geochemical compositions, two types of lithologies are identified. First, a texturally immature, medium to coarse grained, light-coloured rock distinguished as Arkose. Second, a fine grained, dark coloured metapelitic rock containing adequate amount of mafic minerals, identified as greywacke. CIA (chemical index of alteration) and CIW (chemical index of weathering) values and Th/U ratios suggest that the source area of these sedimentary rocks had only been weekly weathered. ICV (Index of compositional variability) values of these rocks are <<1, suggesting that the sediments are generally immature. Low degree of weathering in their source region, immature nature and minor sorting influence on the detritus are the features which suggest high rate of erosion, rapid sedimentation, potentially marked relief and short distance transportation of the debris, derived from a tectonically active source region. Th- Sc- Zr systematic suggests insignificant degree of recycling. Assessment of provenance composition using Al_2O_3 - TiO_2, Sc-Th/Sc and (CaO+MgO) - SiO_2 – (Na_2O_+ $K_2O_)$, variation diagrams, REE patterns and (La/Yb)n ratios suggest that the studied sedimentary rocks were derived from mixing of debris of felsic and mafic composition in different proportions. The provenance modelling using REE data indicates that the arkoses can be best modelled with an 80% TTG and 20% granite mixture. On the other hand the greywacke can be best modelled with a mixture having 50% TTG, 40% basaltic rocks and 10% granite. It is suggested that the basin experienced contemporaneous sedimentation of immature detritus derived from a young craton comprising TTG and granitic batholiths and syn-depositional volcanic centres in an active tectonic environment.

Key words: Bundelkhand, metasediments, geochemistry, provenance.

Introduction

Compositional characteristics of source rocks are generally preserved in the sedimentary products and thus provide valuable information about nature of their source terrain (Van de Kamp and Leake, 1985; Armstrong-Altrin et al., 2004; Armstrong-Altrin and Verma, 2005; Sinha et al., 2007; Nagarajan et al., 2007; Maravelis and Zelilidis, 2009). Many studies have revealed that the chemical composition of the clastic sedimentary rocks is controlled by various factors including source rock composition, the extent and duration of weathering, mode of transportation and post depositional processes such as diagenesis (Taylor and McLennan, 1985, McLennan et al., 1993; Hayashi et al., 1997; Purevjav and Roser, 2013). Therefore, the elemental compositions of sedimentary rocks have been widely used to determine the provenance characteristics of sedimentary rocks and the tectonic conditions prevailing at the time of their deposition (Nesbitt, 1979; 1994; Cullers et al., 1987, 1988; McLennan et al., 1990, 1993; Wronkiewicz and Condie, 1990; Condie et al., 1995; Cox et al., 1995; Cullers and Podkovyrov, 2000; Cullers 2000; Condie 2001; Hofmann 2005; Manikyamba, et al., 2008; Absar et al., 2009; Raza et al., 2010; Absar and

sreenivas, 2015; Fatima and Khan, 2012). In recent years, the origin of the continental crust has received wide attention amongst the Precambrian geologists (Taylor and McLennan, 1985; Windley, 1995 and Condie, 1997). To understand the origin of continental crust it is important to know the composition of early crust. Clastic sedimentary rocks have been demonstrated to represent the average chemical composition of exposed crust from which they were derived (Taylor and McLennan, 1985). Therefore, the geochemical characteristics of the sedimentary formations, particularly those from Archaean greenstone belts, may provide important clues to estimate the composition of the early crust (Wronkiewicz and Condie, 1987; McLennan, 1989; Cullers, 2000; Condie, 2001; Hofmann, 2005; Absar et al., 2009; Raza et al., 2010). Most of our present knowledge regarding composition and evolution of early crust is based on geochemical and isotopic composition of Precambrian sedimentary records.

Sedimentary successions comprising clastic sedimentary rocks are important components of Archaean greenstone belts of the Indian shield. Although enough amount of Precambrian sedimentary record is available in Indian shield, the application of sediment geochemistry to the crustal evolution studies did not catch up widely. Despite early beginning by Naqvi and his co-workers (Naqvi and Hussain, 1972; Naqvi and Rogers, 1987 and references therein) in the field, comprehensive work on the geochemical aspects of the Archaean sedimentary rocks of the Indian shield are lacking. In this shield area, most of the work on the geochemistry of sedimentary rocks has been carried out on the Archaean sequences of Dharwar craton of south Indian shield (Naqvi et al., 1983; Naqvi and Rogers, 1987 and references therein; Naqvi et al., 2002). The present work deals with the major and trace element geochemistry of clastic sedimentary rocks of an Archaean greenstone belt, referred to as Mauranipur- Babina greenstone belt of the Bundelkhand craton occurring to the north of Central Indian Shear Zone (CISZ) in the central part of the Indian shield.

Although the geochemistry of mafic rocks of the Archaean greenstone belt of this area has been examined (Malviya et al., 2006), the geochemical data on associated sedimentary rocks are not available in literature. The Bundelkhand craton thus remains unrepresented in any model proposed for the evolution of the Archaean continental crust. The present study is the first, to report major and trace element (including REE) characteristics of previously unrecognized clastic sedimentary rocks from volcanic-sedimentary sequence of greenstone belt occurring in the Mauranipur-Babina section of the Bundelkhand Craton. Our aims are to report and utilize the textural and geochemical data of these Archaean sedimentary rocks to constrain the composition and weathering history of their source terrain. This would also help to understand the tectonic scenario prevailing during the Archaean in this part of the Indian Shield.

Geological setting and field occurrence of the studied sedimentary rocks

Bundelkhand cratonic block

The Bundelkhand cratonic block, occurring in the central part of the Indian Shield, covers an area of about 29,000km^2, and is bounded by the Great Boundary Fault (GBF) in the west and the Central Indian Tectonic Zone in the south. It consists predominantly of Proterozoic granites containing linear slivers of gneisses of tonalite-trondhjemite- granodiorite composition

(TTG) and volcanic-sedimentary sequences of Archaean age. The western, eastern and southern margins of the craton are marked by the presence of Proterozoic basins hosting sedimentary successions of Bijawar Group and Vindhyan Supergroup. (Fig.1). The Bundelkhand craton experienced multiple phase of mafic and felsic magmatism during the Archaean and Proterozoic time. The dominant magmatic event was the emplacement of a series of Proterozoic granitoids exposed at various places within the craton. The TTG magmatism in the Bundelkhand craton occurred from ~3.59 Ga to ~2.6 Ga (Verma et al., 2016; Saha et al., 2015; Kaur et al., 2014; Mondal et al., 2002). Based on various associated magmatic events the lithological units of the Bundelkhand massif can be divided into: i) Archaean gneisses of tonalite, trondhjemite and granodiorite (TTG) composition (Basu, 1986; Mondal and Zainuddin, 1996; Mondal et al., 2002), ii) metamorphosed supracrustal basement rocks (BIF, interbedded quartzite, schist, amphibolite and/or clac-silicate rocks) exposed along the E-W trending Bundelkhand linear Tectonic Zone (BTZ). This lineament is a major brittle ductile shear zone extending along Mauranipur-Babina section and iii) undeformed younger granitoids including hornblende granitoids, biotite granitoids and leucogranitoids (Mondal and Zainuddin, 1996). These granitoids are intrusive in nature within Archaean gneisses and metamorphosed supracustal rocks. NE-SW trending quartz reefs (2.0- 1.8 Ga, Pati et al., 2007) and NW-SE trending dolerite dykes (2.0-0.9Ga, Rao et al., 2005) have also been observed within massif (Basu, 1986). Dolerite dykes cut across the quartz reefs, suggesting it to be the youngest magmatic phase of the Bundelkhand craton. Based on the structural analyses three generation of deformation within Muaranipur supracrustal rocks were suggested (Malviya et al., 2006). The D_1 deformation phase is marked by moderately plunging tight to isoclinal fold (F_1), the second generation of deformation is marked by refolded fold and the formation of pucker lineation on S_1 plane and the third generation of deformation are represented by low amplitude broad warps.

Mauranipur-Babina Greenstone belt

Although, coharent greenstone belts similar to those of Dharwar craton are not found in the Bundelkhand block, the sporadic occurrences of volcanic-sedimentary sequences, along linear zones within the gneissic complex, are considered as greenstone belts (Basu, 1986; Prasad et al., 1999; Ramakrishnan and Vaidyanadhan, 2010). Two east-west trending zones comprising many greenstone sub- belts have been recognized (Fig.1). These are (i) Mauranipur- Babina greenstone belt in the north and (ii) Madaura –Girar greenstone belt in the south. The Mauranipur- Babina greenstone belt consists of metamorphosed assemblages of mafic and felsic volcanics, banded iron formations and minor sedimentary components. The samples for present study were collected from Naugao, Jugalpur and Baruasagar where the metasedimentary rocks are associated with basaltic to basaltic andesitic rock (Malviya et al., 2006) and constitutes a small portion of the Archaean greenstone belt in the major shear zone along Mauranipur-Babina section. Two distinct metasedimentary rocks were identified based on their mineralogical and textural characteristics; immature medium to coarse grained gritty quartzite dominantly composed of quartz and feldspars and fine grained dark coloured metapelitic rocks with abundant mafic components in addition to quartz grains.

Field Occurrences of clastic sedimentary rocks

The clastic metasedimentary rocks occur as minor but distinct components of volcanic –sedimentary greenstone succession of Mauranipur-Babina belt. The clastic metasedimentary rocks are best exposed in and around Naugao, Jugalpur and Baruasagar, where they are found interlayered with volcanic flows of basaltic to basaltic andesitic composition (Malviya et al., 2004) and constitutes a small portion of the Archaean greenstone belt in the major shear zone along Mauranipur-Babina section. Two distinct metasedimentary rocks were identified based on their mineralogical and textural characteristics. These are: (i) fine grained metapeletic rocks consisting predominantly of mafic minerals in association with quartz grains and (ii) medium to coarse grained, quartzites consisting predominantly of quartz and feldspars.

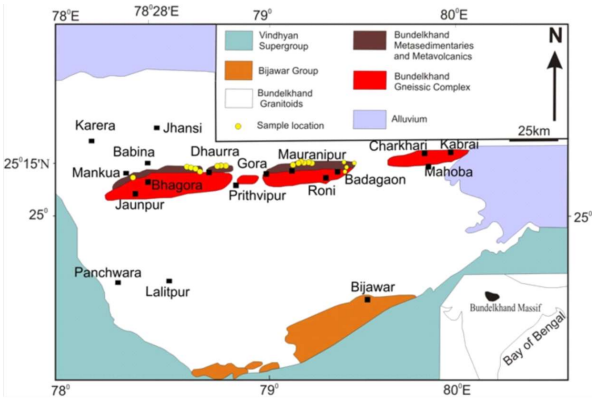

Figure1: Generalized geological Map of the Bundelkhand massif, illustrating marginal basins and East-West trending Bundelkhand tectonic zone (after Ramakrishnan and Vaidyanadhan, 2010)

Sampling procedures and Analytical Techniques

In the present study samples were collected from the isolated outcrops of the volcano-sedimentary successions of the greenstone belt of the Bundelkhand craton from Dhaurra, Prithvipur, Naugao, Baruasagar, Badagao and Mauranipur areas (Fig.1).

Samples were collected from fresh and unweathered outcrops to avoid weathering and alteration effects. All the samples were examined petrographically. In order to Obviate grain size compositional dependence of coarse grain metasedimentary rocks modal analysis was carried out by counting more than 500 points per thin sections using the Dickinson-Gazzi point counting methods (Dickinson, 1970). For

	Bundelkhand metasediments							
			Greywacke			Arkose		
Sample Name	M 219	M 220	M 221	N 205	MR 142	MR 144	N 209	N 210
SiO_2	64.55	58.47	58.71	58.37	87.18	82.04	76.65	73.53
TiO_2	0.51	0.67	0.65	0.73	0.1	0.03	0.09	0.14
Al_2O_3	15.78	13.02	12.39	14.63	8.15	10.83	13.38	14.78
Fe_2O_3 T	3.37	5.32	5.42	7.68	1.6	0.5	0.79	1.31
CaO	9.68	14.34	10.22	5.53	0.66	0.27	0.38	1.61
MgO	3.17	5.1	8.82	5.15	0.06	0.08	0.09	0.29
Na_2O	0.97	1.44	2.01	4.2	0.5	4.6	3.86	5.4
K_2O	1.37	1.4	1.56	3.52	0.71	2.51	5.62	3.28
MnO	0.41	0.33	0.2	0.06	0.03	0.01	0.02	0.03
P_2O_5	0.11	0.11	0.09	0.33	0.02	0.01	0.02	0.04
Sum	99.92	100.2	100.07	100.2	99.01	100.88	100.9	100.41
Sc	5.261	9.142	9.769	4.691	2.579	1.044	1.209	1.939
V	31.537	51.571	56.618	35.773	4.881	3.07	3.453	4.708
Cr	7.837	19.917	24.762	5.883	6.379	4.054	4.286	4.075
Co	20.425	28.495	32.872	20.084	21.9	18.247	25.43	27.378
Ni	11.357	35.043	43.839	14.202	7.528	5.621	3.21	3.114
Cu	1.051	1.163	1.051	3.354	1.327	1.33	0.718	0.919
Zn	41.981	57.551	68.666	28.149	11.132	17.141	13.84	9.115
Ga	13.267	11.125	11 .123	12.307	3.738	5.445	11.22	13.621
Rb	54.383	38.858	57.981	71.247	21.821	52.66	222.9	85.419
Sr	72.052	65.577	61.853	440.59	33.617	58.189	43.48	153.11
Y	28.423	23.868	20.926	17.363	5.642	8.068	8.554	6.345
Zr	238.61	161.18	142.317	140.89	69.971	67.02	69.73	87.044
Nb	12.756	7.289	6.584	5.284	2.236	6.249	7.49	5.957
Cs	1.636	0.825	0.881	0.824	0.221	0.206	1.186	1.2
Ba	202.58	160.02	100.469	891.99	123.75	542.36	220.3	407.97
La	32.73	21	16.921	42.821	10.474	7.392	12.754	14.063
Ce	61.052	40.532	33.986	83.065	18.226	15.804	25.54	23.89
Pr	6.178	4.235	3.614	11.243	1.94	1.478	1.99	2.214
Nd	23.245	16.441	14.353	44.955	7.037	5.259	6.337	7.612
Sm	4.587	3.364	3.155	6.949	1.301	0.994	1.028	1.197
Eu	0.96	0.686	0.666	1.844	0.385	0.282	0.191	0.368
Gd	4.024	3.226	2.832	4.939	1.046	0.859	0.899	1.009
Tb	0.697	0.564	0.508	0.632	0.162	0.157	0.146	0.14
Dy	4.663	4.067	3.574	3.332	1.019	1.143	1.068	0.864
Ho	0.545	0.467	0.402	0.353	0.113	0.139	0.123	0.104
Er	1.795	1.591	1.374	1.202	0.388	0.558	0.506	0.381
Tm	0.226	0.201	0.178	0.137	0.055	0.08	0.083	0.053
Yb	2.231	2.013	1.823	1.401	0.601	0.932	0.998	0.593
Lu	0.355	0.338	0.293	0.225	0.109	0.166	0.205	0.113
Hf	6.59	4.601	4.013	4.012	2.013	2.639	3.08	3.008
Ta	1.737	0.946	0.922	0.562	0.961	2.124	2.353	1.85
Pb	10.857	7.851	8.126	12.674	9.21	15.141	21.89	21.551
Th	12.541	6.73	5.824	8.143	3.185	13.289	18.66	10.853
U	2.84	2.047	1.557	2.51	0.687	3.236	4.515	1.725

Table 1: Major (wt%) and Trace element concentra for metasedimentary rocks of the Bundelkhand gre (BGB)

geochemical studies samples were powdered to -200 mesh size by using agate pulveriser. Major element oxides were determined by X-Ray fluorescence Spectrophotometry (XRF) technique in geochemical laboratory of Wadia Institute of Himalayan Geology, Dehradun. The accuracy and precision was ± 1-3%. Trace element and REE were analysed by Inductively Coupled Plasma-Mass Spectrometry (ICP-MS, Perkin-Elmer, SCIEXELAN DRC II) at National Geophysical Research Institute (NGRI), Hyderabad with <10% precision (Roy et al., 2007). International rock standards SCo-1 and GSR-4 were also analyzed and the results agree with the reported values (Govindaraju, 1994). The precision is better than 10% RSD. The data are given in Table 1.

RESULTS

Petrography

The collected samples of metasedimentary rocks of the Mauranipur- Babina greenstone belt are of two distinct types. First, the texturally, immature medium to coarse grained, light-coloured sedimentary rocks appearing as quartzite. Another set of metasedimentary rocks are fine grained volcaniclastic type sediments containing adequate amount of mafic minerals along with quartz. The frame work grains of our medium to coarse grained, light coloured samples of metasedimentary rocks are dominantly feldspars (plagioclase + microcline) and quartz among which monocrystalline quartz (Q_m) are in abundance than polycrystalline quartz (Q_p). In contrast, the fine grained, dark coloured samples of the metasediments are rich in pyroxenes (Table 2). Since first type of sediments are medium to course grained they were studied under the microscope to determine their modal compositions. The QFR classification diagram (Folk, 1980) defines arkosic nature of these sediments (Fig. 2B). The mineralogical compositions were also plotted in triangular diagrams in accordance with Dickinson (1985) scheme. In QtFL diagram our samples are plotted in the field of uplifted basement provenance (Fig. 2A). It can thus be suggested that an uplifted basement complex can be the source for these metasedimentary rocks.

Samples	Qt	Qm	Qp	F	L
N210	210	150	60	313	0
N209	207	177	30	401	0
MR144	220	190	30	375	0
MR142	200	156	64	405	0

Table 2: Framework modes (after Dickinson,1985) of the metasediments of the Bundelkhand greenstone Belt (BGB). Qt, Total quartz; Qm, Monocrystalline quartz; F, Total feldspar grains; Lt, total lithic fragments

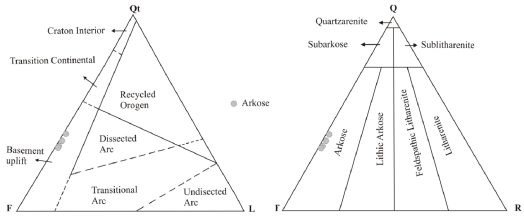

Figure 2: Studied metasediments plotted in (**A**) Basement uplift field in Dickinson and Suczek, (1979), framework mode diagram discriminating between different tectonic depositional settings Qt= total quartz (monocrystalline and polycrystalline); F= feldspar (plagioclase and K-feldspar); L= lithic fragments. (**B**) Arkose field in Folks's classification (1980) of sandstone based on QFR ternary diagram (Q= total quartz; F= total feldspar; R= total rocks fragments including chert.

Geochemistry

Because most of the rocks under study have undergone metamorphism up to the amphibolite facies, it is possible that some or many of the major and trace elements will have been variably remobilized (Taylor & McLennan 1985; Tarney & Weaver 1987; Barovich & Patchett 1992; Pearce 1996; Tran *et al.* 2003). The alteration of original composition, if any, would obviously reduce the effectiveness of the

geochemical parameters. The degree of mobility during high grade metamorphism is controversial. It is generally agreed that major changes in composition of sedimentary rocks can occur even before the onset of granulite facies metamorphism (e.g. Taylor & McLennan 1985). However, some studies have suggested that elemental mobility in high grade rocks is insignificant (Ferry 1983; Roser & Korsch 1986; Passchier et al., 1990). In recent years, various studies have shown that REEs, high field strength elements (HFSEs) and even transition elements are not generally affected even beyond amphibolite facies metamorphism (Barovich & Patchet 1992; Crichton & Condie, 1993; Payne et al., 2006). However, large ion lithophile elements (LILE) are expected as being variably mobile during metamorphism. The elements Rb, Sr and Ba are highly mobile during secondary processes (Nesbitt et al., 1980), and thus the abundance of these elements in sedimentary rocks does not always represent the composition of their source rock. Th is considered immobile during sedimentation and weathering and has very low residence time in seawater (McLennan et al., 1980).

Many authors have suggested the use of immobile or relatively immobile elements as discriminant tools (Cann, 1970; McLennan, 1989; Taylor and McLennan, 1985). These elements include Al_2O_3, TiO_2, HFSE such as Zr, Y, Nb, Hf, Ta and Ga and transition elements such as Sc, Ni, and V. The REEs are also considered to be relatively immobile during chemical weathering and digenesis (Nesbitt, 1979; Humphris, 1984) such that provenance information may not be lost even after considerable alteration of framework grains (Johnsson, 1993). For these reasons, selected major, minor and trace elements are increasingly being employed as tools in igneous discrimination and sedimentary provenance characterization studies.

Although exceptions occur (Cullers, 1994), the REE are generally regarded as immobile. The smoothness and parallel nature of REE patterns (Fig. 3) and multielement profiles (Fig. 4) of the studied rocks together with the facts that the samples are from different parts of the belt, suggest that REE and other elements have not been affected significantly during the process of metamorphism. The similarity in the patterns is maintained over a large range of composition (SiO_2=58.37-87.18%). In the present study, although all the

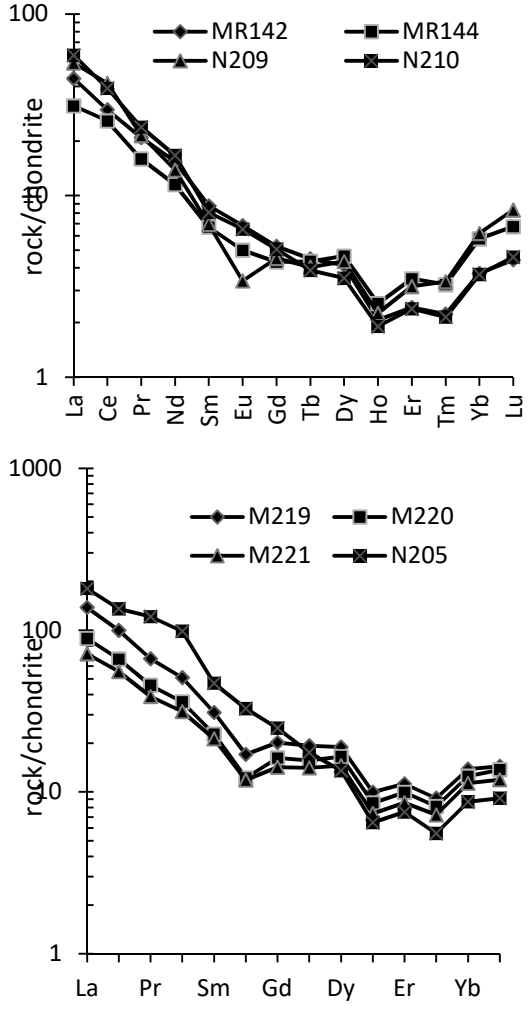

Figure 3: Chondrite- normalized rare earth elements (REE) pattern. Normalizing values after McDonough and Sun (1995) (**A**) Greywacke with fractionated REE pattern and slight negative Eu anomaly and enriched Heavy rare earth elements (HREE). (**B**) Arkose with fractionated REE pattern and no to negligible Eu anomaly.

elements analyzed are used for geochemical characterization of metasediments, more weight is given to the immobile elements. In the present study, with the exception of a few major element fingerprints, our interpretations and conclusion heavily rely on the immobile or less mobile trace elements.

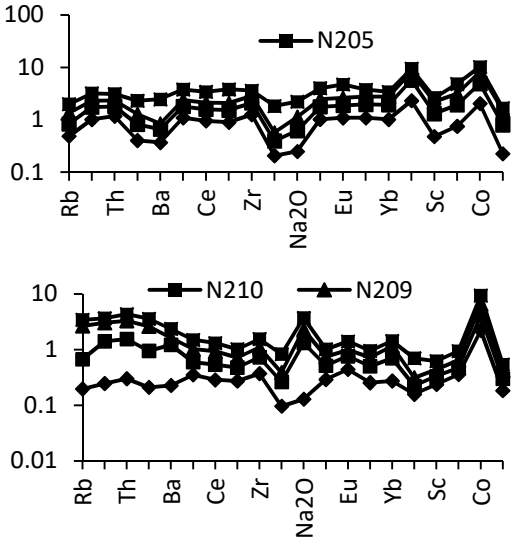

Figure 4: Average Upper Continental Crust (AUCC) normalized multielement spidergram of (**A**) greywackes and (**B**) Arkose from Mauranipur- Babina greenstone belt of the Bundelkhand craton. Normalized values after Taylor and McLennan (1985).

Geochemical classification

Major and trace element contents of our samples show large variations. Many of the geochemical differences between the samples of fine grain metapelites and medium to course grained quartzites of Mauranipur-Babina belt are due to different mineralogy of the two types of the sediments. On SiO_2/ Al_2O_3 versus K_2O /Na_2O bivariant diagram (Fig. 5) our samples are plotted within or very near to the field of Archaean greenstone shale. However the samples of metapelites show more restricted range of SiO_2/ Al_2O_3 than those of quartzites.

Geochemical composition of clastic sedimentary rocks has been widely used to distinguish the rock types (e.g. Pettijohn et al., 1972; Herron, 1988). On chemical classification diagram of Herron (1988), the analysed samples of metapelites plot in the field of greywacke and those of quartzite in the field of arkose (Fig. 6). On this diagram the samples, identified as greywacke appear to show heterogeneous geochemical signatures in comparison to homogenous composition of arkose samples. Taking into consideration the above mentioned diagrams, the studied clastic sedimentary rocks of Mauranipur-Babina greenstone belt are described herein as greywacke and arkose in our further discussion.

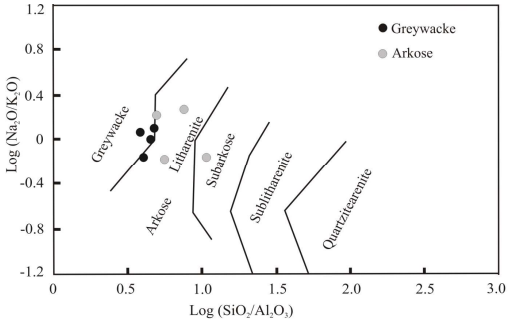

Figure 5: Chemical classification scheme diagram of Pettijohn (1972), analysed samples are plotted within or very near to the field of greywacke and arkose.

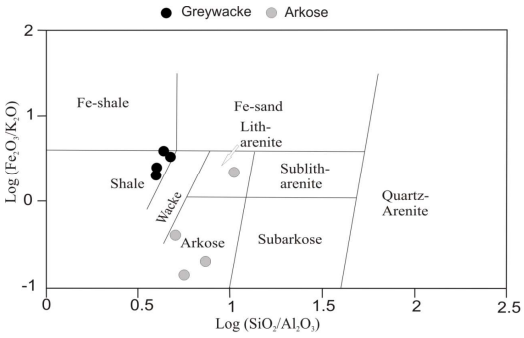

Figure 6: Chemical classification diagram of Herron (1988), the analysed samples of metapelites are plotted in the field of greywacke and those of quartzite in the field of arkose

Geochemical characterization

Comparison of major elements composition between the greywacke and arkose samples indicates that the latter are enriched in SiO_2 (avg.~80%) and depleted in Al_2O_3 (avg. ~12%) relative to the former (~60% and 14% respectively). However MgO and CaO

contents of the greywacke (avg. 5.56% & 9.94% respectively) are greater than those of arkose (avg. 0.13% & 0.73 respectively). Greywacke are also enriched in TiO_2 (avg. 0.64%) relative to arkose (avg.0.09%). Other major elements do not show much variation. The SiO_2 contents of greywacke and arkose show a strong negative correlation with Al_2O_3 (r = - 0.76; - 0.99 respectively). Such correlation is expected, because in sedimentary rocks the Al_2O_3 and SiO_2 contents are controlled by aluminous clay and quartz contents respectively. The strong positive relationship between Al_2O_3 and K_2O (r = 0.77) is shown by samples of arkose, indicating illite control. Such a relationship is not exhibited by the samples of greywacke (r= 0.23). It is observed that the increasing trend of textural maturity in sandstones leads to an increase in the amount of quartz at the expense of primary clay size material. As a result, the SiO_2/Al_2O_3 ratios are increased and concentrations of other elements are decreased due to quartz dilution. Therefore, the maturity of sandstone can be assessed by using SiO_2/Al_2O_3 ratios (McLennan et al., 1993). The average SiO_2/Al_2O_3 ratio of studied arkoses and greywacke are lower > 10 (7.2 and 4.3 respectively), thus suggesting that they are immature sediments. However the greywacke appear to be more immature than the samples of arkose.

The studied greywacke are relatively more enriched in ferromagnesian trace elements such as (Avg. Ni= 26 ppm; Cr= 15ppm; V= 44ppm and Sc= 7ppm) relative to arkose (Avg. Ni=5 ppm; Cr= 5 ppm; V=4 ppm and Sc= 2 ppm) indicating a significant proportion of mafic material in their source terrain. Similarities and dissimilarities among various samples of greywacke and arkose in major and trace elements are shown in multi element spidergrams in Fig. 4. In this diagram, the arrangement of the elements is in the order of increasing compatibility from left to right. In comparison with average upper continental crust (AUCC), the greywacke are enriched in MgO, CaO and TiO_2 and depleted in Na_2O, K_2O and P_2O_5. On the other hand the arkose are generally depleted in TiO_2, CaO, Fe_2O_3, MgO and P_2O_5 (Table 1). Enrichment of MgO, CaO and TiO_2 in the former can be attributed to the higher amount of mafic minerals as shown by petrographic study. In comparison with AUCC, the samples greywacke are generally depleted in almost all the elements except in Large Ion Lithophile Elements (LILE) Rb, Th, U and K which show more concentration in arkose.

The overall total REE concentrations as shown by our samples of arkoses vary from 35 ppm to 53 ppm with an average of 46 ppm. The greywacke samples are more enriched in total REE showing variation from 84 ppm to 203 ppm with an average of 132 ppm. However, the total REE contents of arkose as well as greywacke remain lower than that of AUCC (~ 143 ppm; Taylor and McLennan, 1985). Chondrite- normalized REE patterns of our greywacke and arkose samples are sub-parallel, characterized by LREE enrichment and no to minor Eu anomalies (Fig. 3). These rocks also exhibit concave- upward REE patterns between Dy and Lu, This feature is more prominent in the REE patterns of arkose samples. Such type of REE patterns are characteristically shown by TTG (e.g. Huang et al., 2010) and considered as a characteristic feature of arc magma (Van Boening and Nabelek, 2008).

Discussion

Weathering history of the source terrain

The degree of weathering in the source area of sedimentary rocks can be quantified by using geochemical indices such as chemical index of alteration

[CIA= {Al_2O_3 / (Al_2O_3+CaO* + Na_2O + K_2O)}X 100] (Nesbitt and Young, 1982) and chemical index of weathering [CIW= {Al_2O_3 / (Al_2O_3+CaO* + Na_2O)}X 100] (Cullers, 2000) where all the major oxides are expressed in molecular proportions and CaO* is the content of CaO incorporated in silicate fraction. The CIA values of greywacke are lower (30- 43; avg 37) than those of arkoses (49- 74; avg. 56). Similarly the CIW values of greywacke (31-46; avg 40) are lower than those of arkoses (56-80; avg 65) (Table 3). Collectively these values are intermediate between those of unweathered igneous rocks and typical shales (i.e. <50 and 70-75 respectively) and therefore suggest that the source area of these sedimentary rocks had only been weekly weathered.

Elements Ratio	**Bundelkhand Metasediments**		**Mixing end members (Condie 1993)**			**Mixing result for Greywacke**	**Mixing result for Arkose**
	Greywacke	**Arkose**	**TTG**	**Basalt**	**Granite**	**T60:B40:G10**	**T80:G20**
La_N	119.6	47.13	126.58	31.65	210.97	150.8439	143.4599
Ce_N	89.16	34.03	91.35	31.05	155.23	110.8731	104.1289
Nd_N	54.15	14.35	48.14	23.55	98.50	65.82591	58.21225
Sm_N	30.49	7.63	22.97	19.61	41.18	29.91786	26.61367
Eu_N	18.45	5.44	17.76	17.24	14.66	16.4672	17.14063
Gd_N	18.87	4.79	14.97	15.86	22.73	18.16384	16.52491
Tb_N	16.62	4.18	12.47	14.71	17.38	14.65515	13.44823
Yb_N	11.59	4.85	6.21	13.53	11.76	9.164414	7.321885
Lu_N	12.30	6.02	6.91	14.96	12.60	9.990718	8.04814
Eu/Eu*	0.73	0.89	-	-	-	-	-
$(La/Lu)_N$	10.44	8.49	-	-	-	-	-
La/Sc	4.84	7.23	-	-	-	-	-
Th/Sc	1.36	8.75	-	-	-	-	-
La/Co	1.24	0.47	-	-	-	-	-
Th/Co	0.35	0.50	-	-	-	-	-
Cr/Th	2.13	0.72	-	-	-	-	-
$(La/Sm)_N$	3.88	6.18	-	-	-	-	-
$(Gd/Yb)_N$	1.71	1.06	-	-	-	-	-
$(La/Yb)_N$	11.03	10.50	-	-	-	-	-
Th/U	3.67	4.79	-	-	-	-	-
Zr/Sc	26.89	48.47	-	-	-	-	-
CIA	37	56	-	-	-	-	-
CIW	40	65	-	-	-	-	-
ICV	13.9	11.8	-	-	-	-	-

Table 3: Average values of elemental ratios of the greywacke and arkose metasedimentary rocks of the Bundelkhand craton and mixing calculation of the Archaean rocks (Condie 1993).

The weathering history of source area of sedimentary sequences can also be evaluated by using their Th/U ratios. The Th/U ratios of sedimentary rocks are increased with increasing weathering due to oxidation and loss of U (Taylor and McLennan, 1985; McLennan et al., 1995). The average Th/U ratio of Upper crustal rocks is around 3.8 (Taylor and McLennan, 1985). Th/U ratios above 4 are considered to be related to weathering history. The Th/U ratios of studied samples range from 3.24 to 6.29 and averages at 4.2. The average Th/U ratio of greywackes is lower (3.67) than

that of arkose (4.79) (Table 3). In Figure 7(A**)**, Th/U is plotted against Th abundances (McLennan et al., 1993). Most of the samples of greywacke plot below the value for upper continental crust (UCC), only one sample (N220) plot slightly above the line representing UCC. The samples of arkoses plot slightly above the line. The plot of greywacke near the field of depleted mantle sources indicates their derivation from non-recycled arc magmatic rocks. As a whole the Th/U values of studied rocks suggest that these sediments were derived from source rocks with weak weathering and/or from debris which suffered least recycling. This result is consistent with interpretation drawn from CIA and CIW values.

A number of studies carried out on Archaean sedimentary sequences indicate severe chemical weathering of their source areas (McLennan et al., 1983; Wronkiewicz and Condie, 1987; Kasting, 1993; Fedo et al., 1996; Hofmann et al., 2003; and Hofmann, 2005). Elevated surface temperature, CO_2– rich atmosphere and humid climate during the Archaeans are the factors which have been related to intense weathering during that period (Kasting, 1993; Knauth and Lowe, 2003; Hessler et al., 2004). The intensity of chemical weathering is mainly controlled by source rock composition, duration of weathering, climate and tectonic conditions (Wronkiewicz and Condie, 1987). The rate of erosion and the climate are the main control of weathering. If rate of erosion is high it will not leave enough time for severe chemical weathering. Therefore, low degree of weathering in the source region of our samples may be due to high rate of erosion, rapid sedimentation and short distance transportation of the debris in a tectonically active setting of sedimentation. These conditions are compatible with non-steady state weathering where active tectonism and uplift allow erosion of all soil horizons and rock surfaces.

Provenance

Although overall composition of source region essentially controls the chemical composition of the clastic sedimentary rocks, there are certain surface processes such as sediment recycling, hydraulic sorting and palaeoweathering which may greatly modify the provenance memory (Lahtinen, 2000; Hofmann, 2005; Roddaz et al., 2006). Therefore, to identify the source of sedimentary sequences it is important to consider first the effect of these processes on the overall composition of sediments. The Th/Sc-Zr/Sc variation diagram is a useful measure to assess the contribution of pre-existing sedimentary sources. A Th/Sc ratio >1 of sedimentary rocks reflects input from fairly evolved crustal igneous rocks (Taylor and McLennan, 1985). Th/Sc ratio <0.8 indicates source of the sedimentary rocks other than the typical continental crust, probably a mafic source or input from mature or recycled source if coupled with higher ratio of Zr/Sc (>10). Average values of Th/Sc and Zr/Sc ratios of our samples are low (greywacke= 1.36 and 26.9; arkose= 8.75 and 48.47 respectively, Table 3). The Th/Sc ratio of sedimentary rocks characterizes the composition of their source rocks, whereas an increase in the Zr/Sc ratio alone would indicate the increase of zircon by sorting and recycling to sediments. Our samples of Greywacke and arkose, both display a positive linear correlation between Zr/Sc and Th/Sc (r= 0.98; 0.92 respectively), that is consistent with provenance dependent igneous differentiation trend. The compositional variation and the degree of sediment reworking and heavy mineral sorting can be illustrated in Zr/Sc versus Th/Sc plot of McLennan et al. (1993). In Zr/Sc versus Th/Sc diagram (Fig. 7B) the studied samples

are plotted along linear trend, suggesting insignificant degree of recycling.

The major element composition of pelitic rocks can be used to suggest their detrital mineralogy (Cox et al., 1995). The index of compositional variability [ICV = (Fe_2O_3+K_2O+Na_2O+CaO+MgO+ TiO_2)/Al_2O_3] has been effectively used in this regard (Cox et al., 1995). Basic idea behind the calculation of this parameter is that the non-clay minerals have higher ratios of the major cations to Al_2O_3 than clay minerals, so the non-clay minerals have higher ICV values. For example ICV decreases in the order of pyroxene and amphibole (~10-100)-biotite (~8)-alkali feldspar (~0.8-1)-plagioclase (~0.6)-muscovite and illite (~0.3)-montmorillionite (~0.15-0.3), and kaolinite (~0.03-0.05) (Cox et al., 1995). Immature shales with high percentages of non-clay silicate minerals will thus have ICV values greater than one. Such shales are often found in tectonically active settings in first cycle deposits (Van de Kamp and Leake, 1985). In contrast, more mature mud rocks rich in clay minerals ought to have lower ICV values of less than one (Cox et al., 1995). Such shales are derived from stable cratons with quiescent environments (Weaver, 1989). Low ICV values have also been found, however, in some first cycle material that was intensely weathered (Barshad, 1966). The average ICV values of studied greywacke (13.9; range- 12.39-15.78) and those of arkoses (11.78; range- 8.15-14.78) are >>1, thus suggest that these sediments are generally immature, derived from a tectonically active source region.

The geochemical composition of clastic sedimentary rocks is primarily related to that of their source terrain. Therefore, the major and trace element compositions are widely used to determine the composition of their source region (Roser and Korsch, 1988;

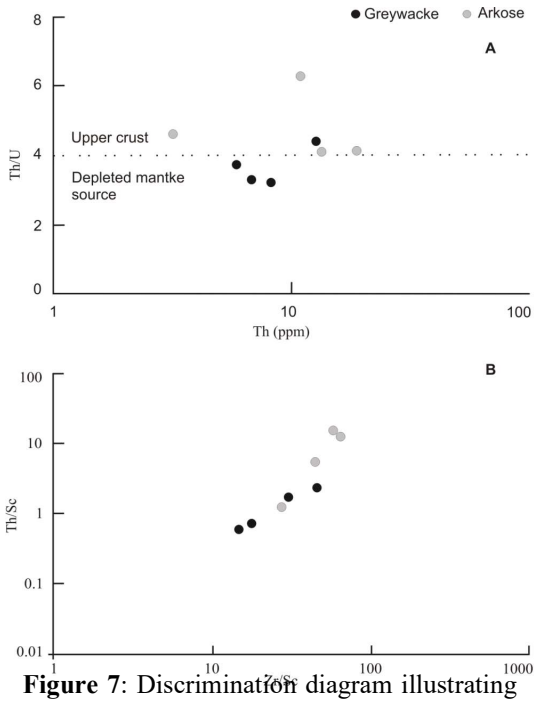

Figure 7: Discrimination diagram illustrating weathering and recycling; (**A**) Th/U vs Th diagram after McLennan et al., (1993), (**B**) Th/Sc vs Zr/Sc diagram after McLennan et al. (1993).

Fedo et al., 1997; Culler, 2000; Gu et al., 2002; Roddaz et al., 2007; Manikyamba, 2008; Absar et al., 2009; Raza et al., 2010; Absar and Sreenivas, 2014). It is observed that Ti and Al remain essentially immobile and behave similarly during weathering and fluvial transport (Nesbitt and Young, 1982; Sugitani et al., 1996; Chen et al., 2010, 2013). The Al/Ti ratio of clastic sedimentary rocks is considered to be similar to their magmatic source rocks (Yamamoto et al., 1986; Hayashi et al., 1997), therefore can be used as an important indicator of source composition. In igneous rocks, Al resides mostly in feldspars and Ti in mafic minerals such as olivine, pyroxene, hornblend biotite and ilmenite). Therefore, the Al/Ti ratio of igneous rocks gradually increases from mafic to more felsic rocks. The Al_2O_3/ TiO_2 ratio of our samples of greywacke varies from 19.06 to 30.94 and averages at 22.36, therefore suggest their derivation from source of mafic to intermediate composition. The average value of Al_2O_3/ TiO_2 of studied arkose

samples is 174.18 (range 81.50- 361.00) reflecting a felsic source. In Al_2O_3 - TiO_2 diagram (Fig. 8**),** the studied samples of arkose are plotted near the granite field and those of greywacke near the basalt field with an inclination towards granite field. This relationship indicates the derivation of our greywacke samples from a source region comprising a mixture of mafic and felsic rocks. On the other hand the studied arkose samples appear to have been derived from a source of predominantly felsic composition. On the (CaO+MgO) - SiO_2 – (Na_2O_+ $K_2O_)$ ternary diagram (Taylor and McLennan, 1985), our samples of greywacke and arkose again plot near the fields of basalt and granite respectively (Fig. 9) thus indicating the derivation of debris from sources of contrast composition.

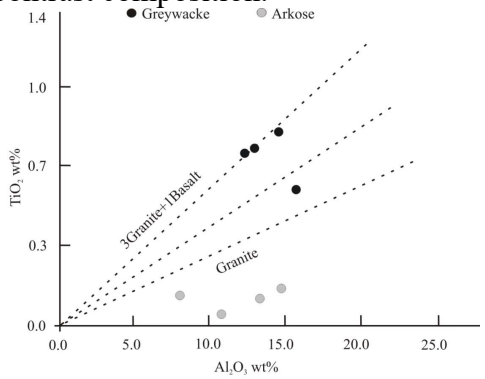

Figure 8: TiO_2 wt% versus Al_2O_3 wt% bivariate diagram (after McLennan et al., 1980). The 'granite line' and '3granite+ 1basalt' line are after Schieber (1992).

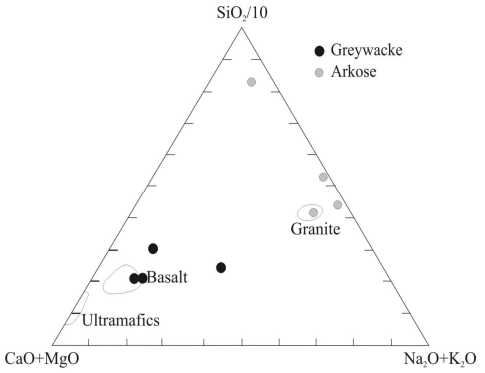

Figure 9: SiO_2/10- CaO+MgO- Na_2O diagram after Taylor and McLennan (1985), analyzed greywacke and arkose samples occupying basalt and granite field respectively.

REE and their ratios are most sensitive geochemical parameters influenced by source rock composition. The REE patterns are the most reliable indicators of sedimentary provinces (Taylor & McLennan, 1985). The degree of LREE vs HREE enrichment may be accessed through the $(La/Yb)_N$ values. The degree of differentiation of LREE from HREE is a measure of proportion of felsic to mafic rocks in the provenance. All of our samples reveal LREE enrichment with $(La/Yb)_N$ ratio ranging from 6.30 to 20.73 in greywacke and from 5.38 to 16.11 in arkose. The $(La/Yb)_N$ ratios, as shown by some of our samples e.g. N205 of greywacke and N210 of arkose are very high (20.73-16.11 respectively) in comparison to North American Shale Composite (NASC= 7.17; Gromet et al., 1984) and Post- Archaean Australian Shales (PAAS= 8.2). Amongst older crustal components, Tonalite-Trondhjemite-Granodiorite (TTG) and adakite suites are characterized by high $(La/Yb)_N$ ratios (TTG=42, Martin, 1994; Adakite= 24, Defant et al., 1991). Therefore, the high values of $(La/Yb)_N$ ratio as shown by some of our samples point towards a possible TTG/adakite component in their source terrain.

The negative Eu anomaly is a reflection of recycled crustal material characterizing evolved crustal cratons (Gao and Wedepohl, 1995; Meinhold et al., 2007). REE patterns of studied rocks do not exhibit significant negative Eu anomalies. They exhibit either minor Eu anomalies with (Eu/Eu*= 0.64-0.68) or no Eu anomalies with Eu/Eu* values ranging from 0.61 to 1.02. Out of four samples of arkose three samples show no Eu anomalies (Eu/Eu*= 0.93-1.02) and one sample show minor Eu anomaly (Eu/Eu*= 0.61). Amongst the greywacke samples, one sample shows no Eu anomaly (Eu/Eu*= 0.96) and rest of the three samples show minor Eu anomaly (Eu/Eu*= 0.64-0.68).

Significantly the samples of greywacke (N205) and arkose (N210) having high values of Eu/Eu* (0.96 and 1.02 respectively) also have high values of $(La/Yb)_N$ ratios (21.92 and 17.01). These relationships could indicate the contribution of TTG ({$La/Yb)_N$ = 0.97; Condie, 1993) source for both of the sedimentary types. The large variation in Eu/Eu* (greywacke: 0.64-0.96; arkose: 0.61-1.02) together with more mafic nature of greywackes and more felsic nature of arkose could be explained by invoking mixing of TTG, granite and mafic rocks in different proportions. It appears that the studied sedimentary rocks were derived from mixing of debris of felsic composition from distal sources to that of mafic composition from local sources, probably derived from a magmatic arc. These characteristics suggest the derivation of debris from young undifferentiated arc material (McLennan et al., 1990).

With the identification of mafic rocks, granite and TTG as possible source rocks of studied sedimentary sequence, an attempt can be made to constrain the contribution of these components. In recent years simple mixing calculation have been performed by many workers (e.g. Osae et al., 2006; Roddaz et al.,2007; Absar et al., 2009; Raza et al., 2010a, 2010b) using REE data. To determine the relative contribution of these end members to overall composition of studied Greywackes and arkoses, simple mixing calculations are performed. The purpose is to search for best fit solution to reproduce the observed REE patterns of these rock types. The greywacke samples are best modelled with a mixture of 50% TTG, 40% basalt, and 10% granite (Fig. 10). To constrain the contribution of various source rocks, the trace element modelling is attempted, also for the studied arkose samples. The shape of trace element pattern (Fig. 11) of average arkose samples is closely similar to that of modelled pattern. However, the overall trace element abundances are lower in arkose relative to modeled mixture. This is because of the fact that the trace element abundances have been reduced due to quartz dilution.

Although the modelling gives only an idea about the approximate contribution by possible end members, it provides convincing evidence to distinguish the types of rocks which supplied the debris to the sedimentary basin. Our modelling suggests that minor amount of granitic (or Rhyolitic) material must have been in existence during the time of deposition of sedimentary rocks of Mauranipur-Babina greenstone belt.

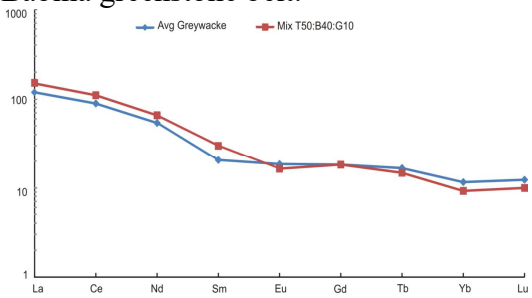

Figure 10: Chondrite –normalized REE patterns of greywacke from Mauranipur-Babina greenstone belt of the Bundelkhand craton compared with estimated best- fit source composition (Mixing results : 50%TTG, 40% basaltic rocks, 10% granites) See table 3.

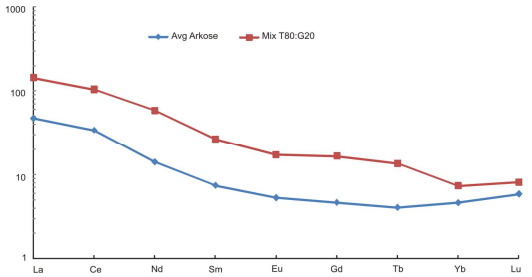

Figure 11: Chondrite –normalized REE pattern of Arkoses from Mauranipur-Babina greenstone belt of the Bundelkhand craton compared with estimated best- fit source composition (Mixing results : 80%TTG and 20% granites), See table 3.

Tectonic setting

The immature nature of studied rocks, low degree of weathering in their source region and minor sorting influence on the detritus are the features which suggest high rate of erosion, rapid sedimentation, potentially marked relief and short distance transportation of the debris. These features indicate a tectonically active setting of sedimentation where the sedimentary basin received detritus from terrains that were actively being eroded during the entire period of sedimentation. According to K_2O/ Na_2O versus SiO_2 diagrams (Fig.12) of Roser and Korsch (1988) and Th-Sc-Zr/10 triangular diagram (Fig.13) of Bhatia and Crook (1986), our samples appear to have been deposited predominantly in an active continental arc setting. High values of $(La/Yb)_N$ ratios and concave upward patterns of HREEs, shown more prominently by the samples of arkoses, further attest the derivation of studied sedimentary rocks from a source containing TTG (e.g Huang et al., 2010) that are thought to form above subduction zones (Drummond and Defant, 1990; Van Boening et al., 2008).

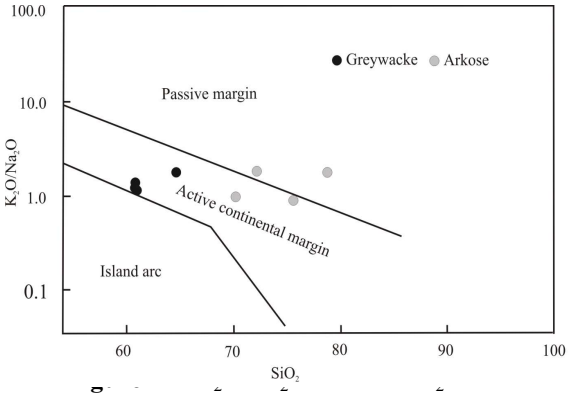

Roser and Korsch (1988), the analysed greywacke and arkose sediments of the Bundelkhand craton predominantly occupies active continental arc settings.

These features lead to suggest that the basin evolved through contemporaneous sedimentation of immature sediments derived from 1) A young craton evolved through accretion and tectonic amalgamation of continental arcs consisting TTG and granitic batholiths and 2) Mafic volcanic rocks derived from syn-depositional volcanic centres in an active tectonic environment.

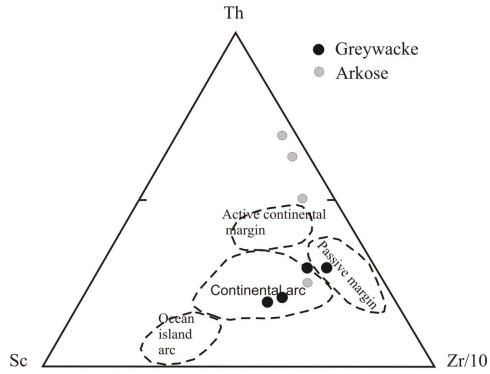

Figure 13: Th-Sc-Zr/10 after Bhatia and Crook (1986), the analysed greywacke and arkose sediments of the Bundelkhand craton predominantly occupies active continental arc settings.

Conclusions

The Archaean clastic sedimentary rocks, occurring in parts of Mauranipur-Babina greenstone of the Bundelkhand craton of the central India are geochemically classified as greywacke and arkose.

The source terrain suffered low degree of weathering indicative of non steady weathering conditions where active tectonism and uplift lead erosion of all soil horizons and rock surfaces. These trends indicate high erosion rate coupled with short distance rapid sedimentation in a tectonically active basin.

The provenance analyses based on geochemical characteristics suggest the derivation of greywacke from a terrain comprising 50%TTG, 40% mafic volcanic rocks and 10% granite. The arkose were derived from a source region consisting 80%TTG and 20% granite.

The basin experienced contemporaneous sedimentation of immature detritus derived from a young craton consisting TTG and granitic batholiths and syn-depositional volcanic centres in an active tectonic environment.

Acknowledgements:

The authors are thankful to the Chairman, Department of Geology, Aligarh Muslim University for providing necessary facilities for this work. First author is also thankful to Dr. P.R. Golani, Deputy Director General, Geological Survey of India, for his immense guidance. The financial assistance provided by the Department of Science and Technology, Ministry of Science and Technology, Government of India is thankfully acknowledged (SR/S4/ES 469/2009).

References:

Absar, N., Raza, M., Roy, M., Naqvi, S.M., and Roy, A.K. (2009). Composition and weathering conditions of Paleoproterozoic upper crust of Bundelkhand craton, Central India: Records from geochemistry of clastic sediments of 1.9 Ga Gwalior Group: Precambrian Research, v. 168, p. 313–329. doi:10.1016/j.precamres.2008.11.001.

Absar, N. and Sreenivas B. (2015). Petrology and geochemistry of greywackes of the ~1.6 Ga Middle Aravalli Supergroup, northwest India: evidence for active margin processes. Intern. Geol. Rev. DOI: 10.1080/00206814.2014.999355

Armstrong-Altrin, J.S., Lee, Y.I., Verma, S.P., Ramasamy, S. (2004). Geochemistry of sandstones from the upper Miocene KudankulamFormation, southern India: Implications for provenance, weathering,and tectonic setting: Journal of Sedimentary Research, 74(2), 285-297.

Armstrong-Altrin, J.S., Verma, S.P. (2005). Critical evaluation of six tectonic setting discrimination diagrams using geochemical data of Neogene sediments from known tectonic setting: Sedimentary Geology, 177(1-2), 115-129.

Barovich, K.M. and Patchett, P.J. (1992). Behaviour of isotopic systematics during deformation and a metamorphism; an Hf, Nd and Sr isotopic study of mylonitized granite. Contrib. Mineral. Petrol., 109 (3), 386-393.

Barshad, I. (1966). The effect of a variation in precipitation on the nature of clay minerals formation in soils from acid and basic igneous rocks. Proceedings International Clay Conference, Jerusalem., 167-173.

Basu, A.K. (1986). Geology in parts of Bundelkhand granite massif, central India. Rec. Geol. Surv. India, v. 117 (part-2), pp. 61-124.

Bhatia, M.R. and Crook, K.A.W. (1986). Trace element characteristics of graywackes and tectonic setting discrimination of sedimentary basins. Contribution to Mineral. Petrol., 92, 181-193.

Cann, J.R. (1970). Rb, Sr, Y, Zr and Nb in some ocean floor basaltic rocks. Earth Planet Sci. Lett., 10, 7-11.

Chen, H. F., Song, S. R., Lee T. Q., Lowemark, L., Chi, Z. Q., Wang, Y., Hong, E. (2010). A multiproxy lake record from inner Magolia displays a late Holocene teleconnection between Central Asian and North Atlantic climate. Quaternary International, 227, 170-183.

Chen, H. F., Yeh, P. Y., Song, S. R., Hsu, S.C., Yang, T. N., Wang, Y., Chi, Z., Lee T. Q., Chen, M., T., Cheng, C. L., Zou, J.,and Chau Y. P. (2013). The Ti/Al molar ratio as a new proxy for tracing sediments transportation processes and its application in Aeolian and sea level change in East Asia. Jour. Asian Earth. Sc.73, 31-38.

Condie, K.C. (1997). Plate Tectonics and Crustal Evolution (4^{th}ed.). Butterworth Heinemann, Oxford., 282p.

Condie, K.C. (1993). Chemical composition and evolution of the upper continental crust: Contrasting results from surface samples and shales. Chem. Geol., 104, 1–37.

Condie, K.C. (2001). Mantle Plumes and Their Record in Earth History. Oxford, UK: Cambridge Univ. Press. 306 p.

Condie, K. C., Dengate, J. and Cullers, R. L. (1995). Behavior of rare earth elements in a Paleoweathering profile on granodiorite in the Front Range, Colorado, USA. *Geochimica et Cosmochimica Acta*, 59: 279-294.

Cox, R., Lowe, D.R. and Cullers, R.D. (1995). The influence of sediment recycling and basement composition on evolution of mudrock chemistry in the southwestern United States. Geochim. Cosmochim. Acta., 59, 2919-2940.

Crichton, J. G. and Condie, K. C. (1993). Trace-elements as source indicators in Cratonic

sediments – a case study from the Early Proterozoic Libby Creek Group, Southeastern Wyoming. Jour. Geol., 101 (3), 319-332.

Cullers, R.L., Barrett, T., Carlson, R., Robinson, B. (1987). Rare-earth element andmineralogic changes in Holocenesoil and stream sediment: a case study in the Wet Mountains, Colorado, USA. Chem. Geol. 63, 275–297.

Cullers, R.L., Basu, A., Suttner, L. (1988). Geochemical signatureof provenance in sand-size material in soils andstream sediments near the Tobacco Root batholith, Montana, USA. Chem. Geol. 70, 335–348.

Cullers, R.L. (1994). The control on the major and trace element variation of shale, siltstones and sandstones of Pennsylvanian-Permian age from uplifted continental blocks in Colorado to platform sediment in Kansas, USA. Geochim. Cosmochim. Acta., 58, 4955-4972.

Cullers, R.L., Podkovyrov, V.M. (2000). Geochemistry of the mesoproterozoic Lakhanda shales in southeastern Yakutia, Russia: implications for mineralogical and provenance control, and recycling. Precambrian Res. 104, 77–93.

Cullers, R.L. (2000). The geochemistry of shales, siltstones, and sandstones of Pennsylvanian–Permian age, Colorado, USA: implications for provenance and metamorphic studies. Lithos 51, 181–203.

Defant, M.J., Recherson, P.M., de Boer, J. Z., Stewart, R. H., Maury, R. C.,Bellon, H., Drummand, M. S., Feigenson, M.D. and Jackson, T. E. (1991). Dacite genesis via slab melting and differentiation : petrogenesis of La YeguadaVolcanic Complex, Panama. Jour. Petrol. 32, 1101-1112.

Dickinson, W.R. (1970). Interpreting detrital modes of greywacke and arkose. Jour. Sedi. Petro., v. 40, pp. 695-707.

Dickinson, W.R. (1985). Interpreting provenance relations from detrital modes of sandstone.
In: Zuffa, G., (*ed*.), Provenance from Arenites, pp. 333-361, Reidel, Dordrecht.

Dickinson, W.R. and Suczek, C.A. (1979). Plate-tectonics and sandstones composition. Amer. Assoc. Pet. Geol. Bull., 63, 2164-2182.

Drummand, M. S., Defant, M. J. (1990). A mode for trondhjemite-tonalite –dacite genesis and crustal growth via slab melting : Archaen to modern comparison. Jour. Geophys. Res. 95 B, 21503- 21521.

Fatima, **S**., and Khan, M.S. (2012). Petrographic and geochemical characteristics of Mesoproterozoic Kumbalgarh clastic rocks, NW Indian shield: Implications for provenance, tectonic setting, and crustal evolution: International Geology Review, v. 54, p. 1113–1144. doi:10.1080/00206814.2011.623032.

Fedo, C. M., Eriksson, K. A. and Krogstad., E. J, (1996). Geochemistry of shales from the Archaean (~3.0) Bhuwa Greenstone belt, Zimbabwe: Implications for provenance and source - area weathering. Geochim. Cosmochim. Acta., 60, 1751-1763.

Fedo, C.M., Young, G.M., Nesbitt, H.W. and Hanchar, J.M. (1997). Potassic and sodic metasomatism in the Southern Province of the Canadian Shield: Evidence from the Paleoproterozoic Serpent Formation, Huronian Supergroup, Canada. Precamb. Res., 84, 17-36.

Ferry, J.M. (1983). Mineral reactions and element migration during metamorphism of calcareous sediments from the Vasseboro formation, South-Central Maine. Amer. Mineral., 68, 224-354.

Folk, R.L. (1980). Petrology of Sedimentary Rocks. Hemphill Austin, Texas, 182p.

Gao, S. and Wedepohl, K. H. (1995). The negative Eu anomaly in Archean sedimentary rocks: implications for decomposition, age and importance of their granitic sources. Earth Planet. Sci. Lett., 133, 81–94.

K. Govidaraju, (1994). Compilation of working values and sample discrimination for 383 geostandards. Geostandard newsletter, volume 18, issue supplement S1, pages 1-158, July 1994.

Gromet, L. P., Dymek, R.F., Haskin, L. A. and Korotev, R. I. (1984). The North Amerikan shale composit: Its composition, major and trace element characteristics Geochim. et Cosmochim Acta, 48, 2469- 2482.

Gu, X. X., Liu, J. M., Zheng, M. H., Tang, J. X. and Qi, L. (2002). Provenance and tectonic setting of the Proterozoic turbidities in Hunan, South China: Geochemical evidence. Jour. Sed. Res., 72, 393–407.

Hayashi, K., Fujisawa, H., Holland, H., Ohmoto, H. (1997). Geochemistry of ~ 1.9 Ga sedimentary rocks from northeastern Labrador, Canada. Geochim. Cosmochim. Acta., 61, 4115-4137.

Herron, M. M. (1988). Geochemical classification of terrigenous sands and shales from core or log data: Journal of

Sedimentary Petrology, v. 58, no.5, p. 820- 829

Hessler, A. M., Lowe, D. R., and Jones, R. L. (2004). A lower limit for atmospheric carbon dioxide levels 3.2 billion years ago. *Nature* 428, 736-738.

Hofmann, A. (2005). The geochemistry of sedimentary rocks from the Fig Tree Group, Barberton greenstone belt: Implications for tectonic, hydrothermal and surface processes during mid-Archaean times. *Precamb. Res.* 143-23-49.

Hofmann, A., Bolhar, R., Dirks,P. H. G. M. Jelsma, H. A. (2003). The geochemistry of Archaean shales derived from a mafic volcanic sequence , Belingwe greenstone belt , Zimbabwe: pprovenance, source area unroofing and submarine versus subaerial weathering. Gechim. Cosmochim. Acta 67, 421-440

Huang, X. L., Niu, Y., Xu, Y. G., Yang, J. Q., Zhong, J. W. (2010). Geochemistry of TTG and TTG- like gneisses from Lushan- Taihua Complex in the southern North China craton: implications for late Archaean crustal accretion. Precamb. Res. V. 182, pp. 43-56.

Humphris, S.E. (1984). The mobility of rare earth elements in the crust. In: Henderson P. (Edit.) Rare Earth Element Geochemistry. Amster. Elsev., 317 -342.

Johnsson, M.J. (1993). The system controlling the composition of clastic sediments. In: Processes Controlling the Composition of Clastic Sediments (Eds. M.J. Johnsson and A. Basu), Geol. Soc. Amer. Spec. Paper., 284, 1–19.

Kasting, J. af. (1993). Earth's early atmosphere Science, 259, 920-926.

Knauth, L. P. and Lowe, D. R. (2003). High Archaean climatic temperaturesinferred from oxygen isotope geochemistry of chert in the 3.5 Ga Swaziland Supergroup South Africa. Gel. Soc. Amer. Bull. 115, 566-580.

Kaur, P., Armin Zeh, Naveen Chaudhri. (2014). Characterisation and U–Pb–Hf isotope record of the 3.55 Ga felsic crust from the Bundelkhand Craton, northern India. Precambrian research, V. 255, page 236-244

Lahtinen, R. (2000). Archaean-Proterozoic transition: geochemistry, provenance and tectonic setting of metasedimentary rocks in central Fennoscandian Shield, Finland. Precamb.Res., 104, 147-174.

Malviya, V.P., Arima, M., Pati, J.K. and Kaneko, Y. (2004). First report of metamorphosed basaltic pillow lava from central part of Bundelkhand craton, India: An Island arc setting of possible Late Archaean age. Gond. Res. v. 7, pp. 1338-1340.

Malviya, V.P., Arima, M., Pati, J.K. and Kaneko, Y. (2006). Petrology and geochemistry of metamorphosed basaltic pillow lava and basaltic komatiite in Mauranipur area: subduction related volcanism in Archean Bundelkhand craton, Central India. Jour. Mineral. Petrol. Sci., v. 101, pp. 199-217.

Manikyamba, C., Kerrich, R., González-Álvarez, I., Mathur, R., and Khanna, T.C. (2008). Geochemistry of Paleoproterozoic black shales from the Intracontinental Cuddapah basin, India: Implications for provenance, tectonic setting, and weathering intensity: Precambrian Research, v. 162, p. 424–440. doi:10.1016/j.precamres.2007.10.003.

Maravelis and Zelilidis, (2009). Petrography and geochemistry of the late Eocene–early Oligocene submarine fans and shelf deposits on Lemnos Island, NE Greece. Implications for provenance and tectonic setting. Volume 45, Issue 4, pages 412–433, July/August 2010.

Meinhold, G., Kostopoulos, D. and Reischmann, T. (2007). Geochemical constraints on the provenance and depositional setting of sedimentary rocks from the islands of Chios, Inousses and Psara, Aegean Sea, Greece: implications for the evolution of Palaeotethys. Journal of the Geol. Soc. London., 164, 1145–1163.

McDonough, W.F. and Sun, S.-S. (1995). Composition of the Earth. Chemical Geology 120: 223-253.

McLennan, S.M. (1989). Rare earth elements in sedimentary rocks. Influence of provenance and sedimentary processes. Reviews in Mineralogy., 21, 169-200.

McLennan, S.M., W.B. Nance and S.R. Taylor. (1980). Rare earth element-thorium correlations in sedimentary rocks and the composition of the continental crust. Geochim. Cosmochim. Acta., 44, 1833-1839.

McLennan, S.M., Taylor, S.R. and Kroner, A. (1983). Geochemical evolution of Archean shales from South Africa I, the Swaziland and Pogola Supergroups. Precamb. Res., 22, 93-124.

McLennan, S.M., Hemming, S., McDaniel, D.K. and Hanson, G.N. (1993). Geochemical approaches to sedimentation, provenance and tectonics. In: Johnsson M.J. and Basu A,(eds.) Processes controlling the

composition of Clastic sediments. Geol. Soc. Amer. Spec. Paper., 284, 21-40.

McLennan, S.M., Hemming, S., Taylor, S.R. and Erikson, K.A. (1995). Early Proterozoic crustal evolution: Geochemical and Nd-Pb isotopic evidence from metasedimentary rocks southwestern North America. Geochim. Cosmochim. Acta., 59, 1153-1173.

McLennan, S.M., Taylor, S.R., McCulloch, M.T., and Maynard, J.B. (1990). Geochemical and Nd-Sr isotopic composition of deep sea turbitites: crustal evolution and plate tectonic associations. Geochim. Cosmochim. Acta., 54, 2015-2050.

Mondal, M.E.A., Goswami, J.N., Deomurari, M.P., Sharma, K.K. (2002). Ion microprobe $^{207}Pb/^{206}Pb$ ages of zircon from the Bundelkhand massif, northern India: implications for crustal evolution of the Bundelkhand-Aravalli protocontinent. Precamb. Res., v. 117, pp. 85-100.

Mondal, M.E.A. and Zainuddin, S.M. (1996). Evolution of Archean-Palaeoproterozoic Bundelkhand massif, Central India-evidence from granitoid geochemistry. Terra Nova, v. 8, pp. 532-539.

Nagarajan,R., Madhacaraju, J., Nagendra, R., Amstrong-Altrin, J.S., Moutte, J. (2007). Geochemistry of Neoproterozoic shales of the Rabanpalli Formation, Bhima basin, Northern Karnataka, Southern India: Implication for provenance and paleoredox conditions. Revista Mexicana de Ciencias Geologicas 24(2). 150-160.

Nesbitt .H. W. (1979). Mobility and fractionation and rare-earth elements during weathering of a granodiorite. *Nature* 279, 206-210.

Naqvi, S. M., Condie, K. C., and Allen, P. (1983). Geochemistry of some unusual early Archaean sediments from Dharwar craton, India. Precamb. Res., *22*(1), 125-147.

Naqvi, S.M. and Hussain, S.M. (1972). Petrochemistry of early Precambrian metasediments from the central part of the Chitradurga schist belt, Mysore, India. Chem. Geol., 10, 109-135.

Naqvi, S.M. and Rogers, J.J.W. (1987). Precambrian Geology of India. Oxford monographs on Geology and Geophysics, 6, Oxford University press, Oxford, New York., 223.

Naqvi, S.M., Uday Raj, B., Subba Rao, D.V., Manikyamba C., Nirmal Charan, S., Balaram, V., Sarma, D.S. (2002). Geology and geochemistry of arenite-quartzwacke from the Late Archean Sandur schist belt - implications for provenance and accretion processes. Precamb.Res., 114, 177-197.

Nesbitt, H. W. (1979). Mobility and fractionation of rare earth elements during weathering of a granodiorite. Nature., 279, 206–210.

Nesbitt, H.W., Markovics, G. and Price R.C. (1980). Chemical processes affecting alkalies and alkaline earths during continental weathering. Geochim. Cosmochim. Acta., 44, 1659-1666.

Nesbitt, H.W., Young, G.M. (1982). Early Proterozoic climates and plate motion inferred from major element chemistry of lutites. Nature., 299, 715-717.

Osae, S., Asiedu, D., K., Banoeng-Yakubo, B., Koeberl, C. Dampare, S.B. (2006). Provenance and tectonic setting of Late Proterozoic Buem sandstones of southeastern Ghana: Evidence from geochemistry and detrital modes. Journal of African Earth Sciences 44, 85-96.

Passchier, C.W., Myers, J. S., Kroner, A. (1990). Field Geology of High grade Gneiss Terrains. Springer – Verlag., 150p.

Purevjav and Roser, (2013). Geochemistry of Silurian–Carboniferous sedimentary rocks of the Ulaanbaatar terrane, Hangay–Hentey belt, central Mongolia: Provenance, paleoweathering, tectonic setting, and relationship with the neighbouring Tsetserleg terrane. Chemie der Erde - Geochemistry (Impact Factor: 1.27). 12/2013; 73(4):481–493. DOI: 10.1016/j.chemer.2013.03.003

Pati, J.K., Patel S.C., Pruseth, K.L., Malviya, V.P., Arima, M., Raju, S., Pati, P. and Prakash K. (2007). Geochemistry of giant quartz veins from the Bundelkhand craton, central India and their implications. Jour. Earth Syst. Sci., v. 116, pp. 497-510.

Payne, J. L., Barovich, K. M. and Hand, M. (2006). Provenance of metasedimentary rocks in the northern Gawler Craton, Australia: implication for Paleoproterozoic reconstructions. Precamb. Res., 148, 275-291.

Pearce, J. A. (1996). A user's guide to basalt discrimination diagrams. In: Wyman, D. A. (ed.) Trace Element Geochemistry of Volcanic Rocks: Applications for Massive Sulphide Exploration. Geol. Asso. Canada., Short Course Notes, 12, 79–113.

Pettijohn, F.J., Potter, P.E. and Siever, R. (1972). Sand and Sandstone (Berlin: Springer-Verlag)., 241p.

Prasad, M.H., Hakim, A., and Krishna Rao, B. (1999). Metavolcanic and Metasedimentary inclusions in the Bundelkhand Granitic Complex in Tikamgarh district, MP: Journal of the Geological Society of India, v. 54, p. 359–368.

Purevjav, N and Barry Roser,B. (2013). Geochemistry of Silurian–Carboniferous sedimentary rocks of the Ulaanbaatarterrane, Hangay–Hentey belt, central Mongolia: Provenance, paleoweathering,tectonic setting, and relationship with the neighbouring Tsetserleg terrane. Chemie der Erde 73 (2013) 481– 493.

Rao, J.M., Rao, G.V.S.P., Widdowson, M. and Kelley, S.P. (2005). Evolution of Proterozoic mafic dyke swarms of the Bundelkhand Granite Massif, Central India. Curr. Sci. v. 88, pp. 502-506.

Ramakrishnan, M., and Vaidyanadhan, R. (2010). Geology of India, v. 1: Bangalore, Geological Society of India, 556 p.

Raza M., Bhardwaj V.R., Ahmad A.H.M., Mondal, M.E.A., Khan A. & Khan M. S. 2010.
Provenance and weathering history of Archaean Naharmagra quartzite of Aravalli craton, NW Indian Shield: Petrographic and geochemical evidence. Geochemical journal 44, 331-345.

Raza, M., Bhardwaj, V.R., Dayal, A.M., Rais, S and Khan, A. (2010b). Geochemistry of lower Vindhyan Clastic sedimentary rocks of Northwestern Indian shield: Implications for composition and weathering history of Proterozoic continental crust. Jour. Asian Earth. Sciences, 39, 51-61.

Roddaz, M., Debat, P. and Nikiema, S. (2007). Geochemistry of upper Birimian sediments (major and trace elements and Nd-Sr isotopes) and implications for weathering and tectonic setting of the Late Paleoproterozoic crust. *Precamb. Res*. 159, 197-211.

Roddaz, M., Viers, J., Brusset, S., Baby, P., and Herail, G. (2006). Controls on weathering and provenance in the Amazonian foreland basin: Insights from major and trace element geochemistry of Neogene Amazonian sediments. *Chem. Geol.* 226, 31-65.

Roser B.P. and Korsch R.J. (1986). Determination of tectonic setting of sandstone- mudstone suites using SiO_2 content and K_2O/Na_2O ratio. Jour. Geol., 94, 635-650.

Roser, B.P. and Korsch, R.J. (1988). Provenance signatures of sandstone- mudstone suits determined using discrimination function analysis of major- element data. Chemical geology 67, 119-139.

Roy, P.D., Smykatz-Kloss, W. (2007). REE geochemistry of the recent playa sediments from the Thar desert, India : an implication to palaya sediment provenance. Chemie der Erde-Geochemistry 67, 55-68.

Saha L., Frei D, Gerdes A., Pati J. K., Sarkar S., Patole V., Bhandari A. and Nasipuri P. (2015) Crustal geodynamics from the Archaean Bundelkhand Craton, India: constraints from zircon U–Pb–Hf isotope studies. Geol. Mag. 153 (1), 2016, pp. 179–192. c_ Cambridge University.

Schieber, J., (1992). A combined petrographical-geochemical provenance study of the Newland Formation. Mid-Proterozoic of Montana. Geol. Mag., 129, 223-237.

Sinha, S., Islam, R., Ghosh, S. K., Kumar, R., anmd Sangode, S. J. (2007). Geochemistry of Neogene Siwalik mudstones along Punjab re-entrant, India: Implications for source-area weathering, provenance and tectonic setting. *Current Science*, 92 (8), 1103-1113.

Sugitani, K., Horiuchi, Y., Adachi, M., and Sugisaki, R. (1996). Anomalously low Al_2O_3/TiO_2 values of Archaean cherts from the Pilbara Block. Western Australia – possible evidence of extensive chemical weathering on the early earth: Precamb. Res., 80, 49-76.

Tarney, J. and Weaver, B. L. (1987). Geochemistry of the Scourian complex: petrogenesis and tectonic models. Geol. Soc., London Spec. Publ., 27, 45-56.

Taylor S. R. and McLennan, S. M. (1985). The Continental Crust: Its Composition and evolution, London, Blackwell., 311p

Tran, H.T., Ansdell, K., Bethune, K., Watters, B. and Ashton, K. (2003). Nd isotope and geochemical constraints on the depositional setting of Paleoproterozoic metasedimentary rocks along the margin of the Archean Hearne Craton, Saskatchewan, Canada. Precamb. Res, 123, 1-28.

Van Boening, A. M. and Nabelek, P.I. (2008). Petrogenesis and tectonic implications of Paleoproterozoic mafic rocks in the Black Hills, South Dakota. Precamb. Res.v.167, pp. 363-376.

Van de Kamp, P.C. and Leake, B.E. (1985). Petrology and geochemistry of feldspathic and mafic sediments of the northeastern Pacific margin. Transactions

of the Royal Society of Edinburg. Earth.

Verma S.K., Verma S.P., Oliveira E.P., Singh V.K. and Moreno J.A. (2016) LA-SF-ICP-MS zircon U–Pb geochronology of granitic rocks from the central Bundelkhand greenstone complex, Bundelkhand craton, India Journal of Asian Earth Sciences 118, 125–137.

Weaver, C.E. (1989). Clays, muds and shales. Amsterdam: Elsevier Newyork., 819p.

Windley, B. F. (1995). The Evolving Continents, 3rd ed. xvii + 526 pp. Chichester, New York, Brisbane, Toronto, Singapore: John Wiley & Sons. Price £19.99 (paperback). ISBN0471 917397.

Wronkiewicz D.J. and Condie, K.C. (1987). Geochemistry of Archean shales from the Witwatersrand Supergroup, South Africa: Source-area weathering and provenance. Geochimica et Cosmochimica Acta 51, 2401-2416.

Wronkiewicz D.J. and Condie, K.C. (1990). Geochemistry and mineralogy of sediments from the Ventersdorp and Transvaal Supergroups, South Africa: cratonic evolution during the early Proterozoic, Geochimica et Cosmochimica Acta 54 (2), 343-354

Yamammoto, K., sugisaki R. and Arai, F. (1986). Chemical aspects of alteration of acidic tuffs and their application to siliceous deposits. Chem.Geol. 55, 61-76

First online volume
Jour. Indian Association of Sedimentologists, Vol. 35, No. 1 (2018), pp.77-88
ISSN 0970-3268

Paleocurrent, Deformation and Geochemical studies of Lower part of the Bagalkot Group of Kaladgi Basin at Ramthal and Salgundi: Implications on Sedimentation History

Meghana Devli* and Kotha Mahender**
*Department of Geology, Parvatibai Chowgule College (Autonomous), Margao Goa 403 602, India.
e-mail: msd00153@gmail.com
**Department of Earth Science, Goa University, Taleigao Goa, India

Abstract: The lithounit **c**onglomerate of the thickness about 6m - 30m is seen exposed at Ramthal and Salgundi belonging to the Salgundi Conglomerate Member of the Ramdurg Formation in the Bagalkot Group of the Kaladgi-Badami sequence of rocks. Even though this basin is studied extensively by many workers on a larger scale, the minute intricacies have remained untouched. This includes studies on individual lithounit with respect to its lithological characters, textural features, provenance, deformation history, paleocurrent directions and mapping on a larger scale of the area. Therefore, this lowermost rock unit provides an opportunity to understand the paleocurrents, provenance and deformation history of the Mesoproterozoic Bagalkot Group. To understand this, field studies were combined with analytical studies to come to a conclusive result. To understand the deformation history of the area, field studies were combined with micro section observations. The deformational mechanisms of grain boundary migration, overgrowths in crystallographic continuity, recrystallisation of quartz, neocrystallisation of micas, indicate the deformation involved a low temperature (<300°C) regime. Further, based on the imbrications of the pebbles observed in the field and reconstruction to a prefolding position of the limbs of the fold based on the dip directions recorded at two places Ramthal (dipping North) and Salgundi (dipping South) suggests the upstream side of the basin to be probably towards the western side of the basin. The rock is mineralogically matured with abundance of silica varieties and lack in feldspars. While percentage of Fe_2O_3 increases along with SiO_2 at both places that of Al_2O_3, K_2O, CaO and Na_2O is much less. The $Al_2O_3+Na_2O+K_2O$ versus SiO_2 plot indicates Compositional Maturity Index is relatively higher at both the study areas suggesting removal or lack of mobile elements like Na_2O and MgO. The lower concentrations of U and Th in the samples with lower ΣREE probably reflects a control by grain size fractionation during transport suggest a contribution from a mafic source with lesser concentration of such elements. Bivariant log/log plot of the ratio of Qp/F + R values represent the region to have been a moderate to low lying plain experiencing hot, tropical, oxidizing, humid climatic conditions.
Keywords: Mesoproterozoic, provenance, deformation, imbrications

Introduction

The rock conglomerate has varied composition both with respect to the matrix as well as the framework clasts. Therefore, this rock can be used to decipher the provenance, paleocurrents, deformation history and thereby the tectonic setting of the area. A geochemical analysis of the matrix can throw more light on the provenances whereas the framework clasts can be used to deduce the paleocurrent directions. Provenance studies and prevailing paleocurrents provide an insight in understanding the physiography and climatic conditions of the region, as also, the geological history of the deposited sediments. A relationship can thus be drawn between the conglomerate composition and the conditions the prevailed in the source area. Penetrative features observed in the field in association with microscopic studies of the rock help to understand the deformation history of a region. A substantial study has been carried out on the Kaladgi-Badami basin occupying the northern part of the state of Karnataka by many workers, but still a lot remains to be studied with respect to individual lithounits, their large scale mapping, mineralogy, provenance and deformational history. Here, we make an attempt in putting forth a detailed study involving field and microscopic observations of the conglomerates from the Mesoproterozoic Member, the Salgundi Conglomerate of

Ramdurg Formation of the Bagalkot Group from the Kaladgi basin. These studies were used to understand how the paleoclimatic conditions that prevailed

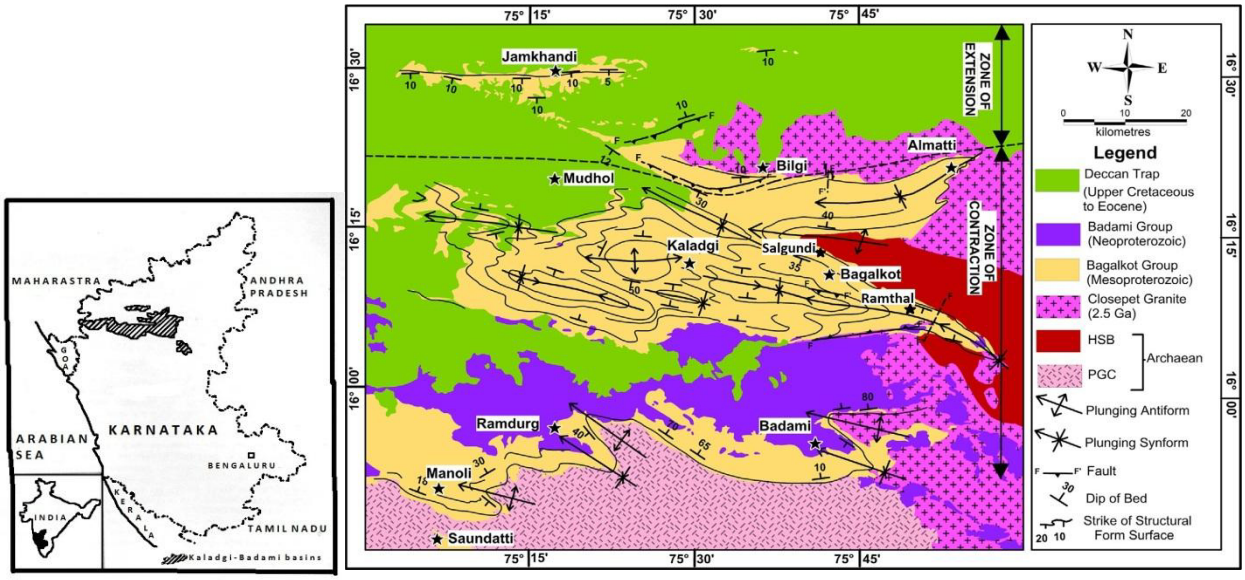

Figure 1: Geological and structural map of the Kaladgi-Badami basin (after Mukerjee et. al, 2016)

been divided into an older Bagalkot Group and an younger Badami Group. The two are separated by an angular unconformity (Kale and Pillai, 2011). Recent geochronological studies (Padmakumari et al, 1998; Balesh Kumar et al 1999) have indicated that the Bagalkot Group was deposited around 1800 + 100Ma supporting a previous suggestion of their Late Palaeoproterozoic age based on stromatolitic studies (Sharma et al., 1998). The Badami Group has been estimated to be of Neoproterozoic age based on trace fossil occurrences (Kulkarni and Borkar, 1997).

during their deposition and the source rock constituents had an effect on the composition of the rock. A geochemical analysis of the rock for the major oxides as well as trace and rare earth element concentrations are used to deduce the provenance based on discriminant functions and to determine the chemical maturity of the rock. An attempt is also made to relate the structural and primary features noted in the field and those observed in microsections to the tectonic history of the region and deduce paleocurrent directions respectively.

Geological setting of the Kaladgi basin

The Kaladgi sequence of rocks cover an area of 8300km2 occupying an East-West trending basin that stretches for nearly 500kms. They unconformably rest over the Archaean Peninsular Gneissic Complex and in turn are overlain by the Deccan Traps of Cretaceous-Eocene age (Jayaprakash et at., 1987; Figure 1).

The sedimentary sequence of the Kaladgi basin situated towards the northern borders of the Dharwar craton has

Basement rock at the study area

The basement rocks for the Kaladgi sequence of rocks include Peninsular Gneissic Complex (PGC) towards the south of the basin, Hungund Schist Belts (HSB) towards the eastern part and Granites (Closepet Granites) towards the North, central and south-eastern parts of the basin. In the study area the Mesoproterozoic sedimentary cover rocks rest unconformably over the Banded Hematite Quartzite of the Hungund Schist Belt (HSB).

The HSB, trending NW-SE extends from Ramagiri in the south to Hungund in the north (Naqvi et al., 2006) and forming one

of the components of the basement cratonic assemblage is exposed in the eastern part of the study area beneath the Kaladgi sedimentary cover rocks. The HSB is an assemblage of (1) metabasalts with minor metaultramafics (2) metasediments with intercalated basic and minor acid metavolcanics and (3) greywacke with intercalated Banded Iron Formations (BIF) (Roy, 1983). The metabasalts of the HSB are now represented by amphibolite, hornblende-chlorite schist, hornblende-plagioclase schist and hornblende-tremolite-actinolite schist. The metasediments (referred as metapelites) occur interbanded with metavolcanics as bands and lenses. They are mainly chlorite schist, quartz-chlorite schists and carbonaceous phyllites. The BIF horizons are 50-100m thick and occur as bands alternating with the metapelites. The components of BIF's include banded hematite quartzite (BHQ), chert and banded hematite jasper (BHJ) and ferruginous meta-argillites. The metapelites occur as thick horizons, exhibit thin compositional bands and are composed of muscovite, chlorite, and quartz. Lensoidal patches of polymictic conglomerates also occur within the metapelites with the long axis of the lens parallel to the compositional bands of the metapelites and are composed of hornblende, chlorite, plagioclase feldspars and minor amounts of quartz and iron oxides. The HSB is intruded by 5-10m thick gabbro dykes that are massive and are oriented E-W.

Mesoproterozoic sedimentary cover rocks at the study area

The areas of Ramthal, situated between latitude 16° 05'13"N to and longitude75° 52'29" E (Figure 2a); and Salgundi, located between 15°40'0"N to and longitude 76°50'0"E (Figure 2b) are chosen for the study as the rocks representing the lower part of the Kaladgi sequence are well exposed and represented here. While, exposures at Ramthal are over a small hillock with scanty vegetation, at Salgundi; the rocks are exposed over a ridge trending E-W.

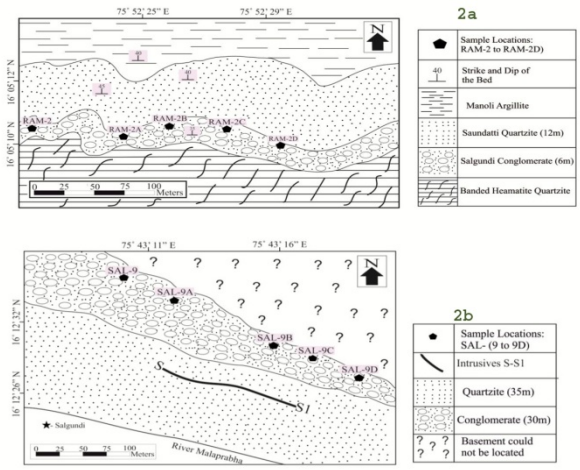

Figure 2: Geological and structural map along with sample locations at (a) Ramthal and (b) Salgundi.

At Ramthal, Banded Heamatite Quartzites of the Archaean Hungund Schist Belt exposed at the base of the hill are overlain successively by Mesoproterozoic conglomerates and quartzites having an East-West strike and a dip due North, while the conglomerate is about 6m thick, the overlying quartzites range upto 13m in thickness (Figure 3a). At Salgundi the underlying conglomerate is about 30m thick maintaining the same strike but dipping due South (Figure 3b).

Large cobbles and elliptical pebbles of jasper, chert, banded chert and banded hematite quartzite that are subrounded to subangular constitute the framework clasts of conglomerate (Figure 4a). These are bound within a ferruginous-siliceous matrix, are found to be clast-supported and show point contacts giving the sediment a grain-support fabric. The matrix has warped around the clasts at a few spots giving a folded structure (Figure 4b). The pebbles appear stretched and are elongated. On the vertical face their longer axis is oriented parallel and also, they are aligned imparting imbrication (Figure 4c). A vertical strike joint cuts through the matrix as well as the clasts of

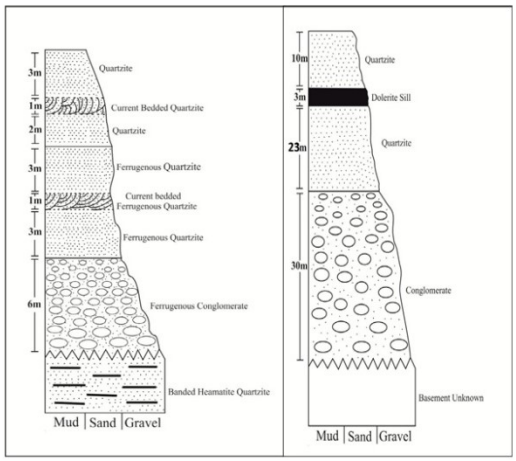

Figure 3: Lithologs at (a) Ramthal and (b) Salgundi

cryptocrystalline varieties of silica. The joint surface is straight and smooth with no evidence of shearing. Bedding joints are also prominent. The overlying quartzites are ferruginous marked by a sharp contact with the conglomerates and display cross-bedded structures on the vertical surface with the cross beds inclined towards west (Figure 4d).

The conglomerate exposed at Salgundi is compact, massive and polymictic with rounded to sub rounded cobbles and pebbles of banded chert, jasper, banded jasper, milky quartz, banded hematite quartzite (Figure 5a). The framework clasts are ovoid and elliptical ranging in size from 1cm to 18cms. These

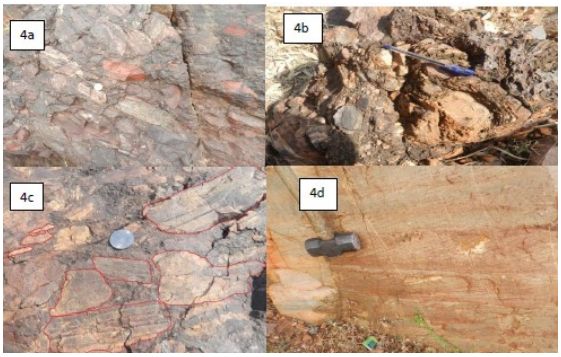

Figure 4: (a) Pebbly conglomerate with preferred orientation of the pebbles and cobbles (b) folding of the matrix around the pebble (c) Imbrications (d) cross bedding in quartzite at Ramthal

appear matrix-supported and oriented with their longer axis along the strike direction with imbrications (Figure 5b). The overlying quartzites constituted of

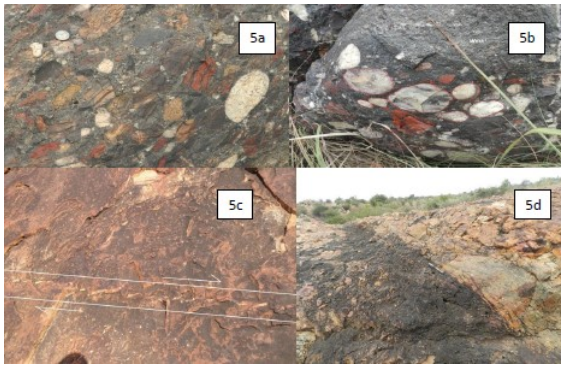

Figure 5: (a) Pebbly conglomerate showing stretched and preferred alignment (b) Imbrications (c) en echelon fractures (d) dolerite sill.

siliceous to ferruginous matrix are about 35m thick and much more massive and resistant. Apart from three prominent joints sets, en echelon fractures (Figure 5c) and box joints are significant. Many of these are filled with secondary silica. A thick vein of quartz cuts through quartzite, while several sills of dolerite ranging upto 3m in thickness (Figure 5d) intrude along the strike joint maintaining sharp contacts with the host rock. Shearing along the margin has led to intense fracturing and blocks of the rock are found trapped within the intrusive sills.

Sampling and Methodology

Fresh rock samples were collected at regular interval of 10 – 15m horizontally along the strata, as well as vertically wherever a change in texture was noticed. The collected field samples were cleaned with distilled water and dried to remove dust contamination for the purpose of analyses. Fifteen samples were selected for the purpose of micro section studies. Part of the matrix portion of selected rock samples was crushed to smaller pieces using a brass pestle and powdered to < 0.004mm size using an agate mortar and pestle, avoiding the larger clasts inorder to attain uniformity for the detection of major, trace and rare earth elements.

Six such powdered bulk rock samples were analyzed for major oxide analysis using X-ray Fluorescence machine; (Make Axios; Model PAN Alytical). For the study of major oxides 0.5gms of the dry powdered sample was weighed using an electronic balance. 5gms of Lithium Metaborate flux was added to the sample in a platinum crucible inorder to lower the temperature of melting. The sample was mixed thoroughly. It was then heated to a temperature of 250ºC for 2minutes inorder to ensure through mixing. Later the temperature was increased by 450ºC and heated for about 7minutes for the sample to melt completely. It was immediately poured into the platinum dish and allowed to cool forming a glass bead which was used for the purpose of analysis. For trace element and Rare Earth Element (REE) analysis six selected representative finely powdered samples were digested using the triple acid digestion (Jarvis, 1988). About 30mg samples were transferred to an acid mixture of HClO4 – HNO3 – HF in a clean Teflon beaker and digested on Q Block system at 200ºC. The addition of acid mixture was repeated to ensure the complete dissolution of samples. The solution was evaporated to incipient dryness. Finally the dry residue was dissolved in 2% HNO3 solution and made to a standard volume of 50ml. blanks were prepared and with addition of all ingredients and processes except for the addition of samples. Geochemical measurements were carried out using an Inductively Coupled Plasma-Mass Spectrometer (Agilent 7700x). Internal Standard Rhodium was added in all samples to estimate the recovery during the digestion process and the recovery was found to be excellent. Calibration was done by Inorganic Ventures Multi element Standards. Analytical precision was estimated using the digestion and analysis of USGS standard reference materials SGR-1b (Green River Shale), GSP-2 (Silver Plume Granodiorite) and NIST 688 (Basalt). Comparison with the certified values revealed excellent quality with the analytical error. Final concentration is given in ppm for all trace elements and for major elements it is given in %.

Petrographic studies

In the microsections of conglomerate from Ramthal subrounded clasts of quartz are seen enclosed within ferruginous matrix, also dispersed are grains of opaque minerals and cryptocrystalline silica. The quartz grains some of which are fractured show point as well as sutured contacts, with a thin film of iron oxide around them.

Microscopic observation of the conglomerate from Salgundi on the other hand shows angular to rounded quartz and cryptocrystalline silica with small flakes of muscovite mica within a ferruginous to siliceous matrix, along with opaque minerals. The mica flakes showing high interference colours are clustered around the larger clasts and appear oriented at high angles to the incipient cleavage (Figure 6a) and the quartz grain show signs of recrystallisation (Figure 6b). The

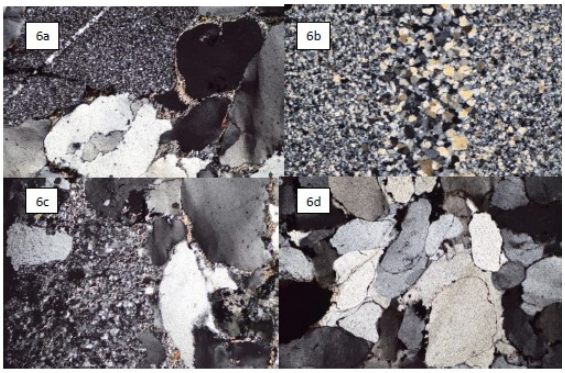

Figure 6: (a) Neocrystallisation of mica around detrital quartz at high angle (b) Recrystallisation of quartz seen as triple junctions at 120° (c) microfolding of mica indicating deformation assisted recrystallisation and neocrystallisation along with undulose extinction (d) overgrowths around quartz grains in crystallographic continuity. (Scale of photograph 10x = 1.54mm base of the photograph).

phyllosilicates are seen developing incipient microfolding seen as sub parallel alignment of the mica flakes (Figure 6c).

Overgrowth on quartz grains in crystallographic continuity is very significant (Figure 6d). Most of these grans exhibit sweeping undulose extinction. Thin sections of the rock from around the margin with the sills show highly angular fragments of quartz.

Bulk rock sample	SiO_2	TiO_2	Al_2O_3	FeOT	Fe_2O_3* adj	FeO adj	MgO	CaO	Na_2O	K_2O	P_2O_5	Total	Al_2O_3+K_2O+ Na_2O
RAM-2	92.12	0.05	0.55	6.32	2.19	4.37	0.06	0.09	0.06	0.13	0.03	99.40	0.74
RAM-2A	92.12	0.04	0.55	6.29	2.18	4.36	0.06	0.10	0.05	0.13	0.01	99.35	0.73
RAM-2B	92.11	0.04	0.55	6.31	2.19	4.37	0.06	0.09	0.07	0.13	0.02	99.37	0.75
RAM-2C	92.12	0.05	0.54	6.29	2.18	4.36	0.05	0.09	0.05	0.13	0.01	99.33	0.72
RAM-2D	92.14	0.05	0.54	6.29	2.18	4.36	0.05	0.08	0.06	0.12	0.02	99.35	0.72
SAL-9	83.32	0.187	3.98	8.21	2.92	5.83	0.48	0.09	0.26	0.28	0.03	105.58	4.52
SAL-9A	83.21	0.19	3.97	8.12	2.89	5.78	0.44	0.08	0.27	0.29	0.02	105.26	4.53
SAL-9B	83.28	0.182	3.89	8.19	2.92	5.83	0.48	0.08	0.26	0.25	0.03	105.39	4.4
SAL-9C	82.98	0.185	3.89	8.19	2.92	5.83	0.45	0.09	0.26	0.23	0.02	105.04	4.38
SAL-9D	83.54	0.179	3.67	8.21	2.92	5.83	0.50	0.08	0.26	0.24	0.03	105.45	4.17

Abbreviations: The subscript 'adj' refers to adjusted data (anhydrous 100% adjusted basis); FeOT = Total iron expressed as FeO. Iron split using Fe_2O_3/FeO ratio after Middlemost (1989).
Fe_2O_3* = Total Fe expressed as Fe_2O_3

Table1: Major oxide concentrations in weight percent (wt. %) for the Ramthal and Salgundi conglomerate

Bulk rock sample	Ag	Ba	Cd	Co	Ni	Cr	Cs	Ga	Mn	Pb	Rb	Sn
RAM-2	1.3167	15.200	0.2667	0.4333	23.05281	6.3000	0.1000	1.5333	3.9333	148.5833	1.4333	43.54785
RAM-2A	1.0500	17.9233	0.5167	0.4167	29.74832	6.7333	0.1167	1.4167	2.9167	182.5500	1.7000	58.28859
RAM-2B	0.6167	17.1833	0.3333	0.4167	28.11075	6.7333	0.1000	1.3333	2.9833	201.4667	1.6667	58.82736
RAM-2C	1.0833	17.3500	0.4833	0.5333	30.36667	7.2167	0.2333	1.7000	3.4167	210.7167	1.8333	64.28333
RAM-2D	1.0278	17.4562	0.4537	0.4125	29.3612	6.7834	0.1341	1.5646	3.5923	195.673	1.6789	58.7842
SAL-9	1.2000	52.7000	0.4500	2.3667	45.428	15.733	0.0667	3.8500	12.7667	234.6500	2.7833	87.24315
SAL-9A	1.3667	55.7333	0.3833	2.4333	42.578	18.050	0.0833	4.1667	12.5167	241.1667	2.7500	82.37113
SAL-9B	2.0667	52.8667	0.3833	2.2833	37.550	15.600	0.0833	3.8500	12.0167	221.9167	2.7000	66.87919
SAL-9C	1.2167	54.2167	0.4333	2.3833	42.897	15.600	0.0833	3.9000	12.7167	239.3333	2.7333	82.9862
SAL-9D	1.3657	55.7453	0.3562	2.4522	42.673	15.453	0.0835	3.8671	12.7682	245.924	2.7143	82.9780
UCC	50	30	0.098	17	44	85	550	17	-	17	112	5.5

Table 2: Trace-element concentrations in ppm for the samples from Ramthal and Salgundi conglomerate.

Bulk rock sample	Yb	Sr	Th	U	V	Cr/Th	Cr/V	Th/U	Th/Co	La/Co
RAM-2	0.082508	6.5833	1.5333	0.4500	2.4500	4.1087	2.571	3.407	3.538	3.807
RAM-2A	0.167785	8.4833	1.8333	0.5167	2.8333	3.6727	2.376	3.548	3.679	4.039
RAM-2B	0.09772	8.0500	1.5667	0.5167	2.7833	4.2977	2.419	3.032	3.759	3.959
RAM-2C	0.23333	8.2167	2.2667	0.6833	3.1000	3.1838	2.327	3.317	4.250	5.312
RAM-2D	0.09356	8.2011	2.1978	0.5280	2.9457	3.0864	2.303	4.1625	5.328	4.053
SAL-9	0.7833	22.4167	3.5500	0.8000	23.9333	4.431	0.657	4.438	1.499	3.619
SAL-9A	0.8167	22.4667	4.0333	0.8667	24.1667	4.475	0.747	4.653	1.657	3.788
SAL-9B	0.6833	22.0167	3.8167	0.8167	23.2667	4.087	0.670	4.673	1.671	3.832
SAL-9C	0.8500	22.6333	3.7167	0.8000	24.4000	4.197	0.639	4.645	1.559	3.699
SAL-9D	0.85612	22.4120	3.5894	0.8000	24.200	4.305	0.638	4.487	1.463	3.626
UCC	-----	-----	10.7	28	1.07					

UCC = Average Upper Continental Crust values, UCC (Taylor and McLennan, 1985)

Table 2 (contd): Trace-element concentrations in ppm for the samples from Ramthal and Salgundi conglomerate

Bulk rock sample	La	Nd	Sm	Eu	Dy	Yb	Gd	ΣREE	(La/Yb)n	(La/Sm)n	(Gd/Yb)n	Eu/Eu*
RAM-2	1.6500	2.9500	0.4333	0.1167	0.314	0.3167	0.37	6.1507	4.344	2.396	0.947	0.87
RAM-2A	1.6833	2.7333	0.5167	0.1500	0.436	0.3667	0.38	6.266	3.828	0.752	0.839	0.99
RAM-2B	1.6500	2.5667	0.5500	0.1000	0.261	0.3167	0.32	5.7644	4.344	1.888	0.251	0.68
RAM-2C	2.8333	3.6667	0.8000	0.3000	0.617	0.5333	0.76	9.511	1.626	2.229	1.155	0.58
RAM-2D	1.6720	2.9675	0.5326	0.1500	0.424	0.3320	0.28	6.358	1.541	1.973	0.68	0.34
SAL-9	8.5667	11.30	2.17	0.5667	1.045	0.599	1.23	25.478	9.66	2.48	1.66	0.97
SAL-9A	9.2167	12.35	2.25	0.6000	1.340	0.687	1.27	27.71	9.07	2.59	1.50	0.99
SAL-9B	8.7500	11.45	2.17	0.5833	1.091	0.587	1.23	25.86	10.07	2.54	1.69	0.99
SAL-9C	8.8167	11.68	2.33	0.6000	1.098	0.598	1.25	26.37	10.00	2.38	1.69	0.99
SAL-9D	8.8912	11.60	2.2	0.5922	1.095	0.600	1.55	26.52	10.01	2.54	2.09	0.93
Chondrite-normalised	0.367	0.711	0.231	0.087		0.248	0.306	1.644				
UCC	64	4.5	0.88	3.8		0.32	3.8	73.5				

Table 3: Rare Earth Elements concentrations in ppm for conglomerate from Ramthal and Salgundi.

Geo chemical studies

Geochemical studies with respect to major oxides, trace element, rare earth element analysis of the samples from Ramthal and Salgundi was used to deduce the provenance and weathering conditions of the source rocks and shown in table 1, 2 and 3 respectively. At both places the percentage content of SiO2 in the conglomerate is quite evidently high; it being 92.12% at Ramthal and 83.21% at Salgundi. While percentage of Fe2O3

increases along with SiO2 at both places that of Al2O3, K2O, CaO and Na2O are much less.

The lesser concentrations of the high-field-strength elements (HFSE) within the rock samples of the studied area were preferentially partitioned into melts during crystallization (Feng and Kerrich 1990), and as a result the mafic rock sources are depleted in these elements rather than felsic rock sources. Additionally, they are thought to reflect provenance compositions as a consequence of their generally immobile behavior (Taylor and McLennan 1985). In the samples analysed, concentrations of U (0.45 – 0.68ppm) and Th (1.53 – 2.2ppm) are found to be very low compared to UCC (U: 28ppm and Th: 10.7ppm; Taylor and McLennan, 1995).

Discussion

The conglomerates exposed in the two localities are resting over the Archaean Banded Iron Formation (BIF) giving the cherry red streak of hematite. Having been dated as of Post Archean age they are found to be matured, polymineralic and clast-supported. The crystalline and cryptocrystalline clasts of silica are well rounded and well sorted. There is also an apparent increase in the content of monocrystalline quartz and decrease in polycrystalline quartz. Microsections of the conglomerate from the study areas revealing the growth of mica around thedetrital quartz display pinning and microfolding. The minute mica flakes appear to be preferentially aligned. A rock cleavage has apparently developed through the interaction of heat and stress. Grains of quartz on being subjected to these factors show overgrowths in structural continuity. The process involving pressure solution transfer, recrystallisation and neocrystallisation subsequently resulted in elongation of the grains with their longer edges aligning parallel thereby generating incipient cleavage plane. The mica during the process has got oriented along an easiest direction to grow which was almost perpendicular to the cleavage. Such grain scale mechanisms are known to occur under low temperatures (<300°C) of deformation (Passchier and Trouw, 2005) suggesting the mega and micro structures observed in the conglomerate to have developed under a low temperature (<300°C) regime.

The percentage of SiO2 is expectedly high with the dominance of varieties of silica in the rock at both Ramthal and Salgundi indicating a mineralogical maturity. The high concentrations of FeO (6.29% at Ramthal and 8.12% at Salgundi as compared to UCC (4.49% , Taylor and McLennan, 2001) is due to dominance of iron oxides in the matrix. Also, lack of feldspars reflects in the neglible amounts of Al2O3, K2O, CaO and Na2O. The K2O/Al2O3 ratios in accordance are found to be low. Further, since the Al2O3+Na2O+K2O versus SiO2 plot indicates Compositional Maturity Index (CMI; Suttner and Dutta 1986; Figure 7) is relatively higher at both the study areas (Ramthal: 7.71 – 11 and Salgundi: 14.7 – 15) suggesting removal or lack of mobile elements like Na2O and MgO. Ti bearing opaque minerals in the conglomerate at Salgundi might be contributing to a relatively higher TiO2 (0.19%) than that at Ramthal (0.05%). The lower concentrations of U and Th in the samples with lower ΣREE probably reflects a control by grain size fractionation during transport, and may also suggest a contribution from a mafic source with lesser concentration of such elements.

Discrimination plots are drawn using various ratios of the oxides to determine the provenance for the sediments. In the discriminant function classification of provenance (Roser and Korsch, 1988) the plots fall in the mafic igneous field (Figure 8a). Based on ternary plots of Q-F-RF

(Quartz-Feldspars-Rock Fragments) of the framework clasts, the plots lie within a metamorphic domain (Figure 8b). In the Bivariant log/log plot of the ratio of Qp/F + R (Sutter and Dutta, 1986; Figure 9) the values represent the region to have been a moderate to low lying plain experiencing tropical humid climatic conditions. The underlying BIF and the hot, humid and oxidizing conditions that might have prevailed during and after the depositional history of the sequence must have been responsible for the ferruginous character of the rocks.

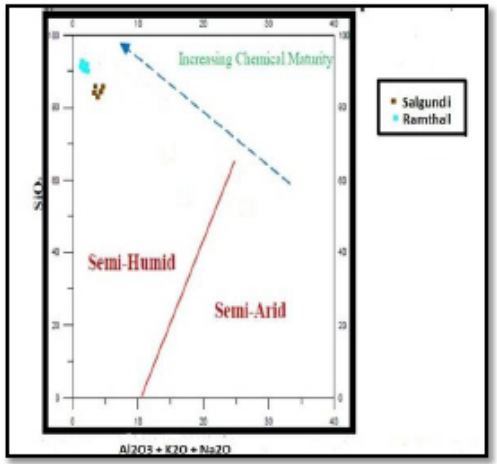

Figure 7: Plot of Al2O3+Na2O+K2O versus SiO2 indicating Compositional Maturity Index (CMI; Suttner and Dutta, 1986).

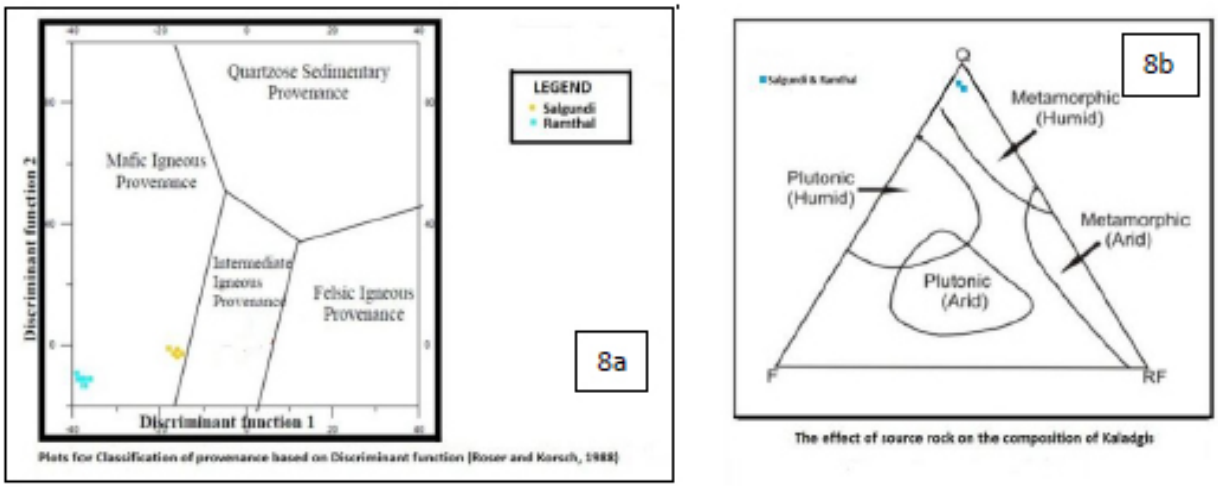

Figure 8: (a) Major element provenance discriminant function diagram for Kaladgi sediments (Roser and Korsch, 1988). The discriminant functions are for the ratio plots are: discriminant function 1 = 30.638 (TiO2/Al2O3) – 12.541 (Fe2O3*/Al2O3) + 7.329 (MgO/Al2O3) + 12.031 (Na2O/Al2O3) + 35.402 (K2O/Al2O3); discriminant function 2 = 56.5 (TiO2/Al2O3) – 10.879 (Fe2O3*/Al2O3)+ 30.875 (MgO/Al2O3) – 5.404 (Na2O/Al2O3) + 11.1112 (K2O/Al2O3) – 3.89 (b) the effect of source rock on the composition of the conglomerate at Ramthal and Salgundi.

The beds at Ramthal dip towards North, while at Salgundi they are inclined towards South. It is envisaged that the sedimentary succession at these two places represent parts of two limbs of a major synclinal fold, the river Malaprabha sinuating along the axis. Field observations of exposures report imbrication created by orientation of elongated pebbles both at Ramthal and Salgundi. At Ramthal the alignment suggests the upstream end to be towards east with paleocurrents flowing down west (Fig 4c &10). The overlying quartzites displaying cross-bedded structures have their cross-beds inclined westwards substantiating the westward flow of currents (Fig. 4d). The conglomerate at Salgundi on the other hand displays elongated pebbles whose orientation based on imbrications is suggestive of an eastward flow of paleocurrents with the upstream end towards west (Fig. 5b & 10).

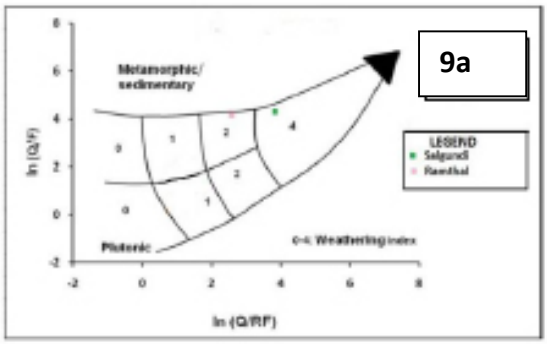

Semi-quantitative Weathering index		Physiography (relief) High (mountains) 0	Moderate (hills) 1	Low (plains) 2
Climate (precipitation) (semi) Arid and Mediterranean	0	0	0	0
Temperate subhumid	1	0	1	2
Tropical humid	2	0	2	4

9b

Figure 9: (a) Bivariant log/log plot of the ratio Qp/F+R versus Qt/F+R of the conglomerates at Ramthal and Salgundi. (Suttner and Dutta, 1986) (b) Log ratio after Weltje et al. (1998) Q=Quartz, F=Feldspar;, RF=Rock Fragments. Fields 1-4 refer to the semi-quantitative weathering indices deduced on the basis of relief and climate as shown in the table respectively.

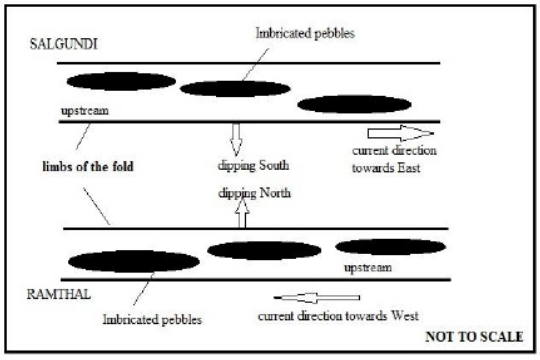

Figure 10 Paleocurrent directions based on imbrications

As observed in the field at Ramthal and Salgundi, the vertical face of the conglomeratic bed exhibits parallelism of the long axes of the elongated (prolate) pebbles. These axes are visibly parallel to the strike of the beds. The shorter axes accordingly, as seen on the surface are oriented in the direction of dip. Such a parallelism of the long axes of the pebbles is generated in water lain deposits. Smoothly flowing streams loaded with large sized pebbles, which are normally dragged along the floor of the channel, orient them during travel and bring about a parallelism of the axes on slowing down. On offloading this will create imbrication and the orientation thus developed will be in line with the direction of flow of the current.

Mukerjee *et al.,* (2016) suggest decoupling effect along a detachment surface, the unconformity acting as one in this case led to separation of the Mesoproterozoic sedimentary cover from the basement rocks in the Kaladgi basin (Fig. 11; Stage 3). A part that got detached from northern block on a regional high slid down southwards under gravity gliding to get compressed against the stable southern margin of the basin producing folds. The stable northern part remained stationary and undeformed maintaining its original tilt towards south. In the folded system that got created, the study areas of Ramthal and Salgundi occupy a synclinal fold. The northern limb of the fold on which Salgundi is located has maintained the original tilt (South) while the other limb (Southern-Ramthal) got rotated to reverse the tilt of the beds towards north as a result of the folding. On unfolding to revert to original prefolding position the southern limb would be in line with the northern limb to dip southwards. In accordance now, the paleocurrent direction at Ramthal deduced from the imbrication should be pointing towards east, in line with that observed at Salgundi where the beds have maintained original tilt. It can thus be inferred that the western side marks the upstream end and the paleocurrents moved down eastwards during the initial deposition of the sediments within the basin (Fig. 11).

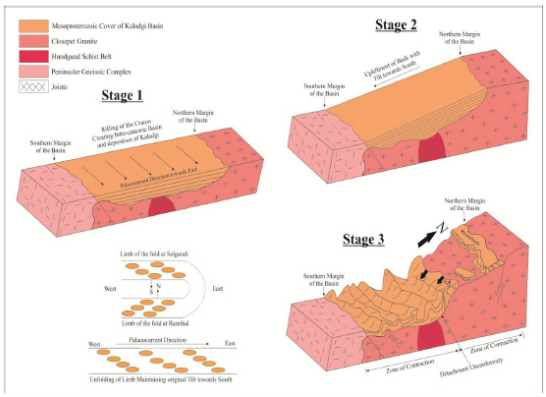

Figure 11 Schematic diagrams representing the depositional history along with paleocurrent directions

Conclusion

The conglomerate from Ramthal as well as Salgundi is oligomictic. It becomes monocrystalline in the direction of dip. The framework clasts of the size of cobbles and pebbles give a textural character to the rock. These are rounded to sub angular in nature and of a varied composition with constituents ranging from varieties of silica to rock fragments of BHQ. The size of the framework clasts suggests deposition having occurred along marginal parts of the basin with a proximity to the source area. The source from which the constituents were drawn must have been originally a mafic igneous rock which was later metamorphosed. Hot, humid and oxidizing conditions must have prevailed during the depositional history of the rock that underwent low temperature (<300°C) deformation The imbrications preserved within the conglomerates indicate paleocurrents to flow from east towards west at Ramthal (South of the basin) whereas at Salgundi (North of the basin) from west to east suggesting the basin to have been at a higher elevation towards the east. The transporting agency, which must have been a swiftly flowing stream having a sufficient velocity, would generally carry pebbles and boulders and align their longer axis in the direction of flow. Presence of cross-bedded feature in the immediately succeeding quartzites is a clear indication of the basin having been shallower at times.

Acknowledgement

The first author is grateful to faculty of Department of Geology, Savitribai Phule Pune University for allowing me to do the presentation of this paper at the National Conference on Sedimentation and Stratigraphy and XXXI Convention of Indian Association of Sedimentologists held on November 12-14, 2014. Gratitude to Prof. H S S Nadkarni, Associate Professor, Chowgule College for helping me with the field studies, discussion and observations. Thankful to the students who accompanied to the field especially Akshay Kelkar who helped in preparing the maps and lithologs. Gratitude to Dr Thamban Meloth and Dr Rahul Mohan, scientist at National Centre for Antarctica and Ocean Research for allowing to work on ICP-MS and SEM-EDS respectively. Sincere thanks to Dr G N Nayak, Professor, Department of Marine Science, Goa University for spending his valuable time in reading and suggesting improvements in the manuscript.

References

Balesh Kumar, B., Das Sharma, S., Dayal, A. M; And Kale, V. S. (1998). Occurrence of Tiny Digitate Stromatolite [Yelma Digitate Grey, 1984].Yargatti Formation, Bagalkot Group, Kaladgi Basin, Karnataka, India. Curr.Sci, 75, 360-365.

Bose, P. K., Sarkar, S., Mukhopadhyay, S., Saha, B And Erikson, P. (2009). Precambrian Basin-Margin Fan Deposits: Mesoproterozoic Bagalkot Group, India. Journal of Asian Earth Sciences, 34 (6)703-715.

Feng, R., and Kerrich, R. (1990). Geochemistry Of Fine-Grained Clastic Sediments In The Archean Abitibi Greenstone Belt, Canada: Implications For Provenance And Tectonic Setting. Geochim. Cosmochim. Acta, 54, 1061–1081.

Jayaprakash, A. V., Sundaram, V., Hans, S.K And Mishra, R. N. (1987) Geology Of The Kaladgi Badami Basin, Karnataka, In: Purana Basins Of Peninsular India (Middle

To Late Proterozoic)., Memoir 6, Gsi , 201-225.

Kale, V. S And Pillai, S. P., (2011). A Reinterpretation Of Two Chertbreccias From The Proterozoic Basins Of India. Jour. Geol. Soc. India., 78, 429-445.

Kulkarni, K. G And Borkar, V. D., (1997). On Occurrence Of Cochlichnus In The Proterozoic Rocks Of Kaladgi Basin. Gondwana Geol. Magz. 12, 55-59.

Taylor, S. And Mclennan, S. (1985). The Continental Crust, Its Composition And Evolution: Oxford, Blackwell, 311.

Tucker, E. M., (2011). Sedimentary Rocks In The Field: A Practical Guide. 4THEDITION, Wiley-Blackwell Publishing Company.

Mclennan, S. M And Taylor, S. R. (1991). Sedimentary Rocks And Crust Evolution: Tectonic Setting And Secular Trends; J. Geol. 99 1–21.

Mclennan, M. S. (2001). Relationships Between The Trace Element Composition Of Sedimentary Rocks And Upper Continental Crust. Geochemistry Geophysics Geosystems, American Geophysical Association. Vol. 2. Paper Number 2000GC000109 [8994 Words, 10 Figures, 5 Tables].

Middlemost, E. A. K. (1989), Iron Oxidation Ratios, Norms And The Classification Of Volcanic Rocks. Chem. Geol., 77, 19-26.

Mukherjee, M. K., Das, S., And Modak, K., (2016). Basement–Cover Structural Relationships In The Kaladgi Basin, Southwestern India: Indications Towards A Mesoproterozoic Gravity Gliding Of The Cover Along A Detached Unconformity. Precambrian Research, 281, 495-520.

Naqvi, S.M., Khan, R.M.K., Manikyamba, C., Rammohan, M., Khanna, T.C., (2006). Geochemistry Of The Neoarchaean High-Mg Basalts, Boninites And Adakites From The Kushtagi–Hungund Greenstone Belt Of The Eastern Dharwar Craton (Edc); Implications For The Tectonic Setting. J. Asian Earth Sci. 27, 25–44.

Padmakumari, V. M., Sambasiva, Rao., V. V And Srinivasan, R. (1998). Model Nd And Sb-Sr Ages Of Shales Of The Bagalkot Group, Kaladgi Supergroup, Karnataka. Nat. Symp. Late Quart. Geol And Sea Level Changes, Cochin University. Kochi Abst;70.

Passchier, C.W. And Trouw, R.A.J. (2005): Microtectonics (Second Ed.). Springer-Verlag, Berlin, Germany.

Roy, A., (1983). Structure And Tectonics In The Cratonic Areas Of North Karnataka. In: Sinha Roy, S. (Ed.), Structure And Tectonics Of The Precambrian Rocks, Hindusthan Publishing Company, New Delhi, 10, 81–96.

Roser, B. P. And Korsch, R. J. (1988). Provenance Signature Of Sandstone–Mudstone Suites Determined Using Discriminant Function Analysis Of Major Element Data; Chem. Geol. 67 119–139.

Sharma, M., Nair, S., Patil, S., Shukla, M., Kale, V.S., (1998). Tiny Digitate Stromatolite, Chitrabhanukot Formation, Kaladgi Basin, India. Current Science. 74, 360–365.

Suttner, L. J., And Dutta, P. K., (1986). Alluvial Sandstone Composition And Paleoclimate, I. Framework Mineralogy: Journal Of Sedimentary Petrology, V. 56, No. 3, P. 329-345.

Weltje, G.J., Meijer, X.D., Deboer, P.L. (1998). Stratigraphic Inversion Of Siliciclastic Basin Fills: A Note On The Distinction Between Supply Signals Resulting From Tectonic And Climate Foreing: Basin Research., V. 10, P. 129-153.

First online volume
Jour. Indian Association of Sedimentologists, Vol. 35, No. 1 (2018), pp.89-98
ISSN 0970-3268

Characterization of carbonaceous matter from sandstone type uranium deposits of Umthongkut-Wahkut, West Khasi Hills District, Meghalaya.

Asoori Latha*, Jitu Gogoi, M.B.Verma** and L.K.Nanda***
Atomic Minerals Directorate for Exploration and Research
AMD Complex, Begumpet, Hyderabad-500016, India.
AMD, Northeastern Region, Nongmynsong, Shillong-79300, India.
Email: asoori.latha@yahoo.com

Abstract: The strong association between uranium and carbonaceous matter, more so in sandstone type uranium deposits world over is well known. In India, sandstone type uranium deposits are mainly located in Meghalaya. Wahkut and Umthongkut constitute two prominent areas in Meghalaya Plateau hosting sandstone type U-mineralization in Lower Mahadek Sandstone of Cretaceous age. In order to evaluate the contribution of carbonaceous matter in U-mineralization in these areas, core samples of Lower Mahadek Sandstone were studied in terms of Total Carbon (TC), Total Organic Carbon (TOC) to understand the relation between uranium mineralization and carbonaceous matter. The carbonaceous matter samples were also taken up for Carbon-Hydrogen-Nitrogen- Oxygen analysis (CHNO) and Functional Group specification by Fourier Transmitted Infrared Spectrometer to decipher the nature of carbonaceous matter that helped in fixation of uranium.

Keywords: Carbonaceous matter, U-mineralization, Lower Mahadek Sandstone, Umthongkut-Wahkut.

Introduction

Sandstone type uranium deposits form significant part of the world uranium resources. They constitute about 18% of world uranium resources and 41% of known deposits (Uranium 2014). Meghalaya is the third uranium rich state in the country after Jharkhand and Andhra Pradesh, accounting for 10% of India's uranium reserves (World Nuclear Association website), with deposits estimated to be around 25,000 tones. The Upper Cretaceous sediments especially the Mahadek Formation of southern Meghalaya plateau of fluvial origin, has been proved as potential host for sandstone type uranium deposit. The area forms a narrow belt extending in the west from Balpakram, Garo Hills to the Lumshong, Jaintia Hills in the east running for almost 180 km and covering about ~1800sq km (Nandy, 2001, GSI, 1974, Sen et.al., 2002). Wahkut and Umthongkut constitute proven areas of U-mineralization in this provenance (Fig.1). Carbonaceous matter is a prime constituent of these sandstones and plays an important role in U-mineralization in these areas Dhanaraju et.al (1989), Kaul Ravi et. al (1990), Sengupta et. al (1991) and Mahendra Kumar et.al (2008). The present studies were carried out to ascertain the nature and role of carbonaceous matter in concentrating uranium mineralization in this particular lithological unit, by estimating Total Carbon (TC) and Total Organic Carbon (TOC) content of the samples and estimation of Carbon-Hydrogen-Nitrogen-Oxygen content. Analysis has been also carried out for the first time for identification of prime Functional Groups by Fourier Transmitted Infrared Spectrometer.

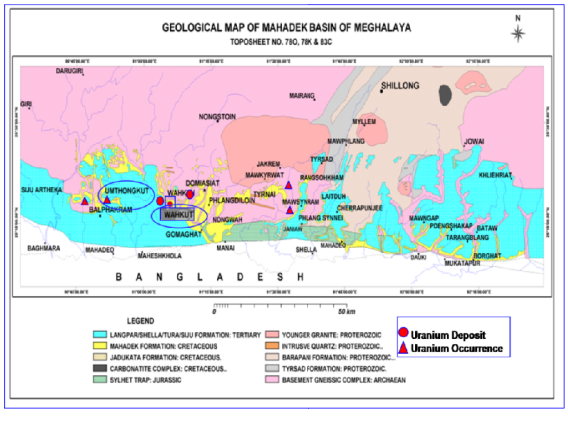

Figure.1 Geological Map of Mahadek Basin with locations of Umthongkut-Wahkut (http://www.amd.gov.in)

The basement rocks for these sediments are constituted by granite-gneisses of Archaean, Shillong Group rocks of Palaeo-Mesoproterozoic, intrusive granites of Neoproterozoic and Sylhet Trap of Jurassic. The lower members of this sedimentary sequence (Jadukata/ Mahadek of Upper Cretaceous period) comprise both fluvial (continental) as well as marginal marine sediments whereas the overlying upper members (Langpar and Shella) are mainly of marine origin (Table.1). The basement rocks are directly overlain by Lower Mahadek Formation at both Umthongkut and Wahkut areas.

Petrography

Lower Mahadek sandstone, based on its predominant clast composition and matrix content characterized as tuffaceous quartz wacke. These are matrix supported having poorly to moderately sorted, framework with angular to sub-angular clasts, fine to medium to coarse sand sized clasts with occasional gravel/ pebble sized clasts. Quartz forms the predominant clast component with subordinate feldspar. The clasts of quartz are mostly mono-crystalline with rare polycrystalline grains. The feldspar is represented by K-Feldspar (microcline, perthite) and minor plagioclase. It's content varies from rock

Geological Age	Group	Formation	Lithology
Miocene	Garo	Chengapara 700m	Sandstone, siltstone clay and marl
		Baghmara 530m	Feldspathic sandstone, conglomerate and clay shale, sandstone and marl
		Koipili-Rewak 500m	Shale, sandstone and marl
Eocene	Jaintia	Shella 600m	Alterntions of sandstone and limestone
Palaeocene		Langpar 50–100m	Calc shale, sandstone and impure limestone
Upper cretaceous	Khasi	Mahadek 215m	Upper: Coarse arkosic sandstone and shale (Purple colour typical)
			Lower: Grey, coarse to fine grained feldspathic sandstone, arkose.
		Jadukata 235m	Sandstone-conglomerate alternations
----------Unconformity----------			
Jurassic	Sylhet Trap		Basalt, Alkali basalt and acid tuff
			Alkaline rocks and carbonatite complexes
----------Unconformity----------			
Neoproterozoic	Mylliem		Coarse porphyritic granite, pegmatite, aplite and quartz vein. Epidiorite and dolerite
Mesoproterozoic	Shillong		Phyllite and quartzite sequence with basal conglomerate
----------Unconformity----------			
Archaean			Granite gneiss, migmatite, mica schist, sillimanite quartz schist, granulite

Table.1 Generalized Stratigraphic Succession of the Meghalaya Plateau (The succession is after Chottapadhyay and Hashimi (1984) and Ghosh et al.,(1991)

sample to rock sample and on the average constitutes ~ 20% of the total clast content (visual estimation). A few spangles of muscovite/ biotite are observed occurring in association with the matrix. The matrix consists of fine sized quartz, feldspar, chlorite, clay, tuffaceous matter and constitutes up to 25% of the rock by volume. It is frequently infiltrated by a hydrated iron oxide (limonite/ goethite). The tuffaceous matter is constituted by quartz of volcanic origin, defined by their shape, angularity and freshness; glass, devitrified shards and fine volcanic ash. The cement is mostly ferruginous with occasional carbonate cement. Zircon, monazite, xenotime, tourmaline, garnet and rutile are the heavy minerals present. Pyrite, ilmenite, magnetite, chalcopyrite, anatase, goethite, limonite, leucoxene and carbonaceous matter are the opaque phases noticed. Radioactivity is attributed to pitchblende replacing carbonaceous matter, coffinite, occurring in association with matrix frequently with pyrite, brannerite occurring as disseminated grains, adsorbed uranium occurring in association with carbonaceous matter/ matrix material/ leucoxenised ilmenite/ hydrated iron oxides.

Carbonaceous matter occurs as irregular streaks (Fig.2), seams and as globules, mostly occupying pore spaces (Fig.3 & 4). It is both radioactive and non-radioactive. Optically these two types show differences in color and reflectance. The non-radioactive carbonaceous matter is grey in color, comparatively lower reflectance, isotropic and takes a smooth polish (Fig.5). The radioactive species is generally brownish grey, comparatively higher reflectivity, shows faint reflection pleochroism and bi-reflectance and have

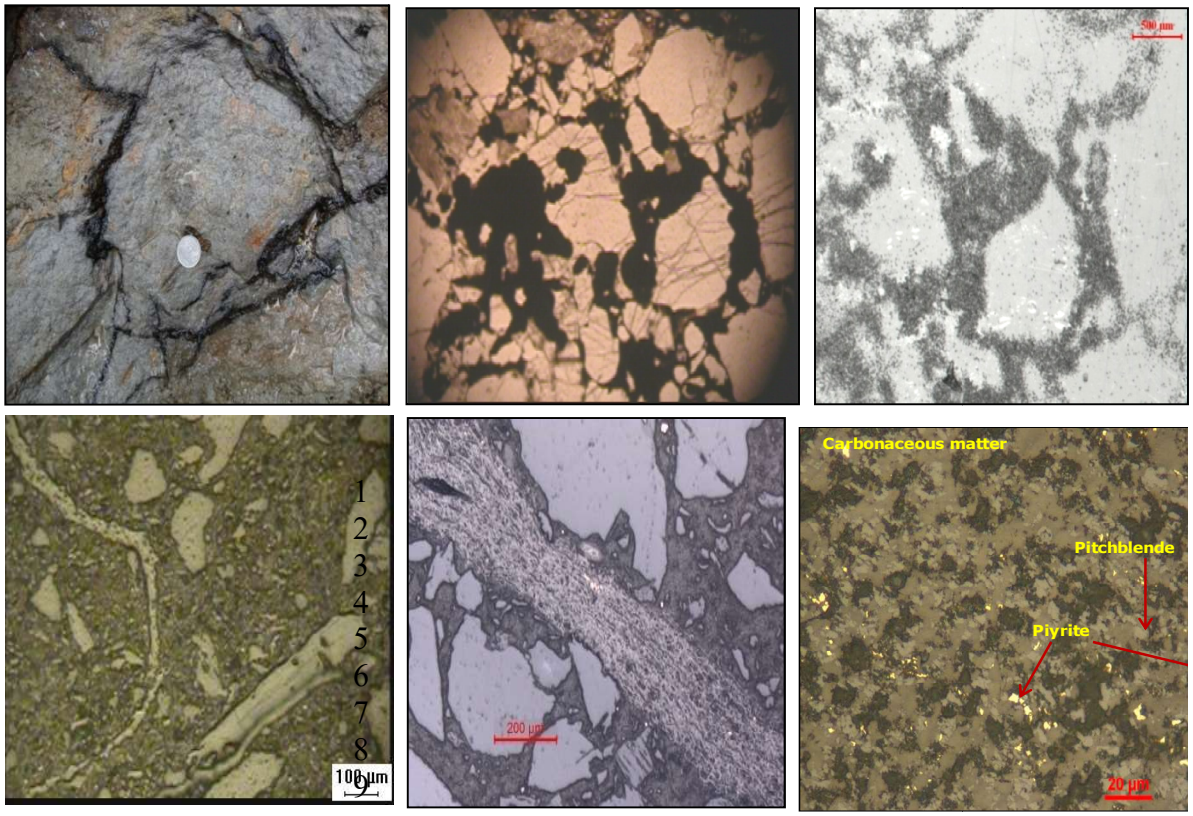

Figure.2 Carbonaceous matter occurring as irregular streaks in Lower Mahadek sandstone.
Figure.3 Radioactive carbonaceous matter along pore spaces of Lower Mahadek sandstone. Transmitted Light, 1 Nicol.
Figure.4 Alpha tracks on CN film corresponds to radioactive carbonaceous matter in Fig.3. Transmitted Light, 1 Nicol.
Figure.5: Non-radioactive carbonaceous matter. Reflected Light 1 Nicol.
Figure.6:Radioactive carbonaceous matter. Reflected Light 1 Nicol.
Figure.7: Pitchblende and pyrite replacing carbonaceous matter. Reflected Light 1 Nicol

Samples & Methodology

Lower Mahadek Sandstone contain variable amount of carbonaceous matter in dispersed state and is intimately associated with uranium bearing minerals. With an intention to ascertain the role of carbonaceous matter in fixing uranium, borehole core samples from different boreholes containing variable content of uranium, including non-mineralized zones were analyzed for Total Carbon (TC) and Total Organic Carbon (TOC). The carbonaceous matter samples were analysed for Carbon-Hydrogen-Nitrogen-Oxygen and Functional Groups by Fourier Transmitted Infrared Spectrometer.

A total of 25 core samples from Wahkut and Umthongkut area were analyzed by Elementar Liqui TOC-B instrument, Chemical Laboratory, AMD Hyderabad for Total Carbon (TC) and Total Organic Carbon (TOC). Sample was heated at 850^0C in a closed furnace in presence of Synthetic Air (Zero Air). Evolved CO2 was estimated by NDIR detector. TOC was estimated after acidolysis of the sample. The precession at 1% TC/TOC is ~10%. Radiometric analysis of borehole core sample for the estimation of uranium, U3O8, is done by beta gamma method, in Physics Lab of AMD, NER, Shillong. In this method, simultaneous beta and gamma radiations are measured. The PC based five channel counting system, consists of NaI (Tl) crystal (solid or well type) for gamma measurement with four single channel analysers and pancake type beta tubes for total beta counting. Based on the U_3O_8 content, the samples were classified into three groups; Group- I containing <100 ppm U_3O_8, Group- II containing 100 to 1000 ppm U_3O_8 and Group- III containing >1000 ppm U_3O_8, so as to understand the correlation between uranium mineralization and carbonaceous matter. Details of total carbon, total organic carbon and uranium content of are given in Table.2.

Sl. No	Sample No	% U_3O_8	% TC	% TOC
Samples with U_3O_8 content <100ppm				
1	WKT/C-43/BOX-1/11	0.003	0.61	0.3
2	WKT/C-43/BOX-1/12	0.003	0.49	0.29
3	WKT/C-43/BOX-3/123	0.006	0.57	0.34
4	WKT/C-43/BOX-3/124	0.005	0.62	0.35
5	WKT/C-43/BOX-4/144	0.002	0.52	0.31
6	WKT/C-43/BOX-4/147	0.002	0.67	0.39
7	WKT/C-43/BOX-5/203	0.002	0.73	0.48
8	UKT/C-57/B-1/20	0.002	0.79	0.49
9	UKT/C-57/B-1/42	0.001	0.74	0.44
10	UKT/C-57/B-1/43	0.001	0.6	0.33
	Av.	0.0027	0.634	0.372
Samples with U_3O_8 content 100 -1000ppm				
1	WKT/C-43/BOX-2/73	0.025	2.08	1.83
2	WKT/C-43/BOX-3/108	0.068	0.65	0.4
3	WKT/C-43/BOX-3/122	0.024	1.83	1.58
4	WKT/C-43/BOX-4/171	0.034	0.63	0.36
5	UKT/C-57/B-1/53	0.025	0.56	0.33
6	UKT/C-57/B-1/54	0.036	0.58	0.35
7	UKT/C-57/B-1/55	0.025	0.63	0.36
8	UKT/C-57/B-1/68	0.015	0.57	0.36

9	UKT/C-57/B-1/69	0.016	0.63	0.38
10	UKT/C-57/B-1/70	0.011	0.69	0.45
	Av.	0.0279	0.885	0.64
Samples with U_3O_8 content >1000ppm				
1	WKT/C-43/BOX-3/110	0.166	0.8	0.53
2	WKT/C-43/BOX-3/118	0.273	1.83	1.61
3	UKT/C-57/B-1/48	0.122	0.92	0.71
4	UKT/C-57/B-1/49	0.32	0.64	0.42
5	UKT/C-57/B-1/50	0.219	0.72	0.46
	Av.	0.22	0.982	0.746

Table.2 Uranium vs Carbon content

Twelve carbonaceous matter samples of radioactive (n=6) and non-radioactive (n=6) sandstone were analysed for Carbon-Hydrogen-Nitrogen and Oxygen (CHNO) at CSIR lab, Jorhat, Assam. The results are given in Table.3

Sl. No.	Sample No	C	H	H/C	N	O	Remarks
1	UKT/C-13/23	56.05	3.86	0.069	0.79	39.3	Samples collected from Radioactive horizon
2	UKT/C-30/16	43.01	2.75	0.064	0.6	53.64	
3	UKT/C-43/6	7.59	1.48	0.19	0.26	90.67	
4	WKT/C-45/95	80.68	4.41	0.06	1.03	13.88	
5	WKT/C-18A/135.20	68.79	4.4	0.064	0.87	24.09	
6	WKT/C-44/176.45	35.77	2.29	0.064	0.54	56.89	
	Average	48.65	3.20	0.085	0.68	46.41	
7	UKT/C-7/11	46.59	3.05	0.065	0.63	49.73	Samples collected from Non-Radioactive horizon
8	UKT/C-1/39	79.94	4.55	0.057	0.95	13.36	
9	UKT/C-15/11	28.86	1.54	0.053	0.42	69.18	
10	WKT/C-38A/B-2/51	61.23	3.82	0.062	0.85	33.18	
11	WKT/C-45/167.80	66.62	3.78	0.057	1.3	28.3	
12	WKT/C-42/228.85	80.63	4.7	0.058	3.8	10.87	
	Average	60.64	3.57	0.058	1.32	34.10	

Table.3 CHNO Analysis of carbonaceous matter

Similarly 12carbonaceous matter samples of Umthongkut (n=6) and Wahkut (n=6) were analysed for identification of Functional Groups by Fourier Transform Infrared Spectrometer (FTIR) at CSIR, laboratory, Jorhat, Assam. The study was carried out to decipher the presence of specific Functional Groups that play a key role in uranium fixation. The sample was ground to −200# BS before using it for FT-IR. The FT-IR spectrum was recorded in FT-IR Spectrophotometer Model 2000 (Perkin Elmer) with KBr pellet. The detector used was deuteratedtriglycinesulphate (DTGS). The total number of scans was 50 with the spectral resolution of 4 cm−1 during the recording of the spectra (Fig.8). The results indicate presence of similar functional groups in all the samples. The Functional Groups in carbonaceous matter are given in Table.4.

Sl.No	Sample No	Radiometric assay % U3O8
1	UKT/C-13/23	0.095
2	UKT/C-30/16	0.080
3	UKT/C-43/6	0.020
4	WKT/C-45/95	0.020
5	WKT/C-18A/135.20	0.045
6	WKT/C-44/176.45	0.085
7	UKT/C-7/11	<0.01
8	UKT/C-1/39	<0.01
9	UKT/C-15/11	<0.01
10	WKT/C-38A/B-2/51	<0.01
11	WKT/C-45/167.80	<0.01
12	WKT/C-42/228.85	<0.01

Absorption (cm^{-1})	Functional groups
3614.9	Phenols (O-H)
3421.5	Amines (N-H bond) & Phenols (O-H)
2959.7	Alkanes (CH_3, CH_2,CH)
2908.0	
2333.3	Alkynes (CΞC)
1632.1	Aromatic C=C, vinylic C=C
1458.0 1384.4	CH_2, and partly O-H, C=C group, Sulfoxide (S=O)
1118.4	C=S thiocarbonyl
1030.8	The peak between 1100 cm^{-1} to 400 cm^{-1} can be assigned to presence of clay minerals, quartz etc.
884.5	
855.9	
801.4	
752.6	
534.7	

Table.4 Functional Groups in carbonaceous matter

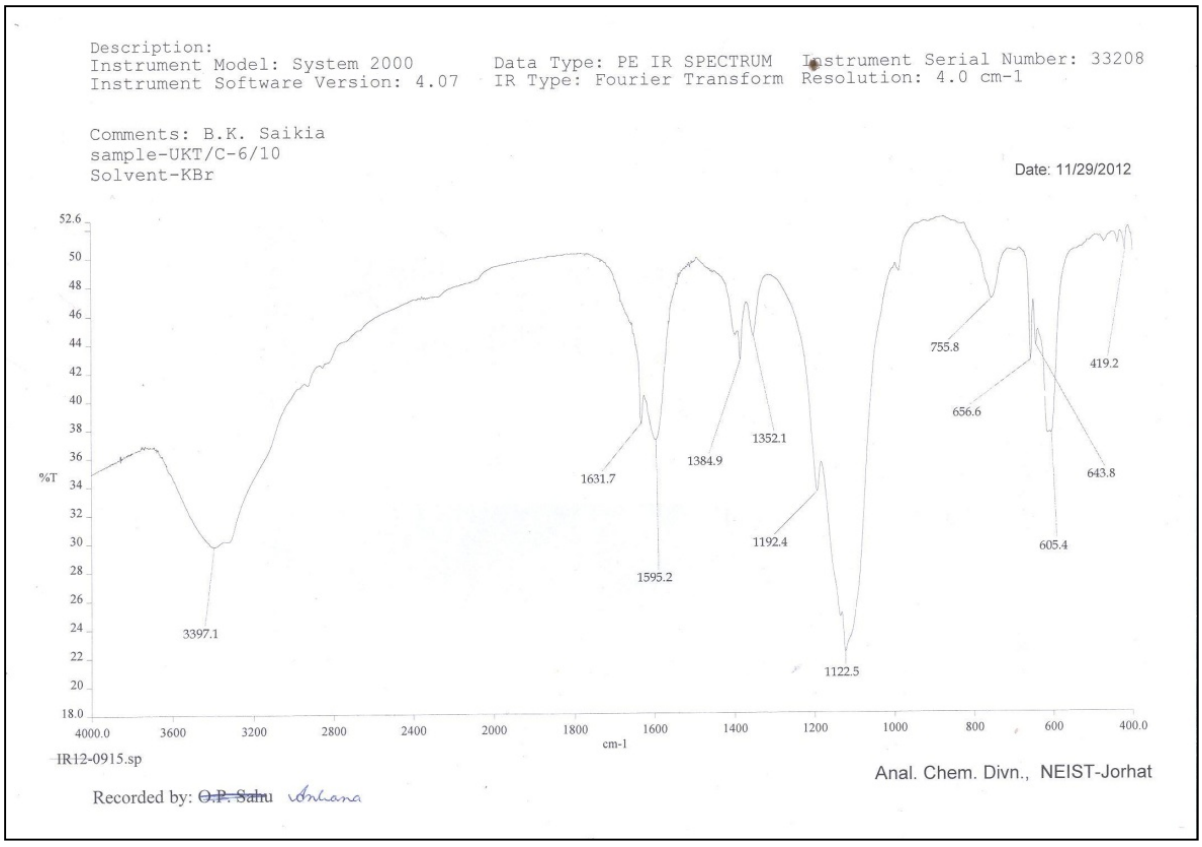

Figure.8 Representative spectra for FTIR

0
1

Discussion

The results obtained from Total Carbon (TC) and Total Organic Carbon (TOC) analysis show a positive correlation with uranium content,Table.5, Fig.9. The results clearly indicate that uranium content is more in the samples having more total carbon as well as total organic carbon. The Hydrogen/ Carbon (H/C) ratio for radioactive samples is more, average 0.085, (n=6), as compared to the non radioactive samples, average 0.058, (n=6), indicating more humic nature for the radioactive samples, which is in corroboration with Nash, 1981, who stated that the uranium has the strongest affinity for humic materials. Besides, the Oxygen/ Carbon ratio is also higher in radioactive samples (2.66) as compared to the non radioactive samples (0.78).

Group	Av % U_3O_8	Av % TC	Av % TOC
Group I (<100 ppm)	0.0027	0.634	0.372
Group II(100-1000 ppm)	0.0279	0.885	0.64
Group III(>1000 ppm)	0.22	0.982	0.746

Table.5 Comparisons between TC, TOC and U_3O_8 results

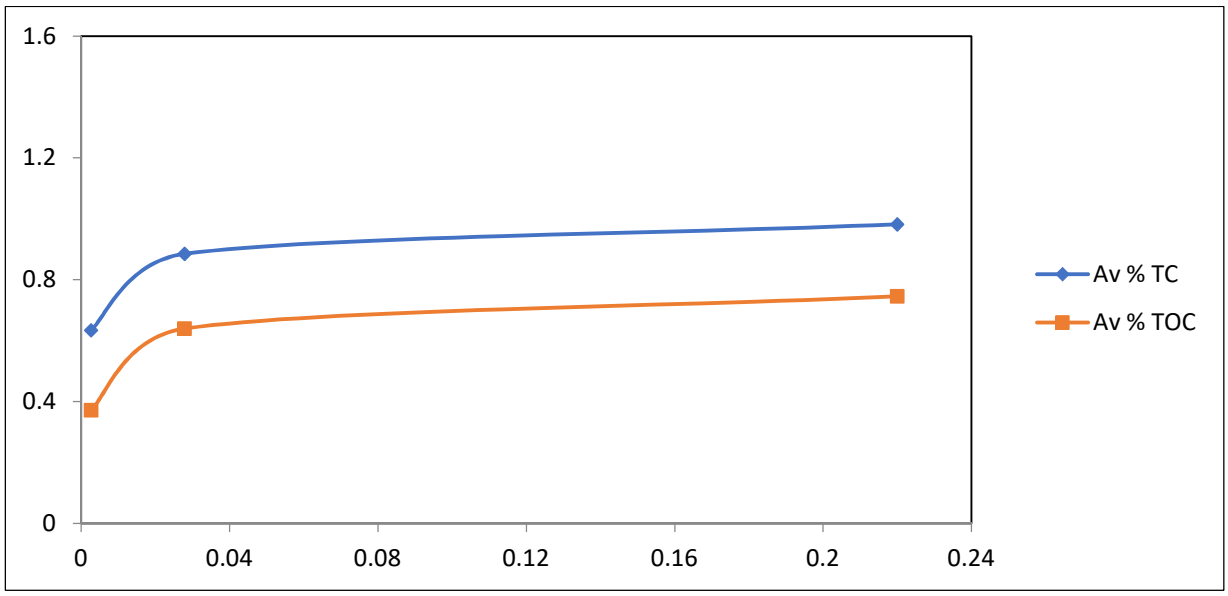

Figure.9 Correlation of Total Carbon (TC) and Total Organic Carbon (TOC) with uranium content

Van Krevelen diagram, a plot of atomic oxygen/carbon (H/C) versus atomic hydrogen/carbon (O/C) derived from elemental analysis of specific type of organic matter can be used to indicate both biological source (type) and thermal maturity. So, accordingly the average value of H/C vs O/C of carbonaceous matter of radioactive samples (Umthongkut & Wahkut) were plotted in Van Krevelen Diagram (1961, 1984) and Jones and Edison (1978) showing the evolution of the four Kerogen Types with maturation, through the stage of diagenesis, catagenesis and meta genesis. The analysed carbonaceous matter falls in the category of Type-III- Kerogen, Fig.9. Type III Kerogen has low H/C (<1.0) and high O/C (up to ~0.3) (Peters and Moldowan, 1993). Such low hydrogen organic matter is polyaromatic and derived mostly from higher plants. Type III kerosene is the chemical equivalent of vitrinite, telinite, collinite, huminite, and so-called humic or woody kerogen (Miles, 1994).

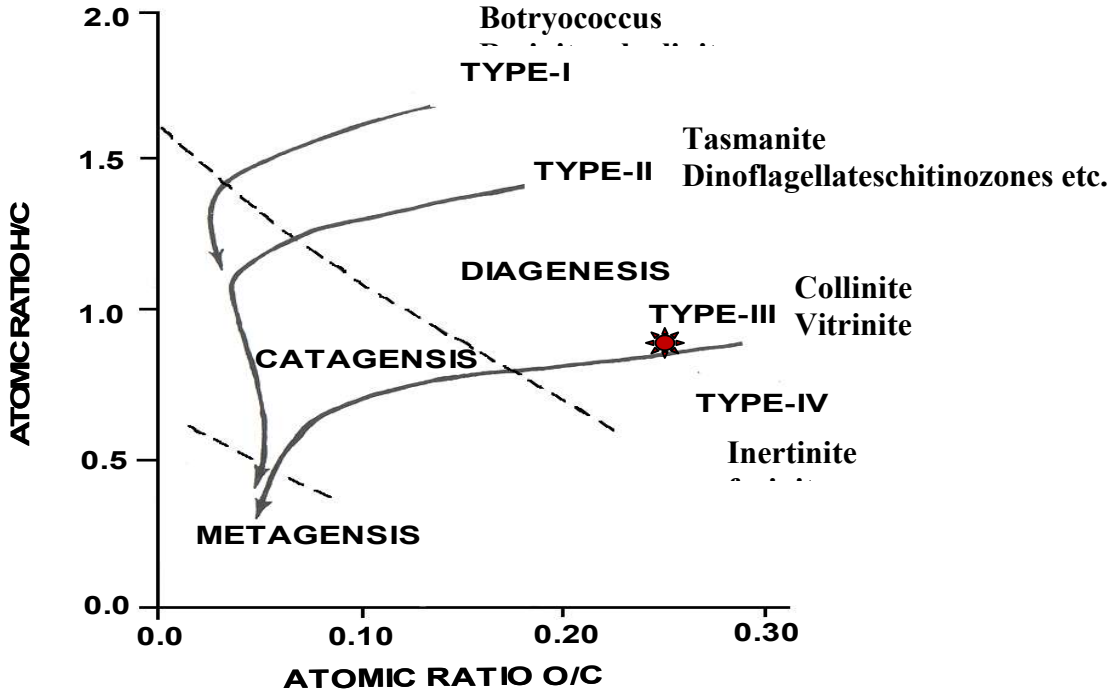

Figure.10 Van Krevelen Diagram (1961, 1984) and Jones and Edison (1978) showing the Kerogen Type of carbonaceous matter of radioactive samples (Umthongkut & Wahkut)

- Average H/C vs O/C of carbonaceous matter of radioactive samples (Umthongkut&Wahkut).

The natural organic materials to which uranium is attracted all contain oxygen bearing function group (Moieties, Nash1981). Organic substance found in decomposing plant decries have many oxygen bearing functional group– principally carboxyl (-COOH), carbonyl (-COO) and hydroxyl or phenolic group (-OH). In the process of complexing uranium, the oxygen sites in these groups can be looked upon as performing a function similar to the oxygen in inorganic ligands such as carbonate, phosphate and hydroxyl. The FTIR study found presence of Functional groups like -OH, -COOH and aromatic C=C groups that play a vital role in fixation of uranium. The mechanism by which uranium forms complex with soluble organic matter ligands are chelation, ion exchange and chemi-sorption, etc., which describe fixing of uranium by both dissolve and solid species.

The association of uranium and organic matter has been primarily attributed to two processes, (i) syngenetic or epigenetic reduction/ fixation of uranium by the organic matter, and (ii) mobile hydrocarbon replacing as well as solubilizing primary uranium minerals (Ekain and Gize, 1992). The nature of association organic matter in Umthongkut and Wahkut areas suggests the first process. Immediate burial of sediments without much sorting, alteration and preservation of organic structures in the carbonaceous matter provided anaerobic sapropelic conditions of degradation, except for some parts where humic conditions might have prevailed due to restricted oxygen supply. Uranium carried by circulating ground waters, partly deposited as pitchblende under anaerobic conditions, due to reduction by bacterogenic H_2S, and part in the form of organo-uranyl complexes by complexion with organic matter. Reduction of organo-

uranyl complex into pitchblende has taken place during diagenetic and radiolysis induced maturation of the organic matter. During the organic acid stage of maturation of organic matter, changes as solubilization of silica, and formation of organo-silica complexes, secondary organic matter and uranium–clay association and precipitation of coffinite as well as partial conversion of early formed uraninite to coffinite took place (Krishna Raoet. al 1995).

Thus, the results indicate that presence of carbonaceous matter in these sandstones has played a significant role in the formation of U-minerals. The dehydrogenation process of organic matter helped in reducing $UO2^{2+}$ complexes to U^{4+}there by precipitating the U-bearing minerals such as pitchblende and coffinite. Besides, the carbonaceous matter functioned as a physical barrier and as a chemical reducing agent, that helped in preserving the reducing conditions even in the presence of oxidizing fluids, over this long period, thereby sustaining these deposits.

Conclusions

Lower Mahadek Sandstone contain significant quantity of carbonaceous matter in dispersed state.

Within the Lower Mahadek Sandstone, uranium content is more in samples having more Total Carbon as well as Total Organic Carbon.

Carbonaceous matter of the radioactive samples is of more humic in nature with high H/C ratio.

When U^{+6} in ground water comes in contact with carbonaceous matter in sediments, it is reduced to U^{+4} and gets precipitated to form uranium mineral.

Presence of functional groups like Aromatic C=C and Phenols (O-H) which acts as U-fixing agents were inferred from FTIR data of carbonaceous matter of mineralized sandstones.

Thus the content and nature of carbonaceous matter has influenced in fixing uranium in these deposits and further preserving them.

Acknowledgements

The authors are grateful to Director, AMD for his kind permission to publish this paper. JORHAT, Assam is thankfully acknowledged for analysis of carbonaceous matter samples.

References

Atomic Minerals Directorate for Exploration and Research website http://www.amd.gov.in/app16/content.aspx?link=35

Chattopadhyay N and Hashmi S (1984). The Sung Valley alkaline carbonatite Complex, East Khasi and Jaintia Hills districts, Meghalaya; Records Geological Survey of India113, 24-33.

Dhana Raju R, Paneer Selvam A and Virnave SN (1989). Characterization of Upper Cretaceous Lower Mahadek Sandstone and its uranium mineralisation in the DomiasiatGomaghatPdengshakap area Meghalaya India Explo. Res. At. Miner. 2, 1-27.

Ekain and Gize(1992). Reflected-light microscopy of uraniferous bitumen; Mineralogical Magazine 56, 85-99.

Ghosh S, Chakravorty S, Bhalla JK, Paul DK, Sarkar A, Bishui PK and Gupta SN (1991). Geochronology and geochemistry of granite plutons from East K. Hills, Meghalaya; J. Geol. Soc. India 37, 331–342.

Geological Survey of India(1974). Geology and Mineral Resources of India; Geol. Surv. India, Misc. Publ. Calcutta 30, 77.

Jones RW and Edison TA (1978). Microscopic observations of kerogen related to geochemical parameters with emphasis on thermal maturation, in D. F. Oltz, ed., Low temperature metamorphism of kerogen and clay minerals; SEPM Pacific Section, Los Angeles, October, 1-12.

Kaul Ravi and Varma HM (1990). Geological evolution and genesis of the sandstone-type uranium deposit at Domiasiat, West Khasi Hills district, Meghalaya, India; Explor. Res. At. Miner. 3, 1-16.

Krishna Rao N, Sunil Kumar T S and Narasimhan D (1995). Uraniferous Organic Matter in the

Sandstone-Type Uranium Ore from Domiasiat, Meghalaya, India. J. Geol. Soc. India 45407-425.

Mahendra Kumar K, Bhattacharjee P and Ranganath N (2008).Uranium mineralization in the Lower Mahadek Sandstones of Laitduh Area, East Khasi Hills District, Meghalaya; Explor. Res. At. Miner. 18, 101-108.

Miles A J (1994).Glossary of Terms Applicable to the Petroleum System. In: The Petroleum System-from source to trap; Edited by Magoon L B and Dow W G. AAPG Memoir 60, 644.

Nandy DR (2001).Geodynamics of Northeastern India and adjoining Region; ACB Publications, 209.

Peters KE and Moldowan JM (1993). The biomarker guide: Interpreting molecular fossil in petroleum and ancient sediments; Prentice Hall, London 363.

Sengupta B, Bahuguna R, Kumar Sunil Singh R and Kaul R (1991).Uranium exploration in the Cretaceous Mahadek sediments of the Meghalaya Plateau; Curr. Sci. 61, 46-47.

Sen DB, Sachan AS, Padhi AK and Mathur SK (2002).Uranium exploration in the Cretaceous Mahadek sediments of the Meghalaya Plateau; Explor. Res. At. Mine.14, 29-58.

Uranium 2014; Resources, Production and Demand- A Joint Report by the OECD Nuclear Energy Agency and the International Atomic Energy Agency.

World Nuclear Association websitehttp://www.world-nuclear.org/information-library/nuclear-fuel-cycle/uranium-resources/geology-of-uranium-deposits.aspx

Van Krevelen D W (1961).Coal; New York, Elsevier, 514.

Van Krevelen D W (1984).Organic geochemistry-old and new;Organic Geochemistry 6, 1-10.

First online volume
Jour. Indian Association of Sedimentologists, Vol. 35, No. 1 (2018), pp.99-106
ISSN 0970-3268

Microfacies analysis and depositional environment of Maastrichtian – Eocene limestone of the Ukhrul district, Manipur, Northeast India

Khumukcham Radhapiyari Devi and Bhagawat. Pran. Duarah

Department of Earth Sciences, Manipur University – 795003
Email: rpiyari@gmail.com
Department of Geological Sciences, Gauhati University, Assam-781014, India
Email: bpduarah@gmail.com

Abstract: Microfacies analysis of the carbonate rocks of Ukhrul were conducted to understand the sedimentological features, microfacies associations and depositional environment of the flyschoidal sediments deposited within Upper Disang Group. These rocks are composed mainly of microcrystalline calcite matrix, sparry calcite cement, skeleton grains and shell fragments. Three microfacies were identified as mudstone, wackestone and packstone. Based on the energy index classification, these limestones can be categorized into Sub-Type II_1 of Type II (Intermittently Agitated), deposition alternately in agitated water and in quiet water. Foraminifera of Upper Cretaceous to Eocene age have been identified in the present study. The recognized microfacies of the present study have been compared and correlated with the standard microfacies association (SMA), and in all probability they falls in Standard Facies Zone 8, Restricted Platforms. The detail microfacies analysis show that the studied limestones are fine-grained and micritic in nature mostly biomicrite, dominantly benthic and planktonic foraminifera deposited in a shallow marine shelf condition with restricted to moderately agitated water within an interior platform basin during the Maastrichtian – Eocene time.

Key words: Microfacies, shallow water Carbonate, depositional environment.

Introduction

The present investigation has been carried out on the samples collected from three sections viz. Paoyi, Ukhrul Town and Hundung sections of Ukhrul district, Manipur. Study of Maastrichtian – Eocene limestone deposits of Ukhrul and reconstruction of their depositional environment is essential and important because of Ukhrul limestones normally occur along or near the western margin of main Ophiolite belt and is considered as one of the deep seated oceanic pelagic sediment of the Nagaland–Manipur Ophiolite Belt (NMOB) by many workers (Singh, 1992; Singh, 2009). Singh (1992) identified microfacies in carbonate rocks of Ukhrul and designated as fossiliferous micrite, sparse biomicrite and packed biomicrite. According to Acharyya *et al.* (1989) the close association of carbonates with the pelagic sediments suggests deposition took place above carbonate compensation-depth. In Manipur limestone deposits are found occuring as scattered pockets within the Disang Group as well as within the oceanic pelagic sediments with Ophiolite suites. Some of the limestone blocks occur within Disang Group and its associated sediments has also been treated as Olistostromal/Exotic deposits. Because of the genetic systematic and occurrence of carbonates in the broader framework of geodynamic evolution of the Manipur – Nagaland Orogenic belt it seems to be difficult and unclear to understand and to study the limestone deposits in detail. As a matter of fact, very few attempts have been made earlier. Inspite of the published account of

earlier workers (Mitra *et al*. 1986; Chungkham *et al.*, 1992; Chungkham and Caron, 1996; Singh, 2011; Singh *et al.* 2013) on this aspect, there are many gaps when one considers the relationship accruing between carbonates and flyschoidal sediment deposits and no record of microfacies study of these limestone. Foraminiferas were recorded earlier from the studied sequence by previous workers (Nandy and Sriram, 1970; Bhattacharyya and Bhattacharyya, 1987; Chunngkham *et al*., 1992; Prithiraj and Jafer, 1998; Singh *et al.,* 2013) however, re-examination is necessary to document the Cretaceous–Tertiary foraminifera from the sediments of Ukhrul in a better and justified manner as they did not mention the importance of benthic foraminifera which are very sensitive to the depositional environment.

In view of this, a detail study of carbonate rocks that occur in scattered pockets in the upper part of the Disang Group of sediments. The objective of the present study is to determined the characteristic of microfacies types and discuss diagnostic features of palaeoenvironmental condition through examination of their sedimentological and palaeontological characteristic. Microfacies types and facies associations are fundamental to the development of models for carbonate sedimentations (Flugel, 2010).

Geological Setting

The study area, Ukhrul district of Manipur, India is a part of Indo-Myanmar Range (IMR) within the Assam-Arakan Basin and represents a complex geological terrain in the subduction zone evolved by ocean–continent collision which gradually transformed into continent–continent collision forming a fold–thrust belt (Ranga Rao, 1983). The basin originated through dextral shear coupling between Indian and Burmese plates resulting to a schuppen belt (Ibotombi, 1998). The sedimentary process involved initial deep sea flysch sedimentation in the basin, namely the Disang Group, which gradually become shallow through sediment filling and tectonic squeezing. There was a shift of sedimentation pattern from finer shaly sediments of Disang Group that gradually transformed into a coarse sandy facies known as Barail Group. This gradual change in marine sedimentation is without any evidence of break in sedimentation. There is probability of getting an intervening neritic environment with favourable carbonate facies deposition (Devi and Duarah, 2015; Devi *et al*., 2016). The sedimentation of the Disang Group commenced during the Late Cretaceous (Maastrichtian) and continued till the end of the Eocene and the sandstone deposition of Oligocene sediments belonging to Barail Group took place conformably on the Disang Group (Kachhara, *et al* 2009). The carbonate rocks of Ukhrul area occupy the upper part of the Disang Group and appear to be of Maastrichtian to Eocene age as evidenced by the occurrences of several microfossils in the carbonate sediments (Devi, 2016). **3.**

Methods

The present study is based on approximately 60 thin sections from samples collected in three section viz. Paoyi, Ukhrul Town and Hundung of Ukhrul district (P_1-P_{16}: U_1-U_9: H_1-H_{33}) shown in Fig. 2. Staining of thin section have been done followed the procedure of Dickson (1965). Insoluble residues (IR) were determined by acid digestion using Hydrochloric acid (HCl) solution to dissolve the carbonate minerals (Carver, 1970). Microfacies studies include the analyses of matrix and grains, textural features, microfossil content, petrographic and energy index classification. The classification of facies types is based on Dunham's (1962) and Folk's (1962) limestone classification scheme. Energy index has been analysed according to Plumley *et al.* (1962) and Catalov (1972). For the identification of facies and

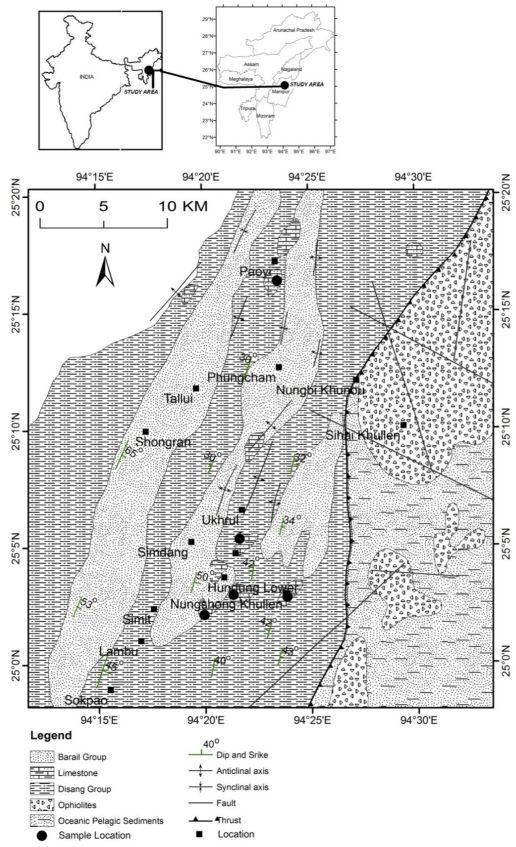

Figure 1: Geological map of the study area (Singh, 2011 and modified on the basis of field study).

interpretation of depositional environments, thin sections were analysed from each sections. The recognition of the "standard microfacies (SMF) types" and the "facies zones" have been defined based on Wilson (1975) and Flugel (2010).

Results and Discussion

Microfacies analysis based on thin-section studies subdivide the different facies into units of similar compositional aspect that reflect specific depositional environment. Basic prerequisites for defining microfacies types (MFT) are based on discrimination of grain categories, limestone classifications based on textural criteria, the recognition of depositional fabrics and the ability to attribute thin section fossils to major systematic groups and taxonomic units (Flugel, 2010). Facies zones (FZ) are limestone belts differentiated according to the changes of their sedimentological and biological criteria across shelf-slope basin transects. These Facies Zones (FZ) described idealized facies belts along an abstract transect from open-marine deep basins to the coast. Carbonates formed within these Facies Zones often exhibit specific Standard Microfacies Types (SMF) assemblages that are used as additional criteria in recognizing the major facies belts The Standard Facies Zones (FZ) describe idealized facies belts.

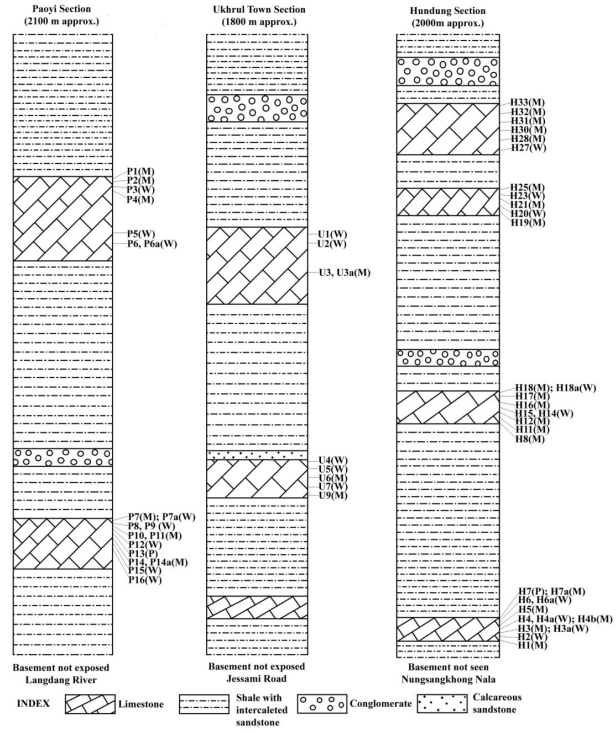

Figure: 2. Lithological column of the sample site of the study area.
W: Wackestone, P: Packstone and M: Mudstone

Classification of microfacies

The petrographic thin section analysis revealed three different types of microfacies viz., mudstone, wackestone and packstone (Fig. 3(A-L). These are described as follows:

(A) Mudstone Microfacies

This microfacies is common within the Ukhrul limestones and found in all the studied sections (Fig. 2). This microfacies

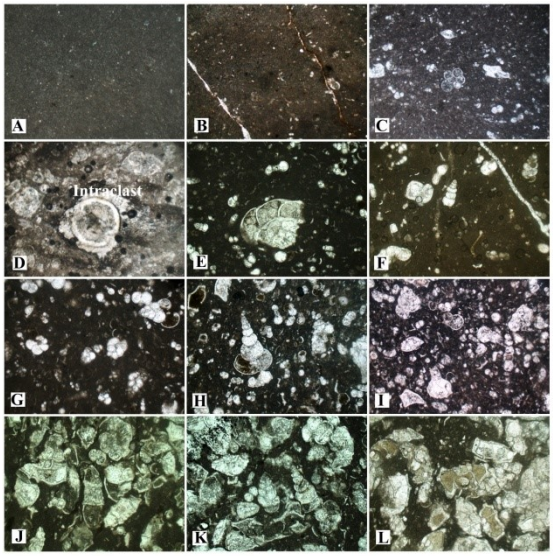

Figure: 3.Photomicrograph of the limestone of the study area: A-C. Mudstone with little allochem, D. Wackestone with Intraclast, E-I. Wackestone with fosil allochem. J-L. Packstone with fossil allochem

consists of lime mud matrix with little or no allochems as shown in Fig. 3(A-C). In the outcrop mud supported limestone is characterized by different shades of light grey to buff colour. Petrographically, it shows a high percentage of mud i.e., microcrystalline calcite matrix reach to 99.12% (P_{11}) in Paoyi section, 97.45% (U_9) in Ukhrul Town and 99.30% (H_{12}) in Hundung section (Table 1).

According to Dunham (1962), mudstone facies are deposited in low energy environment either in protected seas or below fair weather base (calm water). This facies is similar to the Standard Microfacies, SMF-23, Non-laminated unfossiliferous mudstone (Flugel, 2010), which corresponds to the Facies Zone 8 of restricted platform (Wilson 1975; Flugel 2010). Moreover, this facies type also indicates low maturity of the limestone, as the rocks of low maturity are characterized by a high proportion of micrite and low proportion of allochems. High percentage of micrite reflects deposition in a setting where current or wave energy was insufficient to winnow away the fine matrix (Folk, 1962).

(B) Wackestone Microfacies

This is one of the most common microfacies occurring in all the three sections (fig. 2). The grains consist more than 10% of the lithology. It consists of sparry calcite and skeletal remains of foraminifera represented by both panktonic and benthic forms. The planktonic foraminifera include *Globotruncana* sp., *Globotruncanita* sp., *Globorotalia* sp., *Hedbergella* sp., *Heterohelix* globulosa, *Pseudotextularia* sp., *Globigerina* sp., *Globigerinelloides* sp., *Rugoglobigerina* sp. etc. [Fig 4(A-N)] whereas benthic foraminifera include *Textularia* sp., *Valvulina* sp. and other unidentified benthic foraminifera as shown in Fig. 4 (O, P, Q, S & T). Presence of planktonic foraminifera like *Globotruncana* sp., *Pseudotextularia* sp. denotes a Maastrichtian age. The *Globigerina* sp., *Globorotali*a sp. represent Paleocene as Globigerinidae become the most planktonic family in Palaecene time, while planktonic genera Globigerinoides appear in the Eocene (Loeblich and Tappan, 1964). All these fossil records indicate that the age of limestones found in Ukhrul ranges from Upper Cretaceous i.e Maastrichtian to Eocene. The Upper Cretaceous is supported by Prithiraj and Jafar (1998) also. The foraminiferal taxas identified in this facies are very common and similar with those identified by earlier workers from different localities of Manipur. It is generally found that the fossil bearing carbonate rocks occupy the space in the upper part of the Disang Group. The preservation potential of these fossils are mostly poor and in deformed state. Presence of broken skeletal indicates perhaps gentle disturbances in the depositional environment. Intraclasts are found in negligible amount in the present study (only in few rock samples). Its value ranges from 0.02% to 0.9 % as shown in Table 1. Though the amount is negligible, the presence of intraclast (fig. 3D) can be

Sl. No.	*Sample No.	Micrite %	Sparite %	Fossil %	Oolite %	Pellet %	Intra-clast %	Insoluble Residue (IR) %	Dunham (1962)	Folk (1962)
1	P_1	92.07	5.83	2.07	-	-	0.03	27	mudstone	Fossiliferous micrite
2	P_2	96.42	2.39	1.19	-	-	-	24	mudstone	Fossiliferous micrite
3	P_3	89.51	9.44	1.03	-	-	0.02	26	wackestone	Fossiliferous micrite
4	P_4	91.20	7.99	0.81	-	-	-	24	mudstone	Micrite
5	P_5	84.08	12.22	3.70	-	-	-	25	wackestone	Fossiliferous micrite
6	P_6	79.37	16.78	3.85	-	-	-	19	wackestone	Fossiliferous micrite
7	P_{6a}	89.20	6.20	4.60	-	-	-	21	wackestone	Fossiliferous micrite
8	P_7	91.06	6.85	2.09	-	-	-	24	mudstone	Fossiliferous micrite
9	P_{7a}	69.70	21.5	8.80	-	-	-	20	wackestone	Biomicrite
10	P_8	82.12	13.67	4.21	-	-	-	16	wackestone	Fossiliferous micrite
11	P_9	73.81	15.59	10.2	-	-	0.9	36	wackestone	Biomicrite
12	P_{10}	94.40	5.00	0.60	-	-	-	25	mudstone	Micrite
13	P_{11}	99.12	0.88	-	-	-	-	21	mudstone	Micrite
14	P_{12}	87.12	11.5	1.38	-	-	-	18	wackestone	Fossiliferous micrite
15	P_{13}	42.58	44.57	12.85	-	-	-	17	packstone	Sparse Biomicrite
16	P_{14}	92.99	4.66	2.35	-	-	-	18	mudstone	Fossiliferous micrite
17	P_{14a}	98.10	1.80	0.10	-	-	-	16	mudstone	Micrite
18	P_{15}	83.16	4.40	12.44	-	-	-	21	wackestone	Biomicrite
19	P_{16}	86.21	2.98	10.81	-	-	-	24	wackestone	Biomicrite
20	U_1	89.10	1.10	9.80	-	-	-	21	wackestone	Fossiliferous micrite
21	U_2	84.00	4.40	11.6	-	-	-	17	wackestone	Biomicrite
22	U_3	92.00	2.10	5.90	-		-	20	mudstone	Fossiliferous micrite
23	U_{3a}	96.81	2.29	0.90	-	-	-	18	mudstone	Micrite
24	U_4	84.00	5.60	10.4	-	-	-	19	wackestone	Biomicrite
25	U_5	77.80	9.40	12.8	-	-	-	20	wackestone	Biomicrite
26	U_6	92.90	1.70	5.40	-	-	-	16	mudstone	Fossiliferous micrite
27	U_7	89.20	8.20	2.60	-	-	-	18	wackestone	Fossiliferous micrite
28	U_9	97.45	1.80	0.75	-		-	21	mudstone	Micrite
29	H_1	93.21	4.30	2.49	-	-	-	26	mudstone	Fossiliferous micrite
30	H_2	72.90	19.5	7.60	-	-	-	20	wackestone	Fossiliferous micrite
31	H_3	87.67	8.90	3.43	-	-	-	14	mudstone	Fossiliferous micrite
32	H_{3a}	92.38	5.11	2.51	-	-	-	17	mudstone	Fossiliferous micrite
33	H_4	69.45	22.83	7.72	-	-	-	32	wackestone	Fossiliferous micrite
34	H_{4a}	86.31	9.09	4.60	-	-	-	27	wackestone	Fossiliferous micrite
35	H_{4b}	91.04	7.61	1.35	-	-	-	24	mudstone	Fossiliferous micrite
36	H_5	94.01	4.80	1.19	-	-	-	26	mudstone	Fossiliferous micrite
37	H_6	81.64	13.66	4.70	-	-	-	22	wackestone	Fossiliferous micrite
38	H_{6a}	76.05	13.8	10.15	-	-	-	17	wackestone	Biomicrite
39	H_7	45.80	38.6	15.6	-		-	20	packstone	Biomicrite
40	H_{7a}	52.80	31.6	15.6	-	-	-	19	mudstone	Biomicrite
41	H_8	92.35	4.00	3.65	-	--	-	16	mudstone	Fossiliferous micrite
42	H_{10}	95.8	3.69	0.51	-	-	-	11	mudstone	Micrite
43	H_{12}	99.30	0.70	-	-	-	-	28	mudstone	Micrite
44	H_{13}	85.03	4.18	10.79	-	-	-	10	wackestone	Biomicrite
45	H_{15}	89.04	9.61	1.35	-	-	-	18	wackestone	Fossiliferous micrite
46	H_{16}	99.01	0.80	0.19	-	-	-	15	mudstone	Micrite
47	H_{17}	93.84	3.83	2.33	-	-	-	14	mudstone	Fossiliferous micrite
48	H_{18}	95.00	1.60	3.40	-	-	-	21	mudstone	Fossiliferous micrite
49	H_{18a}	87.05	8.35	4.60	-	-	-	20	wackestone	Fossiliferous micrite
50	H_{19}	92.30	4.30	3.38	-	-	0.02	16	mudstone	Fossiliferous micrite
51	H_{20}	80.36	6.57	13.07	-	-	-	24	wackestone	Biomicrite
52	H_{21}	98.21	1.49	0.30	-	-	-	20	mudstone	Micrite
53	H_{23}	89.01	9.79	1.20	-	-	-	17	wackestone	Fossiliferous micrite
54	H_{25}	93.20	4.96	1.84	-	-	-	21	mudstone	Fossiliferous micrite
55	H_{27}	87.60	8.62	3.78	-	-	-	19	wackestone	Fossiliferous micrite
56	H_{28}	98.53	1.43	0.04	-	-	-	22	mudstone	Micrite
57	H_{30}	97.61	1.79	0.60	-	-	-	18	mudstone	Micrite
58	H_{31}	98.01	1.69	0.30	-	-	-	21	mudstone	Micrite
59	H_{32}	92.17	7.80	0.03	-	-	-	25	mudstone	Micrite
60	H_{33}	98.65	0.95	0.40	-	-	-	23	mudstone	Micrite

Table 1: Major constituent components of Ukhrul limestone (in percentage) *Samples with prefix "P" are from Paoyi; "U" from Ukhrul Town and "H" from Hundung sections while "IR" is Insoluble Residue.

evidence of intrabasinal transport and shallow water regime, as the bottom would have shallow enough to be periodically affected by turbulence that causes intraclast formation because even intense storms have little effect below certain depths.

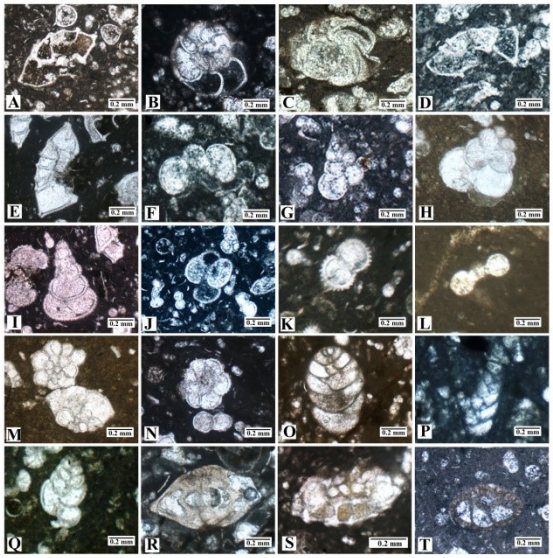

Fig 4: Photomicrograph of the foraminiferal fossils identified from the studied limestone: A-C. *Globotruncana* sp.; D-F. *Hedbergella* sp.; G-H *Heterohelix* sp.; I. *Pseudotextularia* sp.; J-K.*Globigerina* sp.; L. *Globigerinelloides* sp.; M. *Rugoglobigerina* sp.; N. *Globorotalia* sp.; O. *Valvulina* sp.; P-Q. *Textularia* sp.; R. *Robuloides* sp.; S-T. unidentified benthic foraminifera

According to Dunham (1962) wackestone is a mud supported framework carbonate rock implies with low hydraulic energy of deposition. The occurrence of microfossil especially foraminifera locally in great abundance but limited in diversity in the fine grain low energy depositional limestone of the present study can also be correlated to Standard Facies belt 8 i.e. restricted circulation and tidal flates of Wilson's (1975) facies model. The sediments of this belt are characterized mostly lime mud and muddy sand with terrigenous influx common. The biota should be shallow water biota of reduced diversity, but commonly with high number of individuals. Restricted shallow subtidal environments in the inner ramp are indicated by low diversity skeletal fauna in general, abundant of imperforate foraminifera (miliolids and *Archaias*) and lack of subariel exposure features (Hallock, 1984; Buxton and Peddely, 1989; Barattolo *et al*., 2007). Based on the foraminiferal assemblages with abundant miliolids this microfacies can be correlated to the Standard Microfacies (SMF) Type 18 (Wilson, 1975; Flugel, 2010), which fall in FZ 8, because miliolid foraminifera are very common in lagoonal environments of Mesozoic and Cenozoic restricted inner platforms and inner ramps (Flugel, 2010).

(C) Packstone microfacies

This facies is not common in all the studied sections. Exceptionally, only very few samples viz., sample No. P_{13} and H_7 (Table 1) showing such facies [Fig. 3(J,K&L)]. Due to lack of sufficient samples it would not be possible to correlate with standard microfacies. This microfacies is found in Paoyi and Hundung sections (Fig. 2). In this facies the grain percent is more than lime mud, where some of the sparite grains may be due to neomorphism.

Energy Index Classification

The classification proposed by Plumley *et al.* (1962) and Catalov (1972) was adopted for the energy index analysis. From the energy index classification it can be interpreted that limestone genesis is based primarily upon the energy level of depositional environment, which is a function of wave and current action reflecting a fundamental concern with environmental interpretation. These genetic classifications constitute a grading spectrum between quiet water and strongly agitated water. Plumley *et al.* (1962) distinguished five major limestone categories as Type I (quiet water), Type II (intermittently agitated water), Type III (slightly agitated water), Type IV (moderately agitated water) and Type-V (strongly agitated water). Our study

reveals that microcrystalline calcite matrix ranges from 99.30- 42.58% while detrital particles i.e insolule residue % ranges from 36% to 10% (Table-1) and the presence of complex fossil assemblages of both benthic and plantonic type in the studied rocks represent the influence of both quiet and slightly agitated water condition, which fall in subtype II_1 of Type II i.e., mixed types occuring in the transition zone between deep water and very shallow water (Plumley *et al*.1962). According to Catalov (1972) classification the studied rocks fall in Type I, deposited in quiet water as the micrite percent ranges from 42.58% to 99.30% in Ukhrul district limestone.

Conclusion

Dominance of mud supported microfacies indicates the studied rocks were deposited in quiet water and low energy setting environment. Though high amount of micrite reflects a relatively low-turbulent environment however taphonic features of fossils suggest gentle disturbance due to intrabasinal transport. It is also supported by energy index classification. Microcrystalline calcite matrix comprises more than 50% of the rock and presence of complex fossil assemblages representing alternate deposition in agitated and quiet shallow water. Based on the sedimentological and paleontological criteria the identified microfacies types (MFT) were similar with SMF Type 18 and 23, which fall in Standard Facies Zone (FZ) 8, restricted platforms (Flugel, 2010). Associations of MFT occurring within the same lithofacies and deposited in the same general environment suggest local sedimentary sub-environments or local processes (Flugel, 2010). The paleoecological set up of the microfacies and foraminifers observed in the limestone of Ukhrul district of Manipur indicates that the sedimentation take place under marine shelf condition with restricted to moderately water circulation within an interior platform during the Maastrichtian–Eocene Epoch.

Acknowledgements

The authors acknowledge their sincere gratitude to CSIR, New Delhi for the funding this research endeavor (09/059(0053)/2013 EMR-1). Authors also express their sincere gratitude to the unknown reviewers whose suggestions help us greatly to improve the article.

References

Acharyya, S. K., Ray, K. K. and Roy, D. K. (1989). Tectono-Stratigraphy and emplacement history of the Ophiolite assemblage from the Naga Hills and Andaman Island arc India. *Jour. Geo. Soc. of India*, *33, 4-18.*

Barattolo, F., Bassi, D. and Romero, R. (2007). Upper Eocene larger foraminiferal-coralline algal facies from the Klokova Mountain (south continental Greece). *Facies, 53, 361–375.*

Bhattacharyya, A., & Bhattacharyya, U. (1987). Review of the stratigraphy and palaeontology of Upper Cretaceous sediments of northeast India. *Geological Survey of India, Spec. Pub*., No. 11 (1), 367-387.

Buxton, M. W. N., & Pedley, H. M. (1989). Short paper: a standardised model for Tethyan Tertiary carbonates ramps. *Jour. Geol. Soc. of London*, *146, 746–748.*

Carver, R.E. (1970). *Procedure in Sedimentary Petrology*.Wiley Interscience.

Catalov, G. A. (1972). An attempt at energy index (EI) analysis of the Upper Anisian, Ladinian and Carnian carbonate rocks in the Teteven Anticlinorium (Bulgaria). *Sedimentary Geology*, *8, 159-175*.

Chungkham, P., & Caron, M. (1996). Comparative study of a Late Maastrichtian (A. Mayaroensis Zone) foraminiferal assemblages from two distant parts of the Tethys Ocean: Semsales Wildflysch Zone Switzerland and Ukhrul Melange Zone, India. *Revue de biogie, 15(2), 499-512.*

Chungkham, P., Mishra, P. K., & Sahni, A. (1992). Late and terminal Cretaceous foraminiferal assemblages from Ukhrul, Melange zone, Manipur. *Current Science*, *62(6), 478-481.*

Devi, K. R. (2016). Petrography, Geochemistry and Palaeontology of Carbonate rocks occurring in and around Ukhrul, Manipur: An Integrated approach to establish its stratigraphic status in the Indo – Myanmar Ophiolite Belt. Ph. D. Thesis, Gauhati University (Unpublished).

Devi, K. R. & Duarah, B. P. (2015). Geochemistry of Ukhrul limestone of Assam-Arakan subduction basin, Manipur, Northeast India. *Jour. Geol. Soc. of India*, *85, 367-376.*

Devi, K. R., Sing, W. I., Kumar, D. & Duarah, B. P. (2016). Petrography of Upper Cretaceous Eocene limestone deposits of Ukhrul district, Manipur, India: Implication to depositional environment. *Jour. Him. Geology*, *37(2), 165-175.*

Dickson, J. A. D. (1965). A modified technique for carbonates in thin section. *Nature*, *205(4971), 587p*.

Dunham, R. J. (1962). Classification of Carbonate Rocks according to Depositional Texture. In: W. E. Ham (eds.), *Classification of Carbonate Rocks, pp. 108-121.*

American Association of Petroleum Geologist, Memoir No. 1.

Flügel, E. (2010). *Microfacies of Cabonate rocks*, *Analysis Interpretation and Application*. Springer-Verlag, Berlin, 662 p.

Folk, R.L. (1962). Spectral subdivision of limestone types. *Bulletin of American Association Petroleum Geologist,* 1, 62-84.

Hallock, P. (1984). Distribution of selected species of living algal symbiont–bearing foraminifera on two Pacific coral reefs. *Jour. Foraminiferal Research*, *9, 61–69.*

Kachhara, R. P., Soibam, I. and Maonaro, N.J. (2009). Upper age limit of Disang Group in Manipur. Proceeding of XVI Indian colloquium on micropaeontology and stratigraphy NIO, Goa. Bull. Oil and Natural Gas Commission, 37, 215-218.

Loeblich, A. R. Jr., & Tappan, H. (1964). Treatise on invertebrate paleontology; Sarcodina chiefly "Thecamoebians" and Foraminiferida. In: Moore, R. C. (eds.), *Geological Soceity of America* and University of Kansas Press, 1(C).

Mitra, N. D., Vidhyadharan, K. T., Gaur, M. P., Singh, S. K., Mishra, U. K., Joshi, A., Khan, I. K., & Ghosh, S. (1986). A note on the olistrostromal deposits Manipur. Record of *Geological Survey of India*, 114(4), 61-76.

Nandy, D.R., & Sriram K. (1970). Report on Preliminary investigation of limestone prospectsin Nandy Manipur East district. *Geological Survey of India*. Progress Report Field Survey (unpublished).

Plumley, W. J., Risley, G. A., Graver Jr, R.W., & Kaley, M. E. (1962). Energy index for limestone interpretation and classification. *American Association of Petroleum Geologist, Memoirs No. 1. pp. 85-107.*

Prithiraj, Ch., & Jafer, S. A. (1998). Late Cretaceous (Santonian-Maastrichtian) Integrated Coccolith-Globotruncanid Biostratigraphy of Pelagic Limestones from the Accretionary Prism of Manipur, Northeastern India. *Micropaleontology*, *44(1), 69-83.*

Ranga Rao, A. (1983). Geology and hydrocarbon potentials of a part of Assam-Arakan Basin and its adjoining region. Symposium of Petroliferous Basins of India, 127-158.

Singh, A. K. (2009). High-Al chromian spinel in peridotites of Manipur Ophiolite Complex, Indo-Myanmar Orogenic Belt: implication for petrogenesis and geotectonic setting. *Current Science, 96(10), 973-978.*

Singh, N. I. (1992). Petrology and Geochemistry of the carbonate rocks in and around Ukhrul Manipur state, India, Ph. D Thesis, Manipur University (Unpublished).

Singh, N. I., Devi, D., & Chanu, Y. (2013). Depositional Environment of Carbonate Rocks of Ukhrul Area, Manipur Ophiolite Complex, NE India. *Jour. of Him. Geology*, 33, 76-83.

Singh, W. (2011). Petrography and geochemistry of the Barail sandstone in an around Ukhrul area, Ukhrul district, Manipur India. Ph.D. Thesis, Gauhati University (Unpublished).

Singh, Y. K., Jianguo Li., Singh, B. P., & Gurumayum, V. (2013). Microforaminiferal lining from the upper part of the Disang Formation at Gelmoul quarry, Churachandpur, Imphal valley and their bearing on palaeoenvironment. *Current Science*, *105(9), 1223-1226*.

Soibam, I. (1998). Structural and tectonic analysis of Manipur with special reference to evolution of Imphal Valley. Ph. D. Thesis, Manipur University (Unpublished).

Wilson, J. L. (1975). Carbonate facies in geologic history. Berlin–Heidelberg, New York Springer. 471p.

First online volume
Jour. Indian Association of Sedimentologists, Vol. 35, No. 1 (2018), pp.107-118
ISSN 0970-3268

An extended tribute to Professor George Devries Klein (1933-2018): A sedimentologic pioneer and a petroleum geologist

BIOGRAPHY

Introduction

George Devries Klein was an iconic sedimentary geologist. He was born in the Hague, The Netherlands (January 21, 1933), immigrated to the United States in 1947, and passed away in Guam (April 30, 2018). He was one of the foremost sedimentary geologists in the world on the application of many facets of earth science. He was an accomplished process sedimentologist, sequence stratigrapher, sandstone petrologist, tectonics specialist, basin analyst, regional geologist, petroleum geologist, and climate scientist. He had a remarkable career in academia, petroleum industry, and consulting. I had the privilege of getting to know Klein professionally during the past 40 years because of my employment with Mobil Oil Company in Dallas, Texas (1978-2000) and because of our shared interests in subsequent years (2000-2018) on the Ouachita Flysch (USA), submarine fans, tidal currents, deep-water bottom currents, sediment deformation, and climate change. The AAPG Bulletin has accepted a short tribute to Klein for publication (Shanmugam, 2018). However, such a short tribute is not proportional to his monumental contributions with 12 books and edited volumes and over 380 published works. Therefore, this extended tribute, which is a personal reminiscence based on specific publications and events, is offered.

Professional preparation and experience

1954: B.A. in geology, Wesleyan University, Middletown, Connecticut, USA

1957: M.A. in geology, University of Kansas, Lawrence, Kansas, USA

1960: Ph.D. in geology, Yale University, New Haven, Connecticut, USA

1960-1961: Research Geologist, Sinclair Research Laboratories, Inc., Tulsa, Oklahoma, USA

1961-1963: Geology faculty, University of Pittsburgh, Pennsylvania, USA

1963-1970: Geology faculty, University of Pennsylvania in Philadelphia, USA

1970-1993: Geology faculty, University of Illinois at Urbana-Champaign, Illinois,

USA. He was appointed to a full professorship in 1972 and he retired as Professor Emeritus in 1993.

1993-1996: Executive Director, New Jersey Marine Sciences Consortium and director of the New Jersey Sea Grant College, Fort Hancock, New Jersey, USA

1996-2013: President, SED-STRAT Geoscience Consultants, Inc. Houston, Texas, USA

1961-2016: In addition to his teaching undergraduate and graduate courses at various universities, George Klein taught popular short courses on sandstone depositional models and basins analysis for AAPG, SEG and other professional organizations. He presented technical talks at meetings throughout his professional life.

Awards

George Klein was the recipient of 13 awards, including the following:

1969-70: A Visiting Fellowship to Wolfson College at Oxford University, England, UK

1970: SEPM (Journal of Sedimentary Petrology) "Outstanding Paper Award", USA

1980: A Citation of Recognition from the Illinois House of Representatives, USA

1980: The Erasmus Haworth Distinguished Alumnus Award from the University of Kansas Department of Geology, USA

1983: The Japan Society for the Promotion of Science Fellowship, Japan

1989: Fulbright Fellowship to the Netherlands, The Netherlands

2000: The "Lawrence L. Sloss Award" for Sedimentary Geology by Geological Society of America, USA

2013: The "Legend of Sedimentology" award from The Houston Geological Society, Texas, USA.

Retirement in Guam

Following his consulting work in Houston, George Klein and his wife Suyon Cheong, who is originally from Seoul in South Korea, retired to Guam.

SCIENTIFIC CONTRIBUTIONS

Introduction

George Klein was a prolific author with over 380 published works. His research covered a wide spectrum of topics, including tidal sedimentation (Klein, 1970, 1971), estuarine sedimentation (Klein, 1967), lake sedimentation (Klein, 1959), flysch sedimentation (Klein, 1966), Pennsylvanian cyclothems (Klein and Willard (1989), resedimented pelagic carbonate and volcaniclastic sediments (Klein, 1975), DSDP Leg 58 (Klein, Kobayashi et al., 1980), sandstone petrology (Klein, 1961), diagenesis (Klein, 1985), basin analysis (Klein, 1987), tectonics (Klein, 1993), John E. Sanders (Klein, 2000), and climate change (Klein, 2016).

Most of his contributions are archived at the University of Illinois. Details are available at: https://archives.library.illinois.edu/archon/?p=collections/controlcard&id=2148. His contributions during the period 1959-2009 are:

1) Number of published scientific books and edited volumes: 11
2) Number of published articles: 145
3) Number of unpublished technical reports: 49

4) Number of published review articles and abstracts: 141.

Published scientific books and edited volumes

Andrews, J. E., Packham, G. H., Eade, J. V., Holdsworth, B. K., Jones, D. L., Klein, G. D., Kroenke, L. W., Saito, T., Shafik, S., Stoesser, D. G. and van der Lingen, G.J. (1975). Initial Reports for the Deep Sea Drilling Project, v. 30: Washington, U.S. Government Printing Office, 754 p.

Klein, G. D. (Ed.), (1968). Late Paleozoic and Mesozoic continental sedimentation, northeastern North America: Geol. Soc. America Spec. Paper 106, 309 p.

Klein, G. D. (1975). Sandstone depositional models for exploration for fossil fuels: Champaign, IL, Continuing Education Publication Co., 109 p.

Klein, G. D. (Ed.) (1976). Holocene tidal sedimentation. Dowden, Hutchinson & Ross, Inc., Stroudsburg, PA., 425 p.

Klein, G. D. (Ed.) (1977). Sedimentary processes: processes of detrital sedimentation: Soc. Econ. Paleontologists and Mineralogists Reprint Ser . 4, 236 p.

Klein, G. D. (1977). Clastic tidal facies. : CEPCO, Champaign, IL148 p.

Klein, G. D., Kobayashi, K., White, S.M., Chamley, H., Curtis, D.M., Mizuno, A., Dick., H.J.B., Nisterenko, G. V., Marsh, N. G., Waples, D. M., Echols, D. J., Okada, H., Sloan, J. R., Fountain, D. M. and Kinoshita, H. (1980). Initial Reports of the the Deep Sea Drilling Project, v. 58: Washington, U.S. Government Printing Office, 1017 p.

Klein, G. D. (1980). Sandstone depositional models for exploration for fossil fuels, 2nd ed.: Minneapolis, Burgess Pub. Co., 148 p.

Klein, G. D. (1985). Sandstone depositional models for exploration for fossil fuels, 3rd Ed. , IHRDC Press, Boston, MA, 209 p.

Klein G. D. (Ed.) (1994). PANGEA: Paleoclimate, Tectonics and Sedimentation during Accretion, Zenith and Break-up of a Supercontinent: Geol. Soc. America Spec. Paper 288, 295 p.

Klein, G. D. (2009). Rocknocker: A Geologist's Memoir, CCB Publishing, British Columbia, Canada, 431p.

Klein (2003) also published a novel titled "Dissensions", exposing intradepartmental power politics among colleagues in universities.

Tidal sedimentology

George Klein is best known for his pioneering research on tidal sedimentology. His observations and concepts on tidal flats in Bay of Fundy, Canada (Klein, 1963, 1964; Klein and Sanders, 1964) paved a long and illustrious scientific career for Klein. Most importantly, Klein (1971) proposed the "Tidalite" concept for the first time. The genetic term "Tidalites" represents a tidal facies formed in response to global astronomical forcing factors (Klein, 1971, 1977). He showed that increasing shelf width also increased tidal range and thus tidal circulation dominated cratonic seaways. His other work on tidal flats includes the documentation of vertical sequences of rocks and sedimentary structures developed in carbonate banks. Also, he developed new criteria for recognizing features and sediment distribution within tidal flats and the tidal reach in coastal areas. Even today, his publications on tidal sedimentation have a profound impact on facies analysis worldwide (Davies and Dalrymple, 2012).

The Ouachita Flysch, USA: Bottom currents, submarine fans, and sediment deformation

The Pennsylvanian Jackfork Group in the Ouachita Mountains of Arkansas and Oklahoma has conventionally been

interpreted as a classic flysch sequence composed of turbidites in a submarine fan setting (Cline, 1970; Morris, 1977; Moiola and Shanmugam, 1984). In the 1960s, at a time when the turbidite paradigm was in full force, Klein (1966) audaciously advocated an alternative interpretation of sole marks in the classic Ouachita flysch by bottom-current erosion rather than by the orthodoxical turbidity currents. His 1966 publication was a reflection of his courage, innovation, and independence in thinking.

George Klein was the Editor-in-Chief of *Earth-Science Reviews* (ESR) in the late 1980s. After a decade of evaluating submarine fans worldwide, Shanmugam and Moiola (1988) published their review article in ESR. This was my first major encounter with Klein, although his publications had a major impact on my thinking since the 1970s. He liked our ESR paper because it combined sedimentation and tectonics.

Shanmugam et al. (1988) published a paper explaining the origin of sigmoidal deformation structures (i.e., duplex-like structures) by a sedimentary origin in submarine fan channels than by the concentional tectonic origin. This paper caught the attention of George Klein for three reasons. First, the example was from the Ouachita flysch that he studied earlier (Klein, 1966). Second, we explained the origin of duplex-like structures by integrating detailed field observations with sound theory and laboratory experiments. Third, one of his students recognized similar sediment deformation in the modern Matanuska Glacier, Alaska (Lawson, 1981). Soon after our paper was published, we received a complimentary note from George Klein with a field photograph from the Matanuska Glacier showing excellent sediment deformation. The geometrical similarity in sigmoidal sediment deformation among the ancient (Shanmugam et al. 1988, their Fig. 2), modern (Shanmugam, 2016a, his Fig. 20B) and experimental (Shanmugam, 2000a, his Fig. 18B) examples is striking. The point is that George Klein was quick to make the link between modern and ancient environments. After 1988, I started receiving frequent communications from him on sediment deformation (e.g., Shanmugam, 2017) and on deep-water sedimentation. He also began to attend my talks at AAPG and SEPM meetings regularly. Klein (2009, p. 314) acknowledged our long-term friendship in his book "Rocknocker: A Geologist's Memoir" with a statement "*I also visited the Mobil Research Lab to meet Dick Moiola and Shan Shanmugam with whom I developed a long-term friendship*."

In part, following unconventional concepts of Klein (1966), Shanmugam and Moiola (1995) published a controversial reinterpretation of the Ouachita flysch as being composed mostly of debrites and bottom-current deposits. Unlike Newtonian turbidity currents, we argued that plastic debris flows cannot develop typical submarine fans. Our paper resulted in 42 printed pages of five discussions and replies in the AAPG Bulletin (Shanmugam and Moiola, 1997). No other paper in the AAPG Bulletin has generated this much controversy. George Klein, who initiated the Ouachita controversy in the 1960s, was pleased by the AAPG debate in the 1990s.

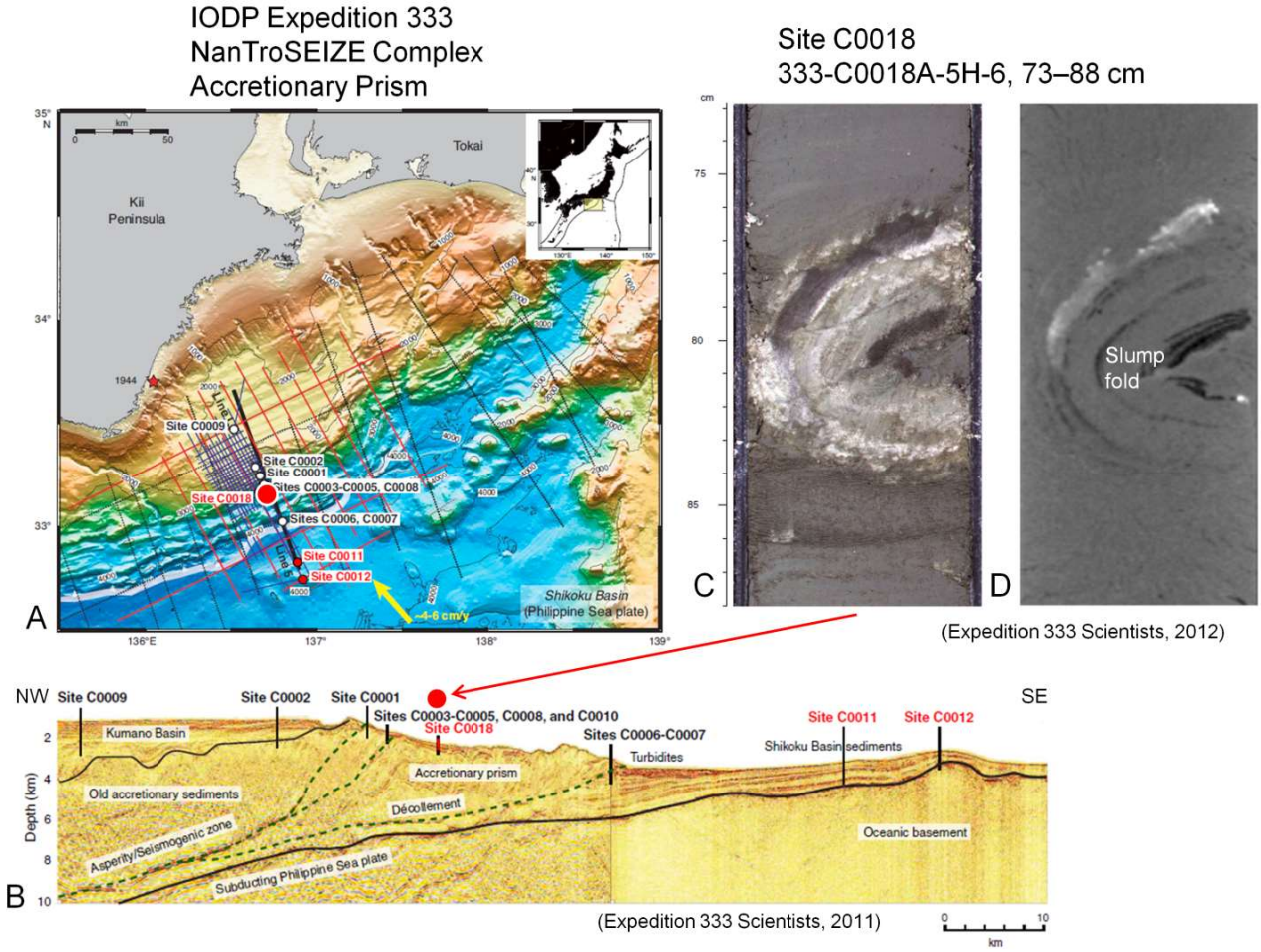

Fig. 1. A - Image showing location of IODP Expedition 333, Site C0018 (filled red circle) in the NanTroSEIZE complex. White barbed line = Position of deformation front of accretionary prism. Yellow arrow = Estimated far-field vectors between Philippine Sea Plate and Japan. Figure from Expedition 333 Scientists (2011), with additional labels by G. Shanmugam. The Shikoku Basin was previously drilled during DSDP Leg 58 (Klein, Kobayashi et al., 1980); B - A NW-SE seismic profile showing position of Site C0018. Note the accretionary prism above the subducting Philippine Sea Plate. Also note location of Site C0012 near the SE end of seismic profile on a Knoll. Figure from Expedition 333 Scientists (2011); C - Core photograph showing slump fold in mudstone. Red arrow points to Site C0018 location; D - CT-Scan image of slump fold in core. Figure from Expedition 333 Scientists (2012), with additional labels by G. Shanmugam. The above composite figure is from Shanmugam, 2017).

George Klein took time to compliment our published works, particularly those that dealt with submarine fans and deep-water sedimentation. After my paper (Shanmugam, 2016b), "Submarine fans: A critical retrospective (1950-2015)" was published, I received an email (5/23/2016 6:20:42 PM Central Standard Time) from him with a note "*Great work Shan and congratulations. Keep the topic moving*."

DSDP Leg 58 and IODP Expedition 333, Shikoku Basin: Sediment deformation

Klein's multifarious scientific activities included a "Co-Chief Scientist" position of the DSDP Leg 58 that drilled the Shikoku Basin in the north Philippine Sea (4 December, 1977 - 30 January, 1978) (Klein and Kobayashi et al., 1980). IODP Expedition 333 cores from this area showed slump folds. In a recent paper, I documented soft-sediment deformation structures (SSDS) from 140 global case studies, including the Shikoku Basin. In this study, I integrated seismic-scale deformation to core-scale deformation (Fig. 1).

After reading this rather long review paper (71 printed pages), I received an email from Klein (Date: 10/26/2017 9:02:04 PM Central Standard Time) with the following comment, "*I scan-read the paper and it appears to be the most comprehensive one I have seen on the subject. I particularly liked where you had illustration showing map, photo of SSDS and a seismic line or cross-section. Places it all in context for easy visualization and understanding. Keep up the good work. I miss academic research but I don't miss the rest of academe*." In 2017, Klein was 84 years old and was suffering from a failing health. And yet, he was keeping up with the literature on sediment deformation, which shows his total dedication to science.

John E. Sanders and the turbidite controversy

The late John E. Sanders was George Klein's Ph.D. advisor at Yale University. Sanders' (1965) seminal paper on turbidity currents and their deposits (i.e., turbidites) is still relevant today. In fact, the crux of the turbidite controversy (i.e., whether the basal high-concentration laminar layer is a truly turbidity current or not) today can be traced back to a comment by Ph. H. Kuenen and a reply by J. E. Sanders published at the end of his paper (Sanders, 1965, p. 217-219). In this context on turbidites, Paul Enos, whose Ph.D. advisor at Yale was also John Sanders, received the "Outstanding Paper Award" from SEPM for his paper "Anatomy of a flysch" (Enos, 1969).

Sanders' (1965) concepts on fluid dynamics of turbidity currents had an indelible impact on all my reinterpretations of "turbidites" as "sandy debrites" (Shanmugam, 1996). In particular, my paper (Shanmugam, 1977) "The Bouma Sequence and the turbidite mins set" was reviewed by John Sanders for the journal *Earth-Science Reviews* by the invitation of the then journal's Editor-in-Chief Gerald M. Friedman. John Sanders passed away in 1999. In honoring Sanders' pioneering contributions and those of selected other geologic pioneers, such as James Hall (1811-1898) who co-founded the Geological Society of America, the late Gerald Friedman organized a "Conference on the History of Geologic Pioneers" at the Rensselaer Center of Applied Geology, Troy, New York in 2000. At that conference, Klein (2000) presented a talk "Research guidelines learned from John E. Sanders". George Klein and Gerald Friedman also invited me to deliver a lecture on the influence of John Sanders on my turbidite research. Following my talk "John

E. Sanders and the turbidite controversy" (Shanmugam, 2000b), Gerald Friedman fondly reminisced the pioneering role played by John Sanders during the early stages of the turbidite paradigm (Sanders, 1965; Shanmugam, 2010; Mutti et al., 2009, 2010).

Deep-water sequence stratigraphy

George Klein ran a successful consulting company for the petroleum industry in Houston, Texas. He authored numerous technical reports on sequence stratigraphy for his clients (see University of Illinois Archives, cited above). Houston was also the birthplace of the paradigm of 'Sequence stratigraphy' introduced by the late Peter Vail and his colleagues at Exxon (Vail et al., 1977). Based on sequence-stratigraphic case studies from the North Sea and Norwegian Sea (Shanmugam et al., 1995), I published a critical paper titled "The obsolescence of deep-water sequence stratigraphy in petroleum geology" (Shanmugam, 2007). George Klein felt that local petroleum geologists in Houston should be exposed to my opposing points of view. Consequently, he made arrangements for me to present a lecture on the topic at SIPES (The Society of Independent Professional Earth Scientists) Houston Continuing Education Seminar on January 12, 2009. My talk stimulated a lively debate. George Klein was always willing to consider opposing points of views.

Krishna-Godavari Basin, Bay of Bengal, India: Sandy debrites and tidalites in submarine canyons

As an editor, George Klein invited me to contribute a chapter on "Submarine canyons" to the McGraw Hill Encyclopedia (Shanmugam, 1992). Preparing this chapter paved the way for my future publications on tidal currents in submarine canyons (Shanmugam, 2003; Shanmugam et al., 2009).

Klein (1975), for the first time, based on studies of DSDP (Leg 30, Sites 288 and 289) cores, suggested that current ripples, micro-cross laminae, mud drapes, flaser bedding, lenticular bedding, and parallel laminae reflect traction and suspension deposition from tidal bottom currents in deep-marine environments. This publication was revolutionary in thinking because traction structures in deep-water deposits were routinely interpreted as "turbidites" in the 1970s. At about the same time, Shepard et al. (1979) measured current velocities of tidal currents in 25 submarine canyons at water depths ranging from 46 to 4200 m by suspending current meters commonly 3 m above the sea bottom. Measured maximum velocities commonly ranged from 25 to 50 cm s^{-1}. Shanmugam et al. (2009) combined the results of Klein (1975) and Shepard et al. (1979) on tidal currents in deep-water environments and applied to the deep-water sands (Pliocene) in the Krishna–Godavari (KG) Basin, Bay of Bengal, India. George Klein served as the primary reviewer for our paper "*Sandy debrites and tidalites of Pliocene reservoir sands in upper-slope canyon environments, offshore Krishna-Godavari Basin (India), implications*" that was published in the *Journal of Sedimentary Research*. The significance is that this case study is a rare example of petroleum-producing debrite-tidalite sandy reservoir.

The contourite problem

Interpretation of traction structures in deep-water deposits has been controversial because their origins have been variously attributed to turbidity currents (Bouma, 1962), contour currents (Hollister, 1967; Shanmugam et al., 1993; Martin-Chivelet et al., 2008), and tidal currents (Klein, 1975).

Furthermore, Lovell and Stow (1981) suggested that contourites can be generated by any kind of bottom currents (i.e., thermohaline, wind, tide or baroclinic) causing additional confusion. I have critically reviewed these issues in a chapter "The contourite problem" (Shanmugam, 2016c) that appeared in the Elsevier Book "Sediment Provenance" edited by Mazumder (2016). Despite his failing health in Guam, George Klein served as the primary reviewer for my chapter. George Klein was chosen as a reviewer because of his established credentials on both bottom currents and provenance.

After his completion of peer review, we exchanged emails on our heath issues. In one of his emails (4/30/2016 1:14:49 AM Central Standard Time), Klein wrote "Just remember, Shan, old age is not for wimps." I will miss his wit!

Climate change

Long before climate change became a fad, Klein (1993) was publishing papers on the role of climate on sea-level changes. Even during his retirement years in Guam, George Klein was very active in pursuing research on "Climate Change". He was disappointed that most scientists have failed to take into account all the available data in presenting a balanced account of climate change. He strongly felt that most publications on climate change promoted a false narrative based on computer models, without a robust set of empirical data. In rectifying this problem, he relentlessly gathered data. As a result, he was invited to present a talk, “Some Geological Aspects of Long- and Short-term Climate Change” at the 2016 University of Guam Island Sustainability Conference. He also presented two other talks on the topic, one at the Western Pacific Water and Environmental Research Institute, and the other at the University of Guam Marine Sciences Laboratory.

Klein (2016) summarized his findings on climate change as follows:

- Geological observations, data and measurements show that throughout the last 600 million years, global temperatures changed independently of changes in CO_2 content.
- The Antarctic Vostok Ice Core shows that during the past 400,000 years increases in temperature occurred ~800-1000 years prior to measured increases in CO_2. Past temperature cycles show that climate always recovered from extremes.
- Evidence for “Tipping Points” and runaway “scenarios” appear absent from the geological record, even though CO_2 content was unusually high during certain past geological periods.
- Pacific Ocean coral reef growth keeps pace with rising sea level; thus barrier and fringing reefs likely can protect islands and island nations from flooding during sea level rise.
- Additional factors contributing to relative sea level change include island thermal subsidence, tectonic uplift, and hydro-isostasy. Mitigation by land-raising is a plausible solution to potentially threatened islands."

George Klein had an uncanny ability to scan through virtually everything that is published on climate change in both print and digital media and to pick out rare nuggets of useful information. He would immediately share the new information with a close circle of 36 scientists worldwide via email. I was fortunate enough to be one among the 36. It was always a delight to

open his frequent emails, expecting some new information on climate change. He was also very sharp in expressing his conservative views on economy, environment, judiciary, media, and politics in the United States.

Petroleum geology

According to Klein (2009), his global consulting work dealing with petroleum reservoirs covered the US Gulf of Mexico, Illinois basin, Appalachian basin, Angola, Senegal, South Africa, East Africa, Brazil, Peru, Venezuela, Mexico, Romania, Russia, and the eastern Mediterranean. It is worthwhile to mention in this context that he discovered on his own or as part of a team some 160 million barrels of oil and some 3 trillion cubic feet of natural gas. By popular demand, a third edition of Klein's (1985) book "Sandstone depositional models for exploration for fossil fuels", was published.

Rocknocker: A geologist's memoir

Klein's (2009) final book appropriately reviewed the life of George Devries Klein. He wa an immigrant who made it through the American System as a geologist. The book chronicled his life from early childhood, graduate school, working as an oil company researcher, university professor, science administrator, and as a geological consultant to the petroleum industry. The book included the highs and lows of George's life. Each chapter also summarizes key lessons learned making the book even more useful to young scientists as a career guide.

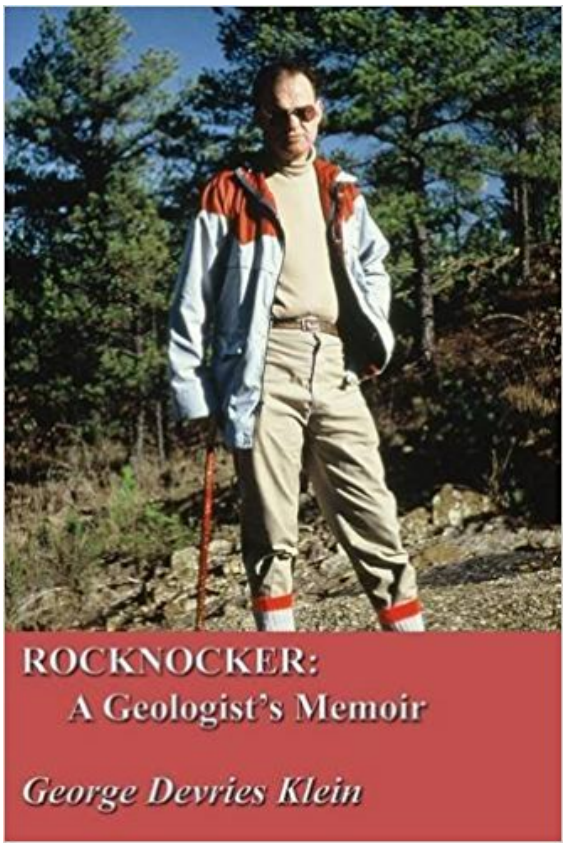

Book cover: CCB Publishing

EPILOGUE

In his passing, the global geology community has lost a great scientist, teacher, friend, philosopher, critic, guide, and patriot. In an era of 'groupthink', George Klein represented a rare tribe of free-thinking scientists. Fortunately, he left us with a legacy rich in enduring doctrines that future generations will ever be grateful.

ACKNOWLEDGEMENTS

I thank Prof. G. M. Bhat, Managing Editor of JIAS, for encouraging me to submit this tribute. I am grateful to my wife, Jean Shanmugam, for her comments. I also thank CCB Publishing for the use of the cover image of Klein's book "Rocknocker: A Geologist's Memoir".

References

Bouma, A.H. (1962). Sedimentology of Some Flysch Deposits: A Graphic Approach to Facies Interpretation. Elsevier, Amsterdam, 168 p.

Cline, L.M. (1970). Sedimentary features of Late Paleozoic flysch, Ouachita Mountains, Oklahoma. In: Lajoie, J. (Ed.), Flysch Sedimentology in North America, The Geological Association of Canada Special Paper 7, pp. 85–101.

Davis Jr., R.A., Dalrymple, R.W. (Eds.), (2012). Principles of Tidal Sedimentology. Springer, Berlin, Germany, 621 p.

Enos, P. (1969). Anatomy of a flysch. Journal of Sedimentary Petrology, 39, 680-723.

Expedition 333 Scientists (2011). Integrated Ocean Drilling Program Expedition 333 Preliminary Report NanTroSEIZE Stage 2: Subduction Inputs 2 and Heat Flow. Texas A&M University, College Station, Texas. http://dx.doi.org/10.2204/iodp.pr.333.2011.

Expedition 333 Scientists (2012). Site C0018. In: Henry, P., Kanamatsu, T., Moe, K., the Expedition 333 Scientists (Eds.), Proceedings of the Integrated Ocean Drilling Program, Volume 333. Texas A&M University, College Station, Texas. http://dx.doi.org/10.2204/iodp.proc.333. 103.2012.

Hollister, C. D. (1967). Sediment Distribution and Deep Circulation in the Western North Atlantic (Ph.D. dissertation). Columbia University, New York, 467 p.

Klein, G. D. (1959). Sedimentary structures in the Blomidon Formation, a Triassic lake deposit (Abs). Geol. Soc. America Bull., 70, 1630.

Klein, G. D. (1961). Depositional environments and sandstone petrology of Triassic sedimentary rocks, western Nova Scotia, Canada. Tulsa, Geol. Soc. Digest, 29, 221-222.

Klein, G. D. (1963). Bay of Fundy intertidal zone sediments. Jour. Sedimentary Petrology., 33, 844-854.

Klein, G. D. (1964). Sedimentary facies in Bay of Fundy intertidal zone, Nova Scotia, Canada. In: Van Straaten, L.M.J.U., (Ed.), Deltaic and shallow marine deposits, Amsterdam, Elsevier, pp. 193-199.

Klein, G. D. (1966). Dispersal and petrology of sandstones of Stanley-Jackfork boundary, Ouachita foldbelt, Arkansas and Oklahoma. AAPG Bulletin 50, 308-326.

Klein, G. D. (1967). Comparision of Ancient and Recent tidal flat and estuarine sediments. In: Lauff, G.H., (Ed.), Estuaries. Am. Assoc. for the Advancement of Science Spec. Pub. 83, pp. 207-218.

Klein, G. D. (1970). Depositional and dispersal dynamics of intertidal sand bars. Jour. Sedimentary Petrology, 40, 1095-1127.

Klein, G. D. (1971). A sedimentary model for determining paleotidal range. Geological Society of America Bulletin, 82, 2585–2592.

Klein, G. D. (1975). Resedimented pelagic carbonate and volcaniclastic sediments and sedimentary structures in Leg 30 DSDP cores from the western equatorial Pacific. Geology, 3, 39-42.

Klein, G. D. (1977). Clastic tidal facies. CEPCO, Champaign, IL, 148 p.

Klein, G. D. (1985). Sediment diagenesis. Am. Scientist, 73, 290-291.

Klein, G. D. (1987). Current aspects of basin analysis. Sed. Geol., 50, 95-118.

Klein, G. D. (1993). Quantitative Discrimination of Tectonic and Climatic Components of Pennsylvanian Sea-level Change. In: Armentrout, J. M., Bloch, R., Olson, H. C., and Perkins, R. F., (Eds.), Rates of Geologic Processes - Tectonics, Sedimentation, Eustasy and Climate: Implications for Petroleum Exploration: Fourteenth Annual Res. Conf, Gulf Coast Section, SEPM Foundation, pp. 77-80.

Klein, G. D. (2000). Research guidelines learned from John E. Sanders. In: Friedman, G.M. (Ed.), Conference on the History of Geologic Pioneers. Rensselaer Center of Applied Geology, Troy, New York, pp.12.

Klein, G. D. (2003). Dissensions. Xlibris, www.Xlibris.com, 370 p.

Klein, G. D. (2009), Rocknocker: A Geologist's Memoir, CCB Publishing, British Columbia, Canada, 431p.

Klein, G. D. (2016). Some Geological Aspects of Long- and Short-Term Climate Change Relevant to Pacific Tropical Islands. Search and Discovery Article #70217 (http://www.searchanddiscovery.com/pdfz/documents/2016/70217klein/ndx_klein.pdf.html).

Klein, G. D., J. E., Sanders., J. E. (1964). Comparison of sediments in tidal flats in the

Bay of Fundy and the Dutch Wadden Zee. Jour. Sedimentary Petrology., 34, 18-24.

Klein, G. D., and Willard, D. A. (1989). Origin of the Pennsylvanian coal-bearing cyclothems of North America. Geology, 17, 152-155.

Klein, G. D., Kobayashi, K., White, S. M., Chamley, H., Curtis, D. M., Mizuno, A., Dick., H. J. B., Nisterenko, G. V., Marsh, N. G., Waples, D. M., Echols, D. J., Okada, H., Sloan, J. R., Fountain, D. M. and Kinoshita, H. (1980). Initial Reports of the the Deep Sea Drilling Project, v. 58: Washington, U.S. Government Printing Office, 1017 p.

Lawson, D. E. (1981). Mobilization, movement and deposition of active subaerial sediment flows, Matanuska Glacier, Alaska. Journal of Geology, 90, 279-300.

Lovell, J. P. B. and Stow, D. A. V. (1981). Identification of ancient sandy contourites. Geology, 9, 347-349.

Martın-Chivelet, J., Fregenal-Martnez, M. A. and Chacón, B. (2008). Traction structures in contourites. In: Rebesco, M., Camerlenghi, A. (Eds.), Contourites, Developments in Sedimentology, vol. 60. Elsevier, Amsterdam, pp. 159-182 (Chapter 10).

Mazumder, R. (Ed.) (2016). *Sediment Provenance,* Elsevier, 614 p.

Moiola, R. J., Shanmugam, G. (1984). Submarine fan sedimentation, Ouachita Mountains, Arkansas and Oklahoma. Transactions-Gulf Coast Association of Geologists Societies, 34, 175–182.

Morris, R. C. (1977). Flysch facies of the Ouachita trough- with examples from the Spillway at the DeGray Dam, Arkansas. In: Symposium on the Geology of the Ouachita Mountains, Arkansas Geological Commission, 1, 158–169.

Mutti, E., Bernoulli, D., Ricci Lucchi, F., and Tineterri, R. (2009). Turbidites and turbidity currents from Alpine 'flysch' to the exploration of continental margins. Sedimentology, 56, 267-318.

Mutti, E., Bernoulli, D., Ricci Lucchi, F., and Tineterri, R. (2010). Reply to the discussion by Ganapathy Shanmugam on "Turbidities and turbidity currents from Alpine flysch to the exploration of continental margins" by Mutti et al. (2009). Sedimentology, 56, 267e-18.

Sanders, J. E. (1965). Primary sedimentary structures formed by turbidity currents and related resedimentation mechanisms. In: Middleton, G.V. (Ed.), Primary Sedimentary Structures and Their Hydrodynamic Interpretation, 12. SEPM Special Publication, Tulsa, OK, pp. 192-219.

Shanmugam, G. (1992). Submarine canyons: 7th Edition of Encyclopedia of Science and Technology. McGraw-Hill Book Company, New York, p. 548-552.

Shanmugam, G. (1996). High-density turbidity currents, are they sandy debris flows? Journal of Sedimentary Research 66, 2-10.

Shanmugam, G. (1997). The Bouma sequence and the turbidite mind set. Earth-Science Reviews 42, 201-229.

Shanmugam, G. (2000a). 50 years of the turbidite paradigm (1950s-1990s): Deep-water processes and facies models -- a critical perspective. Marine and Petroleum Geology, 17, 285-342.

Shanmugam, G. (2000b). John E. Sanders and the turbidite controversy. In: Friedman, G.M. (Ed.), Conference on the History of Geologic Pioneers. Rensselaer Center of Applied Geology, Troy, New York, pp. 19-20.

Shanmugam, G. (2003). Deep-marine tidal bottom currents and their reworked sands in modern and ancient submarine canyons. Marine and Petroleum Geology 20, 471-491.

Shanmugam, G. (2007). The obsolescence of deep-water sequence stratigraphy in petroleum geology. Indian Journal of Petroleum Geology, 16 (1), 1-45.

Shanmugam, G. (2010). Discussion, "Turbidites and turbidity currents from Alpine 'flysch' to the exploration of continental margins" by Mutti et al. (2009). Sedimentology 56, 267-318.

Shanmugam, G. (2016a). The seismite problem. *Journal of Palaeogeorapghy*, 5 (4), 318–362.

Shanmugam, G. (2016b). Submarine fans: A critical retrospective (1950-2015). Journal of Palaeogeography, 5 (2), 110-184.

Shanmugam, G. (2016c). The contourite problem. In: Mazumder, R., (Ed.), *Sediment Provenance, Chapter 9*. Elsevier, pp. 183–254.

Shanmugam, G. (2017). Global case studies of soft-sediment deformation structures (SSDS): Definitions, classifications, advances,

origins, and problems. Journal of Palaeogeorapghy, 6(4), 251-320.

Shanmugam, G. (2018). Professor George Devries Klein (1933-2018): A sedimentologic pioneer. AAPG Bulletin, 102, in press.

Shanmugam, G., and Moiola, R. J. (1988). Submarine fans, Characteristics, models, classification, and reservoir potential. Earth-Science Reviews 24, 383-428

Shanmugam, G., and Moiola, R. J. (1995). Reinterpretation of depositional processes in a classic flysch sequence(Pennsylvanian Jackfork Group), Ouachita Mountains, Arkansas and Oklahoma. AAPG Bulletin, 79, 672-695.

Shanmugam, G., and Moiola, R. J. (1997). Reinterpretation of depositional processes in a classic flysch sequence (Pennsylvanian Jackfork Group), Ouachita Mountains, Arkansas and Oklahoma, reply. AAPG Bulletin, 81, 476-491

Shanmugam, G., Moiola, R. J., and Sales, J. K. (1988). Duplex-like structures in submarine fan channels, Ouachita mountains, Arkansas. Geology 16, 229-232.

Shanmugam, G., Spalding, T.D., and Rofheart, D.H. (1993). Process sedimentology and reservoir quality of deep-marine bottom-current reworked sands (sandy contourites): an example from the Gulf of Mexico. AAPG Bulletin, 77, 1241-1259.

Shanmugam, G., Bloch, R. B., Mitchell, S. M., Beamish, G. W. J., Hodgkinson, R. J., Damuth, J. E., Straume, T., Syvertsen, S. E. and Shields, K. E. (1995). Basin-floor fans in the North Sea, sequence stratigraphic models vs. sedimentary facies. AAPG Bulletin, 79, 477-512.

Shanmugam, G., Shrivastava, S. K., and Das, B. (2009). Sandy debrites and tidalites of Pliocene reservoir sands in upper-slope canyon environments, offshore Krishna-Godavari Basin (India), implications. Journal of Sedimentary Research, 79, 736-756.

Shepard, F. P., Marshall, N. F., McLoughlin, P. A., and Sullivan, G. G. (1979). Currents in submarine canyons and other sea valleys. AAPG Studies in Geoloy 8, 173 p.

Vail, P. R., Mitchum Jr., R. M., and Thompson III, S. (1977). Seismic stratigraphy and global changes of sea level, part 4: global cycles of relative changes of sea level. In: Payton, C.E. (Ed.), Seismic Stratigraphy–Applications to Hydrocarbon Exploration, AAPG Memoir 26, pp. 83–97.

Tribute by
G. Shanmugam
Department of Earth and Environmental Sciences
The University of Texas at Arlington
Arlington, TX 76019, USA
Email: shanshanmugam@aol.com
Submitted May 27, 2018